McGRAW-HILL
INTERNATIONAL
BOOK COMPANY

New York
St. Louis
San Francisco
Auckland
Beirut
Bogotá
Düsseldorf
Johannesburg
Lisbon
London
Lucerne
Madrid
Mexico
New Delhi
Panama
Paris
San Juan
São Paulo
Singapore
Sydney
Tokyo
Toronto

S. RINALDI
Centro Teoria dei Sistemi,
C.N.R.,
Politecnico di Milano,
Italy

R. SONCINI-SESSA
Centro Teoria dei Sistemi,
C.N.R.,
Politecnico di Milano,
Italy

H. STEHFEST
Kernforschungszentrum, Karlsruhe,
Abteilung für angewandte Systemanalyse,
Karlsruhe,
West Germany

H. TAMURA
Department of Precision Engineering,
Osaka University,
Japan

Modeling and Control of River Quality

Riprodotto per gentile concessione dell'Autore
con autorizzazione del 11.3.1991
da CittàStudi S.c.r.l., Milano

This book was set in Times Roman, Series 327

British Library Cataloging in Publication Data

Modeling and control of river quality.
(McGraw-Hill advanced book program)
1. Water—Pollution
I. Rinaldi, S.
628.1'688'1693 TD425 77-30475

ISBN 0-07-052925-6

**MODELING AND CONTROL OF
RIVER QUALITY**

1 2 3 4 W.&J.M. 8 0 7 9 8

Printed and bound in Great Britain

CONTENTS

LIST OF SYMBOLS†

Latin Lower Case

b	biochemical oxygen demand concentration (BOD)
$\bar{b}$	BOD standard
c	dissolved oxygen concentration (DO)
$\underline{c}$	DO standard
c_s	oxygen saturation concentration
$\mathrm{cov}(\cdot)$	covariance
d	dissolved oxygen deficit
$\bar{d}$	DO deficit standard
d_c	critical DO deficit
$\det(\mathbf{A})$	determinant of matrix **A**
$\mathrm{div}(\cdot)$	divergence operator
$\mathbf{e}^{\mathbf{F}(t-t_0)}$	transition matrix
$\mathbf{g}$	input-state vector
$\mathrm{grad}(\cdot)$	gradient operator
h	elevation of the river bottom from a reference level
$\mathbf{h}^T$	state-output row
k_1	deoxygenation (degradation) coefficient
k_2	reaeration coefficient
l	spatial coordinate along the river

---

† This list contains only the symbols which are used in at least two sections of the book. Boldface letters indicate vectors, matrices, or sets. If a vector or matrix degenerates to a scalar, the corresponding italic letter is used.

l_c	location of critical DO deficit
m	mass
$m(t)$	impulse response
p	concentration
$p(A)$	probability density function
$p(A\|B)$	probability density function of A conditioned to B
q	lateral inflow per unit of length
$r(c)$	reaeration rate
s	complex variable (in Laplace transform), substrate concentration
$\mathbf{s}(t)$	sensitivity vector
t	time
$\mathbf{u}(\cdot)$	input function
$\mathbf{u}(t)$	input value at time t
v	velocity
$\mathbf{v}(t)$	process noise
$\mathrm{var}(\cdot)$	variance
w	propagation velocity
$\mathbf{w}(t)$	output (measurement) noise
w_1	easily degradable pollutant concentration
w_2	slowly degradable pollutant concentration
w_3	nondegradable pollutant concentration
$\mathbf{x}(t)$	state at time t
$\mathbf{y}(\cdot)$	output function
$\mathbf{y}(t)$	output value at time t
z	vertical spatial coordinate, decision vector
$\mathbf{z}(t)$	extended state at time t

Greek Lower Case

δ	variation, perturbation
$\delta(\cdot)$	impulse function
$\varepsilon(t)$	estimation error
$\eta(t, \mathbf{x})$	output transformation
$\boldsymbol{\theta}$	parameter vector
λ	eigenvalue, Lagrange multiplier
μ	static gain
ξ	elevation of the river surface from a reference level
ρ	mass density
σ	standard deviation
τ	flow time
$\tau(l, u)$	tax, charge
ϕ	phase
$\phi(\omega)$	phase of frequency response
$\boldsymbol{\phi}(t_0, t, \mathbf{x}_0, \mathbf{u}_{[t_0,t)})$	transition function
$\boldsymbol{\psi}_{t_0,\mathbf{x}_0}$	input-output relationship
ω	frequency

Latin Upper Case

A	cross-sectional area of the river
BOD	biochemical oxygen demand
B	bacterial biomass concentration
$\mathscr{C}$	cost
$\mathbf{C}$	controllability matrix
COD	chemical oxygen demand
$\mathscr{D}$	dispersion term
$\mathbf{D}$	dispersion matrix (coefficient)
DO	dissolved oxygen
E	environmental damage
$E[\cdot]$	expectation operator
$\mathbf{F}(t)$	"state-state" matrix
$\mathbf{G}(t)$	"input-state" matrix
H	river depth
$\mathbf{H}(t)$	"state-output" matrix
$\mathbf{I}$	identity matrix
J	performance index
$\mathbf{K}(t)$	control law matrix
K_L	laboratory BOD decay rate
$\mathscr{L}[\cdot]$	Laplace transform
L	length of river stretch
L_c	limit value of l_c
$L(l, t)$	distributed BOD load
$\mathbf{L}(t)$	Kalman filter gain matrix
$L(z, \lambda)$	Lagrangian
$\mathbf{M}(s)$	transfer function
$\mathbf{O}$	observability matrix
$\mathscr{P}$	pollution index
P	protozoa biomass concentration, oxygen production
Q	flow rate
R	oxygen consumption due to respiration
$R(\omega)$	module of frequency response
S	source term in balance equation
S_Q	rate of water inflow
T	time, temperature
$\mathbf{U}$	input set
$\mathbf{U}(s)$	Laplace transform of $\mathbf{u}(t)$
V	volume
$\mathbf{V}_\varepsilon$	covariance matrix of the estimation error
$\mathbf{X}$	state set
$\mathbf{X}(s)$	Laplace transform of $\mathbf{x}(t)$
Y	river width, output set
$\mathbf{Y}(s)$	Laplace transform of $\mathbf{y}(t)$
$\mathbf{Z}$	feasibility set

CHAPTER

TWO

WATER POLLUTION PROCESSES AND QUALITY INDICATORS

2-1 HYDROLOGIC PHENOMENA

The study of the dynamics of river flow constitutes perhaps the most classical chapter of the hydrological sciences (see, for example, Gray, 1970). This is largely due to the importance of these studies in flood control and water management in general, and partly to the possibility of describing the phenomenon of surface runoff in a reasonably simple way, as shown in Sec. 3-3.

In principle one should consider *surface runoff* as a part of the so-called *water cycle* which starts with *evaporation*, continues with *formation of clouds*, *precipitation*, *interception* by vegetation, *infiltration*, and *percolation* and terminates with *overland flow*, *interflow*, and *groundwater flow* generating surface runoff as shown in Fig. 2-1-1. Some of these phenomena, such as groundwater dynamics, are characterized by very smooth variations over time, while some others, such as overland flow, are almost immediate responses to precipitation. Spatial scale is also very diverse and changes of state occur in many points of the water cycle. Nevertheless, hydrologists often simplify the description of such a complex system by isolating the main mechanisms involved and by neglecting some interactions between them. A typical result of this approach is the block diagram of Fig. 2-1-2 which represents a still general conceptual model of the entire water cycle. Simplified conceptual models for describing particular aspects of the water cycle can be obtained from this general model by further neglecting some of the interactions between the blocks. For example, if river flow must be determined from rainfall data, then evaporation from ground and water surfaces together with interception can be neglected provided that the time period of the investigation is sufficiently short. The model obtained in this way is a so-called *rainfall-runoff* model and can be used to estimate the *peak flow rates* and their times of

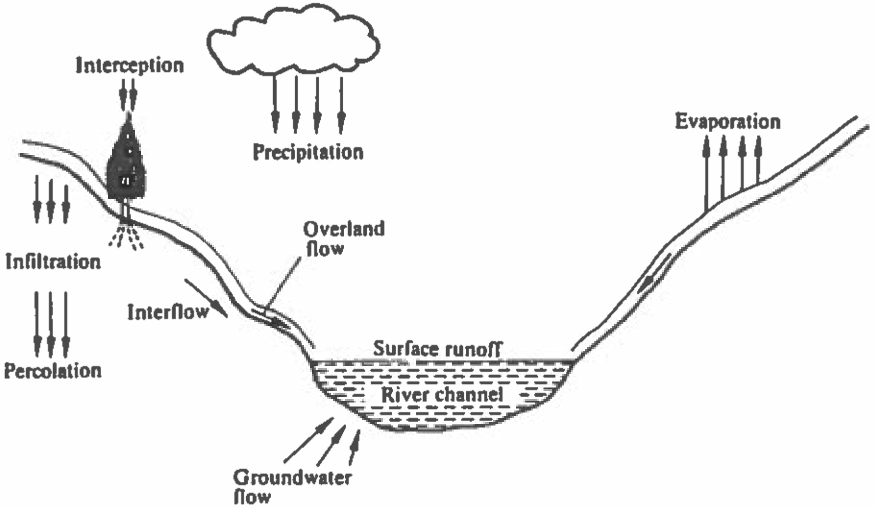

Figure 2-1-1 The water cycle.

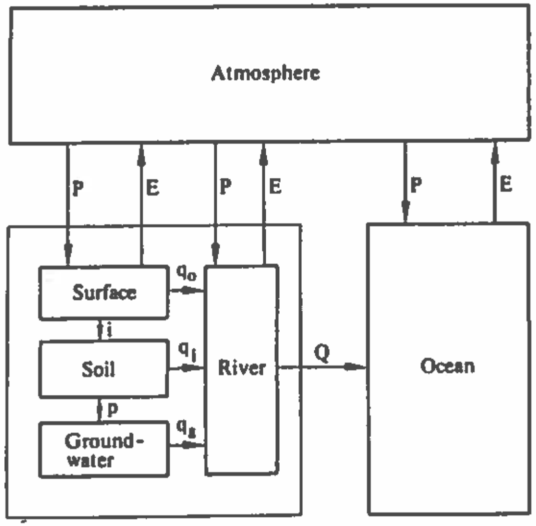

P = Precipitation
E = Evaporation
q_o = Overland flow
q_i = Interflow
q_g = Groundwater flow
Q = River flow
i = Infiltration
p = Percolation

Figure 2-1-2 A general conceptual model of the water cycle.

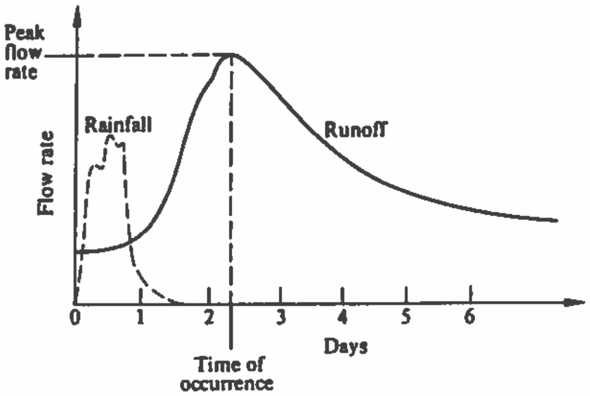

Figure 2-1-3 The runoff hydrograph corresponding to a given rainfall event.

occurrence corresponding to given rainfall events as shown in Fig. 2-1-3 for a particular runoff *hydrograph*. The main properties of this phenomenon are the delay between the rainfall and runoff peaks due to transport time, the smoothing of the rainfall variations due to the diversity among the paths of water particles, and the long tail of the runoff curve due to groundwater flow.

Another problem extensively studied by hydrologists is the propagation of the flood wave in a river stretch. One way of looking at the problem is as follows: suppose a very high variation of flow rate occurs at time t_0 at the upstream end of the river stretch and assume that this variation takes place only during a very short period of time. Subsequent observations at downstream stations show that the wave propagation along the river can be described by a sequence of bell-shaped curves as shown in Fig. 2-1-4. The time of occurrence of the peaks increases with the distance of the station from the upstream end and the bell curves are smoother for downstream stations. The area under each curve is the

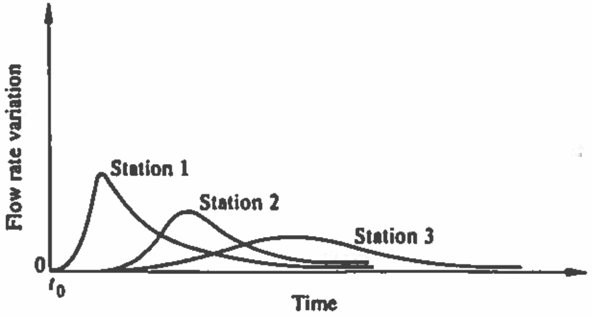

Figure 2-1-4 Time variations of flow rate in three given stations due to an impulse of flow rate at the upstream end of the river.

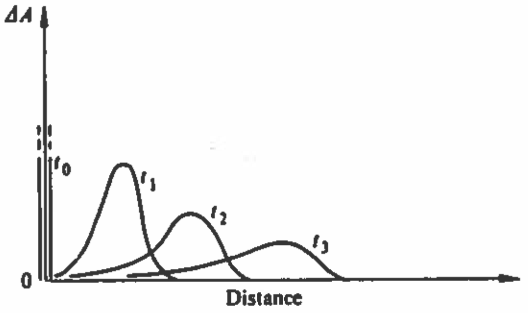

Figure 2-1-5 Spatial variation of the cross-sectional area at different times.

variation of the total volume (or mass) of the water in the river and must therefore be constant if there are no losses in the stretch; thus, the spreading out of the curves implies that the peaks decrease downstream. Another way of looking at the problem is to sample over time the variations of flow rate, or better, of cross-sectional area along the stretch. Again a sequence of bell curves is obtained, as shown in Fig. 2-1-5, and the area underlying the curves is constant since it represents, as before, the total volume of water characterizing the input disturbance. Moreover, quantitative observations show that the bell curves are skewed (steeper at the front of the wave), that the wave propagation velocity is greater than stream velocity, and that the difference between the two velocities increases with the depth of the river.

The relevance of these phenomena in river pollution modeling and control is still relatively limited since for most studies the hydrologic variables can be assumed to be constant in time (this is not the case in estuaries, lakes, and seas). Of course, some relationships between hydrological variables are needed. For example, it is often important to know how the stream velocity is related to the flow rate in steady state conditions. This function, which is increasing and concave, allows one to determine the traveling time of the pollutants between different points on the river when the flow rate is known. Moreover, a hydrologic phenomenon which is very important for river pollution studies is *dispersion*, which is due to the random variations of the velocity in the river (turbulence). Suspended particles and/or dissolved compounds are transferred downstream along different paths so that, on average, pollutants are dispersed in all directions. Although this effect could correctly be explained only by higher dimensional models (models in which there are two or three spatial coordinates), the following will show how dispersion along the axis of the river can be taken into account, together with *molecular diffusion*, by using simple one-dimensional models.

2-2 THERMAL PHENOMENA

An important variable for all river quality considerations is water temperature. Its importance is mainly due to the temperature dependence of many processes through which other quality indicators, like oxygen concentration or pollutant concentration, are determined (these influences will be discussed in the next section). On the other hand, temperature has also to be considered as a quality indicator per se, which affects the kind of fish in the river, the temperature of the drinking water produced from the river water, fog frequency along the river, flow rate, etc. Hence, modeling and control of river quality comprises modeling and control of river temperature, and a prerequisite for this is the understanding of the processes which affect river temperature (see, for example, Krenkel and Parker, 1969; Jobson and Yotsukura, 1972; Heidt, 1975).

These processes are shown symbolically in Fig. 2-2-1, and can be divided into four groups: energy exchange with the atmosphere, energy exchange with the river-bed, internal heat production, and anthropogenic heat addition or subtraction. The radiative energy transport through the water surface consists of three components: short-wave solar radiation, long-wave atmospheric radiation, and long-wave radiation of the river. The *short-wave solar radiation* is that part of the solar radiation which is not absorbed by the atmosphere; it is mainly visible light. The incident energy depends on the atmospheric conditions (e.g., cloudiness) and on the orography of the valley. Part of the incident visible light is reflected, the rest is converted into heat within the river. The proportion reflected depends on the incidence angle, and is usually less than 10 percent. The *long-*

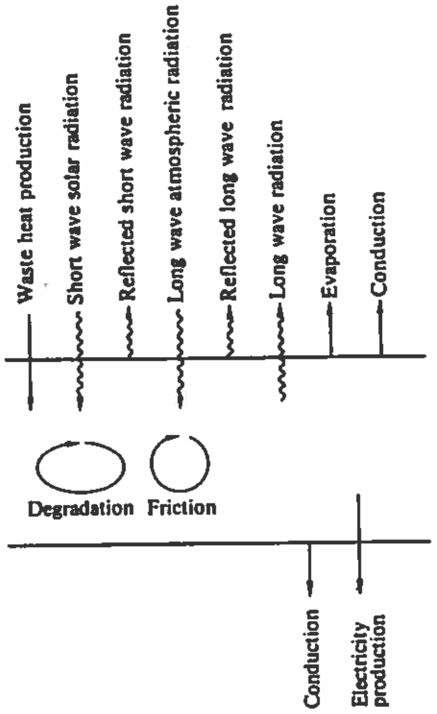

Figure 2-2-1 Heat transfer mechanisms of a river.

wave atmospheric radiation is emitted by the atmosphere above the river (temperature radiation). Its intensity depends on air temperature and humidity. Since the absorption coefficient of air for infrared radiation is low, temperature and humidity in an atmospheric layer of several hundred meters thickness are relevant for this component of the heat balance. About 3 percent of the long-wave atmospheric radiation is reflected. The *long-wave radiation of the water* is emitted only by a very thin surface layer, because the absorption coefficient of water for infrared radiation is high. Hence, the surface temperature is the variable which determines the radiative heat loss of the river.

Energy may also be exchanged between the river and the atmosphere through heat conduction (exchange of *sensible heat*). Pure heat conduction, i.e., heat transport through molecular or atomic collisions, is, however, important only at the air–water interface. Within the two media heat is transported mainly through convection, which occurs in the form of both large scale movement (e.g., advection) and turbulent mixing (*eddy diffusion*, see also Sec. 2-1). The convection in air is primarily forced by the wind. Therefore, the flux of sensible heat through the water surface depends not only on the air and water temperature, but also on wind velocity. Even if no wind is blowing, turbulent mixing is the main transport mechanism for sensible heat in air, because the river flow generates air turbulence through the frictional contact with air. Under particular circumstances *buoyancy forces* may be major sources of convection, for example, if the water temperature is much higher than the air temperature. The convection within the river is, of course, a function of the river flow rate.

The *evaporation* of water from the river also represents a transport of heat, because the change in the state of aggregation requires energy. The heat abstracted from the water through evaporation does not correspond to an increase of air temperature, but occurs as heat only when the water vapor condenses again; that is why one speaks of a flux of *latent heat* from the water to the air. The net evaporation rate is the sum of microscopic evaporation and condensation processes. Thus, the net flux of latent heat obviously depends on the water vapor pressure in the air and on the surface temperature of the water. (The latter determines the saturated vapor pressure of the water.) The dispersion of the evaporated water is governed by the same processes as the dispersion of the sensible heat. Therefore, the dependence of the latent heat flux on wind velocity can be expected to be the same as that of sensible heat. In rare cases the net evaporation is negative, i.e., water vapor condenses at the river surface. The sensible heat carried away by the evaporated water can be neglected. Similarly, the addition of heat through rain, which is not shown in Fig. 2-2-1, is usually negligible.

The heat exchange with the river bed is determined by the heat conductivity of the soil. Since this is very small and also the temperature gradients which occur are moderate, the heat exchange with the river bed can usually also be neglected.

The internal heat production in the river is mainly due to two effects: conversion of potential energy of the water into *frictional heat* and biochemical conversion of chemical energy into heat. The latter plays a minor role even in heavily polluted rivers.

The direct impact of human activities on river temperature consists mainly in the discharge of *waste heat* and in the abstraction of energy, which otherwise would be converted into heat, through *hydropower plants*. Waste heat is a by-product of numerous industrial processes, and the easiest way to dispose of it is by discharging it into rivers (see Sec. 7-2). The main waste heat sources are electric power plants; other sources include chemical plants which have to be cooled, river navigation, or domestic sewage. The abstraction of energy through hydropower plants can often be neglected.

If waste heat is discharged into a river, and one follows the water as it flows downstream, one observes an extra flux of energy from the river to the atmosphere which tends to establish the *natural river temperature*, i.e., the temperature which the river would have if there were no waste heat sources. This extra flux is usually desirable. It can be enhanced by choosing an appropriate outlet structure which influences the way in which the waste heat is admixed to the river. Figure 2-2-2 shows three admixture modes to aim for. The extra heat flux is certainly highest with mode (a), where one is attempting to distribute the heated water quickly over the river surface. But this option has the drawback of hindering the diffusion of oxygen into the water (see Sec. 2-3). The difference between the extra heat fluxes of solution (b) and (c) is small. If rapid mixture is achieved, the heated surface is large but the temperature increase is small; with slow transverse mixing the opposite is the case.

Finally, it should be mentioned that the natural temperature of a river may be changed drastically through hydraulic engineering constructions, which change the heat convection within the river. An extreme example is the construction of a big reservoir with the outlet at the bottom of the dam; then the river temperature immediately downstream of the dam is practically constant throughout the year, while before the construction there may have been large annual and diurnal variations.

Summarizing the discussion of the various heat transfer processes, one can

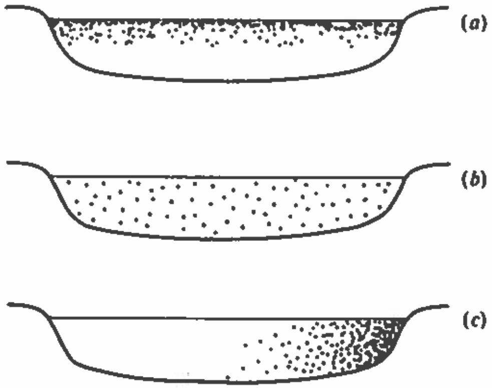

Figure 2-2-2 Admixture modes for waste heat:
(*a*) heated surface layer
(*b*) rapid mixing
(*c*) slow transverse mixing
(The density of the dots represents the temperature distribution over the river cross section).

state that for both the natural river temperature and the additional heat flux due to an artificial temperature increase the most relevant quantities are the convection characteristics of the river and the meteorological parameters which affect the energy transfer through the water surface. The importance of the meteorological parameters has led to the concept of the *equilibrium temperature*, which is defined as the temperature which a completely mixed water column has if the net heat flux through its surface is zero; the column is assumed to be thermally insulated laterally and at the bottom. The equilibrium temperature is determined uniquely by the meteorological conditions; it may be lower or higher than the air temperature. Roughly speaking, one can say that at each moment the energy transfer processes through the river surface tend to establish this temperature level.

2-3 BIOCHEMICAL AND SELF-PURIFICATION PHENOMENA

Most river quality problems are generated by matter which is discharged into the river as a consequence of human activities. Many of these problems are related to the interactions between the discharged matter and river organisms, such as bacteria, rooted plants, and fish; these interactions are now discussed.

A Laboratory Experiment

The impact of a pollutant discharge on river biology can be studied qualitatively through the following laboratory experiment. A sample of river water containing a representative biological community (*biocenosis*) is placed in a reaction tank. A given amount of pollutants at a given instant of time is added, and the resultant processes in the sample are observed. The processes observed correspond to the processes going on in a volume of river water which is flowing downstream; the addition of the pollutant in the experiment corresponds to a single wastewater effluent on the river. While the observations along the river would be disturbed by other effluents and varying hydrology and temperature, in the laboratory experiment described the biochemical processes can be studied under well-defined, constant conditions. That is why observations from such an experiment, which are shown in Fig. 2-3-1 (Münch, 1970), are used as a guide-line for the following discussion. Peptone, which is a mixture of protein fragments, was added at $t = 0$. Hence the "pollutant" was made up of amino acids, which contain considerable amounts of organically bound nitrogen. The development of both the biocenosis and several chemical characteristics was observed. The groups of organisms present other than the bacteria all belong to the subkingdom of *protozoa*, i.e., only unicellular organisms were observed in this experiment. Each group comprises a great variety of species; as an example, Fig. 2-3-2 shows the disaggregation of the class *Ciliata* into single species. Detailed descriptions of the various organisms may be found in textbooks on water biology, e.g., in Liebmann (1962).

Looking at the curves of Figs. 2-3-1 and 2-3-2 it is apparent that peptone stimulates the growth of the species present in the sample. The energy source for this so-called *succession* must be the electrochemical energy of the peptone, since no other energy source is available (the experiment was run in the dark). The appearance of inorganic forms of nitrogen indeed indicates that peptone has been decomposed. The sequential occurrence of ammonium (NH_4^+), nitrite (NO_2^-), and nitrate (NO_3^-), and the subsequent decline of ammonium and nitrite suggest that the primary decomposition product is ammonium, which is then oxidized to nitrate (via nitrite). The concentrations of the dissolved gases carbon dioxide (CO_2) and oxygen (O_2) are at saturation level at the beginning, i.e., the diffusion currents of the gas molecules through the water surface are equal in both directions.

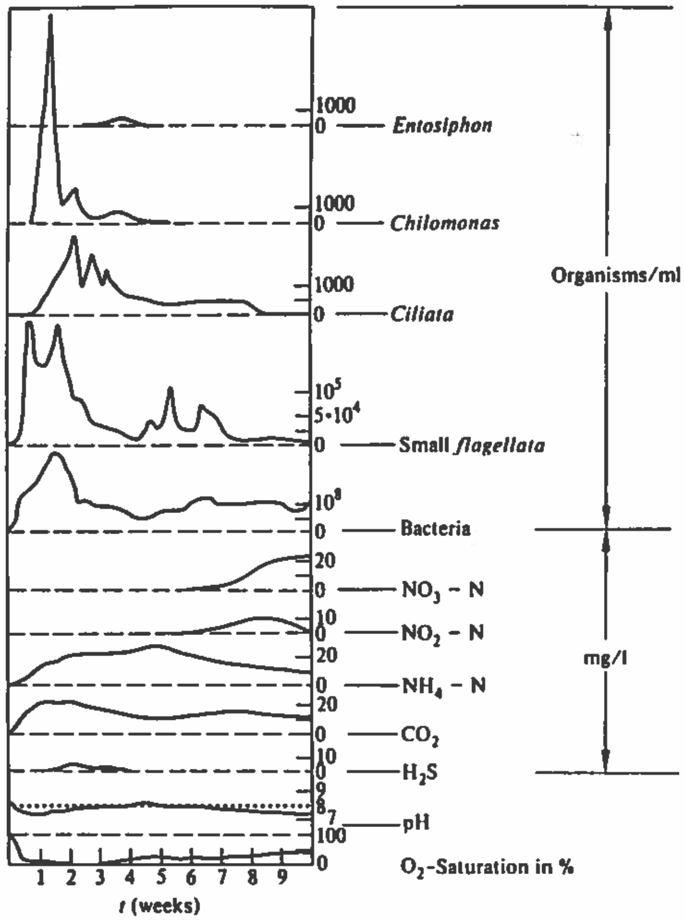

Figure 2-3-1 Changes induced in a natural water sample through the addition of peptone at $t = 0$ (after Münch, 1970, $T = 10\,°C$. The inorganic nitrogen compounds are represented through their nitrogen content).

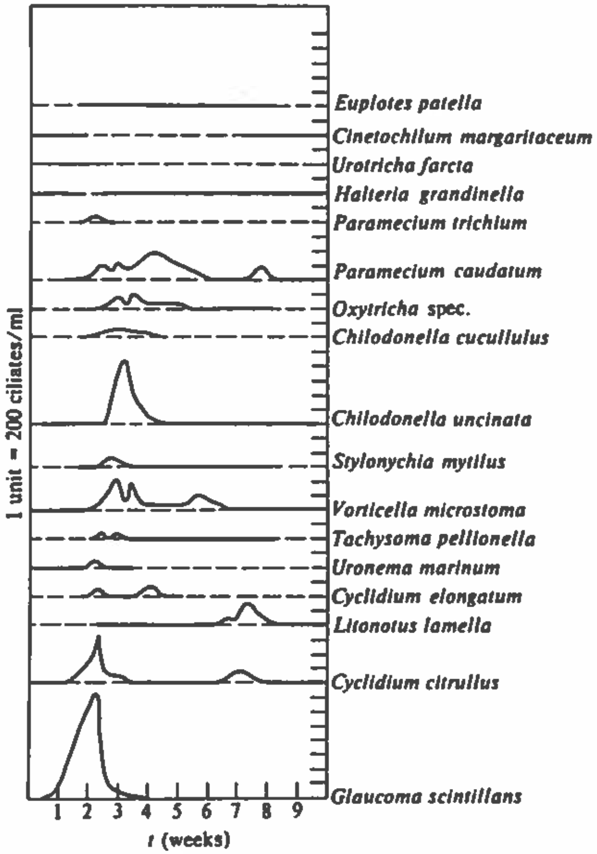

Figure 2-3-2 Development of species of *Ciliata* during the experiment shown in Fig. 2-3-1 (after Münch, 1970).

Hence, the oxygen and carbon dioxide curves in Fig. 2-3-1 indicate that the processes induced by the peptone consume oxygen and liberate carbon dioxide. The curves result from the superposition of these consumption and liberation processes, respectively, and the diffusion, which tends to re-establish the initial equilibrium. Around the third week complete oxygen depletion is observed. The occurrence of hydrogen sulfide (H_2S), which is toxic to most of the organisms, seems to be related to this depletion.

On further inspection of the metabolic activities of the organisms it can be seen that at first the peptone added serves as nutrient for certain bacterial species. The *bacteria* decompose the peptone and use the energy released for growth, multiplication, and maintenance of their life function. They excrete certain organic or inorganic substances, which they cannot use any more. The most relevant of these substances is ammonium. Ammonium is used by some other bacterial species, the *nitrifiers*, as an energy source, the ammonium itself being oxidized (*nitrification*). The organic bacterial excrements are used by *saprozoic flagellates*, to which the groups of small flagellates, *Chilomonas*, and *Entosiphon* in Fig. 2-3-1 belong. These flagellates also decompose the organic matter released after the death of bacteria. The living bacteria and flagellates serve as prey for many ciliates, and these ciliates are eaten by *raptorial ciliates* (e.g., *Litonotus lamella* is a raptorial ciliate, see Fig. 2-3-2). The ciliates also excrete various substances which may be utilized by flagellates or bacteria. Thus, there exists a complex system of nutritional interrelations between the species, which is called *food web* or (less aptly) *food chain*. The population dynamics in Figs. 2-3-1 and 2-3-2 are mainly determined by these interrelations and by competition between species for food.

With all feeding activities chemical energy of the food compounds is set free and used for synthesis of biomass or maintenance of life functions. Hence, part of the released energy is bound again as chemical energy, the rest being converted into heat. The food compounds are thereby oxidized, which means that oxygen is used and organic compounds are converted mainly into carbon dioxide and water. (If no free oxygen is available (*anaerobic conditions*) oxygen from sulfate may be used by some bacteria, resulting in the formation of hydrogen sulfide; see Fig. 2-3-1.) If there is not enough food available, organisms oxidize part of their own matter in order to obtain energy for the maintenance of their life functions until they die of hunger or turn into certain dormant and resistant states, like *bacterial spores*. (The energy consumption for maintenance of life functions, like movement or replenishment of spontaneously degenerated protein molecules, is called *endogenous respiration*.) Hence, after a very long time the biomass in the reaction tank will be as small as at the beginning and the overall result of the experiment will be conversion of peptone into mainly water, carbon dioxide, nitrate, and heat. The water, which may have been fairly turbid during the experiment, becomes as clear as at the beginning. That is why the processes described are designated biochemical *self-purification* (Wuhrmann, 1972). The ability of rivers to purify themselves is an extremely important factor in almost all river quality considerations and plays a major role throughout this book. The importance of self-purification for river quality is illustrated in Fig. 2-3-3 in which the actual organic pollution of the Rhine river, measured as *Chemical Oxygen Demand* (COD) concentration (see Sec. 3-5) is compared with the pollution which would result if the pollutants discharged into the river section shown just accumulated (see Sec. 5-3). The concentration at the downstream end would already be of the same order of magnitude as the concentration in domestic wastewater. Since biochemical self-purification is such an important factor, the most important aspects of it are now discussed in more detail. It will also be necessary to work out the differences between our illustrative experiment and an actual river.

Degradation of Pollutants by Bacteria

The first and most important step in the self-purification process is the degradation

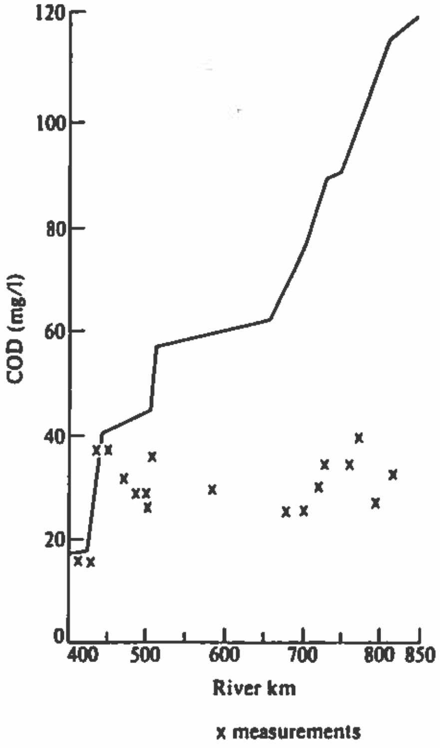

Figure 2-3-3 Organic pollution of the Rhine river: comparison of actual measurements with the pollution which would occur if there were no self-purification.

of the originally discharged pollutants by bacteria (and lower order *fungi*). *Degradation* denotes any chemical change of a pollutant which releases electrochemical energy. Bacterial degradation is the most important step because the proportion of the energy of the pollutants which is dissipated is obviously greatest at this level. (Assuming the same efficiency for all energy conversions connected with feeding, and assuming also a strict chain-like structure of the food web, the chemical energy is reduced from link to link of the food chain in a geometric progression.)

The processes related to bacterial degradation are schematically shown in Fig. 2-3-4, in which the energy donors (pollutants) are assumed to be organic molecules. The degradation processes are usually long chains of reactions which are catalyzed by *enzymes*, i.e., degradation takes place practically only if certain highly specific proteins or proteids (enzymes) are present. These enzymes are not changed by the chemical reactions they catalyze. The energy yielding processes during degradation are transfers of electrons such that the potential energy of the electrons is lowered. In the reactions most important for energy deliberation, the electrons are carried by hydrogen (*dehydrogenation* of the energy donor). The energy released is partly bound again through the formation of *adenosine triphosphate* (ATP) from *adenosine di-phosphate* (ADP) and inorganic phosphorus.

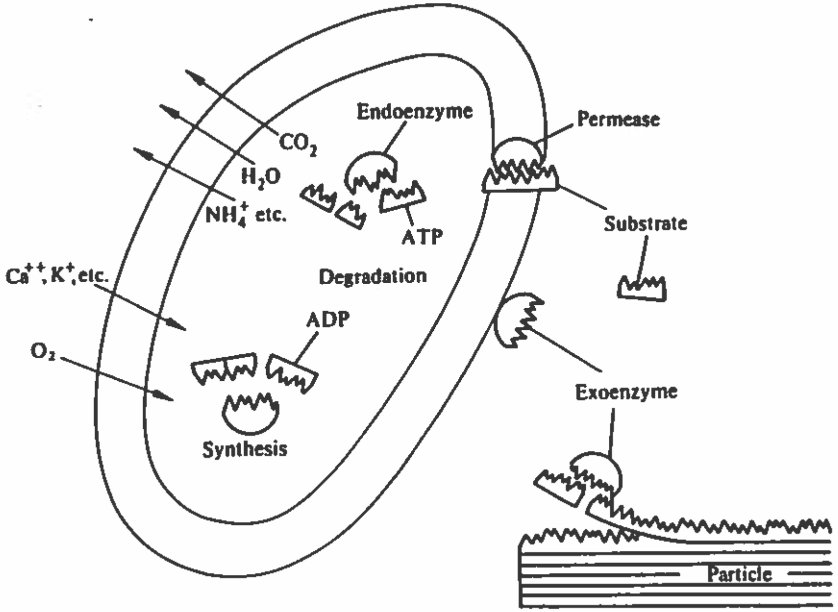

Figure 2-3-4 Schematic representation of bacterial enzyme action.

New bacterial mass is synthesized also by chains of enzymatic reactions. The energy required for this is taken from ATP which is thereby converted into ADP. The building materials for the biomass synthesis (carbon, hydrogen, and small amounts of various other elements) are partly taken from the environment, but also fragments of the pollutants may be integrated directly into the new biomass. The rate at which new bacterial mass is formed is usually limited by the amount of energy which can be gained through degradation rather than by the availability of building materials.

The enzymes mentioned so far are all *endoenzymes*, since they catalyze reactions within the cell. There are particular enzymes, called *permeases*, by which the transport through the cell wall (or, more precisely, through the cytoplasmic membrane) is achieved (diffusion plays no significant role because the transport through the cell wall has to be accomplished against a concentration gradient). If the pollutant molecules are very large (e.g., starch, cellulose, protein), a direct transport into the cell is impossible. In this case, the molecules are decomposed outside the cell into fragments which are small enough. These decompositions are catalyzed by so-called *exoenzymes*. They can be attached to the cell walls as well as be released into the surrounding medium. They differ from the endoenzymes by their small molecular weight (10^4–10^5 as opposed to 10^5–10^6 of the endoenzymes) and by their extremely low cystin and cystein content (Pollock, 1962).

The ability of a bacterium to utilize a pollutant, i.e., to synthesize enzymes which catalyze the degradation of the pollutant, is genetically determined. That is why only those compounds which have been present for a long time in nature are biologically degradable. Compounds which have appeared during the last few decades through the development of chemical technology, cannot often be degraded or can only be partially degraded; among those, for example, are the *chlorinated hydrocarbons* (see, for instance, Eichelberger and Lichtenberg, 1971). Only part of the enzymes, the so-called *constituent enzymes*, is synthesized independently of the available nutrients. The other enzymes are *inducable*, that is, the genetically fixed ability to synthesize them is only realized when the specific substrate (or sometimes other structurally similar compounds) are present.

Four major groups of bacteria, which are defined by the two binary notions *autotrophic–heterotrophic* and *aerobic–anaerobic*, may be distinguished according to the kind of degradation and synthesis processes. A few energy yielding processes which are representative for these groups are shown in Fig. 2-3-5. The distinction between autotrophic and heterotrophic is made according to whether the carbon for synthesis of biomass is of organic or inorganic origin. Autotrophic bacteria get their carbon from carbonic acid or its salts. By and large, this distinction coincides with the distinction as to whether the energy source is inorganic or organic, respectively. The distinction aerobic–anaerobic is based on whether or not oxygen is the final electron acceptor in the degradation process. The two reaction examples given in Fig. 2-3-5 for autotrophic, aerobic organisms are the oxidation of sulfur and ammonium, which can be performed, for example, by the genera *Beggiatoa* and *Nitrosomonas*, respectively. The latter belong to the nitrifying bacteria already mentioned. The autotrophic, anaerobic example is also a sulfur oxidation; since no free oxygen is available nitrate is stripped of oxygen, hence the process is called *denitrification*. *Thiobacillus denitrificans* is an example of a bacterium which is able to denitrify. The two examples in the heterotrophic–aerobic quadrant are the processes performed by baker's yeast and vinegar producing bacteria, respectively. The first example given for heterotrophic–anaerobic organisms is the well-known alcoholic fermentation; the second one, which can be performed by the genus *Desulfovibrio*, reduces sulfate. A reaction similar to this must have occurred around the third week of the experiment shown in Fig. 2-3-1. Although any bacterial species is adapted to one of the quadrants in Fig. 2-3-5, in many cases bacteria may survive or even reproduce in other quadrants.

	Autotrophic (C from CO_2 or H_2CO_3)	Heterotrophic (C from organic compounds)
Aerobic	$2S + 2H_2O + 3O_2$ $- 2H_2SO_4$ $2NH_4OH + 3O_2$ $- 2HNO_2 + 4H_2O$	$C_6H_{12}O_6 + 6O_2$ $- 6CO_2 + 6H_2O$ $C_2H_5OH + O_2$ $- CH_3COOH + H_2O$
Anaerobic	$5S + 6HNO_3 + 2H_2CO_3$ $- 5H_2SO_4 + 2CO_2 + 3N_2$	$C_6H_{12}O_6 - 2C_2H_5OH + 2CO_2$ $2C_3H_6O_3 + 3H_2SO_4$ $- 3H_2CO_3 + 3H_2O + 3H_2S + 3CO_2$

Figure 2-3-5 Basic types of microbial metabolism and typical energy yielding reactions.

The most important type of bacterial metabolism for river quality problems is heterotrophy under aerobic conditions. Anaerobic conditions are avoided whenever possible, because usually unpleasant metabolic by-products, like hydrogen sulfide, occur. And autotrophy is of minor importance because most of the anthropogenic waste discharged into rivers (in terms of electrochemical energy) is organic material. The only important autotrophic bacteria are the *nitrifiers*, because ammonium is a common component of wastewater as well as a common end product of heterotrophic bacterial metabolism. The growth rate of the nitrifiers is, however, quite low, as can be seen from Fig. 2-3-1. Therefore, they play an important part only in slow flowing (e.g., impounded) or overgrown rivers: in overgrown bodies of water the nitrifiers may settle on water plants; if there are no water plants and the river velocity is high, the flow time is too short for the development of a high nitrifier population (Liebmann, 1962; Wezernak and Gannon, 1970; Wolf, 1971; Goering, 1972). Moreover, the growth of the nitrifiers is inhibited by numerous pollutants, so that the influence of nitrification on the self-purification process is often negligible.

The number of different organic compounds which may be found in rivers is immense, and is rapidly increasing as chemical technology develops. Nevertheless, most of these compounds can be decomposed by microorganisms. Because of the great variety of pollutants the bacteria found in rivers are not specialists but show great flexibility in their use of pollutants (see, for example, Hopton, 1970). Most of them belong to the genera *Bacillus*, *Aerobacter*, *Pseudomonas*, *Flavobacterium*, *Escherichia*, *Achromobacter*, *Alcaligenes*, *Micrococcus*, *Sphaerotilus*, and *Chromobacterium* (Liebmann, 1962; Hopton, 1970; Frobisher, 1974).

The many degradation pathways which the river bacteria are able to follow are so arranged that with progressing degradation more and more pathways coincide. This is the natural result of evolution, which minimizes the expenditures on enzyme production.

If different bacterial species are able to utilize a certain substance the degradation pathways are in most cases the same. This means, a bacterial community composed of those species behaves similarly to a homogeneous population as far as the degradation of that substance is concerned (see, for example, Gaudy, 1962; Wilderer, 1969). Therefore, the river bacteria, which are so versatile, act to a good approximation like a homogeneous bacterial population against the organic pollutants. This may even be true if just a few species are able to decompose a substance, because often metabolic intermediates are available for the other species. This is especially the case with the end products of reactions catalyzed by *exoenzymes*. Similarly, the small flagellates living on organic bacterial excrements may be looked upon as part of the bacterial population as far as self-purification is concerned, because their population dynamics follow so closely the bacterial population dynamics (see Fig. 2-3-1).

The kinetics of degradation of a certain substance is often specifically influenced by other nutrients or by nondegradable compounds. This influence can consist of the *repression* of the production of an enzyme. Thus, numerous inducible enzymes, especially exoenzymes, are only formed when other more easily degradable nutrients have been used up (Pollock, 1962; Stumm-Zollinger, 1966). Also the activity of enzymes already present may be regulated. This kind of regulation can be achieved through the binding of the regulator molecule to the active site of the enzyme molecule, which is then no longer able to catalyze (*competitive inhibition*, see, for example, Laidler, 1958); in this case the regulator molecule and the substrate molecule are usually structurally similar. [The special case of competitive inhibition in which regulator and substrate molecule are the same occurs if the metabolic pathways of two substrates merge and the slowest (i.e., rate determining) reaction is in the common part of the pathways (Wilderer, 1969).]

In many cases, the regulator molecules are attached to some other part of the enzyme molecule and activate or inhibit it by changing the form of the molecule (*allosteric inhibition*, Laidler, 1958); in these cases there is, in general, no structural similarity between substrate and regulator molecule. Measurement results of a laboratory self-purification experiment in which the degradation of one substance (sorbitol) is inhibited allosterically by another will be shown in Fig. 3-5-7. In competitive inhibition the enzyme activity depends upon the ratio of the concentrations of substrate and regulator; if the substrate concentration is high enough the inhibition can be overcome. On the other hand, in allosteric regulation the enzyme activity depends only on the regulator concentration. Allosteric inhibitions and activations also play an important role in the endogenic regulation of metabolism: the end product of a metabolic pathway acts as an allosteric regulator of the first reaction (feedback). Many substances which occur in wastewaters influence the bacterial metabolism so seriously, even at relatively small concentrations, that bacteria die. *Heavy metals* are an example of such toxic materials.

Great differences in mobility exist within the realm of bacteria. There are attached types as well as various types of flagella. For self-purification considerations, however, the question whether a bacterial species is sessil or motile is less important than the question how many bacteria are actually attached to the river bottom (*benthic*) and how many are suspended in the flowing water (*planctonic*). (The latter category also comprises sessil bacteria, which may be attached to suspended particles or ripped off from the river bottom.) The importance of this distinction, which will be elaborated in the following chapters, can be easily seen. If the conditions for benthic bacteria are favorable downstream of a wastewater inlet (e.g., water weed on which the bacteria may settle) the bacterial degradation activity can be very intense immediately downstream of the inlet. If, however, only planctonic bacteria can grow, and the river upstream of the inlet is quite clean, the maximum of the bacterial degradation may be far downstream because of the time needed to adapt to the wastewater (produce the appropriate enzymes) and to reproduce.

The Role of Higher Order Consumers and of Phototrophs in Self-Purification

Through the bacterial degradation the electrochemical energy of the pollutants has been converted into electrochemical energy of bacterial mass with an efficiency which usually lies between 10 and 60 percent (Servizi and Bogan, 1964; Burkhead and McKinney, 1969; McCarty, 1972). Thus the self-purification cannot be considered finished even if the bacteria have removed all pollutants. The newly created bacterial mass, which must still be considered a kind of pollution (which can be filtered off or sedimented out, however) would decline only very slowly due to *endogenous respiration*; the death rate would become significant only relatively late. But usually self-purification proceeds considerably faster because the bacteria are consumed by protozoa, in particular by ciliates.

The role of *protozoa* in the self-purification process was greatly disputed up to a few years ago, but after several convincing experiments their importance is now an established fact (Javornický and Prokešová, 1963; Bick, 1964; Bhatla and Gaudy, 1965; Straskrabová-Prokešová and Legner, 1966; Münch, 1970; Gaudy, 1972). As an example Fig. 2-3-6 shows the dynamics of bacterial density and oxygen consumption in a laboratory experiment with a river water sample with, and without, the addition of protozoa (Javornický and Prokešová, 1963). One can see that the accumulated oxygen consumption, which can be considered a measure of the pollutants energy which has been converted into heat, is much larger in the first case. The bacterial density is thereby clearly smaller. (After the first day bacterial and protozoan densities are of the order of magnitude of those measured in the river. The smaller bacterial density at the beginning resulted from the fact that in eliminating the natural protozoa many bacteria were inevitably eliminated as well.) Whether the additional oxygen consumption is due solely to the digestion of the bacteria by protozoa, has not yet been clarified. Straskrabová-Prokešová and Legner (1966) suppose, on the basis of their measurements, that the protozoa secrete a substance which enhances the degradation activity of the bacteria. The reason for the high additional oxygen consumption could also be that protozoan grazing, which reduces the competition among the bacterial species, favors the bacteria with high degradation activity more than the others. However, the importance of the protozoa lies mainly in the fact that they control the bacterial density through grazing, and only this aspect is included in the considerations which follow. For example, protozoan grazing should be the main reason for the reduction of the bacterial concentration in the Rhine river between Mainz and Köln which is observed during summer. Figure 2-3-7a shows the bacterial concentration along a section of the Rhine river during summer, calculated as the geometric mean of the measurements taken by the Rhine Water Works during the six summer months of 1967 (ARW, 1969). (Similar values were measured for other years.) Figure 2-3-7b gives the corresponding curves for the six winter months. The opposite behavior between Mainz and Köln in winter (when the self-purification processes are slowed down, see page 39) shows that

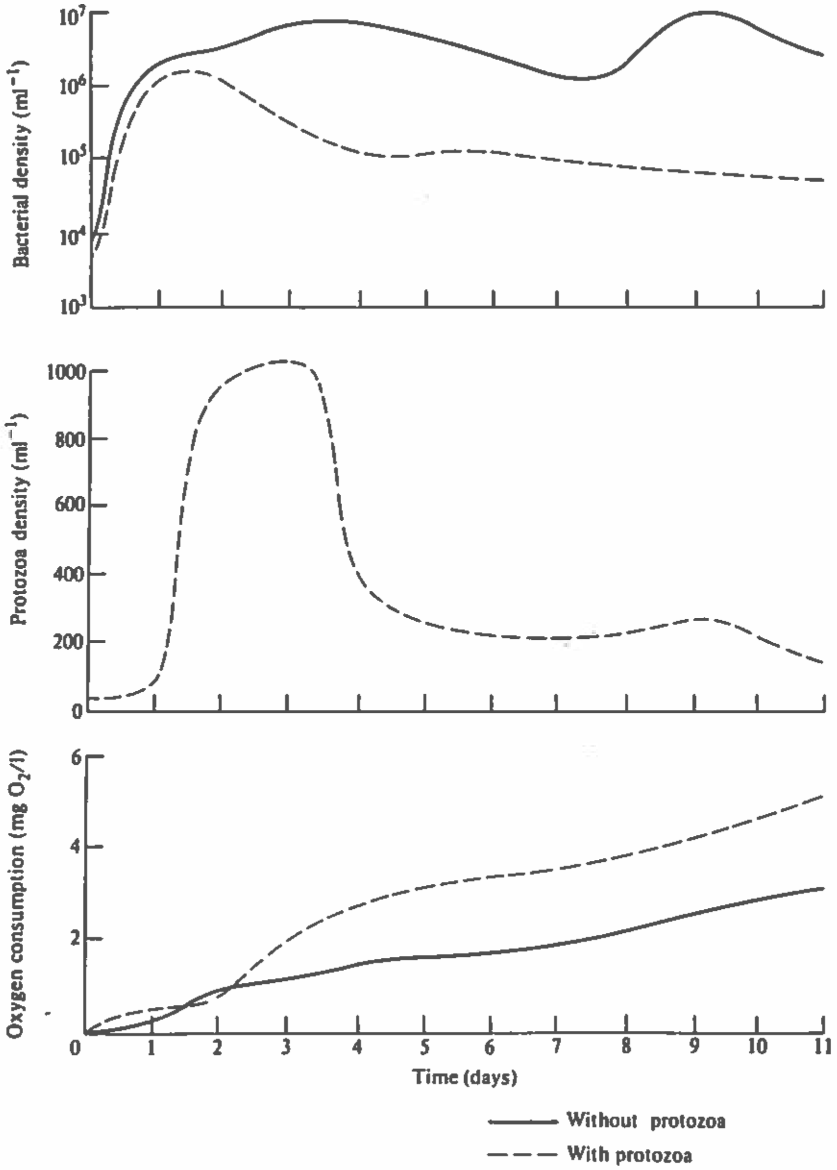

Figure 2-3-6 Influence of protozoa on bacterial density in a laboratory experiment with river water.

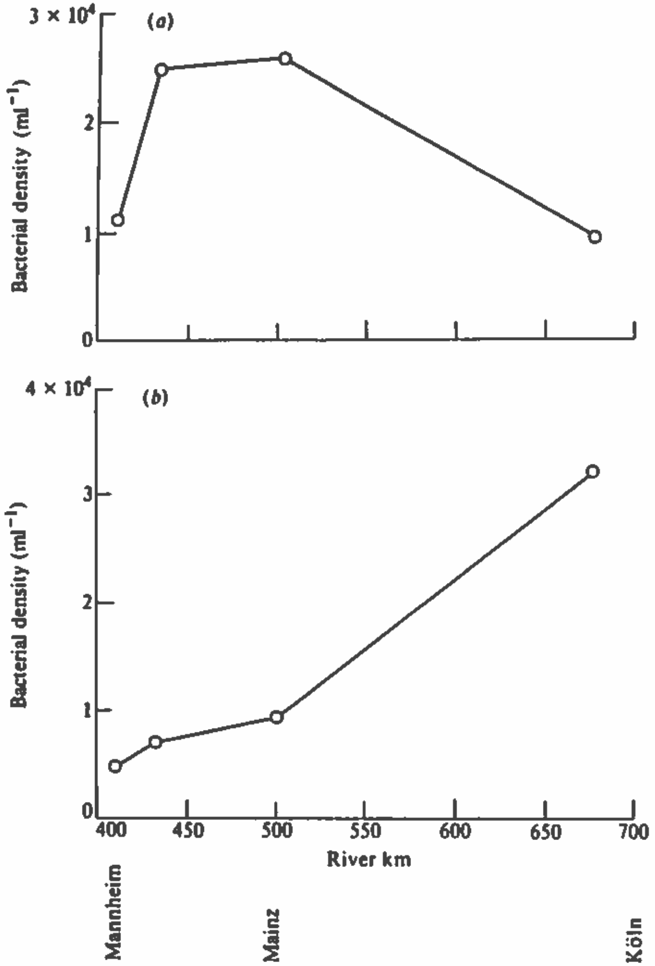

Figure 2-3-7 Measured values of bacterial density in the Rhine river: (*a*) in summer (*b*) in winter.

the decline in summer is certainly not caused by differences in the measuring technique. (The plate count technique was used, so one may suspect that the shape of the curve in Fig. 2-3-7a is determined by slight differences in the culture media which are used in the different measurement points.)

The growth rates of bacteria in rivers may vary widely due to the great differences in degradability of their food. For protozoa feeding on bacteria this source of variability of growth rates is much less important, because the protozoan food has essentially always the same composition.

As already mentioned above, the protozoa feeding on bacteria are in turn eaten by higher organisms. Beside the raptorial ciliates, which were involved in the experiment of Fig. 2-3-1, primitive worms (phylum *Nemathelminthes*) and fish are the major predators. Other prey–predator interrelations follow up to the raptorial fish, which lie at the top of the food web.

As with the bacteria, so with higher order consumers *benthic* and *planctonic* organisms must be distinguished, and again among the planctonic organisms there may be sessil forms, which are living on suspended matter or which have been ripped off from the river bottom. Fish can in some cases be assumed to live stationary, i.e., they act like benthic organisms. For other species of fish it might be necessary, however, to take migration into account.

The part of the original electrochemical energy which the higher order consumers dissipate becomes smaller and smaller as one ascends the food web. Nevertheless, the influence of the higher order consumers upon the dynamics of self-purification could be considerable, because they reduce the consumers of lower orders. This, however, is not normally the case, for two reasons. Firstly, the growth rates decrease toward the top of the food web. Therefore those higher consumers which are stream-borne do not have enough time to reach the high population density which could be supported by the nutritional base—the pollutants. Secondly, organisms become, in general, more and more exacting toward the top of the food web, so that many of them cannot survive or breed in heavily polluted water.

Unlike the laboratory experiment described at the beginning, in real rivers the electrochemical energy on which the food web is based, stems not only from the pollutants discharged into the river, but also from *phototrophic* organisms, i.e., organisms which are able to use sunlight as an energy source in building new biomass. The net effect of the phototrophs is practically the inverse of degradation: carbon dioxide, water, and some other substances are combined to energy-rich organic matter, and oxygen is liberated. This organism group contains, beside a few bacteria and many flagellates, algae and higher aquatic plants. Although the phototrophs can use sunlight as an energy source, they often use, either indispensably or facultatively, organic substances. In some cases, growth is possible even in the dark (Round, 1965). The inorganic and organic substances which the phototrophs take up are to a large extent by-products of the degradation processes described above (carbon dioxide, nitrate or ammonium, phosphates, etc.). Thus, the pollutants in fact act as fertilizers for the aquatic flora. This effect, which causes *eutrophication* in lakes, may lead to similar phenomena in slowly flowing rivers, e.g., algal blooms or huge amounts of dying algae in autumn.

In producing new organic matter the phototrophs counteract the self-purification. On the other hand, they may also enhance self-purification. The oxygen released by photosynthesis can prevent anaerobic conditions, which cause the self-purification to proceed much more slowly than under aerobic conditions. However, if the light intensity is not sufficient (during night or in winter) the phototrophs represent an additional oxygen demand because of their endogenous respiration. Figure 2-3-8 gives an example of how the activity of phototrophs influences the oxygen balance of a river. It shows the diurnal variations of oxygen concentration in the Rhine river at Gernsheim during a bright summer day (Schulze-Rettmer and Böhnke, 1973). It can be seen that the oxygen production through photosynthesis is so intense that oversaturation even occurs. The measurements were taken, however, near the river bank, where the influence of littoral plants and of almost stagnant river branches can be felt. The variations of the cross-sectional mean value are much smaller (see Sec. 5-3). Another beneficial effect on self-purification is that phototrophs provide surfaces for bacteria to attach to, so that the bacterial degradation activity can be very intensive immediately downstream of a wastewater inflow (see page 32). This effect is particularly important for the slowly growing nitrifiers. It should also be mentioned that some species of algae produce compounds which are toxic to higher animals, and which, therefore, disturb drinking water production in particular. These species grow preferably at high temperatures (> 30 °C).

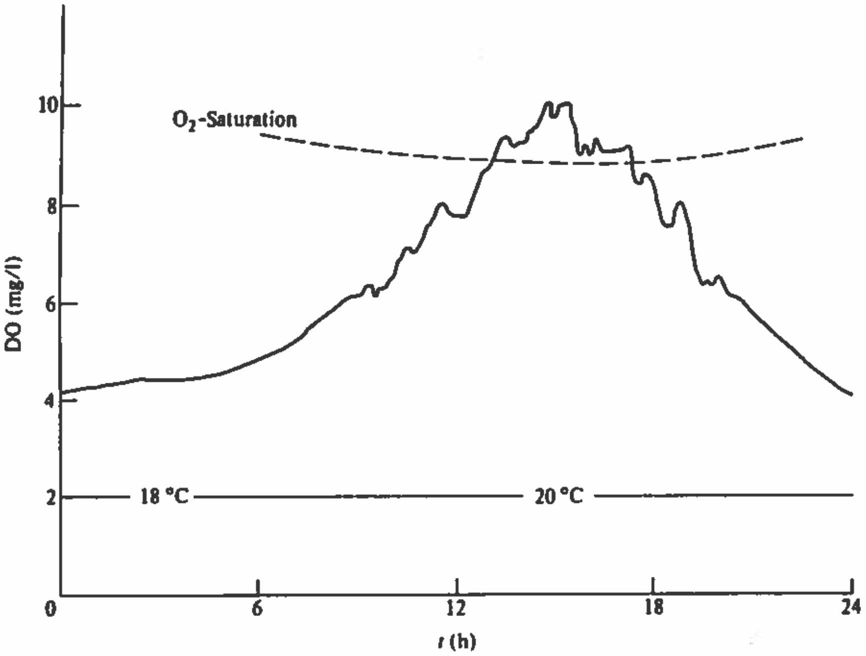

Figure 2-3-8 Diurnal variations of oxygen concentration in the Rhine river at Gernsheim during a bright summer day (after Schulze-Rettmer and Böhnke, 1973).

Like the *chemotrophic* organisms, the phototrophic organisms may be benthic or planctonic; the higher plants are without exception stationary. Since the growth rate of most phototrophs is quite small (compared with bacteria, for example), the species which live planctonic are of importance only in very slowly flowing (e.g., impounded) rivers. Phototrophs do not play a major role in deep rivers, because the light intensity in greater depths is not sufficient for their growth; this may be true even for relatively shallow rivers, if they are turbid enough. In general, phototrophs are more exacting than lower order consumers, therefore they cannot grow in heavily polluted rivers. Hence, there are many cases in which the influence of phototrophs on self-purification may be neglected.

Phototrophs serve as food for many animal species, some of which may be able to utilize other kinds of food as well (*omnivores*), while others live exclusively on phototrophs (*herbivores*). The most important group among the latter is the class *Crustacea* (mainly phyllopods and copepods, see Liebmann, 1962). The organisms feeding on phototrophs are subject to the same predatory processes as the organisms mentioned above.

All self-purification processes described up to now are summarized in Fig. 2-3-9 in the form of a food web. The arrows indicate flows of material. The arrows at the compartments "O_2" and "excrements, detritus, etc." which do not end at another compartment symbolize oxygen consumption and waste matter production, respectively, by all living organisms. The slanted lines indicate the environment of the river. It should be appreciated that Fig. 2-3-9 gives only a very approximate picture of reality. The substances and organisms shown are highly aggregated, and only the most important ones are depicted. Nevertheless, it is believed that this picture can be used as a starting point for the second step in conceptualization (see Sec. 1-3), namely formulation of quantitative, mathematical models of self-purification. This will be done in the following chapters. The distinction between benthic and planctonic variables, which has been omitted from Fig. 2-3-9, will also be made.

Each compartment in Fig. 2-3-9 represents one aspect of what is called *water quality*. Too few fish may be perceived as a river quality problem as well as too

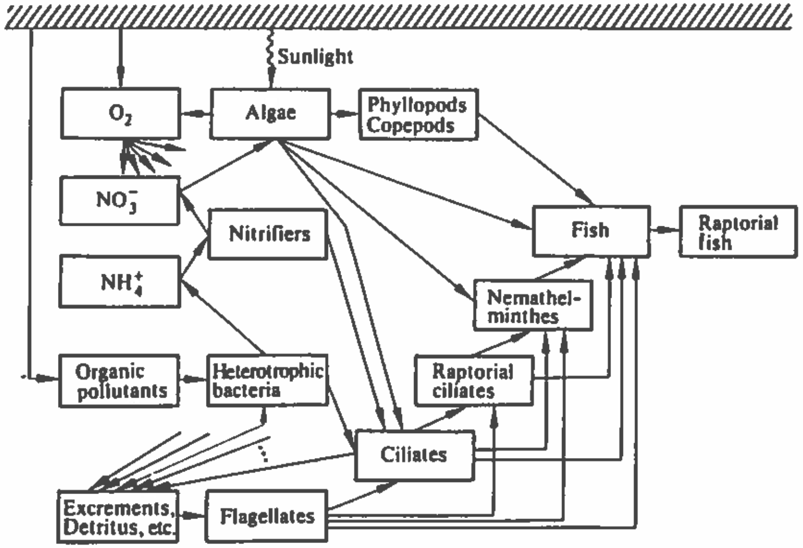

Figure 2-3-9 Food web of the self-purification process.

many bacteria, to give only two examples. Thus, water quality ought to be measured through a quantitative specification of all the compartments in Fig. 2-3-9 (and possibly physical and chemical characteristics, see, for example, Sec. 2-2). This is essentially the way in which Kolkwitz and Marsson (1902) defined water quality when they introduced their *saprobial system* (see also Liebmann, 1962). They defined different categories of water quality through specification of typical *biocenoses*. While this way of measuring water quality is appropriate for descriptive purposes, it is less well suited for anticipatory investigations, because the impact of a pollutant on the whole river biocenosis cannot be evaluated quantitatively. Therefore, water quality is now usually defined through a few elementary variables which characterize the living conditions for the aquatic organisms (Stehfest, 1972). Hence, the quality indicators most frequently used are temperature, oxygen concentration, and pollutant concentration. For the latter, very global measures may be used (see Sec. 3-5) as well as measures which comprise single compounds (e.g., toxins).

The Influence of Physical and Chemical Agents on Self-Purification

The physical river parameters which are most important for self-purification are temperature and flow rate, which have been discussed in the previous sections. If the temperature increases all chemical reactions, and hence all metabolic conversions, are accelerated, unless the temperature is so high that essential compounds of the organisms (e.g., enzymes) denature. If in the experiment of Fig. 2-3-1, for example, the temperature is increased from 10°C to 20°C, the curves of Fig. 2-3-10 are observed (Münch, 1970). If one compares Figs. 2-3-1 and 2-3-10 one can see that self-purification proceeds about twice as fast at 20°C as at 10°C. At 20°C the oxygen curve has two clearly distinct minima, the second one obviously being due to nitrification. Some types of organisms occur which have not been observed at 10°C, even multicellular organisms (e.g., *Rotatoria*). They were probably also present in the 10°C experiment, but could not reproduce up to an observable population size during the measurement time. In general, not only the growth rates but also the relative abundance of the various species is changed if temperature changes. Each species is adapted to a particular temperature, and, if the actual temperature deviates from this, other species may become superior in the competition for food.

The temperature dependence of the photosynthesis activity of aquatic plants can be much weaker than that of degradation processes if the light intensity is low. The reason is that at low light intensity the limiting reaction is a photochemical one, which should not be influenced by moderate temperature variations. The *endogenous respiration* of the phototrophs, however, depends on temperature as strongly as with the other organisms. This implies that at low light intensities the net growth rate of phototrophs may increase if the temperature is lowered (Round, 1965). The oxygen saturation concentration decreases if the temperature increases, while the decay rate of a given deviation from saturation increases.

It is not clear a priori whether all temperature dependencies mentioned so

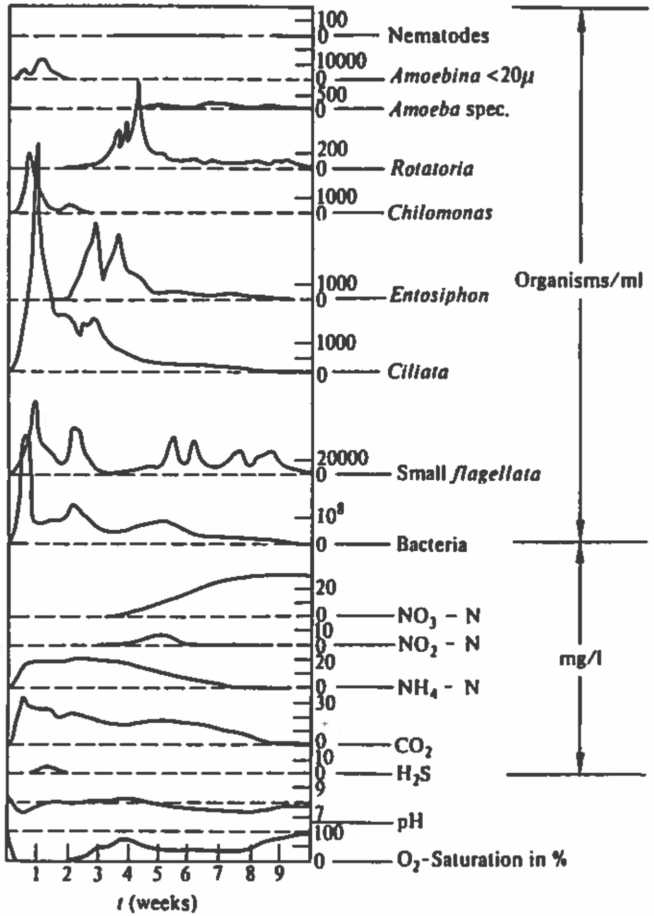

Figure 2-3-10 Laboratory self-purification experiment of Fig. 2-3-1 with increased temperature (after Münch, 1970, $T = 20\,^{\circ}C$).

far result in an increase or a decrease of oxygen concentration if temperature changes. And, in fact, the river quality models described in the following chapters are such that the oxygen concentration may increase or decrease with decreasing temperature, depending, for example, on the location (see Secs. 4-1 and 5-3).

The main effects of a variation in flow rate are the variations of the flow time between the pollution sources and the variation of the dilution ratio. Again, it is not obvious whether the sum of these effects is a reduction or an increase of the pollutant concentration. Usually a reduction of the pollutant concentration is observed if the flow rate increases; only at very low flow rates, where river velocity increases very quickly with flow rate, may the opposite be observed. A third consequence of flow rate variations, which seems to be less important, is that the ecological interactions within the food web change because the turbulence changes. It is obvious, for example, that the efficiency of bacterial degradation processes which involve exoenzymes drops if turbulence increases.

No general statement can be made about the variation of oxygen concentration with flow rate. Even the influence of flow rate on physical reaeration alone cannot be derived easily, because two consequences have to be considered which compensate each other to a certain extent. If flow rate increases, diffusion of oxygen from air into water is enhanced because of higher turbulence. On the other hand, the oxygen which diffuses through a certain surface area has to be distributed over a greater volume, because the depth has increased.

There are many factors other than temperature and flow rate, which are largely determined externally, and which influence the self-purification processes in rivers. Several of them, such as light intensity and quality of river-bed, have already been mentioned. Another one is the pH value (see Fig. 2-3-1). Its main impact consists in shifting some important chemical equilibria. The equilibrium between ammonia (NH_3) and ammonium (NH_4^+), for example, is shifted toward ammonia if the pH-value is increased; then ammonia may escape and less inorganically bound nitrogen is available (e.g., for phototrophs). But in real rivers this and numerous other possible effects are of minor relevance and are therefore not discussed in detail here.

2-4 OTHER PHENOMENA

There are several processes beside the ones described in Secs. 2-1–2-3 which may be relevant to one or other aspect of river quality. The most important among them are *sedimentation* and *resuspension*, which are obviously closely related to the hydrologic phenomena discussed in Sec. 2-1. If turbulence in a river is weak, which usually happens when river velocity is low, suspended particles may settle. The river water becomes cleaner, so we may speak of *physical self-purification* of the river. Substances which can be degraded biochemically as described in Sec. 2-3 may be degraded within the sediment as well, although the biological species involved are different. Anaerobic conditions are much more likely to occur within the bottom deposits, however, because the oxygen consumed can be replenished only through molecular diffusion, while within the water body turbulent mixing is the dominant oxygen transport mechanism. This implies that biochemical self-purification within the sediments usually proceeds at a slower rate than in the stream above it. Sedimentation of degradable suspended matter has been observed to be relevant only for (cross-sectional mean) velocities smaller than about 0.5 m/s (see, for example, Velz, 1958 and Benoit, 1971). If sedimentation occurred in a river and the flow rate of the river increased considerably, the sediments may be stirred up again. Through this resuspension, large amounts of biodegradable matter can be released into the water instantaneously, which may cause a serious deterioration of the oxygen concentration. The resuspended matter is usually even more easily degradable than the material which has settled out before, due to the slow anaerobic degradation processes within the sediments.

Another phenomenon important for river quality is *sorption*, i.e., the binding of dissolved molecules or ions to solid particles (see, for example, Benoit, 1971). Obviously, this process in conjunction with sedimentation also acts as physical self-purification. The binding forces for sorption are van der Waals' forces in the case of molecules (*adsorption*) and electrostatic forces in the case of ions. When an ion is bound to a particle, another ion, which is less strongly bound, may be displaced into solution (*ion exchange*). Ions of heavy metals, for example, usually displace the common ions of the alkali and alkaline earth metals (like sodium and calcium); this is an important fact for water quality considerations since many heavy metals are extremely toxic (Förstner and Müller, 1974). The particles on which sorption occurs may be either organic or inorganic. The larger the total solid surface, the greater becomes the purification effect, i.e., small particle size enhances this kind of self-purification.

A third, though less important, aspect of physical self-purification is *flocculation*, i.e., destabilization of colloids and formation of flocs which may subsequently settle (see, for example, Singley, 1971). Flocculation is enhanced by high turbulence, and by neutralizing with ions the repulsive charges on the colloidal particles.

There are also purely chemical phenomena which may be said to contribute to self-purification of rivers, the main one being *precipitation*. The insoluble compounds may be formed through both polar and covalent bonds. Precipitation, like ion exchange, is particularly important for the removal of heavy metals. Under the usual chemical conditions in rivers, hydroxides, carbonates, and sulfides of heavy metals have very low solubility, and the formation of these compounds in natural rivers is fairly likely (Förstner and Müller, 1974). The numerous other chemical processes which may possibly influence river water quality, for example, the escape of ammonia (NH_3) in the case of increase in the pH value (see page 41), are not believed to be important in rivers.

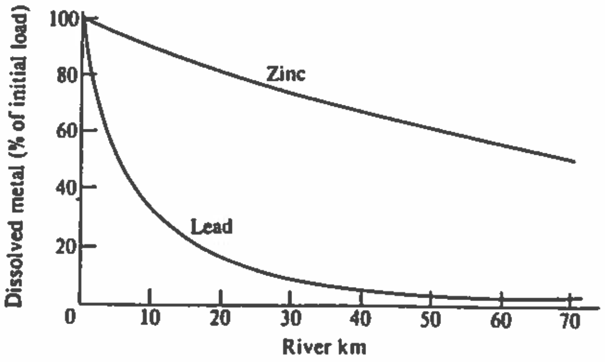

Figure 2-4-1 Removal of dissolved lead and zinc along a section of the Ruhr river (after Koppe, 1973).

No general statements can be made about the relative importance of the phenomena described in this section so far, because they are heavily dependent on the physical and chemical characteristics of the river. The main factors are turbulence, temperature, and pH value. And if one or more of these characteristics change, pollutants which have already been fixed in the sediments may be redissolved or resuspended. Heavy metals, for example, which have been precipitated may easily be dissolved when the pH value is lowered.

An example of how the phenomena described affect the concentration of dissolved heavy metals (zinc and lead) along a river is shown in Fig. 2-4-1 (Koppe, 1973). The measurements were taken on the Ruhr river in West Germany. They show that heavy metals may be fixed to suspended or settled solids almost completely over relatively short distances (lead), but in other cases removal may be much slower (zinc). If a heavy metal is removed quickly the enrichment of that metal in the sediments may yield concentrations which are comparable to concentrations in mineable ores.

Finally, it should be mentioned that all the phenomena described in this section are utilized in both water and wastewater treatment plants (see Sec. 7-1).

2-5 INTERRELATIONSHIPS BETWEEN THE PHENOMENA

All the phenomena presented in the preceding sections will be described in the next chapter by means of differential equations. The resulting set of relationships (the river quality model) may be partitioned into three subsets (namely, the hydrologic, the thermal, and the biochemical submodels), coupled together as

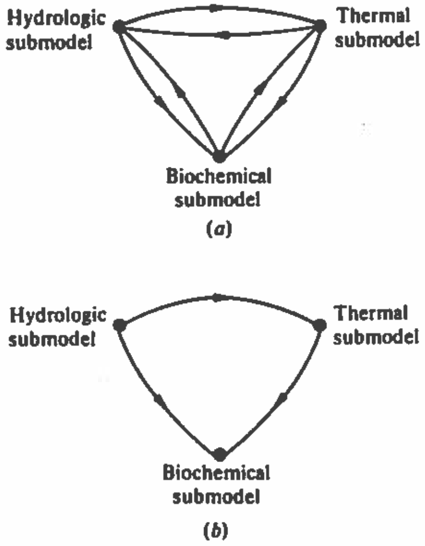

Figure 2-5-1 The links among the three submodels:
(*a*) in the general case
(*b*) when minor effects are neglected.

shown in Fig. 2-5-1a. The state variables of the hydrologic submodels influence all other variables, since all phenomena take place in the fluid medium. The water temperature strongly influences the biochemical processes. It also has an impact on hydrology because of evaporation and buoyancy. The biochemical processes (which are understood to also comprise the processes described in Sec. 2-4) may influence the hydrology through sedimentation or growth of water weed, for example. They may also affect the temperature through heat production or changes of the heat transfer characteristics. In most practical cases, however, the influences of the biochemical processes on hydrology and temperature, and of the temperature on hydrology may be neglected. Then the relations between the submodels are the ones indicated in Fig. 2-5-1b. One can see that the three groups of equations can be solved in cascade, starting from the hydrologic submodel and ending with the biochemical one.

REFERENCES

Section 2-1

Gray, D. M. (1970). *Handbook on the Principles of Hydrology.* Water Information Center, Inc., Port Washington, New York.

Section 2-2

Heidt, F. D. (1975). Heat Exchange Processes at the Surface of Stagnant and Flowing Waters (in German). In *Wärmeeinleitungen in Strömungen* (C. Zimmermann, H. Kobus, and P. Geldner, eds.). Technischer Verlag Resch, München, W. Germany.

Jobson, H. E. and Yotsukura, N. (1972). Mechanics of Heat Transfer in Nonstratified Open-Channel Flows. In *Environmental Impact on Rivers (River Mechanics III)* (H. W. Shen, ed.). H. W. Shen, Fort Collins, Colorado.

Krenkel, P. A. and Parker, F. L. (1969). Engineering Aspects, Sources, and Magnitude of Thermal Pollution. In *Biological Aspects of Thermal Pollution* (P. A. Krenkel and F. L. Parker, eds.). Proceedings of the National Symposium on Thermal Pollution, Portland, Oregon, 3–5 June 1968. Vanderbilt University Press, Nashville, Tennessee.

Section 2-3

ARW (Arbeitsgemeinschaft der Rheinwasserwerke) (1969). Annual Report No. 24. Karlsruhe, W. Germany.

Bhatla, M. N. and Gaudy, A. F. (1965). Role of Protozoa in the Diphasic Exertion of BOD. *J. San. Eng. Div., Proc. ASCE*, 91, 68–87.

Bick, H. (1964). *Succession of Organisms during Self-Purification of Organically Polluted Water under Various Conditions* (in German). Ministerium für Ernährung, Landwirtschaft und Forsten des Landes Nordrhein-Westfalen, Düsseldorf, W. Germany.

Burkhead, C. E. and McKinney, R. E. (1969). Energy Concepts of Aerobic Microbial Metabolism. *J. San. Eng. Div., Proc. ASCE*, 96, 253–268.

Eichelberger, J. W. and Lichtenberg, J. J. (1971). Persistence of Pesticides in River Water. *Environ. Sci. Technol.*, 5, 541–544.

Frobisher, M. (1974). *Fundamentals of Microbiology.* W. B. Saunders, Philadelphia.

Gaudy Jr., A. F. (1962). Studies on Induction and Repression in Activated Sludge Systems. *Applied Microbiology*, 10, 264–271.

Gaudy Jr., A. F. (1972). Biochemical Oxygen Demand. In *Water Pollution Microbiology* (R. Mitchell, ed.). John Wiley, New York.

Goering, J. J. (1972). The Role of Nitrogen in Eutrophic Processes. In *Water Pollution Microbiology* (R. Mitchell, ed.). John Wiley, New York.

Hopton, J. W. (1970). A Survey of some Physiological Characteristics of Stream-Borne Bacteria. *Water Research*, 4, 493–499.

Javornický, P. and Prokešová, V. (1963). The Influence of Protozoa and Bacteria upon the Oxidation of Organic Substances in Water. *Int. Revue ges. Hydrobiol.*, 48, 335–350.

Kolkwitz, R. and Marsson, M. (1902). Principles of Biological Evaluation of Water according to its Flora and Fauna (in German). *Mitt. Prüf. Anst. Wasserversorg. Abwasserbeseit.* Berlin, 1, 33–72.

Laidler, K. J. (1958). *The Chemical Kinetics of Enzyme Action.* Oxford University Press, Oxford, U.K.

Liebmann, H. (1962). *Handbook of Fresh and Waste Water Biology*, vol. I and II (in German). R. Oldenbourg, München, W. Germany.

McCarty, P. L. (1972). Energetics of Organic Matter Degradation. In *Water Pollution Microbiology* (R. Mitchell, ed.). John Wiley, New York.

Münch, F. (1970). The Influence of Temperature on the Decomposition of Peptone and the Concomitant Succession of Organisms with Special Regard to the Dynamics of the Population of the Ciliates (in German). *Int. Revue ges. Hydrobiol.*, 55, 559–594.

Pollock, M. R. (1962). Exoenzymes. In *The Bacteria: A Treatise on Structure and Function*, vol. IV (J. C. Gunsalus and R. Y. Stanier, eds.). Academic Press, New York.

Round, F. E. (1965). *The Biology of the Algae.* Edward Arnold, London.

Schulze-Rettmer, R. and Böhnke, B. (1973). Contributions to the Oxygen Budget of the Rhine River (in German). *Vom Wasser*, 41, 187–208.

Servizi, J. A. and Bogan, R. H. (1964). Thermodynamic Aspects of Biological Oxidation and Synthesis. *J. WPCF*, 36, 607–618.

Stehfest, H. (1972). Definition and Realization of Quality Standards for Rivers (in German). In *Application of the Polluter-Pays-Principle in the Field of Water Management, Proc. of an International Symposium, Kernforschungszentrum Karlsruhe, 20–21 Nov. 1972.* KFK 1804 UF, 146–160, Kernforschungszentrum Karlsruhe, Karlsruhe, W. Germany.

Straskrabová-Prokešová, V. and Legner, M. (1966). Interrelations Between Bacteria and Protozoa during Glucose Oxidation in Water. *Int. Revue ges. Hydrobiol.*, 51, 279–293.

Stumm-Zollinger, E. (1966). Effects of Inhibition and Repression on the Utilization of Substrates by Heterogeneous Bacterial Communities. *Applied Microbiology*, 14, 654–664.

Wezernak, C. T. and Gannon, J. J. (1970). Evaluation of Nitrification in Streams. *J. San. Eng. Div., Proc. ASCE*, 94, 883–895.

Wilderer, P. (1969). *Enzyme Kinetics as Basis of the BOD Reaction* (in German). Thesis, University of Karlsruhe, Karlsruhe, W. Germany.

Wolf, P. (1971). Incorporation of Latest Findings into Oxygen Budget Calculations for Rivers (in German). *GWF—Wasser/Abwasser*, 112, 200–203 and 250–254.

Wuhrmann, K. (1972). Stream Purification. In *Water Pollution Microbiology* (R. Mitchell, ed.). John Wiley, New York.

Section 2-4

Benoit, R. J. (1971). Self-Purification in Natural Waters. In *Water and Water Pollution Handbook*, vol. I (L. L. Ciacco, ed.). Marcel Dekker, New York.

Förstner, U. and Müller, G. (1974). *Heavy Metals in Rivers and Lakes* (in German). Springer-Verlag, Berlin.

Koppe, P. (1973). Investigation of the Behavior of Waste Water Constituents from Metal-Working Industries in the Water Cycle and their Influence on Drinking Water Supply (in German). *GWF-Wasser/Abwasser*, 114, 170–175.

Singley, J. E. (1971). Chemical and Physical Purification of Water and Waste Water. In *Water and Water Pollution Handbook*, vol. I (L. L. Ciacco, ed.). Marcel Dekker, New York.

Velz, C. J. (1958). *Significance of Organic Sludge Deposits*. U.S. Public Health Service, Robert A. Taft Sanitary Engineering Center, Technical Report W 58-2, Cincinnati, Ohio.

Section 2-5

No references.

CHAPTER

THREE

STRUCTURE OF THE MODELS

3-1 BALANCE EQUATIONS

After having described the relevant hydrologic, thermal, and biochemical phenomena and identified the corresponding variables, the dynamic laws governing the evolution of the variables can now be derived. These laws are all based on the conservation principles for mass, momentum, and energy, regardless of which of the phenomena described in Chapter 2 is dealt with. In other words, the water quality model results from bookkeeping processes for all the relevant variables. Accordingly, the development of model equations follows the same scheme for all variables. This scheme is discussed now, while Secs. 3-3-3-5 are devoted to the more specific problems of deriving the model equations.

Densities and Velocities in a Fluid

There are several points of view from which one may look at a fluid. One possibility for instance, is the *molecular approach*, which considers the fluid to be a huge number of molecules moving around and colliding with each other in the vacuum. The approach best suited to river quality considerations, however, is the *continuum approach*. Following this approach each point in space is associated with the average value of the property considered (for example, energy, momentum, bacterial mass) over a small reference volume. The advantage of using the continuum approach is that a heterogeneous multicomponent fluid can be described as being composed of different continua, interacting with each other and occupying the same position in space at the same instant of time, so that properties of any of these continua may be assigned to every point of the space (*interpenetrating continua*).

In order to clarify this idea, consider a multicomponent fluid, made up of N different components. Let $\mathrm{d}M$ denote the mass contained in a small volume $\mathrm{d}V$, and $\mathrm{d}m_i$ the mass of the i-th component in the same volume (the subscript will be omitted later on, if there is no possibility of confusion). The reference volume $\mathrm{d}V$ is assumed to be large compared with the mean distance between the particles which are to be described as continuum (e.g., molecules, bacteria); but it has to be small compared with the spatial scale of the phenomena being studied. Then the *mass density* (or *concentration*) ρ_i of the i-th component is defined as

$$\rho_i = \frac{\mathrm{d}m_i}{\mathrm{d}V} \qquad i = 1, 2, \ldots, N$$

and

$$\sum_{i=1}^{N} \rho_i = \sum_{i=1}^{N} \frac{\mathrm{d}m_i}{\mathrm{d}V} = \frac{\mathrm{d}M}{\mathrm{d}V} = \rho$$

is the *bulk mass density*.

These notions may be generalized to other characteristics of the fluid which are proportional to the volume, like momentum or energy (*extensive quantities* as opposed to *intensive quantities* like temperature): for any extensive quantity the *concentration* π_i, which is an intensive quantity, may be defined as

$$\pi_i = \frac{\mathrm{d}\Pi_i}{\mathrm{d}V}$$

so that the amount Π_i of the extensive property contained in any volume V is given by

$$\Pi_i = \int_V \pi_i \, \mathrm{d}V \tag{3-1-1}$$

The average velocity ω_i of the particles of the i-th component in a reference volume $\mathrm{d}V$ may, in general, be different from those of the other components. Then, according to the continuum viewpoint, it is necessary to consider, for any point in space, a set of velocities $\{\omega_i\}_{i=1}^{N}$. The *bulk velocity* $\boldsymbol{\Omega}$ may then be defined as

$$\boldsymbol{\Omega} = \frac{\sum_{i=1}^{N} \rho_i \omega_i}{\sum_{i=1}^{N} \rho_i} = \sum_{i=1}^{N} \frac{\rho_i}{\rho} \omega_i$$

which, under normal circumstances, is practically equal to the water velocity. The physical meaning of $\boldsymbol{\Omega}$ is momentum per unit of mass, so that $\rho\boldsymbol{\Omega}$ is the *bulk momentum density* of the fluid.

Three-Dimensional Balance Equation

In a multicomponent fluid consider an arbitrary volume V, invariable in time, and the total amount Π of an extensive property of a given component (e.g., mass of a given pollutant) contained at time t within volume V. As is well known, the rate of change of quantity Π is given by

$$\frac{\partial \Pi}{\partial t} = -\int_S \pi \omega \mathbf{n} \, \mathrm{d}S + \int_V \zeta \, \mathrm{d}V \tag{3-1-2}$$

where S is the surface surrounding V, $\mathbf{n}$ is the unit normal vector directed outward from the surface S, and ζ is the rate of production of the extensive property per unit volume. The first term on the right hand side of Eq. (3-1-2) is the flow of the property out of the volume V, while the second term is the total amount of property generated within the volume. Recalling Eq. (3-1-1) and using Gauss' theorem, Eq. (3-1-2) can be written in the form

$$\int_V \left[\frac{\partial \pi}{\partial t} + \operatorname{div}(\pi\omega) - \zeta \right] \mathrm{d}V = 0$$

from which it follows

$$\frac{\partial \pi}{\partial t} + \operatorname{div}(\pi\omega) = \zeta \tag{3-1-3}$$

since the volume V is arbitrary. Equation (3-1-3) is the formal expression of the *general conservation principle*.

Equation (3-1-3) describes the characteristics of any component of the fluid at a microscopic time scale. However, one is usually not interested in the very rapid fluctuations of densities and velocities which are due to the Brownian movement of the particles and to the turbulent nature of the river flow. Thus, a simplification may be introduced by averaging all the variables over a representative time interval Δt, which is sufficiently large to filter out the high frequency variations, but sufficiently small not to damp the low frequency variations one is interested in.

More precisely, let the average of a variable x over Δt be denoted by

$$\langle x \rangle = \frac{1}{\Delta t} \int_{\Delta t} x \, \mathrm{d}t$$

Then, by definition, for any density π

$$\pi = \langle \pi \rangle + \pi^0 \tag{3-1-4a}$$

and for the velocity of any component

$$\omega = \langle \omega \rangle + \omega^0 \tag{3-1-4b}$$

where π^0 and ω^0 are the random fluctuations around the mean. Inserting Eq. (3-1-4) into Eq. (3-1-3), taking the averages, and using

$$\langle \pi^0 \rangle = \left\langle \frac{\partial \pi^0}{\partial t} \right\rangle = 0$$

and

$$\langle \omega^0 \rangle = \langle \langle \omega \rangle \pi^0 \rangle = \langle \omega^0 \langle \pi \rangle \rangle = 0$$

we obtain

$$\frac{\partial\langle\pi\rangle}{\partial t} + \operatorname{div}(\langle\pi\rangle\langle\omega\rangle) + \operatorname{div}(\langle\pi^0\omega^0\rangle) = \langle\zeta\rangle \qquad (3\text{-}1\text{-}5)$$

The velocity ω can be considered the sum of two terms, the bulk velocity $\mathbf{\Omega}$ and the *diffusive (or migration) velocity* $(\omega - \mathbf{\Omega})$,

$$\omega = \mathbf{\Omega} + (\omega - \mathbf{\Omega})$$

i.e., any movement is seen as a migration with respect to the fluid superimposed on the bulk fluid advection. For simplicity of notation, new symbols are used for the following average values

$$p = \langle\pi\rangle$$

$$\mathbf{v} = \langle\mathbf{\Omega}\rangle$$

$$\mathbf{u} = \langle\omega - \mathbf{\Omega}\rangle$$

$$I = \langle\zeta\rangle$$

Then Eq. (3-1-5) can finally be written as

$$\frac{\partial p}{\partial t} + \operatorname{div}(\mathbf{v}p) + \operatorname{div}(\mathbf{u}p) - \mathcal{D} = I \qquad (3\text{-}1\text{-}6a)$$

where

$$\mathcal{D} = -\left[\operatorname{div}(\langle\mathbf{\Omega}^0\pi^0\rangle) + \operatorname{div}(\langle(\omega - \mathbf{\Omega})^0\pi^0\rangle)\right] \qquad (3\text{-}1\text{-}6b)$$

Equation (3-1-6) is the *general three-dimensional balance equation.*

The role of the different terms in Eq. (3-1-6) is easily identified as follows:

div ($\mathbf{v}p$) represents the advection by the bulk fluid motion. The *flow* $\mathbf{v}p$ introduces a coupling with the hydrologic submodel if p is a variable of the thermal or biochemical submodel.

div ($\mathbf{u}p$) represents the so-called *migration term*. The *flux* $\mathbf{u}p$ is remarkably different from zero only for nondissolved matter. This term may express the sedimentation movements of particulate matter, the rising of bubble gases towards the surface, or the movements due to "the free will" of animals. Usually it is expressed as a function of the particle characteristics by means of empirical formulae.

$\mathcal{S}$ represents the total *dispersion and diffusion term* which is due partly to the random variations of the bulk velocity field (*turbulent dispersion* term $\operatorname{div}(\langle\mathbf{\Omega}^0\pi^0\rangle)$) and partly to the random movements at molecular level (*molecular diffusion* term $\operatorname{div}(\langle(\omega - \mathbf{\Omega})^0\pi^0\rangle)$).

Mixing through molecular diffusion is usually small compared to turbulent mixing, so that the second term of $\mathcal{S}$ can be neglected. The turbulent dispersion term is usually expressed by (see, for example, Sayre, 1972; Holly, 1975; and Yotsukura and Sayre, 1976)

$$\mathcal{S} = \operatorname{div} \mathbf{D} \operatorname{grad} p \qquad (3\text{-}1\text{-}7)$$

with

$$\mathbf{D} = \begin{bmatrix} D_x & 0 & 0 \\ 0 & D_y & 0 \\ 0 & 0 & D_z \end{bmatrix} \qquad (3\text{-}1\text{-}8)$$

I represents the chemical, biochemical, and ecological interactions. This term, in general, introduces a coupling between the density p and other interacting densities.

When Eq. (3-1-7) is used to express dispersion and a dissolved component is considered ($\mathbf{u} = 0$), Eq. (3-1-6) reduces to

$$\frac{\partial p}{\partial t} + \operatorname{div}(\mathbf{v}p) - \operatorname{div} \mathbf{D} \operatorname{grad} p = I \qquad (3\text{-}1\text{-}9)$$

Initial and boundary conditions must be given in order to solve Eqs. (3-1-6) or (3-1-9). The boundary conditions are expressed as functions of the production of the property under consideration outside the fluid (e.g., exchange of oxygen with atmosphere at the surface, oxygen release by macrophytes on the bottom, BOD discharge on river banks, or BOD sedimentation on the bottom). Not only the boundary conditions for p and $\mathbf{v}$ must be given but also the existence of physical frontiers for the fluid must be expressed using boundary conditions. Of course, these frontiers are idealized, i.e., most of the intricacy of the real frontiers is smoothed out. For instance, given a fixed coordinate system x, y, z, with $z = \xi$ and $z = h$ being the equations of the air-water interface and of the bottom, respectively, it is assumed that these *boundary surfaces* satisfy the equations (see Nihoul, 1975)

$$\frac{\partial\xi}{\partial t} + v_x\frac{\partial\xi}{\partial x} + v_y\frac{\partial\xi}{\partial y} = v_z \qquad \text{at } z = \xi \qquad (3\text{-}1\text{-}10a)$$

$$\frac{\partial h}{\partial t} + v_x\frac{\partial h}{\partial x} + v_y\frac{\partial h}{\partial y} = v_z \qquad \text{at } z = h \qquad (3\text{-}1\text{-}10b)$$

Equation (3-1-10) expresses the "model" boundaries as surfaces of an idealized fluid moving with the average bulk velocity $\mathbf{v}$. An equation analogous to Eq. (3-1-10) must also be used to express the existence of the *lateral boundaries* (the river banks).

Two- and One-Dimensional Balance Equations

In rivers, estuaries, and lakes the variations of concentrations in all directions may be important. However, the direct solution of a system of coupled three-dimensional balance equations is beyond the capacity of present-day computers, so that a reduction to the two- or one-dimensional case is necessary. Fortunately, in many situations, variations in one direction are less important than in the others. In rivers, for example, the variations along the vertical line can usually be neglected. This is related to the fact that the width of rivers is much greater than the depth. In these cases one can reduce the dimensionality of the model by averaging the equations over that direction. Even in the most recently developed three-dimensional models of estuaries and lakes (see for instance, Leendertsee et al., 1973, or Chen and Orlob, 1975), the water body is cut horizontally into slices and the equations averaged over the slices are solved slice by slice. Thus, the reduction of three-dimensional balance equations to two or one dimension on the basis of certain simplifying assumptions will now be discussed. An important remark must be made beforehand. A reduction in the dimensionality of the model also curtails the frontiers of the system. If, for instance, one averages over depth, the resulting system has only lateral boundaries, while the surface boundaries have been incorporated in the new balance equation.

Neglecting molecular diffusion and making assumptions (3-1-7, 3-1-8) $\mathcal{D}$ may be written in the form

$$\mathcal{D} = \nabla_h(\mathbf{D}_h\nabla_h p) + \frac{\partial}{\partial z} D_z\left(\frac{\partial p}{\partial z}\right)$$

where

$$\nabla_h = \frac{\partial}{\partial x}\mathbf{i} + \frac{\partial}{\partial y}\mathbf{j}$$

is the two-dimensional gradient operator ($\mathbf{i}$ and $\mathbf{j}$ are the unit vectors in the x and y directions) and

$$\mathbf{D}_h = \begin{bmatrix} D_x & 0 \\ 0 & D_y \end{bmatrix}$$

The z-axis of the coordinate system is assumed to be vertical, while the x-axis is pointing in the longitudinal direction. Let $\mathbf{v}_h$ denote the horizontal component of the velocity $\mathbf{v}$

$$\mathbf{v}_h = v_x\mathbf{i} + v_y\mathbf{j}$$

and assume the horizontal migration term equal to zero (this is always the case except for organisms which can move independently of the stream). Then Eq. (3-1-6) can be written as

$$\frac{\partial p}{\partial t} + \nabla_h(p\mathbf{v}_h) + \frac{\partial}{\partial z}(pv_z) = I - \frac{\partial}{\partial z}(pu_z) + \nabla_h(\mathbf{D}_h\nabla_h p) + \frac{\partial}{\partial z}\left(D_z\frac{\partial p}{\partial z}\right) \quad (3\text{-}1\text{-}11)$$

Moreover, let $\bar{p}$ and $\bar{\mathbf{v}}$ denote the depth-averaged concentration and velocity respectively, i.e.,

$$\bar{p} = \frac{1}{H}\int_h^{\xi} p\,\mathrm{d}z \qquad \bar{\mathbf{v}} = \frac{1}{H}\int_h^{\xi} \mathbf{v}\,\mathrm{d}z$$

where $H = \xi - h$ is the river depth. Then concentration and velocity components in each point can be expressed as the mean value plus a fluctuation:

$$p = \bar{p} + \hat{p}$$

$$\mathbf{v}_h = \bar{\mathbf{v}}_h + \hat{\mathbf{v}}_h$$

These expressions may now be inserted into Eq. (3-1-11) which is then integrated over depth. Application of the rules for changing the sequence of differentiation and integration and use of the boundary conditions (3-1-10) yields the following *two-dimensional balance equation*

$$\frac{\partial(H\bar{p})}{\partial t} + \nabla_h(H\bar{p}\bar{\mathbf{v}}_h) = \mathcal{D}_h + HS_h \quad (3\text{-}1\text{-}12a)$$

where

$$\mathcal{D}_h(x, y) = -\nabla_h\int_h^{\xi}\hat{p}\hat{\mathbf{v}}_h\,\mathrm{d}z + \int_h^{\xi}\nabla_h(\mathbf{D}_h\nabla_h p)\,\mathrm{d}z \quad (3\text{-}1\text{-}12b)$$

is the global dispersion term, and

$$S_h(x, y) = H^{-1}\left[\int_h^{\xi} I\,\mathrm{d}z + \left(D_z\frac{\partial p}{\partial z} - u_z p\right)_{z=\xi} - \left(D_z\frac{\partial p}{\partial z} - u_z p\right)_{z=h}\right] \quad (3\text{-}1\text{-}12c)$$

is the average source term.

The last two terms on the righthand side of Eq. (3-1-12c) represent the fluxes at the air–water interface and at the bottom and must be expressed using the surface boundary conditions for p. Thus, the term HS_h in Eq. (3-1-12a) constitutes the total input in a water column of unit base; if I is a linear function of the concentrations of the different components this term can be expressed as a function of $\bar{p}$ and of the mean concentrations of the interacting constituents. As far as the first term on the righthand side of Eq. (3-1-12b) is concerned, it can be seen that this term describes a dispersion, which is due to the velocity fluctuations in the vertical direction. It would be zero if the velocity were uniform over the depth, but it is well known that this is never the case (the velocity is maximum near the surface and vanishes at the bottom). Assume, for example, the density p to be greater than zero only in a small vertical column, located at the point (x_0, y_0), at a certain instant of time t_0. The distribution of the depth-averaged concentration $\bar{p}$, which is just an impulse in (x_0, y_0) at t_0, would become broader and broader as time goes on, even if there were no turbulent mixing, because the horizontal velocities are different at different depths. Accordingly this term has been incorporated into the dispersion term, and, in analogy with Eq. (3-1-7), this transport can be described by a Fickian type of flow (for example, Sayre, 1972), i.e.,

$$\frac{1}{H}\int_h^{\xi}\hat{p}\hat{\mathbf{v}}_h\,\mathrm{d}z = -\varepsilon\nabla_h\bar{p} \quad (3\text{-}1\text{-}13)$$

with

$$\boldsymbol{\varepsilon} = \begin{bmatrix} \varepsilon_x & 0 \\ 0 & \varepsilon_y \end{bmatrix}$$

Since the variations of v_x are particularly large, *longitudinal dispersion* is dominated by this mechanism, rather than by longitudinal eddy diffusion. For practical purposes, some further simplifying assumptions are usually made for Eq. (3-1-12), which may lead to (see, for example, Holley et al., 1972)

$$\frac{\partial(Hp)}{\partial t} + \nabla_h(Hp\mathbf{v}_h) = \nabla_h(H(\boldsymbol{\varepsilon} + \mathbf{D}_h)\nabla_h p) + HS_h \tag{3-1-14}$$

where the over-bars have been left out for the sake of simplicity.

Integrating Eq. (3-1-12) over the river width one can derive, in a very similar manner, the *one-dimensional balance equation*

$$\frac{\partial(Ap)}{\partial t} + \frac{\partial(Avp)}{\partial l} = \mathcal{S} + AS \tag{3-1-15a}$$

where p and v now denote concentration and velocity averaged over the river cross section A, and the symbol l is used now for the distance along the axis of the river. The terms $\mathcal{S}$ and S are expressed by formulae analogous to Eqs. (3-1-12b) and (3-1-12c) (see also Sec. 3-5). Similarly, as in Eq. (3-1-14), one can write approximately

$$\mathcal{S} \doteq \frac{\partial}{\partial l}\left(AD\frac{\partial p}{\partial l}\right) \tag{3-1-15b}$$

where D is now a scalar, called *longitudinal dispersion coefficient*. As already indicated above, longitudinal dispersion is mainly due to the combined effects of vertical and transverse mixing and the variations of the longitudinal velocity over the cross section. In other words, the transfer coefficient D in Eq. (3-1-15b) is much greater than D_x in Eq. (3-1-8). Since, for practical river studies the one-dimensional balance equation is mainly used, much effort has been devoted to the prediction or experimental determination of the longitudinal dispersion coefficient (see, for example, Bansal, 1971; Sayre, 1972; and McQuivey and Keefer, 1974).

The lateral boundary conditions expressing the exchange of p with the river banks are now included in the source term AS. Thus, considering a river stretch of length L, the only boundary conditions for Eq. (3-1-15a) are now $p(0, t)$ and $p(L, t)$, i.e., the concentrations at the upstream and the downstream end respectively. The cross-sectional average source S(mg/h m^3) is given by

$$S = S_v + \frac{S_s}{H} + \frac{S_l}{A} \tag{3-1-15c}$$

where S_v is the average volume source (mg/h m^3), S_s the average surface source (mg/h m^2) and S_l the lateral source (mg/h m). Finally, it is worth knowing that Eq. (3-1-15) can be rearranged in the form

$$\frac{\partial p}{\partial t} + v\frac{\partial p}{\partial l} = -\frac{S_Q}{A}p + \frac{\partial}{A\,\partial l}\left(AD\frac{\partial p}{\partial l}\right) + S \tag{3-1-16a}$$

where

$$S_Q = \frac{\partial A}{\partial t} + \frac{\partial(vA)}{\partial l} \tag{3-1-16b}$$

is the rate of water inflow (see Sec. 3-3).

Limitations of One-Dimensional Models

In river quality studies Eq. (3-1-15) is generally believed to be sufficiently detailed, while the two-dimensional equation (3-1-14) is generally used for estuaries (Chen and Orlob, 1975; Orlob, 1976). However, it must be kept in mind that the one-dimensional equation is an approximation which may lead to severe errors if its limitations are not carefully considered (Ward and Fischer, 1971). For example, only if a quasi-equilibrium between lateral and vertical dispersion on the one hand, and differential convection on the other, has been established, are the average concentrations good indices and does Eq. (3-1-15b) correctly describe the dispersion effects (Sayre, 1972). In general, wastewaters are injected in single points, so that Eq. (3-1-15) is not adequate in the immediate vicinity of the outlet. Hence, before using a one-dimensional equation it is necessary to estimate the distance required by a tracer, injected in a point, to become well mixed and only if this distance comes out to be short with respect to the spatial scale of the phenomena under analysis, can the use of a one-dimensional model be considered to be justified.

Often the application of Eq. (3-1-15) is unjustified since there are pockets of little or no flow on the river banks. A tracer pulse released in the river can be partially trapped in these pockets. Thus, a sensor located in the stream sees first a large bulk of material and then a long tail until the pockets along the side are completely emptied of the tracer. In this case, the river may be divided into a main stream and a *stagnant zone* and the dynamics of each variable be described by two coupled one-dimensional equations (see Hays, 1966; Thackston and Schnelle, 1970; Sayre, 1972):

$$\frac{\partial(A_m p_m)}{\partial t} + \frac{\partial(A_m v p_m)}{\partial l} = \frac{\partial}{\partial l}\left(A_m D\frac{\partial p_m}{\partial l}\right) - \alpha(p_m - p_s) + A_m S_m$$

$$\frac{\partial(A_s p_s)}{\partial t} = \alpha(p_m - p_s) + A_s S_s$$

where indices m and s refer to main stream and stagnant zone respectively.

Benthal Constituents

So far only constituents flowing with the stream (*planctonic constituents*) have been considered, but sometimes matter and organisms settling on the bottom (*benthal constituents*) are also important (e.g., water weed and sediments). Their main characteristic is the absence of transportation mechanism, so that the evolution of the cross-sectional mean concentration of a benthal constituent is described by an equation of the type (3-1-15) with v and D equal to zero (see also the above mentioned equation for stagnant zones). Sources and sinks for benthal constituents, in addition to internal processes, are sedimentation and scour.

The Method of Characteristics

Solutions of the various balance equations can usually be obtained only numerically, and much scientific effort has been devoted to the development of efficient and reliable solution techniques. With most of them a discretization of independent variables is introduced, and hence, the main problem these techniques have to cope with is numerical dispersion. Since the numerical integration schemes usually have no physical interpretation, they are not discussed here; the interested reader is referred to the literature (see, for example, Hirsch, 1975) for a general discussion of the particular properties of the different solution schemes.

A particular integration method, the *method of characteristics*, is described briefly because of its stimulating interpretation and because it is the only one which allows analytical results to be obtained sometimes (see, for instance, Li, 1962; Di Toro, 1969; and Chapter 4). The method of characteristics can be applied only if all model equations are of type (3-1-15) and if the dispersive components of the flow are negligible with respect to the advective component, i.e., if $\mathscr{D} = 0$. Under this hypothesis the one-dimensional balance equation (3-1-15) can be written as

$$\frac{\partial p}{\partial t} + v\frac{\partial p}{\partial l} = -\frac{S_Q}{A}p + S \qquad \text{(3-1-17a)}$$

where

$$S_Q = \frac{\partial A}{\partial t} + \frac{\partial (vA)}{\partial l} \qquad \text{(3-1-17b)}$$

Equation (3-1-17) can be solved if the boundary conditions at $l = 0$

$$p(0, t) = p_b(t) \qquad t \geq 0 \qquad \text{(3-1-18a)}$$

and the initial conditions at $t = 0$

$$p(l, 0) = p_i(l) \qquad 0 \leq l \leq L \qquad \text{(3-1-18b)}$$

are given. Since Eqs. (3-1-17) and (3-1-18) are a Cauchy problem a solution exists for a large class of functions v, A, S_Q, and S.

The boundary conditions $p_b(t)$ are known if the cross-sectional average concentration p at $l = 0$ for $t \geq 0$ can be measured, while the initial conditions $p_i(l)$, corresponding to a "picture" of the river at time $t = 0$, are rarely known in practice.

The central idea of the method of characteristics is to substitute Eqs. (3-1-17) and (3-1-18) by the following three ordinary differential equations

$$\frac{dt}{d\tau} = 1 \qquad \text{(3-1-19a)}$$

$$\frac{dl}{d\tau} = v(l, t) \qquad \text{(3-1-19b)}$$

$$\frac{dp}{d\tau} = -\frac{1}{A(l, t)}S_Q(l, t)p + S(p, l, t) \qquad \text{(3-1-19c)}$$

and the initial conditions (see point A of Fig. 3-1-1)

$$t(0) = 0, \quad l(0) = l_0, \quad p(0) = p_i(l_0) \qquad \text{for } 0 \leq l_0 \leq L \qquad \text{(3-1-20a)}$$

and (see point B of Fig. 3-1-1)

$$t(0) = t_0, \quad l(0) = 0, \quad p(0) = p_b(t_0) \qquad \text{for } t_0 > 0 \qquad \text{(3-1-20b)}$$

The line $(t(\tau), l(\tau), p(\tau))$ in the (t, l, p) space, which is a solution of Eq. (3-1-19) with a given initial condition $t(0) = t_0$, $l(0) = l_0$, $p(0) = p_0$, is called the *characteristic line*. In the hydrologic literature the term is also used to denote the line $(t(\tau), l(\tau))$ in the (t, l) plane, a practice which will be followed in this book.

It is obvious that Eq. (3-1-19) subject to conditions (3-1-20) is equivalent to Eq. (3-1-17) subject to conditions (3-1-18) (see Fig. 3-1-1). The main point is that

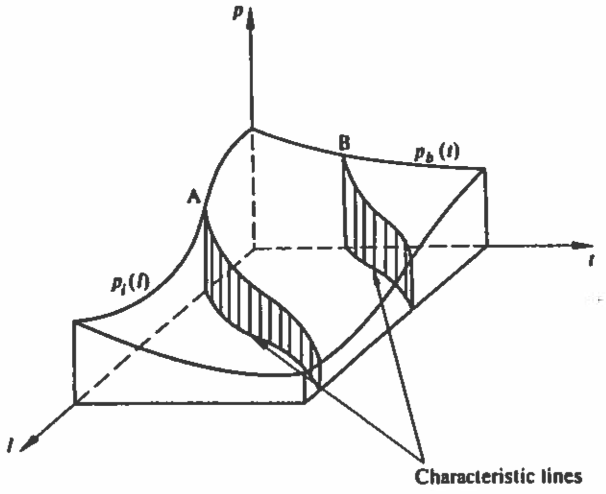

Figure 3-1-1 Cauchy problem and characteristic lines.

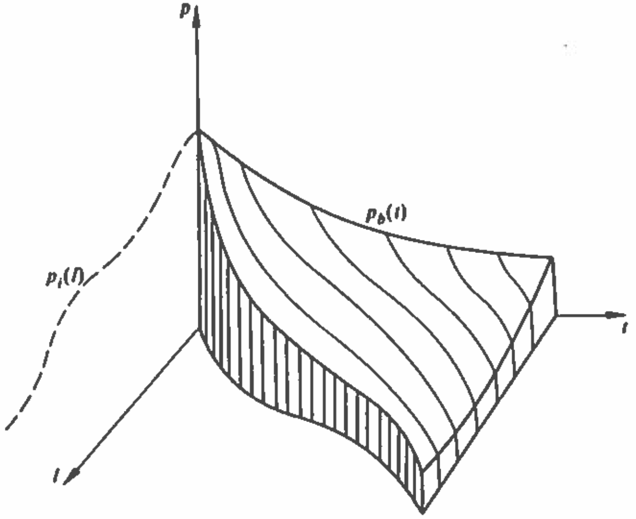

Figure 3-1-2 The solution of Eq. (3-1-17), when only boundary conditions are known.

Eq. (3-1-17), in contrast to the more general balance equations, has only one family of characteristic lines, all of which propagate in the downstream direction. Hence, the solution along each characteristic line can be obtained independently of the solution along a neighboring characteristic line. From a physical point of view this is quite understandable since dispersion was assumed to be insignificant, i.e., plugs of water of differential thickness in the l-direction retain their identity as they flow downstream. Hence, models (3-1-17, 3-1-19) are called *plug flow models*. Equation (3-1-19) describes the dynamics of the variable p as an observer, moving with this plug, sees them. The variable τ, which is called *flow time*, represents the time elapsed since the start of the plug at $l(0)$.

The consequence of unknown initial conditions $p_i(l)$ is now evident and is shown in Fig. 3-1-2: the solution $p(l, t)$ can be determined only for the pairs (l, t) lying on characteristic lines starting from a point on the t axis ($l = 0$).

Later on, when the method of characteristics is employed, Eqs. (3-1-19a) and (3-1-19b) are often omitted for the sake of simplicity. Only Eq. (3-1-19c) is used and the corresponding models, called *flow time models*, are written in the form

$$\dot{p} = -\frac{S_Q}{A} p + S \tag{3-1-21}$$

3-2 ATTRIBUTES OF THE MODELS

The river quality models analyzed in this book are composed, as already pointed out, of several equations of the kind (3-1-15) coupled together. As shown in Sec. 2-5, this set of equations can be partitioned into three subsets constituting the hydrologic, the thermal, and biochemical submodels. The hydrologic submodel is coupled with all other models since the velocity v and the cross-sectional area A enter all other equations. The temperature interacts with the biochemical variables through the source terms S. Finally, biochemical variables are mutually coupled through the source terms S.

According to the assumptions made for specifying the model equations various attributes of the model or submodels result. Since these attributes are used quite often below, it seems worthwhile listing the definitions of all the corresponding types of models although some of those have already been introduced.

linear model: all equations are linear in the state variables
nonlinear model: at least one equation is nonlinear
plug flow model: the diffusion coefficient D is equal to zero in all equations
dispersion model: the diffusion coefficient D is different from zero
steady state model: partial derivatives with respect to time are missing (equal to zero)
unsteady state model: at least one equation contains a time derivative
time-invariant model: all the parameters are constant in time
time-varying model: at least one parameter is time varying
lumped parameter model: the equations are ordinary differential equations (the independent variable may be time or space)
distributed parameter model: at least one equation is a partial differential equation
flow time model: a lumped parameter model with flow time as independent variable
ecological model: at least one state variable is the biomass of some living compartment of the food web
chemical model: no state variable of the biochemical submodel is the biomass of a living compartment of the food web

It is important to notice that some of these attributes are not independent. For instance, time-varying models are unsteady state models and steady state models are lumped parameter models. Moreover, these attributes can be different when looking at the model as a whole or at the single submodels. For example, a river quality model is always nonlinear because of the terms Ap and Avp appearing in Eq. (3-1-15) (recall that v and A are functions of the state variables of the hydrologic submodel), while the biochemical submodel, in which v and A have to be considered as parameters, may be a linear model (see, for instance, Sec. 4-1).

3-3 THE HYDROLOGIC SUBMODEL

The hydrologic submodel is, in the most general case, constituted by two coupled partial differential equations, namely the water *mass* and *momentum balance* *equations*. These equations can be written in three, two, and one dimensions as already shown in Section 3-1. Nevertheless, the following discussion is restricted to one-dimensional models since only these models have been used extensively in river pollution modeling, while higher dimensional models have been employed for studies of estuaries and lakes (see, for instance, Chen and Orlob, 1975, and Orlob, 1976).

In the general one-dimensional balance equation (3-1-15)

$$\frac{\partial(Ap)}{\partial t} + \frac{\partial(Apv)}{\partial l} - \frac{\partial}{\partial l}\left(DA\frac{\partial p}{\partial l}\right) = AS \tag{3-3-1}$$

p is identified with the water density ρ (constant in space and time). Defining flow rate $Q = Av$

$$\frac{\partial A}{\partial t} + \frac{\partial Q}{\partial l} = AS$$

is obtained, which is the so-called *continuity equation*. The term

$$S_Q = \frac{\partial A}{\partial t} + \frac{\partial Q}{\partial l}$$

appears in all one-dimensional balance equations (see Eq. (3-1-16)), where it can be replaced by the rate AS of water inflow. If there is no lateral inflow and/or outflow along the river stretch ($S = 0$), the continuity equation becomes

$$\frac{\partial A}{\partial t} + \frac{\partial Q}{\partial l} = 0 \tag{3-3-2}$$

Equation (3-3-2) can be integrated only if it is coupled with the momentum balance equation or if the river discharge Q at any point l is assumed to be a known function of the depth H of the river at that point, i.e.,

$$Q = Q^*(H, l) \tag{3-3-3}$$

This function, called *stage-discharge relation*, is in general a convex function as shown in Fig. 3-3-1 and usually corresponds to the real behavior of the stream when the river flow is varying relatively slowly in time. From Eq. (3-3-3) and from the knowledge of the geometry of the river bed a function

$$Q(l, t) = \tilde{Q}(A(l, t), l) \tag{3-3-4}$$

can be derived which is also convex. If the continuity equation (3-3-2) is multiplied by the velocity

$$w = \frac{\partial \tilde{Q}}{\partial A}$$

which is well defined because of Eq. (3-3-4), the new equation

$$\frac{\partial Q}{\partial t} + w\frac{\partial Q}{\partial l} = 0 \tag{3-3-5}$$

is obtained. This expression corresponds to the so-called *kinematic approximation* and implies that the river discharge is constant along the characteristic line $\mathrm{d}l/\mathrm{d}t = w$, i.e., the wave is propagating downstream at velocity w and there is no spreading effect. In other words, the stretch can be considered, from a functional point of view, as a pure time delay: an impulse variation of flow rate at one point produces a delayed impulse variation downstream, while a bell-shaped hydrograph as shown in Fig. 2-1-4 should be expected. Nevertheless, this model reproduces the observed fact that the velocity of propagation increases with depth. Indeed, since $\tilde{Q}(A, l)$ is convex with respect to A and A is increasing with H, it follows that w is an increasing function of the depth.

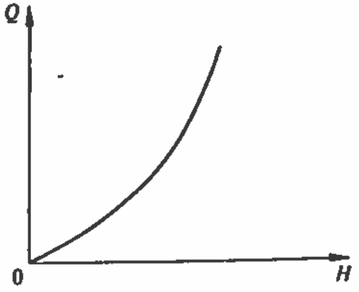

Figure 3-3-1 Stage-discharge relationship at a given point.

If the kinematic approximation described by Eq. (3-3-5) seems to be unreasonable, the natural alternative is to make use of the momentum balance equation which can be derived from Eq. (3-3-1) by neglecting the dispersion term ($D = 0$). Thus, Eq. (3-3-1) with $p = \rho v$ becomes

$$\frac{\partial(Av)}{\partial t} + \frac{\partial(Av^2)}{\partial l} = \frac{AS}{\rho}$$

or, by eliminating v,

$$\frac{\partial Q}{\partial t} + \frac{\partial}{\partial l}\left(\frac{Q^2}{A}\right) = \frac{AS}{\rho} \tag{3-3-6}$$

The term S at the righthand side of Eq. (3-3-6) takes into account the distributed sources and losses of momentum which are, respectively, the component of the gravity forces in the direction of the river and the force induced by hydrodynamic friction. The first of these two terms, say S_1, can be given the form

$$S_1 = -\rho g\left[\frac{\mathrm{d}h}{\mathrm{d}l} + \frac{1}{A}\frac{\partial}{\partial l}(AH_c)\right] \tag{3-3-7}$$

where g is the acceleration of gravity, h is the elevation of the bottom from a reference level, $\mathrm{d}h/\mathrm{d}l$ is the bottom slope and H_c is the depth from the free surface to the centroid of the cross section. The second term S_2 is usually written as

$$S_2 = -\rho g i_f \tag{3-3-8}$$

where i_f is the so-called *friction slope* and is, in general, a function of the river flow Q and of the river depth H.

If we now deal, for simplicity, with rectangular cross sections (rectangular channel) of constant width, then

$$A = YH \qquad H_c = \tfrac{1}{2}H$$

where Y is river width, so that Eq. (3-3-7) becomes

$$S_1 = -\rho g\left(\frac{dh}{dl} + \frac{\partial H}{\partial l}\right)$$

which, together with Eqs. (3-3-6) and (3-3-8), gives rise to the momentum equation

$$\frac{\partial Q}{\partial t} + \frac{\partial}{\partial l}\left(\frac{Q^2}{A}\right) = -gA\left(\frac{dh}{dl} + \frac{\partial H}{\partial l} + i_f\right) \tag{3-3-9}$$

It can easily be shown that if the friction slope i_f is constant the momentum equation together with the continuity equation (3-3-2) degenerate into Eq. (3-3-5) (kinematic approximation). This can be easily understood, since if the friction phenomena are independent of Q and H, then a one to one relationship must exist between Q and H at any point (*stage-discharge relation*). Thus, if the model is to describe the attenuation and spreading out of the wave during its propagation, the friction slope i_f cannot be assumed to be constant in Eq. (3-3-9).

Both theoretical and experimental investigations indicate that the terms appearing on the right hand side of the momentum equation are, in general, quite large with respect to the kinetic terms appearing on the left hand side of the equation. Thus, if the kinetic terms are neglected a new approximation of the momentum equation is obtained in the form

$$\frac{\partial H}{\partial l} = -i_f - \frac{dh}{dl}$$

which, when derived with respect to time, gives

$$\frac{\partial}{\partial t}\left(\frac{\partial H}{\partial l}\right) = -\frac{\partial i_f}{\partial t} \tag{3-3-10}$$

This approximation (called *parabolic approximation*) is not so crude as the kinematic one since the friction slope i_f is allowed to vary in time. From the continuity equation and Eq. (3-3-10) a new equation is obtained in the form

$$\frac{\partial Q}{\partial t} + w\frac{\partial Q}{\partial l} = D^*\frac{\partial^2 Q}{\partial l^2} \tag{3-3-11}$$

where the velocity w and the diffusion D^* are suitable positive functions of Q and A. This equation shows that when moving downstream at velocity w the time derivative of Q has the sign of $\partial^2 Q/\partial l^2$. Therefore, a bell-shaped impulse propagating downstream at velocity w will be attenuated (at the peak $\partial^2 Q/\partial l^2 < 0$) and consequently spread out.

In summary, it can be stated that relatively simple versions of the continuity and momentum equations describe quite satisfactorily at least the two main characteristics of the phenomenon, namely propagation and attenuation of the peaks. For this reason, such equations have been employed for years (the first derivation was made by Barré de Saint Venant in 1871) and are still used in simulation studies despite three main disadvantages.

The first disadvantage is that these equations can be integrated (after discretization) only if the function $A(H, l)$ is known in a suitably high number of points l, and obviously this information is not always easily obtainable. Secondly, the solution of the continuity and momentum equations requires a relatively high computational effort. In fact, the method of characteristics (in a version slightly modified with respect to that described in Sec. 3-1) or some *explicit* or *implicit scheme* for integrating partial differential equations must be used. The integration along characteristic lines after discretization in time and space (the river segment is divided into reaches) implies the need to work on a nonregular grid in the (l, t) plane. The space step Δl (length of the reach) must be relatively small in order to give a sufficiently accurate description of the geometry of the river, while the time step Δt is related to Δl through the propagation velocity w ($\Delta t = \Delta l/w$). In real cases this relation implies a very small Δt with

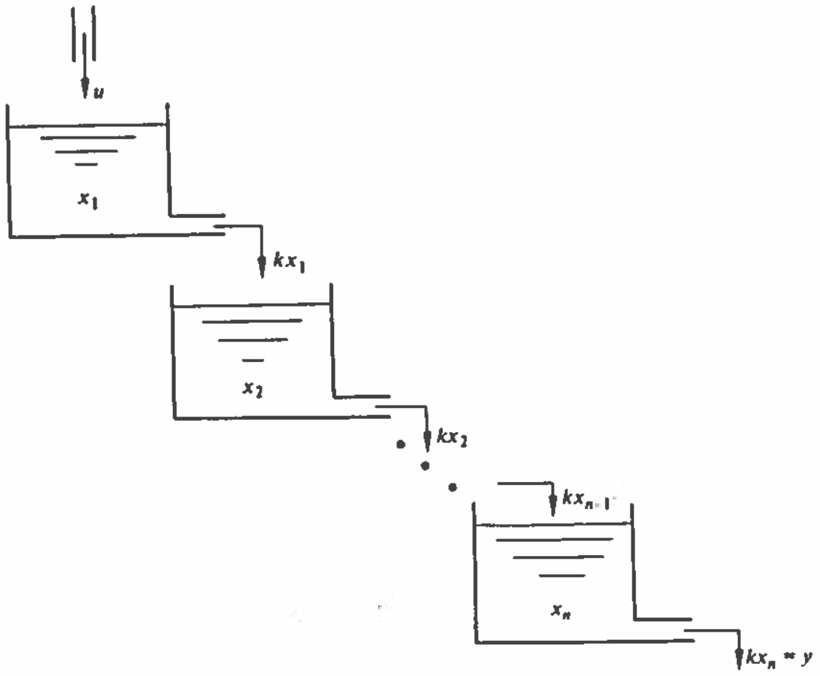

Figure 3-3-2 Description of a river as a sequence of n linear reservoirs.

respect to the duration of the phenomenon so that the method of characteristics turns out to be time consuming. On the other hand, explicit and implicit schemes use regular grids in the (l, t) plane and are therefore more attractive. Explicit schemes are very simple to program but unfortunately they require very small time steps Δt ($\Delta t < \Delta l/w$), since otherwise they become numerically unstable (see Greco and Panattoni, 1977). Implicit schemes are stable for any choice of the space and time intervals, and for this reason they are usually preferred to explicit schemes, even though the latter lead to algebraic equations which are easier to solve. Finally, the third disadvantage which is worth mentioning is that the friction slope i_f is, in general, unknown and must therefore be identified by applying a suitable parameter estimation scheme. Thus, in order to solve this problem it is necessary for some hydrographs to be available.

For all these reasons, simpler models have been proposed and used. Some of these models are derived from the general mass and momentum balance equations following a suitable criterion of approximation, such as space discretization, time discretization, linearization, frequency domain approximation or others. For example, the model obtained with the parabolic approximation (Eq. (3-3-11)) can be further simplified by assuming that w and D are two constant parameters to be estimated by fitting some available hydrograph. Many other models, actually the majority of the models, have been proposed in a very naive way by postulating the mathematical structure of the different blocks constituting a heuristic conceptual model. For example, one of the most classical models of this kind proposed by Nash (1957) corresponds to the model shown in Fig. 3-3-2, where the river is thought of as a sequence of n equal reservoirs.

If the outlet of each reservoir is assumed to be proportional to the volume of the water stored in the reservoir, then the system is described by the following linear equations (mass balance equations):

$$\begin{aligned}
\dot{x}_1 &= u - kx_1 \\
\dot{x}_2 &= kx_1 - kx_2 \\
&\vdots \\
\dot{x}_n &= kx_{n-1} - kx_n \\
y &= kx_n
\end{aligned}$$

where x_i is the volume of water stored in the i-th reservoir, u is the input flow rate of the first reservoir and y is the output flow rate of the last reservoir. In a more compact form the model can be considered to be a finite dimensional linear system of the kind

$$\dot{\mathbf{x}}(t) = \mathbf{F}\mathbf{x}(t) + \mathbf{g}u(t) \tag{3-3-12a}$$

$$y(t) = \mathbf{h}^T\mathbf{x}(t) \tag{3-3-12b}$$

where

$$\mathbf{x} = [\begin{matrix} x_1 & x_2 & x_3 & \dots & x_{n-1} & x_n \end{matrix}]^T$$

$$\mathbf{F} = \begin{bmatrix} -k & 0 & 0 & \dots & 0 & 0 \\ k & -k & 0 & \dots & 0 & 0 \\ 0 & k & -k & \dots & 0 & 0 \\ \vdots & \vdots & \vdots & & \vdots & \vdots \\ 0 & 0 & 0 & \dots & k & -k \end{bmatrix} \qquad \mathbf{g} = \begin{bmatrix} 1 \\ 0 \\ 0 \\ \vdots \\ 0 \end{bmatrix}$$

$$\mathbf{h}^T = [\begin{matrix} 0 & 0 & 0 & \dots & 0 & k \end{matrix}]$$

The impulse response (*unit hydrograph*)

$$\tilde{y}(t) = \mathbf{h}^T e^{\mathbf{F}t}\mathbf{g}$$

of this model can be explicitly determined since the matrix $\mathbf{F}$ has a very simple form (Jordan canonical form), and turns out to be

$$\tilde{y}(t) = \frac{1}{T(n-1)!}\left(\frac{t}{T}\right)^{n-1} e^{-t/T} \tag{3-3-13}$$

where $T = 1/k$ is the so-called *time constant* of the reservoirs. The impulse response $\tilde{y}(t)$ is plotted in Fig. 3-3-3 for different values of n. Obviously the curves in Fig. 3-3-3 can also be interpreted as the flows at the end of the intermediate reaches (reservoirs), so that by comparison with Fig. 2-1-4 it can be concluded that this model can take into account both propagation and attenuation of the peaks. The time of occurrence of the peak can immediately be derived from Eq. (3-3-13) and is given by

$$t^* = (n-1)T$$

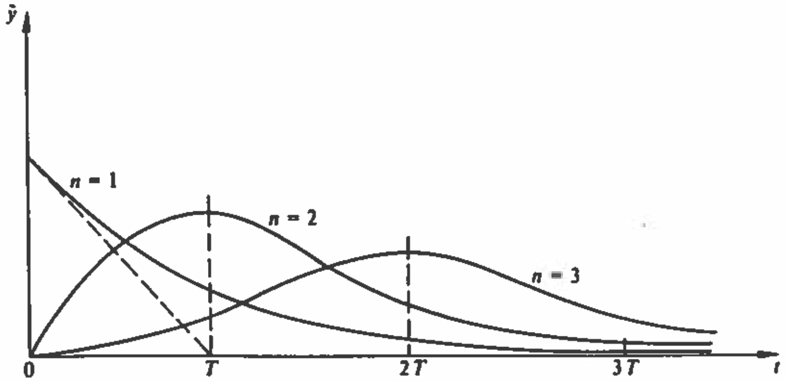

Figure 3-3-3 The impulse response of the Nash model for different values of n.

while the value y^* of the peak is

$$y^* = \frac{1}{T}\frac{(n-1)^{n-1}}{(n-1)!}e^{-(n-1)}$$

If the impulse response of the real system were available, these two expressions could be used to estimate the two parameters, n and T, such that the time of arrival t^* and the height y^* of the peak would be exactly the same in reality and in the model. In practice, however, the two parameters are selected such that a good fit with some available hydrograph is obtained.

Although there is no particular advantage in doing so, the *Nash model* and similar linear models are often presented in terms of *transfer functions*. The transfer function $M(s)$ associated with a linear system of the kind (3-3-12) is the *Laplace transform* of its impulse response and is given by

$$M(s) = \frac{Y(s)}{U(s)} = \mathbf{h}^T(s\mathbf{I} - \mathbf{F})^{-1}\mathbf{g} \qquad (3\text{-}3\text{-}14)$$

where s is the complex variable, $U(s)$ and $Y(s)$ are the Laplace transforms of $u(t)$ and $y(t)$, and $\mathbf{I}$ is the identity matrix. Substituting the expressions for $\mathbf{F}$, $\mathbf{g}$, and $\mathbf{h}^T$ corresponding to the Nash model into Eq. (3-3-14)

$$M(s) = \frac{1}{(1+sT)^n}$$

is obtained, which states that the transfer function of the system is simply the product of n transfer functions $m_i(s)$, which, in this particular case, are all equal to $1/(1+sT)$. On the other hand, the transfer function of a single reservoir described by

$$\dot{x} = -kx + u$$

$$y = kx$$

is given by (see Eq. (3-3-14))

$$m(s) = k \cdot (s+k)^{-1} \cdot 1 = \frac{1}{1+sT}$$

which proves that the transfer function of the Nash model is the product of the transfer functions of the n reservoirs, as should be expected, recalling that the transfer function of two systems connected in series is the product of the two transfer functions (see Sec. 1-2). This means that if the reservoirs were allowed to be different a transfer function would be obtained of the kind

$$M(s) = \prod_{i=1}^{n} m_i(s) = \prod_{i=1}^{n} \frac{1}{1+sT_i}$$

which is characterized by n parameters to be estimated.

Moreover, if the conceptual model is modified and the river considered a sequence of channels and reservoirs, and each channel characterized by a transport time τ_i, then a transfer function would be obtained of the following form (recall that a system characterized by a pure time delay τ_i has a transfer function given by $\exp(-\tau_i s)$)

$$M(s) = \frac{\prod_{i=1}^{n} e^{-\tau_i s}}{\prod_{i=1}^{n}(1+sT_i)} = \frac{e^{-\tau s}}{\prod_{i=1}^{n}(1+sT_i)}$$

where τ is the sum of all time delays introduced by the channels.

Another possible conceptual model consists of n reservoirs connected in parallel as shown in Fig. 3-3-4, where the coefficients λ_i satisfy the conditions

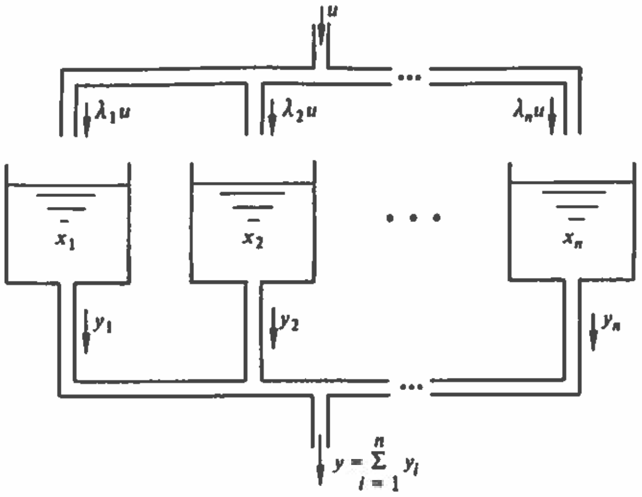

Figure 3-3-4 Description of a river as a bunch of parallel connected linear reservoirs.

$$0 \le \lambda_i \le 1 \qquad \sum_{i=1}^{n} \lambda_i = 1$$

in order to conserve the total mass. Since each reservoir is characterized by a transfer function

$$m_i(s) = \frac{\lambda_i}{1+sT_i}$$

and the transfer function of n systems connected in parallel is the sum of the single transfer functions we have

$$M(s) = \sum_{i=1}^{n} m_i(s) = \frac{\prod_{j=1}^{n-1}(1+st_j)}{\prod_{i=1}^{n}(1+sT_i)} \qquad (3\text{-}3\text{-}15)$$

where the time constants t_j are suitable functions of the λ_i's and T_i's. The transfer function given by Eq. (3-3-15) is the most general one which has the property of conserving the mass between input and output of finite dimensional systems. In fact, given a function $f(t)$ its Laplace transform is given by

$$F(s) = \int_0^\infty e^{-st} f(t)\,dt$$

so that

$$F(0) = \int_0^\infty f(t)\,dt$$

Thus, the conservation of mass between input and output of a given system can be expressed as $U(0) = Y(0)$, which implies (recall that $Y(s) = M(s)U(s)$) that $M(0) = 1$, and this property is indeed satisfied by Eq. (3-3-15). This shows that the model structure given in Fig. 3-3-4 does not really impose any particular constraint on the input–output relationship of the system, since the corresponding transfer function is the most general one satisfying the principle of mass conservation. Hence, even if a model structure has been postulated which seems to be highly specific, it may turn out that the corresponding mathematical model is the most general one.

A discussion of other hydrological models such as those in which overland flow and/or underground flow are involved, which would somehow make the survey complete, is not undertaken since it would represent too great a departure from the main goal of the book. However, the problems, the difficulties, and the different approaches already discussed with reference to wave propagation, are quite representative of any other field in hydrology and the interested reader should therefore be able to enlarge his knowledge by referring to the most recent books and treatises on this fascinating field (Gray, 1970). Of course, after this short and crude introduction to the art of modeling hydrological phenomena the reader cannot be expected to be familiar with this topic. For this reason, detailed descriptions of the dynamics of river flow will not be used in the remainder of the book. This is actually quite normal, since almost all studies on river pollution make reference to steady state hydrological conditions.

3-4 THE THERMAL SUBMODEL

Heat can be considered to be one of the dispersing substances for which the equations of Sec. 3-1 were derived. This means that the distribution of heat in a river is governed by an equation of the type (3-1-6) with

$$p = \theta\rho T$$

where θ, ρ, and T are the specific heat capacity, the density, and the temperature of the water respectively. This equation establishes the thermal submodel. As

discussed in Chapter 2, the hydrological variables in it may be considered to be externally imposed, since the influence of the temperature distribution on hydrology is small. Moreover, as in Sec. 3-3, our considerations will be confined to the one-dimensional balance equation which is usually sufficient for temperature investigations in ordinary rivers. Only for estuaries and river impoundments is the solution of the full two- or three-dimensional model often necessary (see Orlob and Selna, 1970; Leendertsee et al., 1973; Orlob, 1976). (The expressions given below for the components of the air–water heat exchange could also be used in the higher dimensional case if T is understood to be the local surface temperature rather than the cross-sectional mean temperature.) Hence, if it is assumed, for the sake of simplicity, that there is no water added to or subtracted from the river section considered, the *one-dimensional heat balance equation* reads (see Eq. (3-1-16))

$$\frac{\partial T}{\partial t} + v\frac{\partial T}{\partial l} - \frac{1}{A}\frac{\partial}{\partial l}\left(AD\frac{\partial T}{\partial l}\right) = \frac{1}{\theta\rho}\left(\frac{\lambda}{A} - \frac{Y}{A}F(T, M)\right) \qquad (3\text{-}4\text{-}1)$$

where λ = amount of heat added per length and time unit by man
Y = river width
F = flux of heat from the river to the atmosphere per unit surface area
M = set of meteorological conditions which determine the heat exchange between water and atmosphere

The less important components of the heat budget, like heat exchange with the river bed and frictional heat (see Sec. 2-2), are omitted, and θ and ρ are assumed to be constant.

The simplest way to specify the function $F(T, M)$ in Eq. (3-4-1) is to assume that the net heat flux through the air–water interface is proportional to the deviation of the water temperature from the equilibrium temperature T_E (see Sec. 2-2). If, in addition, the longitudinal dispersion is disregarded and the characteristic method applied by introducing the flow time τ (see Sec. 3-1) the equation

$$\frac{dT}{d\tau} = \frac{1}{\theta\rho}\left(\frac{\lambda}{A} - \frac{Y}{A}k(T - T_E)\right) \qquad (3\text{-}4\text{-}2)$$

is obtained, which has been used quite often (see, for example, Edinger et al., 1968). However, the simplicity of Eq. (3-4-2) is deceptive, because T_E is a complicated function of the meteorological conditions, and because k cannot be considered constant if the model is to be realistic.

Therefore, the most common approach to specify $F(T, M)$ is to develop separate expressions for each component of the heat flux through the air–water interface and to replace $F(T, M)$ by the sum of those expressions, i.e.,

$$F(T, M) = -F_s(M) + F_{sr}(M) - F_a(M) + F_{ar}(M) + F_w(T) + F_l(T, M) + F_c(T, M) \qquad (3\text{-}4\text{-}3)$$

where F_s = incoming solar radiation
F_{sr} = reflected solar radiation
F_a = long wave atmospheric radiation
F_{ar} = reflected long wave atmospheric radiation
F_w = long wave radiation of the water
F_l = latent heat flux
F_c = sensible heat flux

Expressions for the incoming *solar radiation* F_s are usually based on empirical formulae which describe the diurnal and seasonal variations of this heat budget component in the case of clear sky. The data necessary to set up such a formula can easily be measured. The values which the formula yields are then corrected for cloudiness, for example, according to the following equation

$$F_s = (1 - 0.65b^2)F_{so} \tag{3-4-4}$$

where F_{so} is the solar radiation from the clear sky and b is the proportion of the sky covered with clouds (*cloudiness ratio*). The *reflected proportion of the solar radiation* depends on the altitude of the sun and on cloudiness and is also calculated through empirical formulae which give the ratio F_{sr}/F_s as a function of cloudiness and altitude of the sun (see, for example, Anderson, 1954). Quite often the reflectivity is simply assumed to be constant, 6 percent being a typical value.

The *long-wave radiation of the atmosphere* F_a is mainly governed by the *Stefan-Boltzmann law*, which says that the radiation intensity is proportional to the fourth power of the temperature, i.e.,

$$F_a = \varepsilon_a \sigma T_a^4 \tag{3-4-5}$$

where ε_a is the *emissivity* of air, which depends strongly on humidity e_a, σ is the Stefan-Boltzmann constant, and T_a is the air temperature. As emphasized in Sec. 2-2, temperature and humidity distribution over a relatively thick layer are relevant for the long-wave atmospheric radiation, and these distributions ought to appear in the expression for F_a. But values of T_a and e_a measured at a height of a few meters (usually 2 m) have proved to be sufficiently representative for the calculation of F_a. The dependence of ε_a on humidity e_a (measured as water vapor pressure in the air) is again expressed with reference to clear sky, and then corrected for cloudiness. A typical example of an expression of this kind is (see Anderson, 1954)

$$\varepsilon_a = (0.74 + 0.0065e_a)(1 + 0.17b^2) \tag{3-4-6}$$

where e_a is measured in mmHg and b is the cloudiness ratio. The proportion of the long wave atmospheric radiation which is reflected is usually assumed to be constant; a typical value is 3 percent.

The *long-wave radiation of the water* F_w is also proportional to the fourth power of the absolute temperature. The emissivity ε_w is constant and slightly smaller than 1 because the river water is not a black body. Hence a reasonable expression for F_w is

$$F_w = 0.95\sigma T^4 \tag{3-4-7}$$

This component of the heat budget is the least problematic one.

The heat exchange through evaporation is governed by the turbulent mixing processes in the air layer above the water surface (see Sec. 2-2). Therefore, it should be described in principle by equations like the balance equations of Sec. 3-1. In practice, however, simple, semiempirical formulae are used, which give the heat flux as a function of a very few meteorological parameters. The most common formula for the flux of *latent heat* is

$$F_l = \beta(w)(e_s(T) - e_a) \tag{3-4-8}$$

where $\beta(w)$ is a function describing the influence of the wind velocity w on evaporation, and $e_s(T)$ is the saturated water vapor pressure at the water temperature T. The proportionality between F_l and the water vapor difference can be justified in the following way: the flux of water vapor is proportional to the gradient of the water vapor pressure (see Sec. 3-1), and this gradient is approximately proportional to the difference in Eq. (3-4-8). (See also Sec. 3-5, where a formula for physical reaeration which is analogous to Eq. (3-4-8) will be explained.) Many different expressions for the wind function $\beta(w)$ have been reported in the literature (LAWA, 1971); a linear one is mostly used:

$$\beta = a + bw \tag{3-4-9}$$

where a and b are suitable constants and w is usually measured at the same height as e_a and T_a. The ratio between a and b is about 1 if w is measured in m/s. The saturated water vapor pressure $e_s(T)$ is very well known and may be expressed in the model by a convenient empirical formula. An example, given by Jobson and Yotsukura (1972), is

$$e_s(T) = 0.75 \exp(54.721 - 6788.6T^{-1} - 5.0016 \ln T)$$

where e_s is in mmHg and T in Kelvin. In analogy to Eq. (3-4-8) the flux of *sensible heat* is written as

$$F_c = \alpha(w)(T - T_a) \tag{3-4-10}$$

where α is the wind function for convective heat transport. Since the transport mechanisms for both latent and sensible heat are the same, a close correlation between α and β can be expected. In fact, Bowen (1926) has shown that approximately

$$\frac{F_c}{F_l} = 0.524 \frac{T - T_a}{e_s - e_a} \tag{3-4-11}$$

(*Bowen ratio*), where T is in °C and e_a in mmHg. This relationship has been confirmed by many experiments.

Considering the expressions (3-4-4–3-4-10) it can be seen that Eq. (3-4-1) is nonlinear because of expressions (3-4-7) and (3-4-8), and that the meteorological parameters involved are air temperature, humidity, and wind speed at a certain height, cloudiness, and altitude of the sun. The local conditions around the river are reflected by the parameter values in the various expressions.

Sometimes only the difference $\Delta T = T' - T$ between the river temperature T' which results from anthropogenic waste heat discharges and the natural river temperature T is of interest. This is the case for example, if a river temperature standard is formulated as a maximum permissible deviation from the natural river temperature (which is common practice). For ΔT a model can be derived which is considerably simpler than Eq. (3-4-1), because all terms which do not depend on T are eliminated. If diffusion is disregarded and the balance equation written in flow time

$$\frac{\mathrm{d}\Delta T}{\mathrm{d}\tau} = \frac{v}{\theta\rho Q}(\lambda - Y\{0.95\sigma[(T+\Delta T)^4 - T^4] + \beta(w)[e_s(T+\Delta T) - e_s(T) + 0.524\,\Delta T]\}) \qquad (3\text{-}4\text{-}12)$$

is obtained, by subtracting the balance equation for T from the one for T'. If ΔT is small (which is usually the case) $(T + \Delta T)^4$ and $e_s(T + \Delta T)$ can be linearized around T and Eq. (3-4-12) becomes

$$\frac{\mathrm{d}\Delta T}{\mathrm{d}\tau} = \frac{v}{\theta\rho Q}\left\{\lambda - \Delta T Y\left[3.8\sigma T^3 + \beta(w)\left(\frac{\mathrm{d}e_s}{\mathrm{d}T} + 0.524\right)\right]\right\} \qquad (3\text{-}4\text{-}13)$$

Equation (3-4-13) is a linear ordinary differential equation which can easily be solved. It can be used to calculate the effect of the heat discharge λ on river temperature T if measurements of T are available (Faude et al., 1974). Equation (3-4-13) even remains a good approximation if instead of the "natural" temperature T a reasonable reference temperature is used, because the first derivatives of the functions which were linearized in Eq. (3-4-12) do not vary greatly over the range over which T usually varies. Even in the full equation (3-4-1) the terms dependent on T are sometimes linearized around a reasonable reference temperature (see, for example, Jobson and Yotsukura, 1972), although in this case the variations of the linearized functions themselves (rather than the derivatives) are important.

Finally, it should be stressed that the empirical and semiempirical formulae (3-4-4–3-4-10) are only typical examples from a great variety of similar expressions (see, for instance, Eckel and Reuter, 1950; Anderson, 1954; Parker and Krenkel, 1970; LAWA, 1971; Jobson and Yotsukura, 1972; Harleman et al., 1973). There is no set of formulae which could clearly be considered superior to all others. In view of their simplicity the degree of accuracy with which they can predict the actual river temperature is surprising. Figure 3-4-1 compares, for example, the predictions of a temperature model of type (3-4-1) for the Rhine river with measured data at Andernach, which is about 500 km downstream from the point where the boundary condition is imposed. The results shown in Fig. 3-4-1 are taken from Motor Columbus (1971), while the model is described in Bøgh and Zünd (1970). The figure shows that the calculated values follow the actual measurements almost perfectly. The way in which diffusion is taken into account in this model is worth mentioning (see also Jaske and Spurgeon, 1968): the river is appropriately split up into two fictitious channels which flow parallel with different velocities. The flow within the channels is without longitudinal dispersion, but the two channels are completely mixed with each other transversely from time to time. This computational scheme corresponds directly to the statement in Sec. 3-1 that longitudinal dispersion is mainly due to the combined effect of longitudinal stream velocity differences across the river and transverse turbulent mixing.

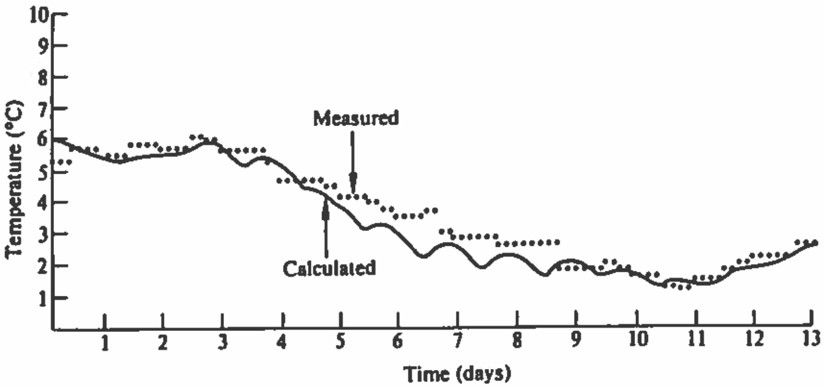

Figure 3-4-1 Comparison of measured Rhine river temperatures at Andernach with computer simulation results (after Motor Columbus, 1971).

3-5 THE BIOCHEMICAL SUBMODEL

As pointed out in Sec. 1-3, one of the first steps in building a mathematical model is the selection of the variables relevant to the problem. For the self-purification processes this is not as easy as for the thermal submodel, where temperature is the natural choice. The only variable which occurs as naturally in self-purification models is the oxygen concentration c, which was explained in Sec. 2-3 to be an important criterion for water quality. As in the previous section, the discussion in this section is confined to the one-dimensional case without addition and extraction of water, and since the source term of Eq. (3-1-16) is the essential point the dispersion term is even omitted. Then the *balance equation for the oxygen* concentration c can be written as

$$\frac{\partial c}{\partial t} + v\frac{\partial c}{\partial l} = r(c) - R + P \qquad (3\text{-}5\text{-}1)$$

where r is the *reaeration rate* and the terms R and P stand, respectively, for consumption and production of oxygen by all kinds of biochemical processes in the river, which may under certain circumstances also be a function of c. The variable $c(l, t)$ denotes the cross-sectional mean of the oxygen concentration. When, in the following, the oxygen concentration averaged over other space coordinates is referred to the same symbol c is used and the coordinates which have not been averaged out are listed. Anthropogenic source terms have not been included in Eq. (3-5-1) and will not be included in the model equations throughout this section.

Physical Aeration

The term $r(c)$ in Eq. (3-5-1) reads

$$r(c) = \frac{1}{H}\left[D_z \frac{\partial c(l, z)}{\partial z}\right]_{z=\xi} \tag{3-5-2}$$

where H = water depth
D_z = vertical diffusion coefficient
ξ = mean z value of the water surface at (l, t)

As shown in Sec. 3-1, the source term (3-5-2) appears after averaging the three-dimensional balance equation over y and z. Equation (3-5-2) corresponds to the second term on the right hand side of Eq. (3-1-12c) (the migration velocity u_z is zero since the oxygen is truly dissolved). The term $r(c)$ has to be expressed now in terms of the actual boundary condition

$$c(l, \xi) = c_s \tag{3-5-3}$$

where c_s is the *oxygen saturation concentration*.

The usual way to account for condition (3-5-3) through expression (3-5-2) is

$$\frac{1}{H}\left[D_z \frac{\partial c(l, z)}{\partial z}\right]_{z=\xi} = k_2(c_s - c) \equiv k_2 d \tag{3-5-4}$$

where k_2 is called the *reaeration coefficient* and d denotes the *oxygen deficit*. A possible justification of (3-5-4) is based on the assumption that there is a thin *water surface layer* in which the diffusion of oxygen is much slower than in the remaining body of water. In order to keep the discussion as simple as possible the aeration process in an open tank, which is assumed to be completely homogeneous in any horizontal cross section, is considered. If the volume of the layer is small compared to the total water volume we can assume that the oxygen transport through the layer is governed by a steady state *diffusion equation*

$$\frac{\partial^2 c(z)}{\partial z^2} = 0 \tag{3-5-5}$$

with boundary conditions

$$c(\xi) = c_s \qquad c(\xi - \Delta) = c_\Delta \tag{3-5-6}$$

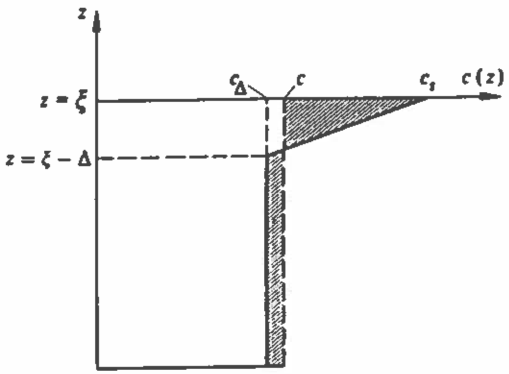

Figure 3-5-1 Idealized vertical oxygen profile in a river.

where Δ is the thickness of the layer, and c_Δ is the oxygen concentration at $z = \xi - \Delta$. The assumption of a steady state within the layer is equivalent to assuming that during the time in which the steady state in the layer is reached the c-value at $\xi - \Delta$ does not change significantly, which is reasonable under the assumptions made above. The solution of the diffusion equation (3-5-5) satisfying the boundary conditions (3-5-6) is a linear function, therefore the vertical oxygen profile is as shown in Fig. 3-5-1 (remember the assumption of practically perfect mixing underneath the surface layer) and

$$\frac{\partial c}{\partial z} = \frac{c_s - c_\Delta}{\Delta}$$

in the layer. Since the volume of the layer was assumed to be very small

$$c_\Delta \simeq c$$

and Eq. (3-5-4) results.

There is some experimental evidence for the existence of that surface layer in which the turbulent mixing is much less effective than in greater depths, but until now no satisfactory quantitative theory for it has been developed. This means that the value of k_2 in Eq. (3-5-4) cannot be calculated accurately from more fundamental river parameters like velocity, depth, etc. There are instead a lot of approximate formulae, derived through different theoretical approaches or directly through regression analysis of measured values of k_2. In the latter case k_2 is usually expressed as

$$k_2 = \alpha_1 v^{\beta_1} H^{-\gamma_1} \tag{3-5-7a}$$

or as

$$k_2 = \alpha_2 D^{\beta_2} H^{-\gamma_2} \tag{3-5-7b}$$

where D is the longitudinal dispersion coefficient (see Sec. 3-1), and quantities symbolized by Greek letters are positive parameters. If such a formula is given with specific values for the parameters it is usually said to be valid only for certain classes of rivers.

Since the theoretical basis for the evaluation of expression (3-5-4) is so weak, its dependence on river flow rate Q and temperature T is practically also only empirically known. The saturation concentration c_s is independent of Q. The *temperature dependence of* c_s is very well known from experiments and may be described by many suitable functions. A second order approximation, used by Beck and Young (1976), for example, is

$$c_s = 14.54 - 0.39T + 0.01T^2 \tag{3-5-8}$$

with T in °C and c_s in mg/l. For the *temperature dependence of* k_2 an expression of the kind

$$k_2(T) = k_2(20)\alpha^{(T-20)} \tag{3-5-9}$$

is quite often used (see, for instance, Sec. 5-2 and Isaacs and Gaudy (1968)), where α is a parameter slightly greater than 1, and T is the temperature in °C. The

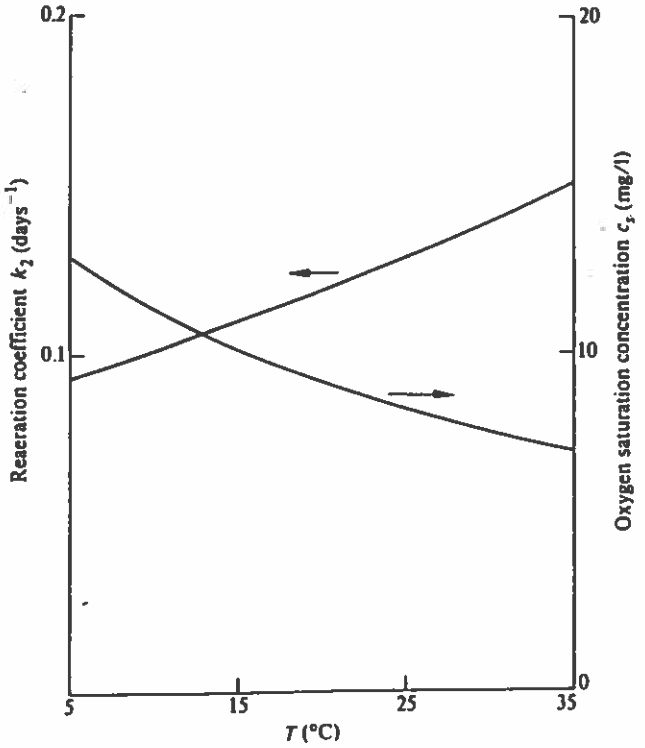

Figure 3-5-2 Temperature dependence of the oxygen saturation concentration and of the reaeration coefficient for a particular river (after Krenkel and Parker, 1969).

temperature dependence of c_s and of k_2 for a particular river (Krenkel and Parker (1969)) is given in Fig. 3-5-2. The dependence of k_2 on Q for a particular river can easily be derived from formulae of type (3-5-7a), if the functions $v(Q)$ and $H(Q)$ are known, which is usually the case (see Secs. 3-3 and 5-3). In general, for a given river this dependence is quite weak. The physical reasons for this is that there are two effects which partly compensate each other: on the one hand the depth H increases with increasing Q, which would result in a smaller k_2 value (see Eq. (3-5-4)); on the other hand, turbulence also increases, which enhances oxygen transport from the surface into greater depths (i.e., the surface layer mentioned above becomes thinner).

Reviews of the different approaches to the calculation of k_2 are given by Thackston and Krenkel (1969), Negulescu and Rojanski (1969), Wilson and MacLeod (1973), and Müller (1975). By and large one can state that the expression (3-5-4) has been proved to describe the physical reaeration term in Eq. (3-5-1) well, but that there is no satisfactory way to calculate k_2 from easily measurable river characteristics like depth and velocity, not to mention nonhydrologic influences like wind or pollution. Hence k_2 should be considered a parameter which has to be estimated from observations of river quality variables (see Chapter 5).

Chemical Models

The processes summarized by R in Eq. (3-5-1) are so complex that it is clear from the beginning that one cannot introduce a state variable for each pollutant and each species, so that the problem emerges how to select appropriately aggregated variables. On the other hand, there may be other quality criteria (beside the oxygen concentration) which are of final interest; for instance the concentration of certain compounds, like phenols or nitrite.

The most direct approach to the problem is to postulate the existence of a chemical reaction between oxygen and the oxidizable matter in the river, without worrying about the organisms involved in the degradation (*Chemical Models*). The great variety of compounds usually present in rivers is reduced to one or a few classes of oxidizable substances, which are treated as fictitious reactants. Because of the actual differences among the constituents of these fictitious reactants, the amount present is best characterized by the amount of oxygen needed for their complete biochemical oxidation. This measure of pollution is the *biochemical oxygen demand* (BOD) (see, for example, Gaudy, 1972) already mentioned in Sec. 2-3, and the corresponding state variable is denoted by b (with an index if there are several components) in the following.

However, this quantity is hard to measure directly, even if all oxidizable matter is looked upon as one reactant, since it takes a very long time until all degradation processes have died away in a river or wastewater sample. Figure 3-5-3 illustrates this fact: the curve, which was given in Wilderer et al. (1970), and which is based on measurements by Gotaas (1948), shows the accumulated oxygen consumption of a wastewater sample over time. After more than a month the

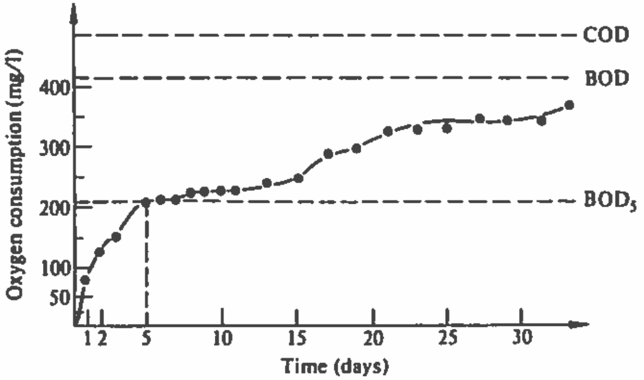

Figure 3-5-3 Oxygen consumption of a wastewater sample over time and relationship to BOD, COD, and BOD$_5$ (curve from Wilderer et al., 1970).

ultimate oxygen demand cannot be ascertained, even though with the temperature as high as 20 °C the reaction rates were fairly high (see page 88). The biodegradable matter originally present may well have disappeared completely after a much shorter time, but part of their chemical energy has been converted into chemical energy of living biomass, which is then released through oxidation very slowly (see Sec. 2-3).

One way to avoid this long measurement time is to observe the oxygen consumption over a reasonable time and then to estimate the BOD by extrapolation. However, this requires a model for the oxygen consumption in the measurement experiment, which is subject to the same kind of discussion as the oxygen consumption models for the river itself (see page 79). If the parameters of this model are assumed to be known it suffices to measure the total oxygen consumption during the measurement period in order to estimate the BOD. Therefore, quite often the oxygen consumption of samples during 2 or 5 days, abbreviated BOD$_2$ or BOD$_5$, is taken as a measure of b. But the assumption that all parameters of the BOD kinetics are known a priori is hardly fulfilled, since, for instance, the oxygen consumption over 2 or 5 days depends strongly on the biological community caught randomly with the sample. And indeed BOD$_2$ or BOD$_5$ measurements are notorious for their bad reproducibility.

Another way of easily obtaining an approximate BOD value is to oxidize chemically all matter and measure the oxygen consumption. This measure is called *chemical oxygen demand* (COD). Since in the ideal case all components are completely oxidized the COD can be higher than the BOD because there may be oxidizable compounds present which are not biodegradable (see Fig. 3-5-3). (The boundary between very slowly degradable and nondegradable cannot be defined precisely, however.) On the other hand, there may be compounds which are not oxidized by the oxidant used. As far as organic matter is concerned this is quite unlikely with *potassium dichromate* ($K_2Cr_2O_7$), which is used nowadays for standard COD measurements. With potassium permanganate however, which was formerly used, often even less than 50 percent of the theoretical COD of the organic matter was measured. The inorganic matter relevant to the oxygen budget, which is essentially ammonium and nitrite, is usually determined separately. Its oxygen demand can be determined stoichiometrically and subtracted from the measured COD value if necessary. (However, ammonium, for example, is not oxidized by either of the oxidants mentioned.)

The simplest and most widely used chemical model reflecting the major characteristics of BOD reaction, such as the one in Fig. 3-5-3, is the first order reaction model

$$\frac{\partial b}{\partial t} + v\frac{\partial b}{\partial l} = -k_1 b \tag{3-5-10}$$

which is part of the well-known *Streeter-Phelps model* (see Sec. 4-1). The parameter k_1 is called *degradation* or *deoxygenation coefficient*, and the biodegradable matter is assumed to be dissolved or suspended. Depending on the circumstances, nonlinear models have also been found useful, for instance,

$$\frac{\partial b}{\partial t} + v\frac{\partial b}{\partial l} = -k_1 bc \tag{3-5-11}$$

$$\frac{\partial b}{\partial t} + v\frac{\partial b}{\partial l} = -k_1 b^2 \tag{3-5-12}$$

(see Sec. 4-2). Because of the definition of BOD, the righthand sides of Eqs. (3-5-10)–(3-5-12), which represent volume source terms (see Sec. 3-1), must directly enter the model equation for c. Hence, for example, Eq. (3-5-1) becomes

$$\frac{\partial c}{\partial t} + v\frac{\partial c}{\partial l} = k_2(c_s - c) - k_1 b \tag{3-5-13}$$

if Eq. (3-5-10) is used. If the total BOD is divided into several components the degradation dynamics are described by as many equations of the types given above with different values of the parameters (see Sec. 4-2). Usually no measurements of the single components are available, so that the number of output variables is smaller than the number of state variables. Nevertheless, *parameter and state estimation* of those models may still be possible, as will be shown in Chapter 5. Sometimes, however, measurements for single components of BOD may be available. An example already mentioned is the oxygen demand of ammonium, which is oxidized to nitrate. Measurements of the concentration of ammonium can be used for estimating a model containing a chemical reaction equation for a fictitious reaction between ammonium and oxygen.

The chemical models given so far were for dissolved or suspended matter only. Their application to benthal BOD, for instance BOD of sediments, is straightforward: if, for the moment, the change of the benthal BOD by sedimentation or resuspension is disregarded, the same kinds of equations described above may be used but without derivatives with respect to l (see Sec. 3-1). The first-order reaction as in Eq. (3-5-10), however, is hardly realistic in this case, since the BOD degradation of sediments is taking place essentially at the water–sediment interface. Conditions in deeper sediment layers are usually anaerobic, which means that degradation there proceeds very slowly. Expressions more appropriate are

$$\frac{\partial b}{\partial t} = -\alpha c^{\beta} \tag{3-5-14}$$

(Edwards and Rolley, 1965) or even the zero-th-order reaction

$$\frac{\partial b}{\partial t} = -\alpha \tag{3-5-15}$$

Thus, using Eq. (3-5-10) for the dynamics of the planctonic BOD (b_1) and Eq. (3-5-14) for the benthal BOD (b_2), the model would read

$$\frac{\partial b_1}{\partial t} + v\frac{\partial b_1}{\partial l} = -k_{11}b_1 \tag{3-5-16a}$$

$$\frac{\partial b_2}{\partial t} = -k_{12}c^{k_{13}} \tag{3-5-16b}$$

$$\frac{\partial c}{\partial t} + v\frac{\partial c}{\partial l} = k_2(c_s - c) - k_{11}b_1 - k_{12}c^{k_{13}} \tag{3-5-16c}$$

where dispersion and external sources have again been left out. Sedimentation and resuspension can be dealt with by adding suitable terms to the righthand sides of Eqs. (3-5-16a) and (3-5-16b), as discussed on page 90 (a review of different approaches to the problem of benthal BOD is given by Müller, 1975).

Little more can be said on the *temperature dependence of the degradation* rate constants used in chemical models than that they increase as T increases. There are numerous empirical formulae to express this dependence, in most cases a formula of type (3-5-9) is used. The dependence on Q is usually neglected.

Ecological Models

It is already obvious from Fig. 3-5-3 that the simple chemical reaction models described so far only very roughly describe the actual oxygen dynamics in a river: the many plateaus which are turnovers of chemical energy from one link of the food chain to another certainly cannot be adequately explained as reactions between BOD components and oxygen. Figure 3-5-4, taken from Gates et al., (1966), illustrates that even the qualitative behavior of the oxygen concentration may be unreproducible by a simple chemical reaction model like the frequently used Streeter-Phelps model, which is given by Eqs. (3-5-10) and (3-5-13) (see Sec. 4-1). In the figure, observed oxygen values from a laboratory self-purification experiment are compared with the model solution. In the course of the experiment organic pollution was added at three time instants, which can easily be identified from Fig. 3-5-4. The parameter k_2 in Eq. (3-5-13) was known, while k_1 in Eq. (3-5-10) was estimated separately for each of the three stages such that the fit to the measured data was optimal in the least square sense (see Chapter 5). The figure shows that in particular the slow rise of the self-purification in the first stage (which is probably due to the low initial bacterial mass) cannot be simulated by the model.

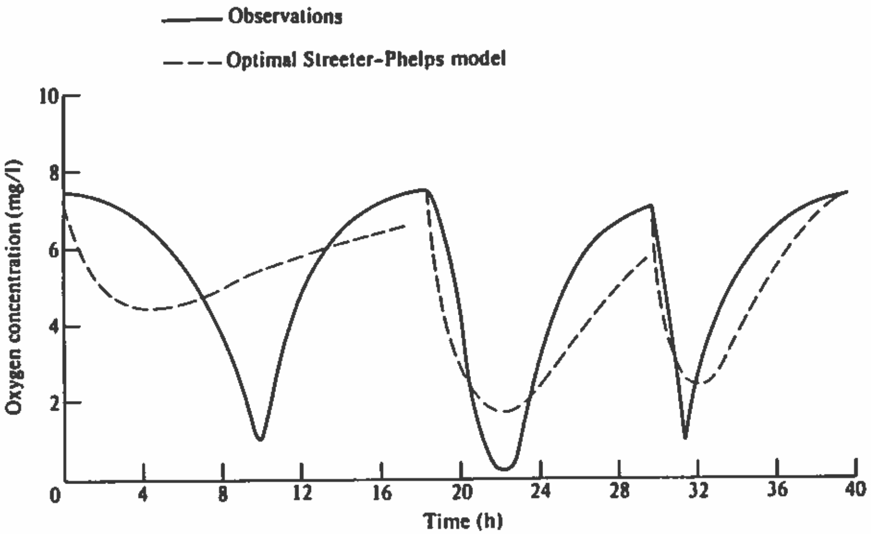

Figure 3-5-4 Reproduction of measured oxygen sag curves by means of the Streeter-Phelps model (after Gates et al., 1966).

Also, for more sophisticated models, which explicitly take into account living organisms, suitably aggregated variables have first to be selected. For single, dissolved pollutants consumed by bacteria the mass concentration will be the natural variable (or any equivalent to it). But for particulate pollutants the surface is more important, since the bacteria can attack the pollutant only at the surface. Hence in this case the available surface is a more appropriate variable (see, for instance, Boling et al., 1975). Usually the number of pollutants in a river is tremendous; for the Rhine river, for instance, the number of organic compounds is estimated to be higher than 10^6 (Kölle et al., 1972). Therefore, one has to aggregate these compounds and use measures which are more meaningful for bacterial growth than just mass or surface. Such a measure could again be the BOD (this time of the bacterial nutrients only), which is correlated with the *free energy* of the reactions the bacteria catalyze (McCarty, 1965, and 1972). Another measure sometimes used is the *total organic carbon* (TOC).

Also, the organisms cannot be dealt with by species, since this would entail a huge number of state variables and severe measurement problems. For the bacteria, for instance, it seems reasonable to lump together all heterotrophic bacteria, as already explained in Sec. 2-3. Having many species in one group the question arises whether one may use the number of individuals as the lumped variable (which is sometimes easier to measure) or whether the biomass has to be used. An example of how different these measures may be is given in Fig. 3-5-5

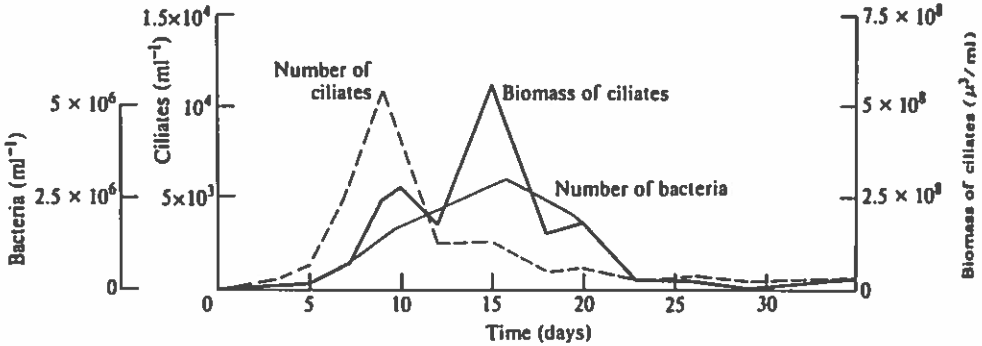

Figure 3-5-5 Development of ciliates feeding on bacteria (after Bick, 1964).

(see Bick, 1964), where the development of the ciliates number and biomass is compared with the abundance of their prey, namely the bacteria. Looking only at the protozoan number it would be hard to understand why the maximum of the curve occurs before the bacterial maximum, while the biomass curve is in agreement with the concept developed in Sec. 2-3 for the ciliata–bacteria interaction. Generalizing these findings, it is important to characterize groups of organisms in the model by their biomass, rather than by their number, because it describes better the activities of the organisms both as predator and prey.

As explained in Sec. 2-3 the most important step in the self-purification process is the interaction between the pollutants and the bacteria. In the case of a single dissolved energy donor, which is assumed to be the growth limiting nutrient, and whose concentration is denoted by s, the degradation can be modeled in the following way

$$\dot{s} = -\frac{\alpha_1 s}{\alpha_2 + s} B \tag{3-5-17}$$

where B is the bacterial mass concentration and α_1 and α_2 are parameters. Eq. (3-5-17) is written in flow time (see Eq. (3-1-21)) since this simplifies the notation considerably. An equation of type (3-5-17) can be derived for a single enzymatic reaction from the *law of mass action*, provided that the enzyme–substrate complex disintegrates slowly into the reaction products and the enzyme (see Laidler, 1958). Thus, the concentration of the enzyme appears first, instead of the bacterial mass density B. For a sequence of enzymatic reactions, the same expression for the rate of degradation of the original substrate can be used given certain assumptions; the reaction parameters and the enzyme concentration in it are those of the slowest reaction in the sequence (see Wilderer, 1969; Boes, 1970). Equation (3-5-17) results if we further assume that the substrate is degraded along a single metabolic pathway, and that the bacterial concentration is proportional to the enzyme concentration. Equation (3-5-17), which is named after *Michaelis-Menten* (1913), is often used in cases where the assumptions which led to it are not fulfilled with certainty. Then, it has to be interpreted as a two-parameter approximation of the real expression of the degradation rate which is assumed to be proportional to the product Bs for low values of s (probability of enzyme–substrate molecular collision) and independent of s and proportional to B for $s \to \infty$ (existence of an upper limit for the feeding activity of a bacterium).

Assuming the absence of predators, the dynamic equation for the bacterial mass may be written as

$$\dot{B} = -\beta_1 \dot{s} - \beta_2 B \tag{3-5-18}$$

where β_1 and β_2 are parameters. The first term on the righthand side of Eq. (3-5-18) is equivalent to the assumption that the ratio between the amount of newly formed biomass and the amount of nutrient degraded (*yield factor*) is constant (see Gunsalus and Shuster, 1961; McCarty, 1965 and 1972). The derivative of s on the righthand side of Eq. (3-5-18) has to be understood only as an abbreviation of the righthand side of Eq. (3-5-17), which facilitates surveying. The term $\beta_2 B$ in Eq. (3-5-18), which may be called *maintenance rate*, accounts for bacterial mass decrease through endogenous respiration, death, and possibly predation (Dawes and Ribbons, 1964; McCarty, 1972). It is obviously only an approximation, since, for example, the death rate ought to depend on the nutrient supply in the past.

The oxygen balance equation in flow time which results from the processes described by Eqs. (3-5-17) and (3-5-18) is

$$\dot{c} = k_2(c_s - c) + \gamma_1 \dot{s} - \gamma_2 \beta_2 B \tag{3-5-19}$$

where γ_1 and γ_2 are the specific oxygen consumptions for removal of s and B, respectively. If s is given as BOD and $\beta_2 B$ in Eq. (3-5-18) includes only endogenous respiration (i.e., self-oxidation of bacterial mass) the following relationship must hold:

$$\gamma_1 + \beta_1 \gamma_2 = 1 \tag{3-5-20}$$

A typical solution of model (3-5-17–3-5-19) is shown in Fig. 3-5-6, together with measurements taken by Gates et al. (1969) from a laboratory experiment in which the energy donor was glucose. The parameters were optimally selected using the *quasilinearization technique* described in Sec. 5-3. The variance of some of the parameters was very high, however, because no measurements of B were available (Stehfest, 1973).

Equations (3-5-17)–(3-5-19) for the pollutant–bacteria interaction may also be used if many pollutants are lumped together in one variable s, and indeed for part of the model described in detail in Sec. 4-4 this has been done. If several pollutants or groups of pollutants are to be taken into account separately one has to distinguish between the various possible interactions mentioned in Sec. 2-3. The pollutants may be degraded independently according to Eq. (3-5-17). This has frequently been observed (Wilderer, 1969), especially if the degradation processes are quite dissimilar, as, for example, with a nutrient combination of carbohydrates and proteins. To obtain the corresponding model one has to replace Eq. (3-5-17)

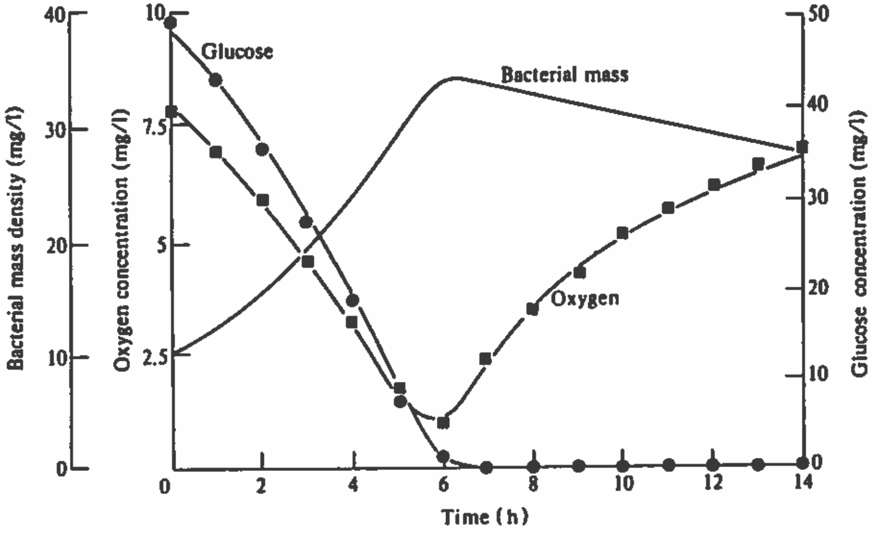

■ ● Measurements from Gates et al.(1969)

—— Optimal model solution

Figure 3-5-6 Simple self-purification model confronted with measurements.

by as many equations of the same kind as there are different pollutants and to add the corresponding terms in Eqs. (3-5-18) and (3-5-19).

In the case of inhibition it is necessary to distinguish between *competitive and allosteric inhibition.* Following the same kind of arguments used to derive the Michaelis-Menten expression one can easily derive expressions to describe the kinetics of single enzymatic reactions which are inhibited by another compound (Laidler, 1958). Similarly, it can be argued that these expressions may be applied to the inhibition of bacterial degradation. The resulting degradation rates are

$$\dot{s} = -\frac{\alpha_1 s}{\alpha_2 + s + \alpha_3 I} B \tag{3-5-21}$$

for competitive inhibition, and

$$\dot{s} = -\frac{\alpha_1 s}{(\alpha_2 + s)(1 + \alpha_3 I)} B \tag{3-5-22}$$

for allosteric inhibition, where I is the concentration of the inhibitor, which may be either a persistent compound (e.g., toxin) or another substrate whose degradation is governed by the Michaelis-Menten equation (Hartmann and Laubenberger, 1968; Stehfest, 1973). The degradation dynamics for large substrate concentrations s in Eqs. (3-5-21) and (3-5-22) can clearly be seen to be as described in Sec. 2-3: the effect of a competitive inhibitor disappears for $s \rightarrow \infty$, while for allosteric inhibition the maximum degradation rate depends on I. Equations (3-5-18) and (3-5-19) are, of course, also valid with inhibition in the degradation equation. The dynamics of a self-purification system where degradation of one pollutant is inhibited by another is shown in Fig. 3-5-7 (Stehfest, 1973). The measurements are essentially from an experiment carried out by Gaudy et al. (1963), using sorbitol and glucose as energy donors and a heterogeneous bacterial population acclimatized to glucose. Inspection of the metabolic pathways and of the observations led to the assumption of allosteric inhibition (Stehfest, 1973); hence the model

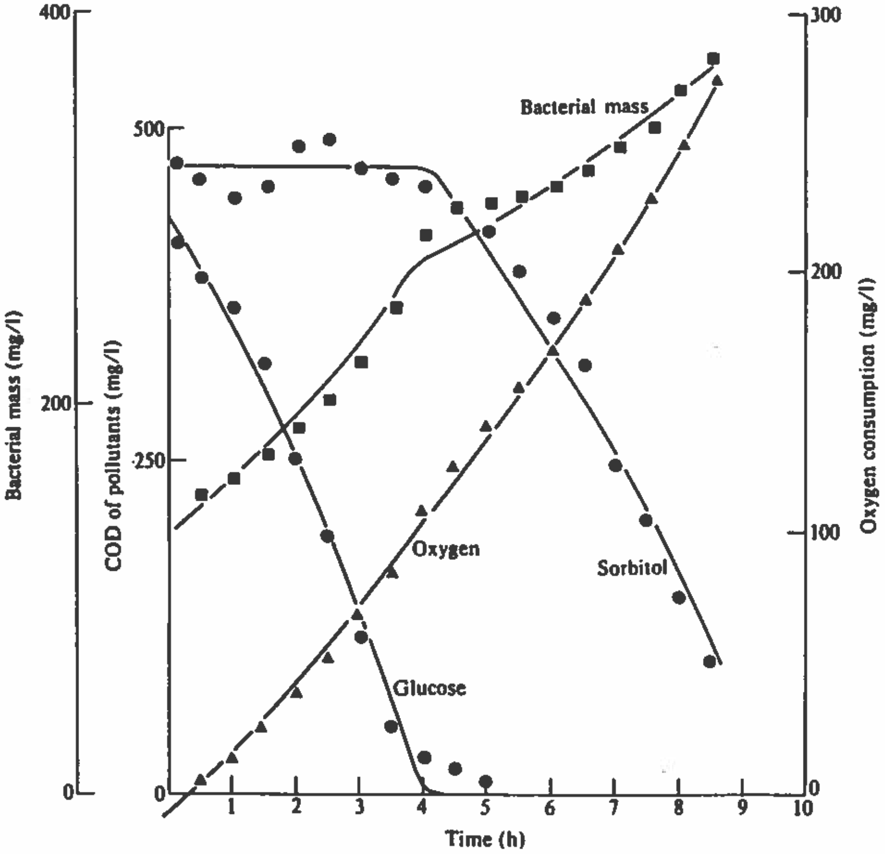

▲ ● ■ Measurements from Gaudy et al. (1963)

—— Optimal model solution

Figure 3-5-7 Two-pollutant self-purification system: model confronted with measurements.

used consists of the following equations

$$\dot{s}_1 = -\frac{\alpha_1 s_1}{\alpha_2 + s_1} B$$

$$\dot{s}_2 = -\frac{\beta_1 s_2}{(\beta_2 + s_2)(1 + \beta_3 s_1)} B$$

$$\dot{B} = -\gamma_1 \dot{s}_1 - \gamma_2 \dot{s}_2 - \gamma_3 B$$

$$\dot{O} = -\delta_1 \dot{s}_1 - \delta_2 \dot{s}_2 + \delta_3 \gamma_3 B$$

where O is oxygen consumption and α_i, β_i, γ_i, and δ_i are parameters which are all positive. Again the parameters were selected optimally through the quasi-linearization technique described in Sec. 5-3. A model including Eq. (3-5-21) for competitive inhibition is described in Sec. 4-4.

In the case of *repression* the most natural modeling approach is to introduce an additional equation for the concentration of the enzyme whose formation is repressed. For an endoenzyme one possibility could be

$$\dot{E} = \frac{\alpha_1 s}{(\alpha_2 + s)(1 + \alpha_3 R)} (\alpha_4 B - E) B - \alpha_5 E - \Delta \frac{E}{B}$$

where E and R are the concentrations of enzyme and repressor, respectively, and Δ is an expression giving the rate of decrease of the bacterial mass due to decay and predation, which may be taken from the model equation for B. The α_i are parameters, α_4 being the maximum of the enzyme–biomass ratio.

For particulate pollutants very sophisticated models could easily be developed using, for instance, variables for different classes of particle size with the particles passing into classes of smaller size as they are degraded. But the data needed for estimating such models are usually lacking, so that a less refined approximation is only possible. Equation (3-5-17) for instance, could also be used since the justification given above applies to particles of small size.

Similar statements can be made about modeling the degradation activity of *bacteria attached to the river bottom*. Here also colonizable surface plays an important role. For a dissolved nutrient which is taken up by attached bacteria as well as by suspended bacteria a possible model (without oxygen balance) is the following

$$\frac{\partial s}{\partial t} + v \frac{\partial s}{\partial l} = -\frac{\alpha_1 s}{\alpha_2 + s} B_1 - \frac{\alpha_3 s}{\alpha_4 + s} \cdot \frac{B_2}{\alpha_5 + B_2} \qquad \text{(3-5-23a)}$$

$$\frac{\partial B_1}{\partial t} + v \frac{\partial B_1}{\partial l} = \beta_1 \frac{\alpha_1 s}{\alpha_2 + s} B_1 - \beta_2 B_1 + \gamma_2 B_2^2 \qquad \text{(3-5-23b)}$$

$$\frac{\partial B_2}{\partial t} = \gamma_1 \frac{\alpha_3 s}{\alpha_4 + s} \cdot \frac{B_2}{\alpha_5 + B_2} - \beta_2 B_2 - \gamma_2 B_2^2 \qquad \text{(3-5-23c)}$$

where s is the energy donor concentration, B_1 and B_2 are the concentrations of planctonic and benthic bacterial biomass respectively, and all Greek letters denote parameters. The second term on the righthand side of Eq. (3-5-23a) accounts for pollutant removal by attached bacteria and may be explained as follows: the number of bacteria getting in touch with the pollutants in the water is for small values of B_2 equal to the number of bacteria present. As B_2 increases the bottom area becomes a limiting factor, bacteria grow in the third dimension, and the number of bacteria being in touch with nutrients and oxygen, i.e., being at the surface of the bacterial layer, becomes constant. Hence the biomass of the bacteria eliminating pollutants may be assumed to be proportional to $\alpha_1 B_2/(\alpha_5 + B_2)$, which is the second factor of the term under discussion. The first factor has an analogous form for the reasons mentioned in connection with Eq. (3-5-17). The same expression times a yield factor appears in Eq. (3-5-23c) for the growth of the attached bacteria. The second term on the righthand side of this equation describes endogenous respiration. The third term is to account for flaking off of bacteria, which only occurs if the bacterial layer becomes too thick. Since the bacteria flaked off continue to reproduce they contribute to B_1 and therefore the term $\gamma_2 B_2^2$ occurs also in Eq. (3-5-23b).

For bacterial degradation of bottom deposits, which also only takes place at the surface (because of anaerobic conditions in greater depths) a model may be derived in a similar way. But in view of the lack of data it may be necessary to use one of the simple chemical models described above. This is sufficient particularly if the processes in the bottom deposits are much less important than the processes going on in the water, which is often the case.

For the interaction between bacteria and protozoa feeding on the bacteria Eq. (3-5-17) may again be used (with B instead of s and protozoa mass density instead of B), and it may even be applied to prey–predator relationships of higher order. If one group of organisms is feeding on n others its *food preferences* for the different preys may be expressed by equations like

$$\dot{s}_i = -\frac{\alpha_i s_i}{1 + \sum_{j=1}^{n} \beta_{ij} s_j} p + (\mu_i - \sigma_i) s_i \qquad \text{(3-5-24)}$$

where s_i and p are prey and predator density, μ_i and σ_i are growth and decay coefficients of the prey, and α_i and β_{ij} are parameters. The similarity of the predation term on the righthand side of Eq. (3-5-24) with Eq. (3-5-21) for competitive inhibition is obvious.

In principle, all parameters determining the ecological processes described above are functions of both temperature and river flow rate. But in most cases the dependencies are small, so that in view of the model structure uncertainties they may be neglected. A temperature dependence which must be taken into account, however, concerns the *maximum specific growth rates*. In the case of model (3-5-17–3-5-19) the maximum specific growth rate of the bacteria is, for instance, $\alpha_1 \beta_1$, in the case of model (3-5-23) it is $\gamma_1(\alpha_3/\alpha_5)$ for the attached bacteria. (Note that endogenous respiration is excluded from the definition of maximum specific growth

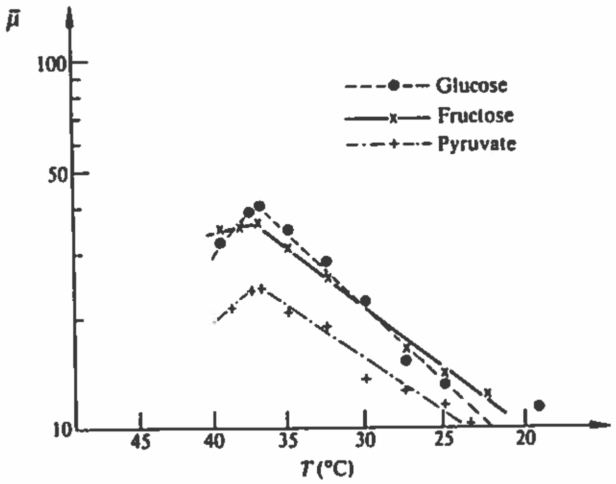

Figure 3-5-8 Maximum specific growth rate of *Escherichia coli* bacteria on various substrates vs. temperature (after Peters, 1973).

rate.) The rate coefficient α of a chemical reaction depends on T according to *Arrhenius' law*

$$\alpha(T) = \beta_1 e^{-\beta_2/T} \tag{3-5-25}$$

where β_1, β_2 are parameters and T is measured in K. Since the growth processes are chains of chemical reactions, their velocity should also depend on T according to Eq. (3-5-25), as long as the temperature is not so high that proteins become denatured. This has indeed been confirmed for many species relevant for self-purification. As an example, Fig. 3-5-8 shows the temperature dependence of the maximum specific growth rate $\bar{\mu}$ of *Escherichia coli* bacteria (Peters, 1973). The units are chosen such that a straight line results if Eq. (3-5-25) applies. It can be seen that Arrhenius' law applies, and similar curves have also been obtained for other organisms (see, for instance, Sudo and Aiba, 1972).

The Arrhenius law should also apply to the *temperature dependence of the endogenous respiration coefficient*, and this has indeed been observed, for example, by Benedek et al. (1972). Since the Arrhenius law describes a strong dependency on T in the temperature region we are interested in, the temperature dependence of endogenous respiration has also to be taken into account. Other temperature or flow rate dependencies are not considered here, although the parameter γ_2 in Eq. (3-5-23) in particular is highly sensitive to changes of Q.

Photosynthesis

Modeling the *biogenic aeration* represented by the term P in Eq. (3-5-1) is in itself a very large field. The underlying processes have been investigated, both experimentally and theoretically, mainly for lakes or impoundments. In polluted rivers, however, processes related to the degradation of anthropogenic wastes dominate. Therefore a few remarks on the subject will suffice.

The simplest way to take the activity of phototrophs into account is to look upon P in Eq. (3-5-1) as an external input. It could be a periodic function of time, in order to account for variations of P due to diurnal variations of light intensity (see Sec. 4-2), or it could even be a constant (see Sec. 5-3). If we want to explicitly model the population dynamics of photosynthesizing organisms, no completely new concepts (compared to the ones discussed above) have to be introduced. The main difference between growth models for bacteria and phototrophs is that for the latter several growth limiting factors have often to be considered, while for the bacteria only the concentration of energy donors is usually important (because in the pollutant degradation processes the other nutrients required by the bacteria occur as by-products anyway). The dependence of the specific growth rate on the limiting factors may again be described by the Michaelis–Menten expression, so that, for example, the growth of planctonic algae (neglecting dispersion) may be modeled through (Chen, 1970)

$$\frac{\partial A}{\partial t} + v\frac{\partial A}{\partial l} = \alpha_1 \cdot \frac{J}{\alpha_2 + J} \cdot \frac{[PO_4^{3-}]}{\alpha_3 + [PO_4^{3-}]} \cdot \frac{[NO_3^-]}{\alpha_4 + [NO_3^-]} \cdot \frac{[CO_2]}{\alpha_5 + [CO_2]} \cdot A - \frac{\beta_1 A}{\beta_2 + A} G - \gamma A$$

where
A = algal density
J = light intensity
G = grazer density
$\alpha_i, \beta_i, \gamma$ = parameters
$[C]$ = concentration of inorganic compound C

The light intensity is also a function of A because of shading. The formulation of the corresponding equations for the nutrients and the grazers and of the terms in the oxygen balance equation is straightforward and need not be discussed here.

The specific growth rate of phototrophs may often be considered independent of temperature, as can be expected for photochemical reactions. On the other hand, endogenous respiration depends on temperature as for chemotrophic organisms, so that the ratio between assimilation and respiration increases as temperature decreases (see Sec. 2-3 and Round, 1965).

Other Self-Purification Phenomena

As in the case of biochemical degradation and synthesis, there is also a great variety of models for the processes of *sedimentation* and *resuspension*. They differ widely in complexity. At one end of the range there are sophisticated statistical models like the one by Shen and Cheong (1974), which try to describe how heavier particles are dragged along the river bottom. At the other end, there are simple first order models: for example, Wolf (1971) gives the following equation for sedimentation of suspended solids (in flow time)

$$\dot{s} = -\alpha_1\left(s - s_0\,\frac{v^4}{\alpha_2 + v^4}\right)$$

where s = concentration of suspended solids
s_0 = initial concentration of suspended solids
α_i = parameters

An analogous model may be formulated for resuspension. Relatively little work has been done on how to include in water quality models the other phenomena mentioned in Sec. 2-4, like *adsorption, precipitation, flocculation*, etc. Models for these processes have been developed, however, in the context of the theory of pollution control facilities (Keinath and Wanielista, 1975), and they may be adapted for inclusion into river quality models.

The discussion of this section may lead to the conclusion that it is easy to develop a fairly detailed water quality model for a given river. The reason for this is that the major problem of how to determine the numerous model parameters uniquely from observations has not yet been discussed. Because of this problem, to which Chapter 5 is devoted, it is usually necessary to use models which are less precise than those developed from a qualitative insight into the problem.

REFERENCES

Section 3-1

Bansal, M. K. (1971). Dispersion in Natural Streams. *J. Hydraulics Div., Proc. ASCE*, 97, HY11, 1867–1886.

Chen, C. W. and Orlob, G. T. (1975). Ecologic Simulation for Aquatic Environments. In *Systems Analysis and Simulation in Ecology*, Vol. 3 (B. D. Patten, ed.). Academic Press, New York.

Di Toro, D. (1969). Stream Equations and Method of Characteristics. *J. San. Eng. Div., Proc. ASCE*, 95, 699–703.

Hays, J. R. (1966). *Mass Transport Mechanisms in Open Channel Flow*. Ph.D. Thesis, Vanderbilt University, Nashville, Tennessee.

Hirsch, C. (1975). Methods of Analysis in Water Quality Simulation Models. In *Modelling and Simulation of Water Resources Systems, Proc. IFIP Working Conference on Computer Simulation of Water Resources Systems*. North-Holland, Amsterdam.

Holley, E. R., Siemons, J., and Abraham, G. (1972). Some Aspects of Analyzing Transverse Diffusion in Rivers. *J. Hydraulics Res.*, 10, 27–57.

Holly, F. M. (1975). *Two-Dimensional Mass Dispersion in Rivers*. Hydrology Paper 78, Colorado State University, Fort Collins, Colo.

Leendertsee, J. J., Alexander, R. C., and Lin, S. K. (1973). *A Three Dimensional Model for Estuaries and Coastal Seas*. Vol. I: *Principles of Computation*. Report 4-1417-OW.RR, Rand Corporation, Santa Monica, California.

Li, W. H. (1962). Unsteady Dissolved Oxygen Sag in a Stream. *J. San. Eng. Div., Proc. ASCE*, 88, 75–85.

McQuivey, R. S. and Keefer, T. N. (1974). Simple Method for Predicting Dispersion in Streams. *J. Env. Eng. Div., Proc. ASCE*, 100, EE4, 997–1011.

Nihoul, J. (1975). Marine Systems Analysis. In *Modelling of Marine Systems* (J. Nihoul, ed.). Elsevier, Amsterdam.

Orlob, G. T. (1976). Estuarial Models. In *Systems Approach to Water Management* (A. K. Biswas, ed.). McGraw-Hill, New York.

Sayre, W. W. (1972). Natural Mixing in Rivers. In *Environmental Impact on Rivers (River Mechanics III)* (H. W. Shen, ed.). H. W. Shen, Fort Collins, Colorado.

Thackston, E. L. and Schnelle, K. B. (1970). Predicting Effects of Dead Zones on Stream Mixing. *J. San. Eng. Div., Proc. ASCE*, 96, 319–331.

Ward, P. R. B. and Fischer, H. B. (1971). Some Limitations on Use of the One-Dimensional Dispersion Equation. *Water Resour. Res.*, 7, 215–220.

Yotsukura, N. and Sayre, W. W. (1976). Transverse Mixing in Natural Channels. *Water Resour. Res.*, 12, 695–704.

Section 3-2

No references

Section 3-3

Chen, C. W. and Orlob, G. T. (1975). Ecologic Simulation for Aquatic Environments. In *Systems Analysis and Simulation in Ecology*, Vol. 3 (B. C. Patten, ed.). Academic Press, New York.

Gray, D. M. (1970). *Handbook on the Principles of Hydrology*. Water Information Center, Port Washington, New York.

Greco, F. and Panattoni, L. (1977). Numerical Solution Methods of the Saint Venant Equations. In *Mathematical Models for Surface Water Hydrology* (T. A. Ciriani, U. Maione, and J. R. Wallis, eds.). John Wiley, New York.

Nash, J. E. (1957). The Form of the Instantaneous Unit Hydrograph. *I.A.S.H.*, vol. 3, n. 45.

Orlob, G. T. (1976). Estuarial Models. In *Systems Approach to Water Management* (A. K. Biswas, ed.). McGraw-Hill, New York.

Section 3-4

Anderson, E. R. (1954). Energy Budget Studies. In *Water Loss Investigations: Lake Hefner Studies*. Prof. Paper 269, 71–119, U.S. Geol. Survey, Washington, D.C.

Bøgh, P. and Zünd, H. (1970). THEDY: A Program for Digital Simulation of the Unsteady Heat Budget of River Systems (in German). *Neue Technik*, 1, 27–31.

Bowen, I. S. (1926). The Ratio of Heat Losses by Conduction and by Evaporation from any Water Surface. *Phys. Rev.*, 27, 785.

Eckel, O. and Reuter, H. (1950). On the Evaluation of Heat Turnover in Rivers during Summer (in German). *Geografiska Annaler Stockholm*, 32, 188–209.

Edinger, J. E., Duttweiler, D. W., and Geyer, J. C. (1968). The Response of Water Temperatures to Meteorological Conditions. *Water Resour. Res.*, 4, 1137–1143.

Faude, D., Bayer, A., Halbritter, G., Spannagel, G., Stehfest, H., and Wintzer, D. (1974). *Energy and Environment in Baden-Württemberg* (in German). Report No. KFK 1966 UF, Kernforschungszentrum Karlsruhe, Karlsruhe, W. Germany.

Harleman, D. R. F., Brocard, D. N., and Najarian, T. O. (1973). *A Predictive Model for Transient Temperature Distributions in Unsteady Flows*. Report No. 175, Ralph M. Parsons Laboratory for Water Resources and Hydrodynamics, MIT, Cambridge, Mass.

Jaske, R. T. and Spurgeon, J. L. (1968). A Special Case, Thermal Digital Simulation of Waste Heat Discharges. *Water Research*, 2, 777–802.

Jobson, H. E. and Yotsukura, N. (1972). Mechanics of Heat Transfer in Nonstratified Open-Channel Flows. In *Environmental Impact on Rivers (River Mechanics III)* (H. W. Shen, ed.). H. W. Shen, Fort Collins, Colo.

LAWA (Länderarbeitsgemeinschaft Wasser) (1971). *Foundations for Evaluating Heat Discharges into Rivers* (in German). Koehler & Hennemann, Wiesbaden, W. Germany.

Leendertsee, J. J., Alexander, R. C., and Lin, S. K. (1973). *A Three-Dimensional Model for Estuaries and Coastal Seas.* Vol. I: *Principles of Computation.* Report 4-1417-OW.RR, Rand Corporation, Santa Monica, California.

Motor Columbus, Ingenieurunternehmung AG (1971). *Study on the Heat-Carrying Capacity of the Rhine River* (in German). Motor Columbus, Baden, Switzerland.

Orlob, G. T. (1976). Estuarial Models. In *Systems Approach to Water Management* (A. K. Biswas, ed.). McGraw-Hill, New York.

Orlob, G. T. and Selna, L. G. (1970). Temperature Variations in Deep Reservoirs. *J. Hydraulics Div., Proc. ASCE,* 96, HY2, Proc. Paper 7063.

Parker, F. L. and Krenkel, P. A. (1970). *Physical and Engineering Aspects of Thermal Pollution.* Butterworths, London.

Section 3-5

Beck, M. B. and Young, P. C. (1976). Systematic Identification of DO-BOD model structure. *J. Env. Eng. Div., Proc. ASCE,* 102, 909–927.

Benedek, P., Farkas, P., and Litheraty, P. (1972). Kinetics of Aerobic Sludge Stabilization. *Water Research,* 6, 91–97.

Bick, H. (1964). *Succession of Organisms during Self-Purification of Organically Polluted Water under Various Conditions* (in German). Ministerium für Ernährung, Landwirtschaft und Forsten des Landes Nordrhein-Westfalen, Düsseldorf, W. Germany.

Boes, M. (1970). *Mathematical Analysis of BOD Kinetics* (in German). Thesis, University of Karlsruhe, Karlsruhe, W. Germany.

Boling, Jr., R. H., Peterson, R. C., and Cummins, K. W. (1975). Modelling of Small Woodland Streams. In *Systems Analysis and Simulation in Ecology,* Vol. III (B. C. Patten, ed.). Academic Press, New York.

Chen, C. W. (1970). Concepts and Utilities of Ecological Models. *J. Sanit. Eng. Div., Proc. ASCE,* 96, 1085–1097.

Dawes, E. A. and Ribbons, D. W. (1964). Some Aspects of the Endogenous Metabolism of Bacteria. *Bact. Rev.,* 28, 126–149.

Edwards, R. W. and Rolley, H. C. J. (1965). Oxygen Consumption of River Muds. *J. Ecol.,* 53, 1–19.

Gates, W. E., Marlar, J. T., and Westfield, J. D. (1969). The Application of Bacterial Process Kinetics in Stream Simulation and Stream Analysis. *Water Research,* 3, 663–686.

Gates, W. E., Pohland, F. G., Mancy, D. G., and Schafie, F. R. (1966). A Simplified Physical Model for Studying Assimilative Capacity. *Proc. 21st Ind. Waste Conf.,* 665–687. Purdue University Extension Service.

Gaudy, Jr., A. F. (1972). Biochemical Oxygen Demand. In *Water Pollution Microbiology* (R. Mitchell, ed.). John Wiley, New York.

Gaudy, Jr., A. F., Komolrit, K., and Bhatla, M. N. (1963). Sequential Substrate Removal in Heterogeneous Populations. *J. WPCF,* 35, 903–922.

Gotaas, J. B. (1948). Effect of Temperature on Biochemical Oxidation of Sewage. *Sewage and Industrial Wastes,* 20, 441–477.

Gunsalus, I. C. and Shuster, C. W. (1961). Energy Yielding Metabolism in Bacteria. In *The Bacteria: A Treatise on Structure and Function,* Vol. II (I. C. Gunsalus and R. Y. Stanier, eds.). Academic Press, New York.

Hartmann, L. and Laubenberger, G. (1968). Toxicity Measurements in Activated Sludge. *J. San. Eng. Div., Proc. ASCE,* 94, 247–256. Corrections in *J. San. Eng. Div., Proc. ASCE,* 96, 607–609.

Isaacs, W. P. and Gaudy, A. E. (1968). Atmospheric Oxygenation in a Simulated Stream. *J. San. Eng. Div., Proc. ASCE,* 94, 319–344.

Keinath, T. M. and Wanielista, M. P. (1975). *Mathematical Modeling for Water Pollution Control Processes.* Ann Arbor Science, Ann Arbor, Mich.

Kölle, W., Ruf, H., and Stieglitz, L. (1972). The Burden of the Rhine River by Organic Pollutants (in German). *Die Naturwissenschaften,* 59, 299–305.

Krenkel, P. A. and Parker, F. L. (1969). Engineering Aspects, Sources, and Magnitude of Thermal Pollution. In *Biological Aspects of Thermal Pollution* (P. A. Krenkel and F. L. Parker, eds.). *Proc. Nat. Symp. on Thermal Pollution, Portland, Oreg., June 3–5, 1968.* Vanderbilt University Press, Nashville, Tenn.

Laidler, K. J. (1958). *The Chemical Kinetics of Enzyme Action.* Oxford University Press, Oxford, U.K.

McCarty, P. L. (1965). Thermodynamics of Biological Synthesis and Growth. *Proc. 2nd International Conference on Water Pollution Research,* 169–199. Pergamon Press, New York.

McCarty, P. L. (1972). Energetics of Organic Matter Degradation. In *Water Pollution Microbiology* (R. Mitchell, ed.). John Wiley, New York.

Michaelis, L. and Menten, M. (1913). The Kinetics of Invertase Action (in German). *Biochem. Z.,* 49, 333–369.

Müller, S. (1975). *Oxygen Budget in Rivers* (in German). Bayer. Landesamt für Umweltschutz, München, W. Germany.

Negulescu, M. and Rojanski, V. (1969). Recent Research to Determine Reaeration Coefficients. *Water Research,* 3, 189–202.

Peters, H. (1973). Thermodynamical Analysis of Oxydative Degradation of Pure Substrates through E. coli (in German). Jahresbericht des Instituts für Ingenieurbiologie und Biotechnologie des Abwassers, Universität Karlsruhe, Karlsruhe, W. Germany.

Round, F. E. (1965). *The Biology of the Algae.* Edward Arnold, London.

Shen, H. W. and Cheong, H.-F. (1972). Dispersion of Contaminants Attached to Sediment Bed Load. In *Environmental Impact on Rivers (River Mechanics III)* (H. W. Shen, ed.). H. W. Shen, Fort Collins, Colo.

Stehfest, H. (1973). *Mathematical Modelling of Self Purification of Rivers* (in German; English translation available as Report IIASA PP-77-11 of the International Institute for Applied Systems Analysis, Laxenburg, Austria). Report KFK 1654 UF, Kernforschungszentrum Karlsruhe, Karlsruhe, W. Germany.

Sudo, R. and Aiba, S. (1972). Growth Rate of *Aspidiscidae* Isolated from Activated Sludge. *Water Research,* 6, 137–144.

Thackston, E. L. and Krenkel, P. A. (1969). Reaeration Prediction in Natural Streams. *J. San. Eng. Div., Proc. ASCE,* 95, 65–94.

Wilderer, P. (1969). *Enzyme Kinetics as a Basis of the BOD Reaction* (in German). Thesis, University of Karlsruhe, Karlsruhe, W. Germany.

Wilderer, P., Hartmann, L., and Janečková, J. (1970). Objections Against the Use of Long-Term BOD for Characterizing Raw Waste Water (in German). *Wasser- und Abwasser-Forschung,* 1, 7–12.

Wilson, G. T. and MacLeod, N. (1973). A Critical Appraisal of Empirical Equations and Models for the Prediction of the Coefficient of Reaeration of Deoxygenated Water. *Water Research,* 8, 341–366.

Wolf, P. (1971). Incorporation of Latest Findings into Oxygen Budget Calculations for Rivers (in German). *GWF–Wasser/Abwasser,* 112, 200–203 and 250–254.

CHAPTER

FOUR

SOME PARTICULAR SELF-PURIFICATION MODELS

4-1 STREETER-PHELPS MODEL

The so-called *Streeter-Phelps model* is not only the oldest (1925) among the biochemical submodels, but also the one most widely used in river quality analysis. Therefore, the properties of this model are studied in detail in this section. As already pointed out in Sec. 3-5, the main assumption underlying the Streeter-Phelps model is that two variables, namely concentration of BOD (biochemical oxygen demand) and DO (dissolved oxygen) are sufficient to describe the biochemical processes. Moreover, Streeter and Phelps (1925) assumed that:

(a) the BOD decay rate is proportional to BOD concentration
(b) the deoxygenation and BOD decay rate are equal
(c) the reoxygenation rate is proportional to the oxygen deficit

The model equations resulting from these assumptions are

$$\frac{\partial b}{\partial t} + v\frac{\partial b}{\partial l} = -k_1 b \tag{4-1-1a}$$

$$\frac{\partial c}{\partial t} + v\frac{\partial c}{\partial l} = -k_1 b + k_2(c_s - c) \tag{4-1-1b}$$

with boundary conditions

$$b(0,t) = b_0(t) \qquad c(0,t) = c_0(t)$$

and initial conditions

$$b(l,0) = b_i(l) \qquad c(l,0) = c_i(l)$$

Longitudinal dispersion was neglected for the sake of simplicity. The parameter k_1 is called *deoxygenation coefficient* and k_2 *reaeration coefficient.*

Equation (4-1-1a) describes the dynamics of the BOD degradation. If finite time BOD_θ (e.g., BOD_5) is measured (see Sec. 3-5) a fixed relationship between BOD_θ and BOD is usually assumed; for example

$$\text{BOD}_\theta = (1 - e^{-K_L\theta})\,\text{BOD}$$

where $K_L(\text{day}^{-1})$ is the coefficient of BOD decay as evaluated by the standard laboratory BOD test. If the dynamics of BOD_θ (b_θ) are to be described, model (4-1-1) has to be modified in the following way

$$\frac{\partial b_\theta}{\partial t} + v\frac{\partial b_\theta}{\partial l} = -k_1 b_\theta$$

$$\frac{\partial c}{\partial t} + v\frac{\partial c}{\partial l} = -\frac{k_1}{(1 - e^{-K_L\theta})} b_\theta + k_2(c_s - c)$$

Sometimes the difference between BOD and BOD_θ is assumed to be small and Eq. (4-1-1) is directly used with b defined as BOD_θ.

As pointed out in Sec. 3-1, model (4-1-1) can be converted into a set of ordinary differential equations

$$\frac{db}{d\tau} = -k_1 b \tag{4-1-2a}$$

$$\frac{dc}{d\tau} = -k_1 b + k_2(c_s - c) \tag{4-1-2b}$$

$$\frac{dl}{d\tau} = v \tag{4-1-2c}$$

$$\frac{dt}{d\tau} = 1 \tag{4-1-2d}$$

with initial conditions

$$b(0) = b_i(l_0) \qquad c(0) = c_i(l_0) \qquad l(0) = l_0 \qquad t(0) = 0 \quad \text{for} \quad 0 \le l_0 \le L$$

and

$$b(0) = b_0(t_0) \qquad c(0) = c_0(t_0) \qquad l(0) = 0 \qquad t(0) = t_0 \quad \text{for} \quad t_0 > 0$$

Equation (4-1-2) describes the self-purification process in *flow time* τ. The time t_0 is called *release time* (Di Toro and O'Connor, 1968).

If $v(l, t)$, $b_0(t)$, $c_0(t)$ are independent of time the steady state case applies, for which the equation could be derived directly from Eq. (4-1-1) by setting all the derivatives with respect to t equal to zero. If in those simplified equations l is replaced by τ according to Eq. (4-1-2c), Eqs. (4-1-2a) and (4-1-2b) result.

Equations (4-1-2a) and (4-1-2b) are linear differential equations which can be written in the form

$$\dot{\mathbf{x}}(\tau) = \mathbf{F}\mathbf{x}(\tau) + \mathbf{g}u$$
$$y(\tau) = \mathbf{H}\mathbf{x}(\tau)$$

where the two-dimensional state vector $\mathbf{x}$ is given by

$$\mathbf{x}(\tau) = [b(\tau) \quad c(\tau)]^T$$

and

$$\mathbf{F} = \begin{bmatrix} -k_1 & 0 \\ -k_1 & -k_2 \end{bmatrix} \qquad \mathbf{g}u = \begin{bmatrix} 0 \\ k_2 c_s \end{bmatrix}$$

The output transformation matrix is given by

$$\mathbf{H} = [0 \quad 1]$$

if DO is considered the only output variable and by

$$\mathbf{H} = \begin{bmatrix} 1 & 0 \\ 0 & 1 \end{bmatrix} \qquad \text{or} \qquad \mathbf{H} = \begin{bmatrix} 1 - e^{-5k_1} & 0 \\ 0 & 1 \end{bmatrix}$$

if BOD or BOD$_5$, respectively, are also considered output variables.

The solution of Eqs. (4-1-2a) and (4-1-2b) (see Sec. 1-2) is given by

$$b(\tau) = b(0)\,e^{-k_1\tau} \tag{4-1-3a}$$

$$c(\tau) = c_s - (c_s - c(0))\,e^{-k_2\tau} + \frac{k_1 b(0)}{k_1 - k_2}(e^{-k_1\tau} - e^{-k_2\tau}) \tag{4-1-3b}$$

The trajectories shown in Fig. 4-1-1 are the solutions $l = l(t - t_0)$ of Eqs. (4-1-2c) and (4-1-2d) and they can be used to define a function $t_0 = t_0(l, t)$ giving the starting (release) time of a particle of water which is at point l at time t. Then, since $\tau = t - t_0$, the solution of Eq. (4-1-1) can be derived by means of Eq. (4-1-3)

giving

$$b(l,t) = b_0(t_0(l,t))\,e^{-k_1(t - t_0(l,t))} \tag{4-1-4a}$$

$$c(l,t) = c_s - [c_s - c_0(t_0(l,t))]\,e^{-k_2(t - t_0(l,t))} + \frac{k_1 b_0(t_0(l,t))}{k_1 - k_2}(e^{-k_1(t - t_0(l,t))} - e^{-k_2(t - t_0(l,t))}) \tag{4-1-4b}$$

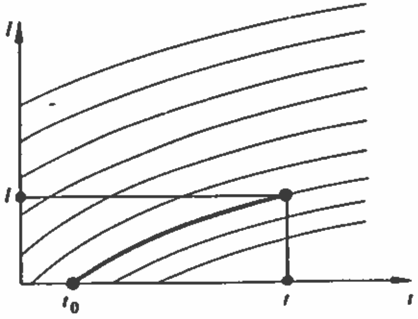

Figure 4-1-1 Trajectories of various water plugs and the function $t_0 = t_0(l, t)$.

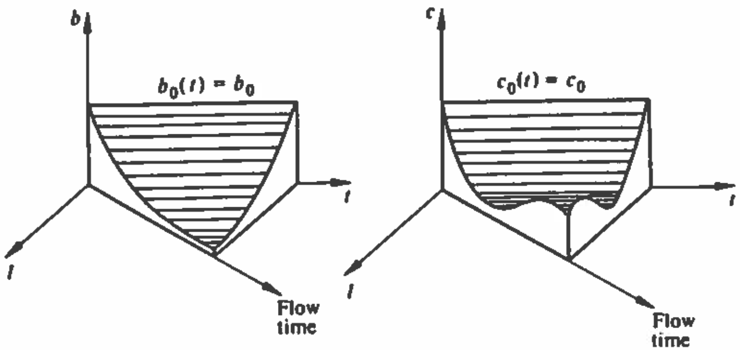

Figure 4-1-2 The surfaces $b(l, t)$ and $c(l, t)$ when the upstream boundary conditions $b_0(t)$, $c_0(t)$ and the stream velocity $v(l, t)$ are constant.

The surfaces $b(l, t)$ and $c(l, t)$ are shown in Fig. 4-1-2 for the steady state case in which v is constant in space and time, while in Fig. 4-1-3 the surface $b(l, t)$ is presented for the case in which a constant BOD load is discharged into a river whose flow rate Q and velocity v vary sinusoidally in time, i.e.,

$$Q = \bar{Q} + \Delta Q \sin(\bar{\omega}t) \qquad (\Delta Q < \bar{Q})$$
$$v = \bar{v} + \Delta v \sin(\bar{\omega}t) \qquad (\Delta v < \bar{v})$$

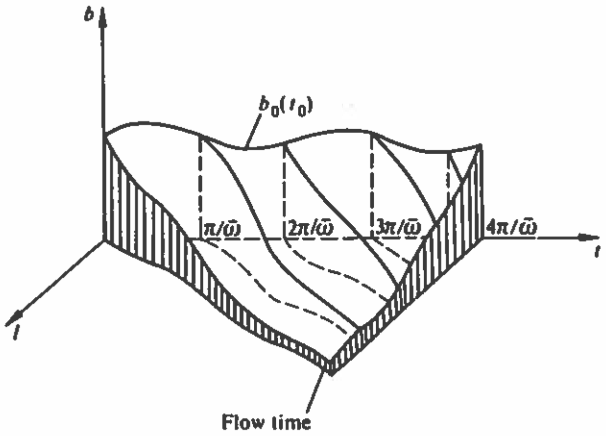

Figure 4-1-3 The surface $b(l, t)$ when a constant BOD load is discharged in a sinusoidally varying flow.

In the steady state case (Fig. 4-1-2) the form of the oxygen profile is that of a *sag curve*, both in flow time and in space, while BOD and DO are constant in time at any given point. For this reason the representation of Fig. 4-1-4 is usually preferred to that of Fig. 4-1-2, since it more clearly shows how biodegradable matter disappears and how oxygen concentration first decreases and then increases as water flows downstream (self-purification of the river). The latter property also applies to the unsteady state case since Eq. (4-1-4) implies that

$$\lim_{t\to\infty} b(l,t) = \lim_{t\to\infty} [c_s - c(l,t)] = 0$$

for all bounded boundary conditions $b_0(t)$ and $c_0(t)$. The self-purification property corresponds to model (4-1-2) to have a unique and asymptotically stable equilibrium state $\bar{\mathbf{x}} = [0\ c_s]^T$ (the matrix $\mathbf{F}$ has negative eigenvalues).

Figure 4-1-4 shows the existence of a *critical point* where the DO deficit reaches its maximum value (*critical deficit*). The position l_c of the critical point and the critical deficit d_c are functions of the boundary conditions since

$$l_c = \frac{v}{k_1(f-1)} \ln \left\{ f\left[1 - (f-1)\frac{d_0}{b_0}\right]\right\} \tag{4-1-5}$$

and

$$d_c = \frac{b_0}{f}\left\{ f\left[1 - (f-1)\frac{d_0}{b_0}\right]\right\}^{1/(1-f)} \tag{4-1-6}$$

where $f = k_2/k_1$ is called the *self-purification rate* (Fair and Geyer, 1965) and $d_0 = c_s - c_0$ is the oxygen deficit at $l = 0$. Equations (4-1-5) and (4-1-6) can easily be found by annihilating the first derivative of $c(t)$ given by Eq. (4-1-3b). A number of interesting properties of these functions are given by Liebman (1965), Liebman and Loucks (1966) and Arbabi et al. (1974). Some of these properties are used in the following (see Sec. 8-2) and are now briefly mentioned. From Eq. (4-1-5), it can be proved that the critical point exists, i.e., that l_c is positive, if and only if

$$\frac{d_0}{b_0} \leq 1/f \tag{4-1-7}$$

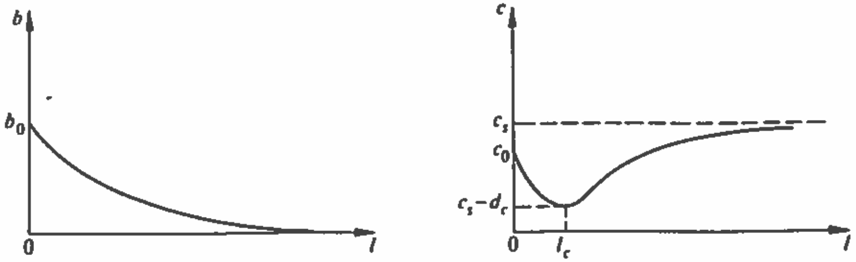

Figure 4-1-4 BOD and DO profiles along the river in steady state conditions.

Moreover, since f, b_0 and d_0 are non-negative, the critical point can never be located downstream the point

$$L_c = \frac{v}{k_1(f-1)} \ln f \tag{4-1-8}$$

In particular l_c tends to L_c for increasing initial loads b_0, while $l_c = L_c$ if the river is perfectly oxygenated at the boundary ($d_0 = 0$). The critical deficit d_c is a nonlinear function of the boundary conditions and this generates some difficulty as will be seen later on (pages 252–254). Equation (4-1-6) may also be written in the form

$$d_c = \frac{b_0}{f} e^{-\frac{k_1}{v} l_c}$$

which shows (recall that l_c is bounded by L_c) that the critical deficit d_c increases without limit with the initial load b_0. In other words, there are initial concentrations b_0, such that $d_c > c_s$, i.e., the oxygen concentration predicted by the model can be negative. This physical nonsense is obviously implied by assumption (a), which says that the deoxygenation rate is independent of the DO concentration. While this assumption is reasonable at high levels of DO, it is at the least doubtful at low values of DO, when anaerobic conditions can occur (see Secs. 2-3 and 3-5). A modified nonlinear model which does not have this disadvantage will be shown in the next section.

The influence on the model of variations in some of the main parameters can now be considered (*sensitivity analysis*). The approach differs depending upon whether large or small variations of the parameters are expected. (There are also other considerations which may be relevant for the selection of the suitable method of sensitivity analysis; see Stehfest, 1975.) In the case of large variations one has, in general, to simulate the model (or look at its analytic solution) for a few representative values of the parameters and then make the comparison (see Lin et al., 1973). On the other hand, if only small variations around some nominal conditions are of interest, the analysis can be carried out by the first order approximation suggested by the so-called *sensitivity theory* (see Rinaldi and Soncini-Sessa, 1976 and 1978). Since this approach is quite efficient and elegant it is now briefly presented and applied to the analysis of the Streeter-Phelps model.

Assume that a continuous, lumped parameter system is described by the differential equation

$$\dot{\mathbf{x}}(t) = \mathbf{f}(\mathbf{x}(t), \theta, t) \tag{4-1-9}$$

where θ is a constant parameter with nominal value $\bar{\theta}$ and let the initial state $\mathbf{x}_0$ of the system depend upon the parameter, i.e.,

$$\mathbf{x}_0 = \mathbf{x}_0(\theta) \qquad (\bar{\mathbf{x}}_0 = \mathbf{x}_0(\bar{\theta})) \tag{4-1-10}$$

The solution of Eq. (4-1-9) with the initial condition (4-1-10) is a function

$$\mathbf{x} = \mathbf{x}(t, \theta)$$

which, under very general conditions, can be expanded in series in the neighborhood of the nominal value of the parameter, i.e.,

$$\mathbf{x}(t,\theta) = \bar{\mathbf{x}}(t) + \left[\frac{\partial \mathbf{x}(t,\theta)}{\partial \theta}\right]_{\bar\theta}(\theta - \bar\theta) + \cdots$$

where $\bar{\mathbf{x}}(t) = \mathbf{x}(t,\bar\theta)$ is the nominal solution. The vector $[\partial\mathbf{x}/\partial\theta]_{\bar\theta}$, namely the derivative of the state vector with respect to the parameter, is called *sensitivity vector* and will be denoted by s from now on, i.e.,

$$\mathbf{s}(t) = \left[\frac{\partial \mathbf{x}}{\partial \theta}\right]_{\bar\theta}$$

Thus, the perturbed solution of Eq. (4-1-9) can easily be obtained as

$$\mathbf{x}(t,\theta) \cong \bar{\mathbf{x}}(t) + \mathbf{s}(t)(\theta - \bar\theta)$$

once the sensitivity vector is known.

When there are many parameters $\theta_1, \theta_2, \ldots, \theta_q$, the knowledge of the sensitivity vectors $\mathbf{s}_1, \mathbf{s}_2, \ldots, \mathbf{s}_q$ allows the association of certain characteristics of the system behavior with certain particular parameters. If, for example, the nominal solution $\bar{x}(t)$ of a first order system is the one shown in Fig. 4-1-5 where $s_1(t)$ and $s_2(t)$ are the sensitivity coefficients of x with respect to two parameters θ_1 and θ_2, then it is reasonable to say that the first parameter is responsible for the overshoot of $\bar{x}$, while the second is responsible for the asymptotic behavior of the system. This characterization of the parameters turns out to be very often of great importance in the phase of the validation of the structure of the system.

It is easy to prove that the sensitivity vector s(t) satisfies the following vector differential equation

$$\dot{\mathbf{s}} = \left[\frac{\partial \mathbf{f}(\mathbf{x},\bar\theta,t)}{\partial \mathbf{x}}\right]_{\bar{\mathbf{x}}}\mathbf{s} + \left[\frac{\partial \mathbf{f}(\bar{\mathbf{x}},\theta,t)}{\partial \theta}\right]_{\bar\theta} \tag{4-1-11}$$

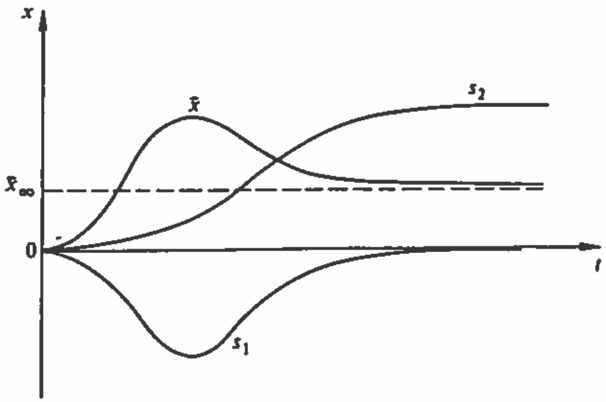

Figure 4-1-5 Nominal solution $\bar{x}$ and sensitivity coefficients s_1 and s_2 of a system.

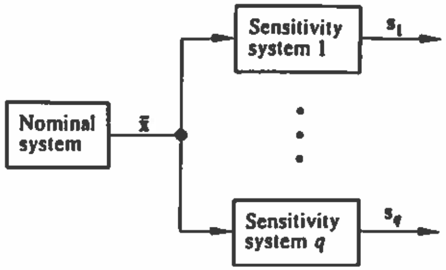

Figure 4-1-6 Computation of the sensitivity vectors.

with initial conditions

$$\mathbf{s}(0) = \left[\frac{\partial \mathbf{x}_0}{\partial \theta}\right]_{\bar\theta} \tag{4-1-12}$$

Thus, the sensitivity vector is the state vector of system (4-1-11), called *sensitivity system*, which is always a linear system, even if system (4-1-9) is nonlinear. Because of this property the sensitivity vectors can often be determined analytically. In any case, they can always be computed by means of simulation following the scheme shown in Fig. 4-1-6.

This methodology is now applied to some very particular but interesting sensitivity problems of river pollution. The model used is the steady state Streeter-Phelps model (4-1-2) or some suitable modification of it. The reader interested in the details of this analysis should refer to Rinaldi and Soncini-Sessa (1976, 1978).

BOD Load Variation

Let us first analyze the effects of a variation of the BOD load discharged at a particular point into the river. By measuring flow time from this point the system is described by

$$\dot b = -k_1 b$$

$$\dot c = -k_1 b + k_2(c_s - c)$$

and the initial conditions are $(\bar\theta = 0)$

$$b_0 = \bar b_0 + \theta \qquad c_0 = \bar c_0$$

Thus, the sensitivity system is given by

$$\dot s_b = -k_1 s_b \tag{4-1-13a}$$

$$\dot s_c = -k_1 s_b - k_2 s_c \tag{4-1-13b}$$

and its initial conditions are

$$s_b(0) = \left[\frac{\partial b_0}{\partial \theta}\right]_{\bar\theta} = 1 \qquad s_c(0) = 0$$

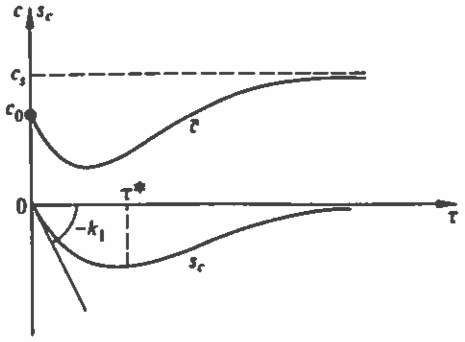

Figure 4-1-7 The sensitivity of dissolved oxygen concentration with respect to BOD load.

The solution of Eq. (4-1-13a) with $s_b(0) = 1$ is given by

$$s_b(\tau) = e^{-k_1\tau}$$

which can be introduced in Eq. (4-1-13b) together with $s_c(0) = 0$, thus giving

$$s_c(\tau) = k_1 \frac{e^{-k_1\tau} - e^{-k_2\tau}}{k_1 - k_2} \tag{4-1-14}$$

The sensitivity coefficient s_c given by Eq. (4-1-14) is always negative. Its behavior is as shown in Fig. 4-1-7 and it has a minimum (see Eq. (4-1-8)) for

$$\tau^* = \frac{\ln(k_2/k_1)}{k_2 - k_1} = \frac{L_c}{v} \tag{4-1-15}$$

This means that a positive perturbation of the BOD load in a point implies that all the river downstream from that point becomes worse as far as its oxygen content is concerned. Of course, this is the conclusion that can be derived from the Streeter-Phelps model which does not represent a priori the behavior of a real river. Indeed, it will be shown in Sec. 5-3 that because of the mechanisms of the food web, it can be expected that the conditions of the river are sometimes improved by an increase of the BOD load (see also Sec. 10-5 for an interesting example of the implications of this fact).

Equilibrium Temperature Variations

The influence of the temperature on the dissolved oxygen of a river will now be discussed. In order to simplify the discussion a constant point source of BOD on a perfectly clean and oxygenated river is assumed. Moreover, suppose that the water temperature T is constant along the river (e.g., equal to the equilibrium temperature, see Sec. 3-4). Thus, the upstream boundary conditions of the stretch are given and depend upon the temperature T of the water since the oxygen saturation level c_s is a (decreasing) function of T. Under these assumptions, the system is described by

$$\dot{b} = -k_1(T)b \tag{4-1-16a}$$

$$\dot{c} = -k_1(T)b + k_2(T)(c_s(T) - c) \tag{4-1-16b}$$

with initial conditions

$$b_0 = \bar{b}_0 \qquad c_0 = c_s(T)$$

The corresponding sensitivity system (4-1-11) is given by

$$\dot{s}_b = -k_1 s_b - k_1' \bar{b}$$

$$\dot{s}_c = -k_1 s_b - k_2 s_c - k_1' \bar{b} + (k_2 c_s)' - k_2' \bar{c}$$

with initial conditions

$$s_b(0) = 0 \qquad s_c(0) = c_s'$$

where ′ denotes derivative with respect to T, and $\bar{b}$ and $\bar{c}$ are the nominal solutions of Eq. (4-1-16). The solution of the sensitivity system can be derived by taking Eq. (4-1-3) into account and is given by

$$s_b(\tau) = -k_1' \bar{b}_0 \tau\, e^{-k_1\tau}$$

$$s_c(\tau) = c_s' + \frac{k_1 k_2' - k_1' k_2}{(k_2 - k_1)^2} \bar{b}_0 (e^{-k_1\tau} - e^{-k_2\tau})$$

$$+ \frac{k_1}{k_2 - k_1} \bar{b}_0 \tau (k_1' e^{-k_1\tau} - k_2' e^{-k_2\tau})$$

From these expressions it follows that

$$\dot{s}_c(0) = -k_1' \bar{b}_0 \qquad s_c(\infty) = s_c(0) = c_s'$$

Hence, since $k_1' > 0$ and $c_s' < 0$ (see Sec. 3-5), the DO sensitivity coefficient s_c is always characterized by the following three properties

$$s_c(0) < 0 \qquad \dot{s}_c(0) < 0 \qquad s_c(\infty) < 0$$

Two possible sensitivity curves s_c are shown in Fig. 4-1-8, the first one (*a*) being negative everywhere and the second one (*b*) showing that along a segment of the river (segment AB) the conditions are improved by an increment of the temperature. A curve of type (*b*) would result if the reaeration coefficient should increase drastically with temperature. Nevertheless, even under this hypothetical condition, the dominant effect is a decrease of the dissolved oxygen concentration with increasing temperature, and hence for reasons of safety, high temperature conditions are often selected as the reference conditions in the design of wastewater treatment plants or other river pollution control facilities. Actually, in these design problems reference is usually made to low flow-high temperature conditions, since similar results can also be proved for flow rate. The only difference is that the sensitivity analysis should be done for the system describing self-purification in space, because flow velocity varies with flow rate (Rinaldi and Soncini-Sessa, 1978).

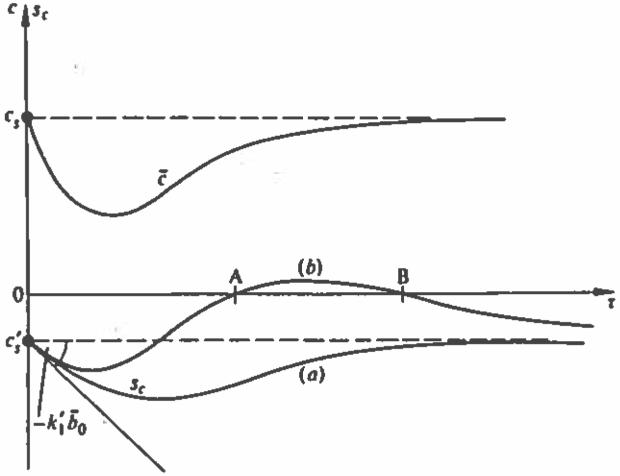

Figure 4-1-8 The sensitivity of dissolved oxygen concentration with respect to equilibrium temperature.

Heat Discharge

As a final example, the effects that heat pollution has on the self-purification processes, as described by the Streeter-Phelps model, is discussed in very simple terms.

The case studied is illustrated in Fig. 4-1-9a, where a river with flow rate Q_1 and temperature T_0^* receives a heat discharge with flow rate Q_2 and temperature $(T_0^* + (Q_1 + Q_2)/Q_2 \Delta T_0)$. Then, after mixing (at the point $l = 0$) a flow rate $Q = Q_1 + Q_2$ and a temperature $T_0 = T_0^* + \Delta T_0$ is obtained. The variation ΔT_0 induced in the river by the heat discharge is the parameter and its nominal value $\overline{\Delta T_0}$ is zero, thus meaning that the nominal conditions refer to the case in which there is no heat discharge. Moreover, the BOD concentration of the discharge is assumed to be the same as that of the river while both the river and the discharge are assumed to be saturated with oxygen (see Sec. 7-2 for justification), as shown in Fig. 4-1-9b, so that the initial conditions are

$$T_0 = T_0^* + \Delta T_0$$

$$b_0 = b_0^*$$

$$c_0 = \frac{Q_1}{Q_1 + Q_2} c_s(T_0^*) + \frac{Q_2}{Q_1 + Q_2} c_s\left(T_0^* + \frac{Q_1 + Q_2}{Q_2} \Delta T_0\right)$$

A thermal submodel must now be coupled with the Streeter-Phelps model considered so far. Thus, assuming that water temperature dynamics can be described by a differential equation (see Sec. 3-4), we obtain

$$\dot{T} = \phi(T) \tag{4-1-17a}$$

$$\dot{b} = -k_1(T)b \tag{4-1-17b}$$

$$\dot{c} = -k_1(T)b + k_2(T)(c_s(T) - c) \tag{4-1-17c}$$

with initial nominal conditions

$$\bar{T}_0 = T_0^* \qquad \bar{b}_0 = b_0^* \qquad \bar{c}_0 = c_s(T_0^*)$$

Thus, the sensitivity system is given by

$$\dot{s}_T = \phi' s_T \tag{4-1-18a}$$

$$\dot{s}_b = -k_1' \bar{b} s_T - k_1 s_b \tag{4-1-18b}$$

$$\dot{s}_c = (-k_1' \bar{b} + k_2' c_s + k_2 c_s' - k_2' \bar{c}) s_T - k_1 s_b - k_2 s_c \tag{4-1-18c}$$

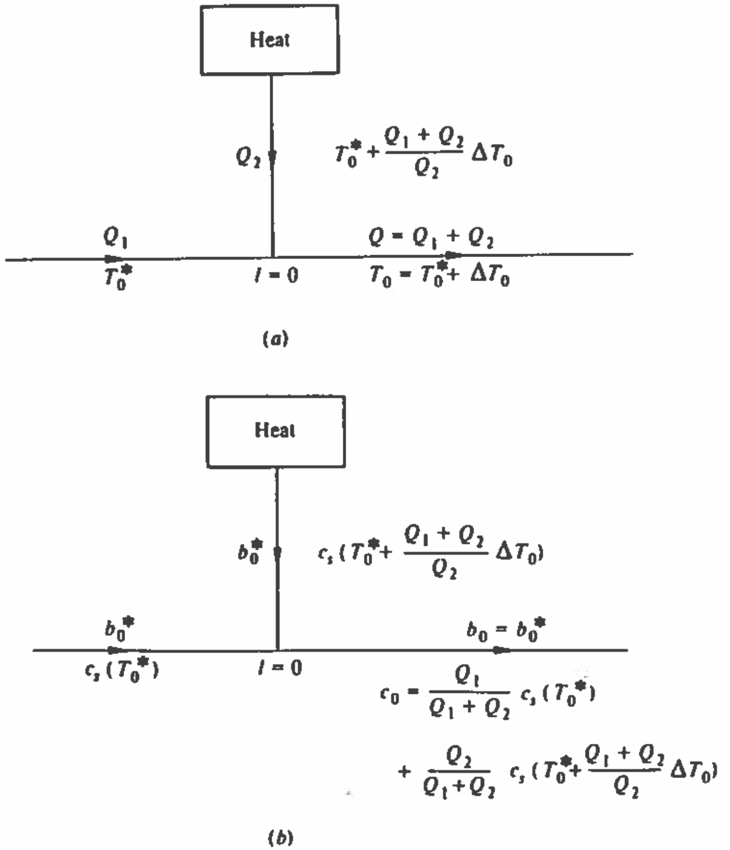

Figure 4-1-9 Balance equations at the discharge point: (*a*) flow rate and temperature (*b*) BOD and DO.

where $\phi' = [\partial\phi/\partial T]_{\bar{T}}$ and the initial conditions are

$$s_T(0) = 1 \qquad s_b(0) = 0 \qquad s_c(0) = c'_s$$

Equations (4-1-17) and (4-1-18) can easily be solved since they are of triangular structure. If $T = T_0^*$ is assumed to be a constant solution of Eq. (4-1-17a) this system of equations can be solved analytically and the solution gives the three sensitivity coefficients

$$s_T = \mathrm{e}^{\phi'\tau}$$

$$s_b = \frac{k'_1}{\phi'}\,\bar{b}_0\,\mathrm{e}^{-k_1\tau}(1 - \mathrm{e}^{\phi'\tau})$$

$$s_c = A\,\mathrm{e}^{-k_1\tau} + B\,\mathrm{e}^{-k_2\tau} + C\,\mathrm{e}^{\phi'\tau} + D\,\mathrm{e}^{(\phi' - k_1)\tau} + E\,\mathrm{e}^{(\phi' - k_2)\tau}$$

where the constants $A, B, \ldots, E$ are given by

$$A = -\frac{k_1 k'_1}{(k_2 - k_1)\phi'}\,\bar{b}_0$$

$$B = -\frac{k_2 c'_s}{k_2 + \phi'} + \frac{k_1 k'_2}{(k_2 - k_1 + \phi')\phi'}\,\bar{b}_0 + \frac{k'_1 k_2}{(k_2 - k_1)(k_2 - k_1 + \phi')}\,\bar{b}_0 + c'_s$$

$$C = \frac{k_2 c'_s}{k_2 + \phi'}$$

$$D = \left[\frac{k_1 k'_2}{k_2 - k_1} - \left(1 - \frac{k_1}{\phi'}\right)k'_1\right]\frac{\bar{b}_0}{k_2 - k_1 + \phi'}$$

$$E = -\frac{k_1 k'_2}{(k_2 - k_1)\phi'}\,\bar{b}_0$$

The corresponding sensitivity curves are shown in Fig. 4-1-10 for realistic values of the parameters; the main conclusion is that the oxygen concentration is lowered everywhere and in particular around the minimum of the DO curve. However, the perturbation introduced by the heat discharge is absorbed along the river, this being the main distinction between this case of temperature perturbation and the preceding one.

4-2 OTHER CHEMICAL MODELS

Since the first work of Streeter and Phelps, the process of natural self-purification has been extensively studied and quite sophisticated mathematical models have been proposed for its description. Most of them are basically the classical Streeter-Phelps model with the source terms suitably modified in order to account for some neglected biochemical phenomena. In all these models the river is assumed to be a chemical reactor in which a reaction between BOD and DO takes place. Since this way of looking at the problem is the fundamental contribution of Streeter and Phelps, these models are often called *modified Streeter-Phelps models*.

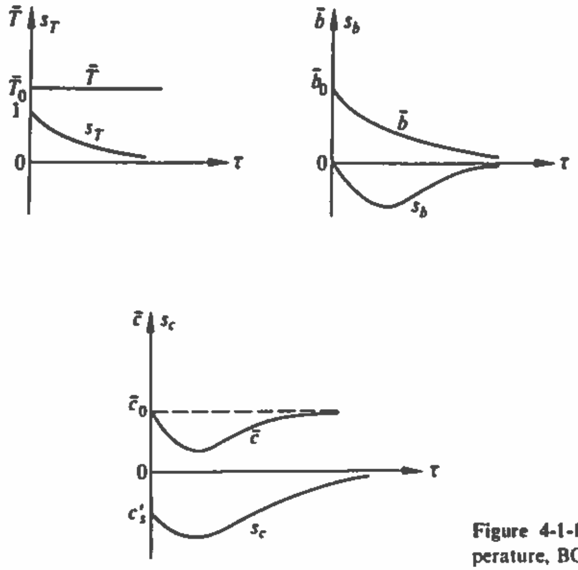

Figure 4-1-10 Sensitivity coefficients of temperature, BOD, and DO to heat discharge.

As stated in the preceding section one of the hypotheses of Streeter and Phelps is that the deoxygenation rate and the BOD decay rate are equal. This is not always true. For example, the decay rate of the stream-borne BOD can be higher than the deoxygenation rate because of sedimentation, or lower because of resuspension. Consequently, Thomas (1948) proposed the following equation for the BOD decay rate

$$\frac{\mathrm{d}b}{\mathrm{d}\tau} = -(k_1 + k_3)b$$

where the new coefficient $k_3 \gtrless 0$ takes into account factors such as sedimentation, flocculation, scour, and resuspension.

Moreover, BOD is entering the river not only from point sources (effluents), but also through distributed sources and local runoff. To account for these distributed sources a term $L(l, t)$ (*distributed BOD load*) has been added by Dobbins (1964) to the righthand side of the BOD equation, which then becomes (recall that A is the cross-sectional area)

$$\frac{\partial b}{\partial t} + v\frac{\partial b}{\partial l} = -(k_1 + k_3)b + \frac{L(l, t)}{A}$$

Again this equation can be written in flow time by defining the BOD load $L(\tau)$ along a characteristic line as (see Fig. 4-1-1 where $\tau = t - t_0$)

$$L(\tau) = L(l(\tau), t(\tau))$$

Thus, the BOD equation becomes

$$\frac{db}{d\tau} = -(k_1 + k_3)b + \frac{L(\tau)}{A} \tag{4-2-1}$$

As far as the DO equation is concerned Camp (1963) and Dobbins (1964) introduced a constant term $(P - R)$ giving

$$\frac{dc}{d\tau} = -k_1 b + k_2(c_s - c) + (P - R) \tag{4-2-2}$$

which represents the difference between P the addition of oxygen due to photosynthetic production (assumed constant in time) and R the DO removal from benthal oxygen demand. The new model can be considered as an ordinary Streeter-Phelps model with a changed oxygen saturation concentration.

O'Connor (1967) proposed the use of two independent terms $P(l, t)$ and $R(l, t)$ to represent oxygen production and oxygen removal, respectively, where $P(l, t)$ is assumed to be a periodic function of time. Moreover, O'Connor (1967) suggested a more relevant modification of the classical Streeter-Phelps model which could explain the existence of different phases appearing in the BOD decay (see Fig. 3-5-3). He assumed that the total BOD is the sum of two components, the carbonaceous BOD (b_c) and the nitrogeneous BOD (b_n), thus writing

$$b = b_c + b_n$$

In accordance with other authors (see, for instance, Gameson, 1959, and Courchaine, 1963) he conjectures that the first two phases of the BOD decay can be explained by assuming that the decomposition reactions for the two different types of BOD proceed with different rates (k_c and k_n respectively) and that a time lag, of increasing length for decreasing degree of treatment, separates these reactions. This time lag could be explained either by an inhibition of carbonaceous BOD over nitrogenous BOD, or by the low growth rate of nitrifiers (see Sec. 2-3). Thus, for the particular case in which the time lag between the two reactions is negligible, as it would be in a stream where all the BOD load comes from biologically treated effluents, O'Connor's model (in flow time) is the following

$$\frac{db_c}{d\tau} = -(k_c + k_3)b_c$$

$$\frac{db_n}{d\tau} = -k_n b_n$$

$$\frac{dc}{d\tau} = -k_c b_c - k_n b_n + k_2(c_s - c) + P(\tau) - R(\tau)$$

where $P(\tau)$ and $R(\tau)$ represent oxygen production and removal along a characteristic line. Obviously the nitrogenous BOD is assumed to be present in dissolved form, since no sedimentation effect is considered in the second equation.

In order to improve the fit to observed data, some authors proposed models with nonlinear source terms. First, on the basis of a suggestion given by Thomas (1953), Young and Clark (1965) proposed a second order reaction equation to model the BOD decay (see Eq. (3-5-12))

$$\frac{db}{d\tau} = -\theta_1 b^2$$

Later on Braun and Berthouex (1970) proposed a Michaelis-Menten expression (see Eq. (3-5-17)) for the BOD decay rate:

$$\frac{db}{d\tau} = -\frac{\theta_1 b}{\theta_2 + b}[B_0 + \theta_3(b_0 - b)]$$

where the bacterial biomass $B(\tau) = [B_0 + \theta_3(b_0 - b(\tau))]$ is assumed to be a linear function of the excerpted BOD. This model has been proved to be of particular interest when the BOD data show an initial lag phase (see Fig. 4-2-1).

Following the chemical engineering tradition, Shastry et al. (1975) suggested modeling the deoxygenation process as a second order reaction where the reaction rate is proportional to the concentration of the two reactants (see Eq. (3-5-11))

$$\frac{db}{d\tau} = -\theta_1 bc \tag{4-2-3a}$$

$$\frac{dc}{d\tau} = -\theta_1 bc + \theta_2(c_s - c) \tag{4-2-3b}$$

Rinaldi and Soncini-Sessa (1974) have shown why this equation can be of particular

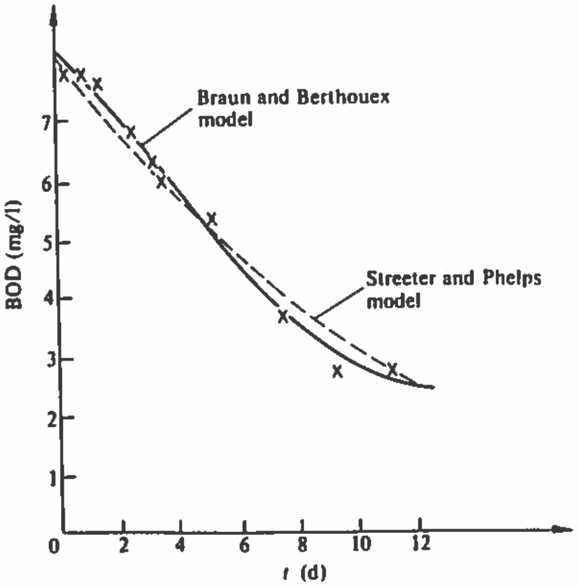

Figure 4-2-1 Comparison of BOD decay profiles of the Braun and Berthouex model and the Streeter-Phelps model on laboratory data.

interest. System (4-2-3) is a nonlinear system of the form

$$\dot{\mathbf{x}} = \mathbf{f}(\mathbf{x}, \mathbf{u})$$

and is still characterized by the unique equilibrium point

$$\bar{\mathbf{x}} = [0 \quad c_s]^T$$

since $\dot{\mathbf{x}} = 0$ implies $b = 0$ and $c = c_s$. Moreover, the linearized system associated with this equilibrium point is given by (see Sec. 1-2)

$$\delta\dot{\mathbf{x}} = \left[\frac{\partial \mathbf{f}}{\partial \mathbf{x}}\right]_{\mathbf{x}=\bar{\mathbf{x}}} \delta\mathbf{x} = \begin{bmatrix} -\theta_1 c_s & 0 \\ -\theta_1 c_s & \theta_2 \end{bmatrix} \delta\mathbf{x}$$

Letting $\theta_1 = k_1/c_s$, $\theta_2 = k_2$ the matrix $[\partial\mathbf{f}/\partial\mathbf{x}]_{\mathbf{x}=\bar{\mathbf{x}}}$ is equal to the **F** matrix of the Streeter-Phelps model. Then, it can be concluded that the two models have the same behavior in the vicinity of the equilibrium point. Nevertheless, model (4-2-3) never generates negative DO concentrations as the Streeter-Phelps model does (see Fig. 4-2-2).

In any one of these modified Streeter-Phelps models, the steady state DO concentration profile is a sag curve. In particular, for a Dobbins' model (see Eqs. (4-2-1)(4-2-2)) with $L(\tau) = \text{const.}$, Liebman and Loucks (1966) have proved that the critical deficit d_c is again a nonlinear function of the initial BOD and DO concentrations, while the limit position ($b_0 \to \infty$ or $c_0 \to c_S$) for the critical point l_c is

$$L_c = \frac{v \ln f}{(k_1 + k_3)(f - 1)}$$

with ($f = k_2/(k_1 + k_3)$) (see Sec. 4-1). However, the limit position L_c is no longer an upper bound of l_c, rather the critical point is located upstream from the point L_c if the distributed BOD load L satisfies the following relationship

$$\frac{L}{A} < \frac{k_1 + k_3}{k_1}(P - R + k_2 d_0)$$

and downstream from the point L_c if the opposite inequality holds.

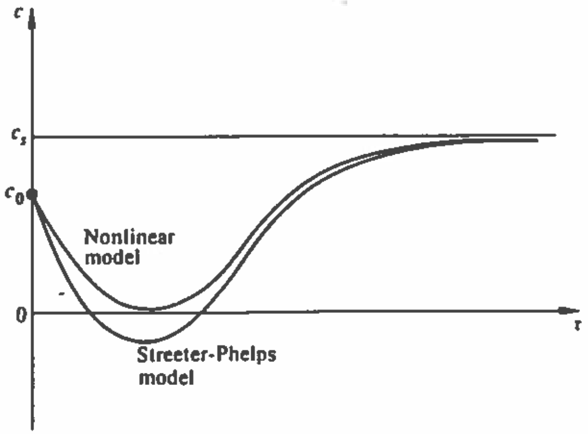

Figure 4-2-2 Comparison of DO sag curves of the Streeter-Phelps model and the nonlinear model (4-2-1).

Numerous particular problems, such as photosynthetic oxygen production, effects of time-varying distributed BOD load, effects of constant BOD load discharged in an oscillating flow, DO deficit due to unsteady point sources of BOD have been extensively discussed in the literature (see, for instance, Di Toro and O'Connor, 1968; O'Connor and Di Toro, 1970; Li, 1972; Li and Kozlowski, 1974; and Rinaldi and Soncini-Sessa, 1974). The first two problems mentioned are discussed in this section in greater detail, not only because they are of a certain interest per se, but also to show how different mathematical techniques can usefully be applied to gain insights into model behavior. In both cases temperature, flow rate, and velocity are assumed to be constant in time and space in order to simplify the discussion.

Photosynthetic Oxygen Production

Downstream from the effluent of a biological treatment plant it is often observed that the growth of benthic algae is stimulated by the nutrients contained in the treated wastewater. The algae may act as both a source and a sink of oxygen, owing to photosynthetic oxygen production and respiration. For the sake of simplicity, the spatial distribution of the algal population is assumed to begin abruptly at $l = 0$ and to remain constant for $l > 0$. Then, the photosynthetic oxygen production P and the oxygen removal R due to algal respiration are constant in space for $l > 0$. Moreover, it can reasonably be assumed that the respiration R is time-invariant, while the photosynthetic oxygen production P varies in the same way as the incident solar radiation (Westlake, 1968). Thus, the oxygen source term $P(t) - R$ can be assumed to be periodic and to have the shape shown in Fig. 4-2-3 (O'Connor and Di Toro, 1970). In other words,

$$P(t) - R = \bar{P} - R + \delta P(t)$$

where $\bar{P}$ is the mean value of $P(t)$ and $\delta P(t)$ is a periodic function with zero mean and period $T = 2\pi/\omega_0 = 1$ day. If sedimentation effects are negligible, the modified Streeter-Phelps model describing the phenomenon is

$$\frac{\partial b}{\partial t} + v\frac{\partial b}{\partial l} = -k_1 b \qquad \text{(4-2-4a)}$$

$$\frac{\partial c}{\partial t} + v\frac{\partial c}{\partial l} = -k_1 b + k_2(c_s - c) + \bar{P} - R + \delta P(t) \qquad \text{(4-2-4b)}$$

In order to solve these equations easily assume time-invariant boundary conditions ($b(0, t) = b_0$ and $c(0, t) = c_0$). Obviously the solution of Eq. (4-2-4a) is the same as

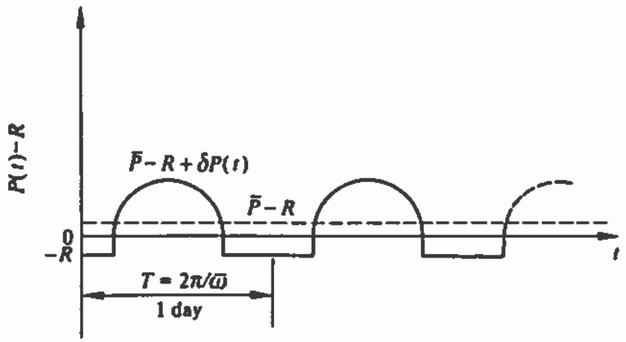

Figure 4-2-3 Idealized daily fluctuations of photosynthetic oxygen production.

that of Eq. (4-1-1a)

$$b(l,t) = b_0\, e^{-k_1 l/v} \tag{4-2-5}$$

As far as the dissolved oxygen is concerned, let us assume that it can be written in the form

$$c(l,t) = \bar{c}(l) + \delta c(t) \tag{4-2-6}$$

with $\delta c(t)$ being a periodic function with zero mean. The validity of this assumption is now verified by actually determining the functions $\bar{c}(l)$ and $\delta c(t)$ in such a way that Eq. (4-2-6) is a solution of Eq. (4-2-4b). By substituting Eq. (4-2-6) into Eq. (4-2-4b)

$$\delta\dot{c}(t) + v\frac{d\bar{c}(l)}{dl} = -k_1 b + k_2(c_s - \bar{c}(l)) - k_2\delta c(t) + \bar{P} - R + \delta P(t) \tag{4-2-7}$$

is obtained. Thus, averaging this equation over the period of one day and remembering that $\delta P(t)$ and $\delta c(t)$ have zero mean yields

$$v\frac{d\bar{c}(l)}{dl} = -k_1 b + k_2(c_s - \bar{c}(l)) + \bar{P} - R \tag{4-2-8}$$

which is of type (4-2-2). This equation can be explicitly integrated, using Eq. (4-2-5) and the boundary condition $\bar{c}(0) = c_0$ (see page 116). The asymptotic value of $\bar{c}(l)$ (note that system (4-2-8) is an asymptotically stable linear system since its eigenvalue is $-k_2$), is

$$c_S + \frac{\bar{P} - R}{k_2}$$

i.e., in points relatively far downstream from the discharge point oversaturated oxygen values are on the average obtained. Substituting Eq. (4-2-8) into Eq. (4-2-7)

$$\delta\dot{c}(t) = -k_2\delta c + \delta P(t) \tag{4-2-9}$$

is obtained, which has a unique periodic solution for each periodic function

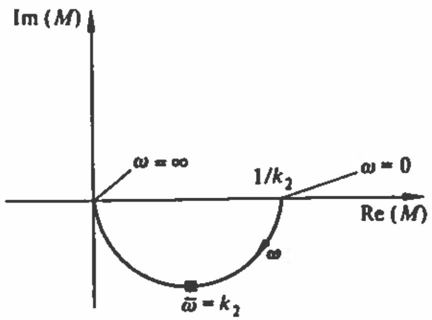

Figure 4-2-4 The DO frequency response to a uniformly distributed oxygen source.

$\delta P(t)$. This periodic solution can easily be obtained by developing the input $\delta P(t)$ in a *Fourier series* (a sum of sine waves) and by determining the corresponding series of δc via frequency response. The transfer function $M(s)$ of system (4-2-9) is given by (see Eq. (1-2-13))

$$M(s) = \frac{1}{s + k_2}$$

and the corresponding frequency response is shown in Fig. 4-2-4 (see Eq. (1-2-18)). Note that $|M(i\omega)|$ is a decreasing function of ω, i.e., the river is acting as a *low pass filter* since high frequency components of $\delta P(t)\,(\omega > k_2)$ are attenuated. Recalling Eq. (4-2-6) it can be concluded that, in the presence of algal population, the classical shape of the dissolved oxygen concentration may still be observed at any instant of time and that the whole sag curve has a diurnal fluctuation around the daily mean concentration $\bar{c}(l)$.

Distributed BOD Load

In this second particular case the effects induced by a time-varying distributed BOD load are analyzed. Again, for the sake of simplicity, it is assumed that downstream of the initial point $l = 0$ the distributed BOD load is constant in space $(L(l,t) = L(t))$ and that at the initial time $t = 0$ the river is perfectly clean and oxygenated $(b(l,0) = d(l,0) = 0)$, while at the initial point $b(0,t) = 0$ for $t > 0$.

The following equations may be used to describe this situation:

$$\frac{\partial b}{\partial t} + v\frac{\partial b}{\partial l} = -k_1 b + \frac{L(t)}{A} \tag{4-2-10a}$$

$$\frac{\partial d}{\partial t} + v\frac{\partial d}{\partial l} = k_1 b - k_2 d \tag{4-2-10b}$$

Even if $L(t)$ is a periodic function, Eq. (4-2-10) can no longer be integrated as in the preceding case, since the form of $c(l,t)$ is now more complex. The notion of *transfer function* can now be of greater help. Applying the Laplace transformation

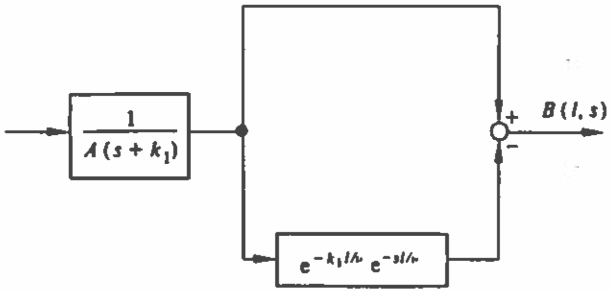

Figure 4-2-5 Block diagram of the transfer function between a uniformly distributed BOD load $L(t)$ and the BOD concentration $b(l, t)$ at a given point l.

to Eq. (4-2-10a) gives (recall that $b(l, 0) = 0$)

$$sB(l,s) + v\frac{dB(l,s)}{dl} = -k_1 B(l,s) + \frac{\hat{L}(s)}{A} \qquad (4\text{-}2\text{-}11)$$

where $B(l, s)$ and $\hat{L}(s)$ are the Laplace transforms of $b(l, t)$ and $L(t)$, respectively. Equation (4-2-11) is an ordinary linear differential equation which gives

$$M_l(s) = \frac{B(l,s)}{\hat{L}(s)} = \frac{1}{A(s+k_1)}\left(1 - e^{-k_1 l/v}\, e^{-sl/v}\right) \qquad (4\text{-}2\text{-}12)$$

where $M_l(s)$ is the transfer function between the distributed BOD load and the BOD concentration at a given point l. The block diagram corresponding to this transfer function is shown in Fig. 4-2-5, while the corresponding frequency response $M_l(i\omega)$ is shown in Fig. 4-2-6, which shows that the river is again acting as a low pass filter.

It is interesting to note that, if the variations of the load are purely sinusoidal, i.e., $L(t) = \bar{L} + \Delta L \sin(\omega_0 t)$, the amplitude and phase of the induced BOD fluctuations are functions of l (see the second block in Fig. 4-2-5). Therefore, this phenomenon is more complex than the photosynthetic oxygen production, where the DO fluctuations were independent of l. Moreover, in this case there are points at which the amplitude of the fluctuation reaches a maximum and points at which it has a minimum. The coordinates of these points can easily be computed by letting the derivative of $|M_l(i\omega)|$ with respect to l be zero

$$k_1 \cos\left(\omega_0 \frac{l}{v}\right) + \omega_0 \sin\left(\omega_0 \frac{l}{v}\right) - k_1\, e^{-k_1 l/v} = 0$$

The function $k_1\, e^{-k_1 l/v}$ tends to zero for increasing values of l, so that, for parts of the river sufficiently downstream, the points characterized by maximum and minimum fluctuations are equally spaced.

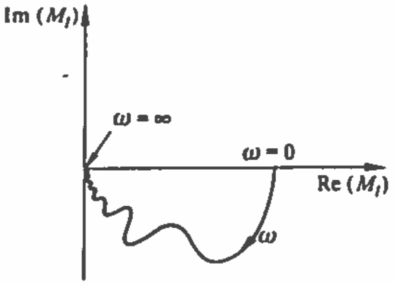

Figure 4-2-6 The BOD frequency response to a uniformly distributed load

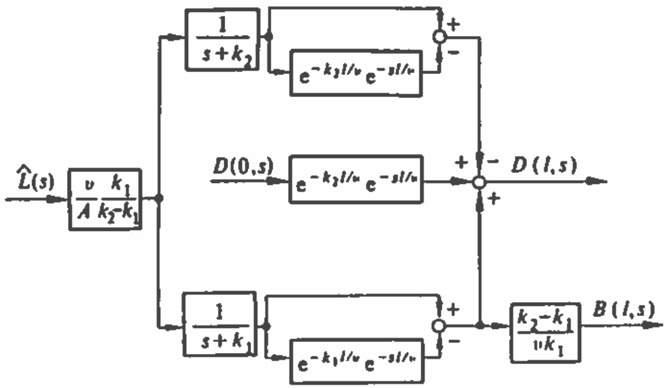

Figure 4-2-7 Block diagram of the transfer function between a uniformly distributed BOD load $L(t)$ and the DO deficit at a given point.

Applying the same procedure to Eq. (4-2-10b) as to Eq. (4-2-10a) the following is obtained

$$D(l,s) = e^{-k_2 l/v} e^{-sl/v} D(0,s) + \frac{vk_1}{A(k_2-k_1)}\left[\frac{1 - e^{-k_1 l/v}\, e^{-sl/v}}{s+k_1} - \frac{1 - e^{-k_2 l/v}\, e^{-sl/v}}{s+k_2}\right]\hat{L}(s)$$

where $D(l, s)$ and $D(0, s)$ are the Laplace transforms of the deficit $d(l, t)$ and of the boundary deficit $d(0, t)$. The block diagram corresponding to the preceding expression is shown in Fig. 4-2-7. Again, it is possible to show that particular points exist at which DO fluctuations reach maximum and minimum values.

Sensitivity Analysis

Finally, it will now be shown how important information on the model behavior can be obtained by employing the simple sensitivity analysis technique presented in the preceding section. Consider, for instance, computing the variations of DO concentration due to an increase in the benthic algal population considered on page 111. This information can easily be obtained by determining the sensitivity of Eq. (4-2-8) with respect to the parameter $(\bar{P} - R)$, since the main consequence of the population increase is a corresponding increase in this parameter.

The sensitivity system associated with Eq. (4-2-8) is

$$v\frac{\mathrm{d}s_c(l)}{\mathrm{d}l} = -k_2 s_c(l) + 1 \qquad (4\text{-}2\text{-}13)$$

If the initial DO concentration c_0 is not affected by the algal bloom ($s_c(0) = 0$) the solution of Eq. (4-2-13) is

$$s_c(l) = \frac{1}{k_2}(1 - \mathrm{e}^{-k_2 l/v})$$

which is represented in Fig. 4-2-8. The conclusion follows that the algal bloom induces a general improvement of the daily mean DO concentration, and that the greatest effects appear far downstream of the BOD source.

As a second example, consider now the case in which the effluent at $l = 0$ contains some non-biodegradable surfactants. These substances do affect the reaeration process so that when they are present the reaeration coefficient k_2 has values which are lower than the normal ones. Thus, the effect of the removal of the surfactants from the wastewater discharge can be analyzed by determining the DO sensitivity with respect to the reaeration coefficient k_2. Using Eq. (4-2-8) once more, the sensitivity system turns out to be

$$v\frac{\mathrm{d}s_c(l)}{\mathrm{d}l} = -k_2 s_c(l) + (c_s - \bar{c}(l)) \qquad (4\text{-}2\text{-}14)$$

where

$$\bar{c}(l) = c_s + \frac{\bar{P} - R}{k_2} - \left(c_s + \frac{\bar{P} - R}{k_2} - \bar{c}_0\right)\mathrm{e}^{-k_2 l/v} + \frac{k_1 b_0}{k_1 - k_2}(\mathrm{e}^{-k_1 l/v} - \mathrm{e}^{-k_2 l/v})$$

is the nominal average DO concentration. Integrating Eq. (4-2-14) with the initial condition $s_c(0) = 0$ (the initial DO level cannot depend upon the surfactant contents of the wastewater discharge), the following equation is obtained

$$s_c(l) = \left[\left(c_S + \frac{\bar{P} - R}{k_2} - c_0\right) + \frac{k_1 b_0}{k_1 - k_2}\right]\frac{l}{v}\mathrm{e}^{-k_2 l/v} + \frac{k_1 b_0}{(k_1 - k_2)^2}(\mathrm{e}^{-k_1 l/v} - \mathrm{e}^{-k_2 l/v}) - \frac{\bar{P} - R}{k_2^2}(1 - \mathrm{e}^{-k_2 l/v})$$

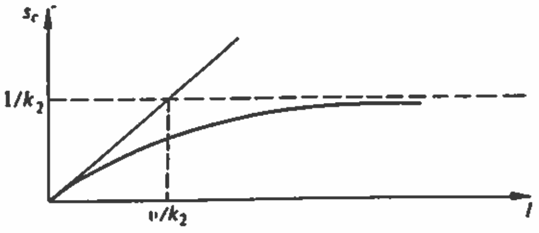

Figure 4-2-8 Sensitivity coefficient of dissolved oxygen with respect to average photosynthetic oxygen production.

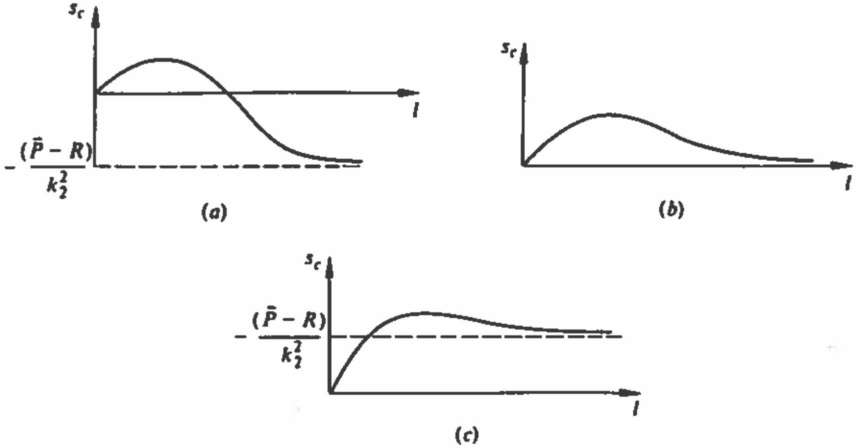

Figure 4-2-9 Sensitivity coefficient of dissolved oxygen with respect to the reaeration coefficient k_2:
(a) when photosynthetic oxygen production is dominant ($\bar{P} > R$)
(b) in absence of sources and sinks of oxygen ($\bar{P} = R$)
(c) when benthal oxygen demand is dominant ($\bar{P} < R$).

Figure 4-2-9 shows three typical profiles of $s_c(l)$ for different values of the oxygen source ($P - R$): positive value (predominance of photosynthetic oxygen production), zero value (absence of sources and sinks), negative value (predominance of benthal oxygen demand). In all cases, the removal of the surfactants generates an improvement in the DO concentration immediately downstream of the discharge. Nevertheless, if photosynthesis predominates, the DO concentration can decrease downstream. This singular phenomenon can be better understood by remembering that, for high values of l, algae create oversaturated DO concentrations. Then, if the oxygen interchange between air and water is improved, lower oversaturation values will be obtained.

4-3 APPROXIMATED STREETER-PHELPS DISPERSION MODELS

The aim of this section is to present BOD-DO models which to some extent take dispersion into account. More precisely, dispersion models are analyzed both in the steady state and in the unsteady state case and, finally, simple lumped parameter models are derived which can be interpreted as approximations of the general dispersion model.

The *Streeter-Phelps model with dispersion* can be written in the form (see Secs. 3-1 and 4-1)

$$\frac{\partial b}{\partial t} + v\frac{\partial b}{\partial l} - D\frac{\partial^2 b}{\partial l^2} = -k_1 b \qquad (4\text{-}3\text{-}1a)$$

$$\frac{\partial d}{\partial t} + v\frac{\partial d}{\partial l} - D\frac{\partial^2 d}{\partial l^2} = k_1 b - k_2 d \qquad (4\text{-}3\text{-}1b)$$

if the cross-sectional area A and the dispersion coefficient D do not depend on l, and if there is no BOD load along the river (recall that d is the DO deficit). The analysis which follows makes reference to this model, but other chemical models like the ones described in Sec. 4-2 could be discussed along the same lines.

Equation (4-3-1) can be simplified by defining the auxiliary variable

$$a = d + \frac{k_1}{k_1 - k_2} b \qquad (4\text{-}3\text{-}2)$$

since from Eq. (4-3-1)

$$\frac{\partial a}{\partial t} + v\frac{\partial a}{\partial l} - D\frac{\partial^2 a}{\partial l^2} = -k_2 a$$

is obtained. Therefore, once Eq. (4-3-1a) has been analytically solved, the solution $a = a(l, t)$ can immediately be obtained by replacing k_1 with k_2, and hence the solution of the DO deficit equation can be deduced from Eq. (4-3-2).

Steady State Analysis

For steady state conditions the following BOD dispersion model is obtained by splitting the second order differential equation (4-3-1a) with $\partial b/\partial t = 0$ into the two first order equations

$$\frac{\partial b}{\partial l} = \beta \qquad (4\text{-}3\text{-}3a)$$

$$\frac{\partial \beta}{\partial l} = \frac{k_1}{D} b + \frac{v}{D}\beta \qquad (4\text{-}3\text{-}3b)$$

while the corresponding *plug flow* model ($D = 0$) is simply

$$\frac{\partial b}{\partial l} = -\frac{k_1}{v} b \qquad (4\text{-}3\text{-}4)$$

Model (4-3-3) is a simple linear model of the form

$$\frac{d\mathbf{x}(l)}{dl} = \mathbf{F}\mathbf{x}(l)$$

with

$$\mathbf{x}(l) = \begin{bmatrix} b(l) \\ \beta(l) \end{bmatrix} \qquad \mathbf{F} = \begin{bmatrix} 0 & 1 \\ \dfrac{k_1}{D} & \dfrac{v}{D} \end{bmatrix}$$

The eigenvalues of the matrix $\mathbf{F}$ are given by

$$\lambda_1 = \frac{v}{2D}\left(1 + \sqrt{1 + 4\frac{k_1 D}{v^2}}\right) \qquad \lambda_2 = \frac{v}{2D}\left(1 - \sqrt{1 + 4\frac{k_1 D}{v^2}}\right)$$

and the corresponding eigenvectors are

$$\mathbf{x}^{(1)} = \begin{bmatrix} 1 \\ \lambda_1 \end{bmatrix} \qquad \mathbf{x}^{(2)} = \begin{bmatrix} 1 \\ \lambda_2 \end{bmatrix}$$

Recalling that any *eigenvector* $\mathbf{x}^{(i)}$ is, by definition, a vector such that $\mathbf{F}\mathbf{x}^{(i)} = \lambda_i \mathbf{x}^{(i)}$, then if the state $\mathbf{x}(l)$ of the system in a point l is given by $\mathbf{x}^{(i)}$, $d\mathbf{x}(l)/dl = \lambda_i \mathbf{x}(l)$, i.e., the tangent to the trajectory describing the evolution of the state vector in the state space is proportional to the vector itself. This implies that in the state space there are two particular straight lines through the origin which correspond to trajectories of the system. The trajectory corresponding to $\mathbf{x}^{(1)}$ is directed away from the origin since $\lambda_1 > 0$, while the trajectory corresponding to $\mathbf{x}^{(2)}$ is directed toward the origin since $\lambda_2 < 0$. Thus, the evolution of BOD (b) and its gradient (β) along the river is that of a *saddle point* in state space as shown in Fig. 4-3-1.

Since there is no BOD load downstream of the initial point ($l = 0$)

$$\lim_{l\to\infty} b(l) = 0$$

must hold, and this can be obtained if and only if the initial state is proportional to the second eigenvector, i.e., if and only if

$$\beta(0) = \lambda_2 b(0)$$

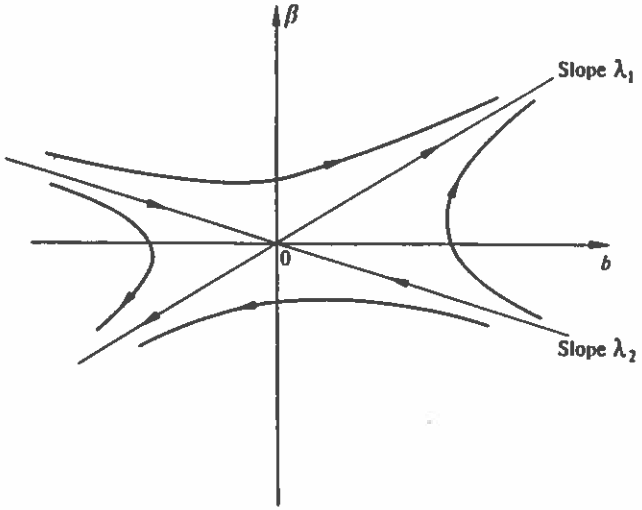

Figure 4-3-1 Trajectories in the state space (b, β).

which implies

$$\beta(l) = \lambda_2 b(l) \qquad (4\text{-}3\text{-}5)$$

for all $l > 0$. Thus, from Eqs. (4-3-3a) and (4-3-5)

$$\frac{\partial b}{\partial l} = \lambda_2 b \qquad (4\text{-}3\text{-}6)$$

is obtained, and by comparing Eq. (4-3-6) with Eq. (4-3-4) the following conclusions can be drawn: the plug flow model (4-3-4) can be used as an equivalent dispersion model under the condition that the stream velocity v is substituted by an *equivalent flow velocity* v_1 such that $\lambda_2 = -k_1/v_1$. This equivalent velocity v_1 turns out to be given by

$$v_1 = v\frac{2k_1 D/v^2}{\sqrt{1 + \dfrac{4k_1 D}{v^2}} - 1} \cong v\left(1 + 2\frac{k_1 D}{v^2}\right)$$

and justifies *Dobbins' criterion* (Dobbins, 1964) which says that if $2(k_1 D/v^2)$ is smaller than $\frac{1}{100}$, the effect of dispersion is negligible. Similarly, for the auxiliary variable a given by Eq. (4-3-2) an equivalent velocity can be defined

$$v_2 = v\frac{2k_2 D/v^2}{\sqrt{1 + \dfrac{4k_2 D}{v^2}} - 1} \cong v\left(1 + 2\frac{k_2 D}{v^2}\right)$$

In conclusion, as far as steady state conditions are concerned the dispersion model (4-3-1) has an equivalent plug flow model given by

$$\begin{aligned} v_1 \frac{\partial b}{\partial l} &= -k_1 b \\ v_2 \frac{\partial d}{\partial l} &= \frac{k_1}{k_1 - k_2}\left(\frac{v_2}{v_1}k_1 - k_2\right)b - k_2 d \end{aligned} \qquad (4\text{-}3\text{-}7)$$

where the velocities v_1 and v_2 depend upon the dispersion coefficient D. The equivalent plug flow model given by Eq. (4-3-7) can be used to analyze steady state situations, since it is much simpler than the dispersion model (4-3-1) with $\partial b/\partial t = \partial d/\partial t = 0$.

Unsteady State Analysis

To obtain approximate dispersion models the dispersion model (4-3-1) is analyzed via transfer function techniques. Let

$$B(l, s) = \mathscr{L}[b(l, t)]$$

be the Laplace transform of $b(l, t)$ with respect to time. Then the Laplace transform of Eq. (4-3-1a) is given by

$$sB - b(l, 0) + v\frac{dB}{dl} - D\frac{d^2B}{dl^2} = -k_1 B \qquad (4\text{-}3\text{-}8)$$

with boundary conditions

$$B(0, s) = B_0(s)\left(= \mathscr{L}[b_0(t)]\right)$$

$$\lim_{l \to \infty} B(l, s) = 0$$

In order to compute the transfer function of the system it is necessary to assume that the initial conditions are zero (see Sec. 1-2), i.e.,

$$b(l, 0) = 0 \qquad \text{for all } l$$

Then, the second order differential equation (4-3-8) can be split into the following two first order differential equations

$$\begin{aligned} \frac{dB}{dl} &= \beta \\ \frac{d\beta}{dl} &= \frac{k_1 + s}{D}B + \frac{v}{D}\beta \end{aligned} \qquad (4\text{-}3\text{-}9)$$

which are formally similar to Eq. (4-3-3). From the preceding results and Eq. (4-3-9) the following is obtained

$$\frac{dB}{dl} = \lambda_2(s)B$$

where

$$\lambda_2(s) = \frac{v}{2D}\left(1 - \sqrt{1 + 4\frac{(k_1 + s)D}{v^2}}\right)$$

Therefore, the Laplace transform of $b(l, t)$ at point l can be written as

$$B(l, s) = B_0(s)\, e^{\lambda_2(s)l}$$

and the transfer function $M_l(s)$ specifying the input–output relationship between $b_0(t)$ and $b(l, t)$ is given by

$$M_l(s) = e^{\lambda_2(s)l} = e^{\frac{vl}{2D}\left(1 - \sqrt{1 + 4\frac{(k_1 + s)D}{v^2}}\right)}$$

Its inverse, which is the impulse response (see Sec. 1-2), is

$$m_l(t) = \frac{1}{2}\frac{lt^{-3/2}}{\sqrt{D\pi}}\, e^{-\frac{1}{4Dt}(l - vt)^2 - k_1 t} \qquad (4\text{-}3\text{-}10)$$

It should be noted, however, that in reality the input function $b_0(t)$ can never be an impulse function. Even if a BOD impulse is discharged at $l = 0$, dispersion will cause $b_0(t)$ to be a function which dies away relatively slowly. But for sufficiently large l expression (4-3-10) is a good approximation to the pollution distribution induced by a BOD impulse discharge.

If a stretch of the river composed of a sequence of n equal reaches of length L/n is considered its transfer function can be written as

$$M_L(s) = [m(s)]^n = [M_{L/n}(s)]^n$$

where

$$m(s) = e^{\frac{vL/n}{2D}\left(1-\sqrt{1+4\frac{(k_1+s)D}{v^2}}\right)}$$

is the transfer function of each reach. Figure 4-3-2 shows the stretch of the river, the n reaches and the corresponding block diagram representation.

The structure of this model is exactly the same as that of the Nash model described in Sec. 3-3. This similarity suggests to approximate the transfer function $m(s)$ of each reach by means of a simple transfer function of the form $\mu/(1 + Ts)$ in order to obtain n *serially connected first order lumped parameter models* for the whole river stretch. The static gain μ and the time constant T can be selected in many different ways, but if the transfer function $m(s)$ is written in the form

$$m(s) = \frac{m(0)}{1 + \dfrac{L/n}{\sqrt{v^2+4k_1D}}s + \dfrac{1}{2}\dfrac{L/n}{\sqrt{v^2+4k_1D}}\left(\dfrac{L/n}{\sqrt{v^2+4k_1D}} - \dfrac{2D}{v^2+4k_1D}\right)s^2 + \cdots}$$

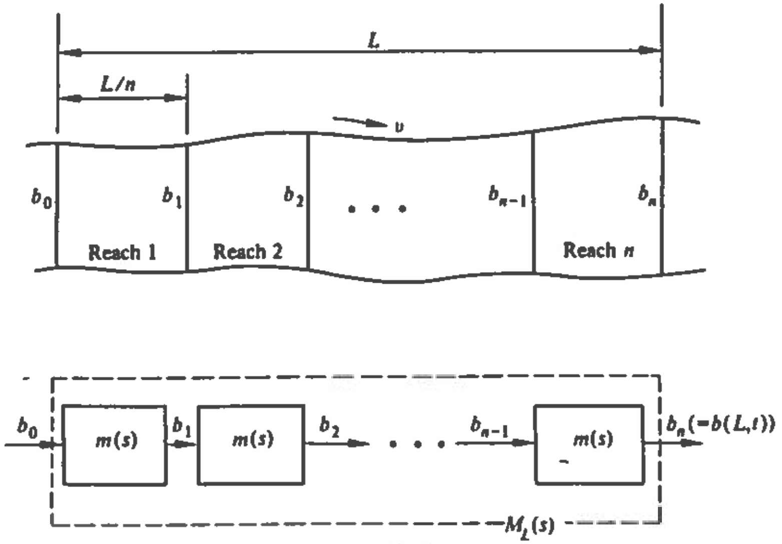

Figure 4-3-2 Subdivision of a stretch of river into n reaches and corresponding block diagram representation.

the most natural approximation, called *low frequency approximation* because it approximates the frequency response of the system (see Sec. 1-2) at low values of the frequency $s = i\omega$, is given by

$$m(s) \cong \frac{m(0)}{1 + \dfrac{L/n}{v\sqrt{1+\dfrac{4k_1D}{v^2}}}s}$$

Assuming that $2k_1D/v^2 \ll 1$, this expression can be further modified to give

$$m(s) \cong \frac{m(0)}{1 + \dfrac{L/n}{v\left(1+2\dfrac{k_1D}{v^2}\right)}s}$$

Similarly, the gain $m(0)$ can be approximated by

$$m(0) \cong \frac{v}{v + k_1L/n}$$

The *approximate dispersion model* can then be written as

$$\begin{aligned}
B_i(s) &= \frac{\mu}{1+Ts}B_{i-1}(s)\\
A_i(s) &= \frac{\mu'}{1+T's}A_{i-1}(s)\\
D_i(s) &= A_i(s) - \frac{k_1}{k_1-k_2}B_i(s)
\end{aligned}\tag{4-3-11}$$

where

$$\mu = \frac{v}{v+k_1L/n} \qquad T = \frac{L/n}{v\left(1+2\dfrac{k_1D}{v^2}\right)}$$

$$\mu' = \frac{v}{v+k_2L/n} \qquad T' = \frac{L/n}{v\left(1+2\dfrac{k_2D}{v^2}\right)}$$

and $B_i(s)$, $A_i(s)$ and $D_i(s)$ are the Laplace transforms of the BOD, of the auxiliary variable $a(t)$, and of the DO deficit, respectively, at the downstream end of the i-th reach. Equation (4-3-11) completely specifies the BOD-DO deficit dynamics of the dispersion model in terms of transfer functions.

It is interesting to note that this approximate dispersion model has the same structure as the so-called *CSTR* (Continuously Stirred Tank Reactor) *model* heuristically proposed by Young and Beck (1974) who joined together two of the most well known simplifying assumptions from hydrology and from chemical engineering. The first consists of imagining the river to be constituted by a sequence of pools (the reaches), and the second corresponds to assuming that each pool is a perfectly mixed reactor. Thus, the mass balance for a single reach (i) of length L/n gives

$$\dot{b}_i(t) = -\left(k_1 + \frac{v}{L/n}\right) b_i(t) + \frac{v}{L/n} b_{i-1}(t)$$

$$\dot{a}_i(t) = -\left(k_2 + \frac{v}{L/n}\right) a_i(t) + \frac{v}{L/n} a_{i-1}(t)$$

$$\dot{d}_i(t) = k_1 b_i(t) - \left(k_2 + \frac{v}{L/n}\right) d_i(t) + \frac{v}{L/n} d_{i-1}(t)$$

The transfer function representation of the *CSTR model* is

$$\begin{aligned} B_i(s) &= \frac{\mu_c}{1 + T_c s} B_{i-1}(s) \\ A_i(s) &= \frac{\mu'_c}{1 + T'_c s} A_{i-1}(s) \\ D_i(s) &= A_i(s) - \frac{k_1}{k_1 - k_2} B_i(s) \end{aligned} \qquad (4\text{-}3\text{-}12)$$

where

$$\mu_c = \frac{v}{v + k_1 L/n} (= \mu) \qquad T_c = \frac{L/n}{v\left(1 + k_1 \dfrac{L/n}{v}\right)}$$

$$\mu'_c = \frac{v}{v + k_2 L/n} (= \mu') \qquad T'_c = \frac{L/n}{v\left(1 + k_2 \dfrac{L/n}{v}\right)}$$

If the number n of reaches could be chosen such that

$$L/n = \frac{2D}{v}$$

then the following would be obtained

$$T_c = T \qquad T'_c = T'$$

i.e., the transfer function of the CSTR model would be the same as that of the approximate dispersion model. However, if $L/n > 2D/v$, as is usually the case, $T_c < T$ and $T'_c < T'$. Thus, it is necessary to add a *time delay* between the adjacent reaches to obtain the same wave propagation velocities (see Sec. 3-3) in both models. The transfer function representation of the *CSTR model with time delay* Δ is simply

$$\begin{aligned} B_i(s) &= \frac{\mu_c}{1 + T_c s} e^{-\Delta s} B_{i-1}(s) \\ A_i(s) &= \frac{\mu'_c}{1 + T'_c s} e^{-\Delta s} A_{i-1}(s) \\ D_i(s) &= A_i(s) - \frac{k_1}{k_1 - k_2} B_i(s) \end{aligned} \qquad (4\text{-}3\text{-}13)$$

and in the time domain the model is described by the following differential equations (see Young and Beck, 1974)

$$\begin{aligned} \dot{b}_i(t) &= -\left(k_1 + \frac{v}{L/n}\right) b_i(t) + \frac{v}{L/n} b_{i-1}(t - \Delta) \\ \dot{d}_i(t) &= k_1 b_i(t) - \left(k_2 + \frac{v}{L/n}\right) d_i(t) + \frac{v}{L/n} d_{i-1}(t - \Delta) \end{aligned} \qquad (4\text{-}3\text{-}14)$$

Choice of the pure time delay Δ as

$$\Delta = T - T_c$$

results in the same wave propagation velocities for the BOD peak in the CSTR model with time delay and in the approximate dispersion model. The CSTR model with time delay can be interpreted as a model describing a river constituted by a sequence of channels and pools, where the biochemical reactions take place only in the pools. Figure 4-3-3 shows the schematic diagram of a single reach of such a river.

If the channels are described by more complex transfer functions taking into account the BOD–DO reactions and the dispersion in the channel, the following

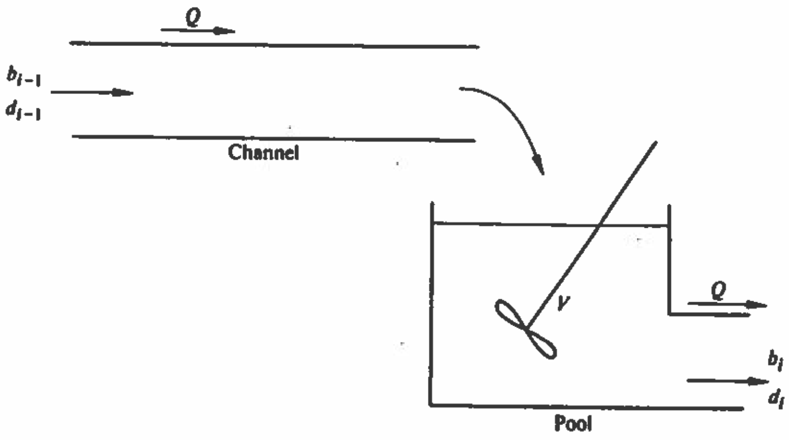

Figure 4-3-3 Schematic diagram of the CSTR model with time delay.

model is obtained

$$B_i(s) = \frac{\mu_c}{1 + T_c s}\Phi(s)B_{i-1}(s)$$

$$A_i(s) = \frac{\mu_c'}{1 + T_c s}\Psi(s)A_{i-1}(s) \qquad (4\text{-}3\text{-}15)$$

$$D_i(s) = A_i(s) - \frac{k_1}{k_1 - k_2}B_i(s)$$

where $\Phi(s)$ is the transfer function of the channel for BOD and $\Psi(s)$ is the one for the auxiliary variable. In the time domain the model (4-3-15) can be written as

$$b_i(t) = -\left(k_1 + \frac{v}{L/n}\right)b_i(t) + \frac{v}{L/n}\int_0^t \phi(\tau)b_{i-1}(t - \tau)\,d\tau$$

$$\dot{d}_i(t) = k_1 b_i(t) - \left(k_2 + \frac{v}{L/n}\right)d_i(t) \qquad (4\text{-}3\text{-}16)$$

$$+ \frac{v}{L/n}\left[\int_0^t \psi(\tau)d_{i-1}(t - \tau)\,d\tau + \int_0^t \phi'(\tau)b_{i-1}(t - \tau)\,d\tau\right]$$

where

$$\phi'(\tau) = \frac{k_1}{k_1 - k_2}(\psi(\tau) - \phi(\tau))$$

and ϕ and ψ are the antitransforms of Φ and Ψ, i.e., the impulse responses of the channel. This is the continuous-time version of the *distributed-lag model* heuristically proposed by Tamura (1974). In this model the river is interpreted as a sequence of channels and pools, and the impulse responses of the channels representing biochemical reactions and distributed-time-delays due to the dispersion in the channel, should appear as shown in Fig. 4-3-4.

The BOD impulse responses of the dispersion model, the approximate dispersion model, the CSTR model, and the CSTR model with time delay are plotted for comparison in Fig. 4-3-5. For the dispersion model (4-3-10) the arrival time of the peak is not exactly an integer multiple of T as shown in Fig. (4-3-5a), but for $l \gg 3D/v$ this is true approximately. For the distributed-lag model it is possible to obtain impulse responses which are as close as desired to those of the dispersion model by suitably selecting $\phi(\tau)$ and $\psi(\tau)$.

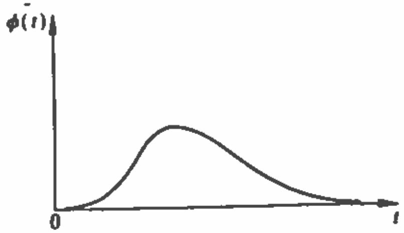

Figure 4-3-4 Impulse response for a channel of the distributed lag model.

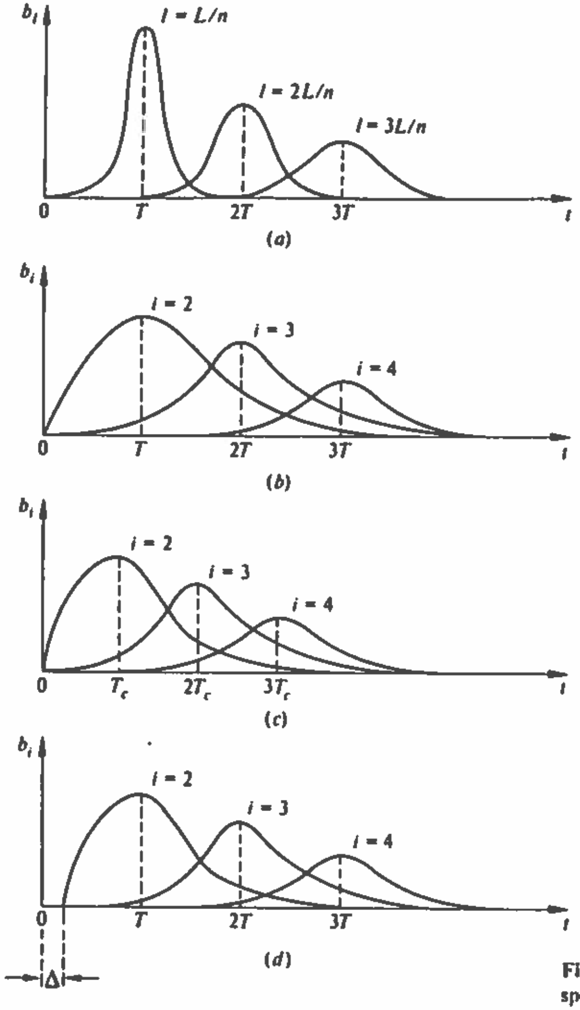

Figure 4-3-5 BOD impulse responses for three river reaches: (*a*) dispersion model (*b*) approximate dispersion model (*c*) CSTR model (*d*) CSTR model with time delay.

Finally, the general block diagram of all the models discussed in this section is shown in Fig. 4-3-6, where $m(s)$ is the BOD transfer function in each reach and $m'(s)$ is the transfer function for the auxiliary variable. The specific forms of $m(s)$ (gain and time constant) are summarized and compared in Table 4-3-1.

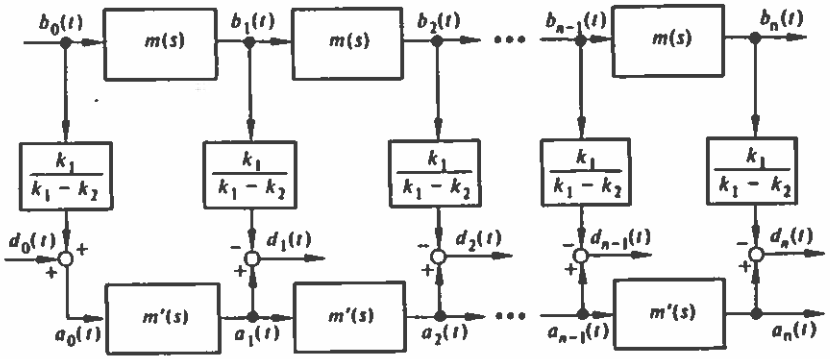

Figure 4-3-6 Block diagram of the n reach river model.

In conclusion, when the value of the dispersion coefficient D of a river is known, Dobbins' criterion can be used to decide whether to take dispersion into account or not. If the answer is positive, the plug flow model with modified velocities can be used as a simple and accurate steady state model, while models (4-3-11, 4-3-12, 4-3-13, 4-3-15) can be used for real time state estimation and control (see Sec. 5-4, 5-5 and 9-3, 9-4). When the value of the dispersion coefficient D is unknown, in general it is necessary to estimate the parameters of one of the models discussed, a procedure considered in Secs. 5-4 and 5-5.

Table 4-3-1 Comparison of approximated Streeter-Phelps models with dispersion (BOD equation)

Model	Transfer function $m(s)$	Gain $m(0)$	Time constant
Dispersion	$e^{\lambda_2(s)L/n}$	$e^{\lambda_2(0)L/n}$	
Approximate dispersion	$\frac{\mu}{1+Ts}$	$\mu = \frac{v}{v+k_1L/n}$	$T = \frac{L/n}{v\left(1+\frac{2k_1D}{v^2}\right)}$
CSTR with time delay	$\frac{\mu_c}{1+T_cs}e^{-s\Delta}$	$\mu_c = \frac{v}{v+k_1L/n}$	$T_c = \frac{L/n}{v\left(1+k_1\frac{L/n}{v}\right)}$
Distributed lag	$\frac{\mu_c}{1+T_cs}\Phi(s)$	$\mu_c\Phi(0)$	$T_c = \frac{L/n}{v\left(1+k_1\frac{L/n}{v}\right)}$

4-4 AN ECOLOGICAL MODEL

As already mentioned in Sec. 3-5 (see Fig. 3-5-4), chemical models, like the Streeter-Phelps model, may be unsatisfactory due to their gross simplifications. These models are problematic, in particular, for investigations anticipating future changes of the wastewater load since the change in parameters cannot be predicted on a theoretical basis. On the other hand, detailed ecological models can avoid this problem, but the parameters involved are hard to estimate, because the necessary measurement effort is tremendous.

In the following, an ecological model is described which is simple enough to be identified with reasonable measurement effort and which is believed to be more realistic than the Streeter-Phelps model for a certain class of rivers (Stehfest, 1973). Beside the assumptions of vertical and lateral homogeneity (see Sec. 3-1), which are made throughout the main part of the book, the following assumptions have to be made for this model

1. river depth and velocity are high
2. longitudinal dispersion can be neglected
3. the river is heavily polluted

The first assumption implies that benthic variables can be neglected, for two reasons. First, sediments and benthic organisms can hardly develop because of the high stream velocity. Second, even if they do, their importance relative to the stream-borne organisms and pollutants will be small, because the water column above the river bottom is high. The latter argument is particularly applicable because the biochemical activity within bottom deposits is relatively small due to the slow material exchange. The insignificance of the benthic variables means that the model consists of equations of type (3-1-16) only (with nonvanishing v and D). If, in addition, the diffusion terms can be neglected (assumption 2) the model can be transformed into a system of ordinary differential equations (see Sec. 3-1). Assumption 2 is only made in order to simplify the following discussion, which is focused on the biochemical aspects. Little change would be required if longitudinal dispersion were to be taken into account in one of the ways described in Sec. 4-3. Assumption 3, in connection with assumption 1, further simplifies the model. The higher organisms of the food web can be neglected because they are fairly exacting, and because their reproduction time is usually comparable to the flow time (see Sec. 2-3). Nitrification and photosynthesis may be neglected for the same reasons. The development of photosynthesizing organisms is in addition hindered by the low mean light intensity, which is due to the great depth and the high turbidity. A river for which the preceding assumptions seem to be approximately fulfilled is the Rhine river in Germany; and in fact, this is the river for which the model was first developed (see Sec. 5-3).

On the basis of the simplifying assumptions the following state variables were selected:

w_1 = easily degradable pollutants

w_2 = slowly degradable pollutants

B = bacteria

P = protozoa

c = oxygen

All variables are defined as mass densities, the pollutants are measured by their chemical oxygen demand (see Sec. 3-5), and hence $w_1 + w_2$ is the biochemical oxygen demand of the pollutants. (The BOD of a water sample, however, also comprises the biochemical oxygen demand of the living matter.) The aggregation of all bacterial and protozoan species into two variables has already been discussed in Sec. 3-5. It is, in any case, more justified than dealing with all pollutants as one variable, because the differences between the pollutants with regard to degradability are certainly larger than the differences among the bacteria or protozoa with regard to growth rate or endogenous respiration.

The model equations chosen are:

$$\dot{w}_1 = -k_{11}g_1B + L_1 \tag{4-4-1a}$$

$$\dot{w}_2 = -k_{21}g_2B + L_2 \tag{4-4-1b}$$

$$\dot{B} = (g_1 + g_2 - k_{36})B - k_{37}g_3P \tag{4-4-1c}$$

$$P = (g_3 - k_{43})P \tag{4-4-1d}$$

$$\dot{c} = k_{51}(c_s - c) - (k_{52}g_1 + k_{53}g_2 + k_{54})B - (k_{55}g_3 + k_{56})P \tag{4-4-1e}$$

with

$$g_1 = \frac{k_{31}w_1}{k_{32} + w_1} \qquad g_2 = \frac{k_{33}w_2}{k_{34} + w_2 + k_{35}w_1} \qquad g_3 = \frac{k_{41}B}{k_{42} + B}$$

All k_{ji}'s are positive parameters, while L_1 and L_2 are pollutant inputs. Obviously, the model is given with flow time as an independent variable (see Sec. 3-1). If it is assumed that there are no flows of material other than those shown in Fig. 4-4-1 (i.e., flows resulting from sedimentation or from interactions of protozoa and bacteria with higher levels in the food web are neglected) then, the three following relationships can be established between the parameters (see the analogous Eq. (3-5-20))

$$\frac{k_{54}}{k_{36}} = k_{11} - k_{52}$$

$$\frac{k_{54}}{k_{36}} = k_{21} - k_{53}$$

$$\frac{k_{56}}{k_{43}} = \frac{k_{54}}{k_{36}}k_{37} - k_{55}$$

However, if the parameters are considered to be independent these relationships may be used as a test for the estimation results (see Chapter 5). All relationships contained in Eq. (4-4-1) have already been discussed in Sec. 3-5. For the easily degradable pollutants the *Michaelis-Menten degradation kinetics* is assumed (Eq. (4-4-1a)), while for the degradation of the slowly degradable pollutants a *competitive inhibition* through the easily degradable pollutants is postulated. The latter assertion is justified by the fact that many enzymes which catalyze the degradation of slowly degradable matter are only formed after the more easily degradable substances have been used up (see Sec. 2-3). Of course, it is not mandatory to use the expression for competitive rather than allosteric inhibition. But it may be argued that for high concentrations of slowly degradable matter bacteria specialized on this matter become abundant, so that the inhibition can be overcome to a certain extent; this effect cannot be described by Eq. (3-5-22) for allosteric inhibition. The terms on the righthand side of Eq. (4-4-1c) stand for increase of bacterial mass by degradation activity, and loss of bacterial mass by endogenous respiration and protozoan predation. Equation (4-4-1d) describes the variation of the protozoan mass as the difference between growth due to digestion of bacteria and endogenous respiration. The latter term with an appropriate parameter value k_{43} may, in addition, approximately account for losses of protozoan mass through predation of higher organisms. Finally, the impacts of the processes just mentioned on the oxygen budget are listed in Eq. (4-4-1e) together with the term for physical reaeration. The structure of the model is shown in Fig. 4-4-1. The compartments correspond to the variables, and the arrows to the flows of material. The slanted lines indicate the surroundings of the river.

Model (4-4-1) contains quite a number of parameters which cannot be determined separately, either through experimentation or through theoretical considerations. The reaeration coefficient k_{51}, for example, cannot be determined

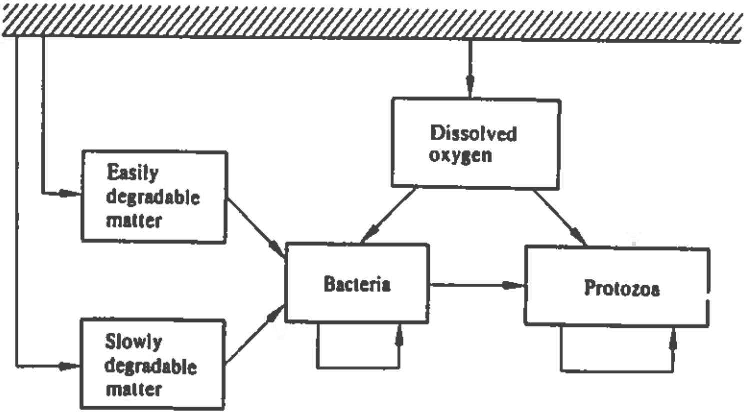

Figure 4-4-1 Structure of the ecological river quality model (4-4-1).

theoretically at sufficient accuracy, as discussed in Sec. 3-5. And it cannot be measured separately, (except for particular cases, see Churchill et al., 1962), because the reaeration process is always superimposed upon the biochemical oxygen consumption processes. Hence, the parameters have to be determined, in general, simultaneously from in situ measurements of the model variables. Various methods of solving this problem are discussed in Chapter 5. Even now, however, it should be intuitively clear that to determine the many parameters of Eq. (4-4-1) it is essential to have accurate measurements of as many variables as possible along the river. The least problematic variable in this respect is oxygen concentration, since it can easily be measured with high accuracy. For the measurement of protozoan mass, however, the only well established method is to determine microscopically number and size of the protozoa, which is rather expensive and not too accurate. For the bacterial mass a similar method could be used, while the traditional plate count (counting the number of colonies developing on a standardized culture medium) is too inaccurate. Another technique, which is not yet widely used, however, consists of measuring the total living biomass through a typical constituent of living matter, for instance, ATP (Jannasch, 1972), and then correcting for the protozoan mass. (Of course, it is also possible to use the observations of $P + B$ directly by defining in an appropriate way the output transformation matrix, see Sec. 1-2. The same applies to the corrections discussed below.) In measurements of the organic pollutants it is, in practice, impossible to differentiate between easily and slowly degradable pollutants. The total organic pollution, however, can be easily measured. One way is to measure the BOD of the water samples and to correct for the BOD of the living matter, so that measurements of $w_1 + w_2$ would be available for the parameter estimation. Another way is to measure the total COD and then correct for both living and undegradable matter (see Sec. 3-5). Quite often the major components of the undegradable organic pollution can be measured separately, e.g., chlorinated carbohydrates. The rest (or even all undegradable organic matter, see Sec. 5-3) may be considered as part of w_2. To summarize, observations of $(w_1 + w_2)$, B, P, and c can be made available at reasonable expense for parameter (and state) estimation of model (4-4-1). Whether this is sufficient or not for the determination of the parameters will be discussed in Sec. 5-3.

Far less can be proved analytically for model (4-4-1) than for the Streeter-Phelps model. But what can be proved is in accordance with what may be expected for an ecological river quality model. Thus, it can easily be shown that the values of w_1, w_2, B, and P can never become negative if the initial values are non-negative. The oxygen concentration may drop below zero (as with the Streeter-Phelps model), but this unrealistic result occurs only in extreme situations.

The *equilibria* of the model can also be easily calculated. In the case of no input ($L_1 = L_2 = 0$) there exists an infinity of non-isolated equilibrium points in the subspace given by $B = 0$, $P = 0$, $c = c_s$. These equilibria are stable, but not asymptotically, in the sense that after a small perturbation of the state, the system returns once more to an equilibrium, not necessarily the same one, though close to it. In other words, B, P, and $(c_s - c)$ tend to zero as τ goes to infinity, while certain amounts of w_1 and w_2 may be left over, depending on the initial values (and on the parameter values, of course). For constant, but non-zero input and realistic parameter values there are two isolated equilibrium points, one with all variables greater than zero, and one in the subspace given by $P = 0$. The assumption of realistic parameter values means, for example, that the maximum protozoan growth rate k_{41} is greater than the protozoan endogenous respiration rate k_{43}, which is certainly reasonable. The dependence of the equilibrium state upon the parameters can easily be determined, but it is not worth giving the formulae here, since they are rather lengthy. The procedure involves putting all derivatives equal to zero in Eq. (4-4-1) and then solving Eqs. (4-4-1d), (4-4-1a), (4-4-1b), (4-4-1c), and (4-4-1e) successively. For this the assumption $P \neq 0$ has to be made, so that the first one of the two isolated equilibrium points results. The other one may be calculated equally simply. It becomes clear during this procedure what the above mentioned realistic assumptions about the parameter values have to be, in order to obtain positive equilibrium values. The equilibrium point with $P \neq 0$ is an asymptotically stable one, as can be seen by inspection of the matrix of the system derived from Eq. (4-4-1) by linearization around the equilibrium. The eigenvalues of the matrix have strictly negative real parts (see Sec. 1-2). The imaginary parts are, in general, different from zero, so that the motions in the vicinity of the equilibrium are damped oscillations, as is typical for prey-predator relationships. Although it has not been proved, it is conjectured that all motions starting with w_1, w_2, B, and P greater than zero tend towards this equilibrium point. Figure 4-4-2 shows how the equilibrium point is approached from arbitrarily chosen initial conditions using realistic parameter values. If L_1 and L_2 are extremely high only B, P, and c reach stationary values, while w_1 and w_2 increase linearly for high τ values.

The *sensitivity* of system (4-4-1) to changes of initial and parameter values has been investigated extensively through numerical experimentation (see Sec. 4-1), but only a few general results have emerged from this study. No dramatically high sensitivities have been observed. Sensitivities show, in general, oscillations, as do the motions toward the equilibrium (see Fig. 4-4-2). It is surprising how far downstream disturbances of the initial values of w_1 and w_2 can be felt (for L_1 and L_2 different from zero the motions are asymptotically stable, which means that the difference between the perturbed and the unperturbed motion goes to zero as we go downstream). Probably the most interesting result is the sensitivity with respect to temperature: if the maximum specific growth rates and endogenous respiration rates are all changed simultaneously in correspondence with a certain temperature variation (see Sec. 3-5) changes of the state variables are remarkably smaller than in the case when only one of these parameters has been changed. Numerical examples of how the model solution for non-constant input varies if flow rate and temperature are changed will be given in Sec. 5-3, where model (4-4-1) is applied to a real case.

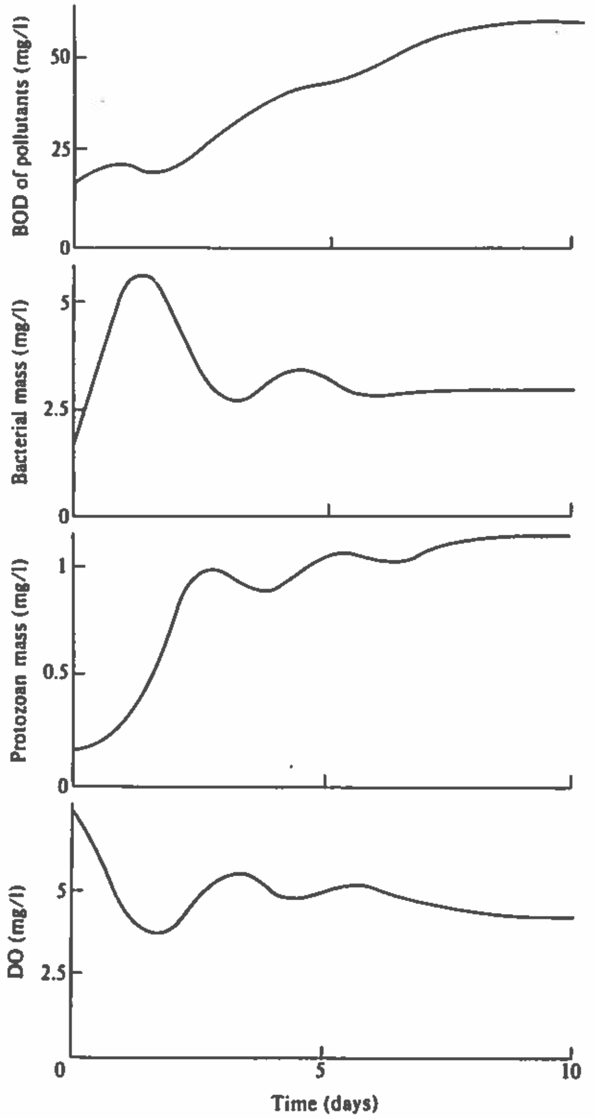

Figure 4-4-2 Typical solution of model (4-4-1) for constant, non-zero input.

4-5 OTHER ECOLOGICAL MODELS

As a representation of reality the ecological model described in the previous section must be considered to be very crude, and of restricted applicability. Many other ecological models can be found in the literature, most of which are much more complicated than the one described in Sec. 4-4. A few of them will be discussed in this section. A complete survey of all ecological river quality models would be beyond the scope of this book, because the material which would have to be presented would be too voluminous. (Since there is no clear distinction between river impoundments and lakes, the very broad field of eutrophication modeling would also have to be discussed.) None of the numerous models which contain ecological quantities, like algal or fish density, but not as dynamical state variables (see Sec. 1-2) are mentioned. In those models the ecological quantities usually do not depend on the pollutant input into the river, but appear as externally given functions in the oxygen balance equation (see, for example, O'Connor, 1967; Wolf, 1971; Willis et al., 1975). In effect, some of the modified Streeter-Phelps models presented in Sec. 4-2 are of this type (see, for instance, Eq. (4-2-2)).

An ecological model, which is even simpler than the one described in the preceding section, is the one by Gates et al., (1969), whose work was already mentioned in Sec. 3-5. Its state variables are the concentrations of organic pollutants, bacterial mass, and oxygen. The model can be derived from model (4-4-1) by removing all expressions related to slowly degradable pollutants, endogenous respiration, and protozoa. Because of its simplicity a formal (graphical) technique for estimating the parameters from measurements could be applied, but the uncertainty of the parameters seems to be high, due to the lack of measurements of the bacterial mass (see Stehfest, 1973, and Chapter 5). The model was used to describe both laboratory and field experiments with glucose as pollutant. This type of model has also been used to describe the nitrification process (Stratton and McCarty, 1967; O'Connor et al., 1976). Since nitrification is a two-stage process (see Sec. 2-3), in which the ammonium substrate is used in sequence by two different types of bacteria, it is necessary to couple two of these models appropriately.

An ecological model considerably more complex than the one in Sec. 4-4 was developed for the Delaware Estuary (USA) by Kelley (1975, 1976). The ecological relationships encompassed by this model are shown in Fig. 4-5-1, in analogy to Fig. 4-4-1 (cf. also Fig. 2-3-9). The mathematical description of the relationships is not worth giving here, especially since the single expressions used have essentially been discussed in Sec. 3-5 already. As one can see from Fig. 4-5-1, eutrophication is a major problem in the Delaware Estuary, while nitrification is considered to be less important. Another remarkable feature of the model is the intention to relate fish abundance to pollutants input. Since fish abundance is an important quality indicator, which also characterizes the recreational benefit of the river, it is very valuable to have it as a state variable of a river quality model. Another interesting aspect is the modeling of the mass transport phenomena in the estuary, which has to cope with tidal movements. Two versions of the model have been investigated: in the first, the river was viewed as a sequence of completely mixed tanks, similar to the CSTR model mentioned in Sec. 4-3. The river flow from reach to reach was averaged over the tidal cycles. As shown in Sec. 4-3, this model reproduces to a certain extent the dispersion phenomena. In the second

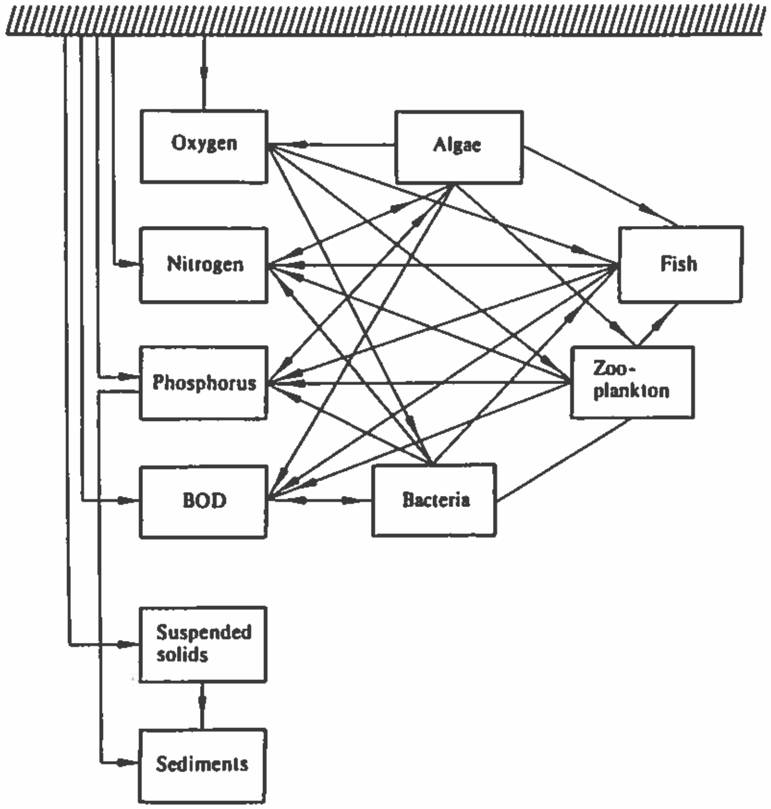

Figure 4-5-1 Structure of the Delaware estuary model.

version, diffusive exchange between the reaches was introduced additionally, mainly to account for tidal mixing. The second version proved to fit measured data better than the first one, but the differences are not dramatic. The model contains a huge number of parameters, so that in view of the scarce measurements for the dependent variables, application of a formal estimation technique would have been hopeless (see Sec. 5-1). Rather, the estimation has been done by playing around with the parameter values within reasonable limits until the model output fitted the measured values. In this way, satisfactory agreement with measurements of oxygen, BOD, phosphate, and nitrogen from one month could be obtained. No measurements were available for the other variables. The application of the model specified in this way to another month, where flow rate and temperature were considerably different from the month used for the parameter estimation, gave very poor agreement with the observations.

Another ecological model, which is of comparable complexity to the model just described, has been reported by Boes (1975). The parameters have been estimated in a similar manner, too. The model was used to predict BOD and oxygen concentrations in the Neckar river in West Germany, while dynamics of the other model variables were not discussed. The BOD and DO predictions have been compared with the corresponding predictions of two other, simpler models (Wolf, 1971; Abendt, 1975) and the differences have turned out to be fairly large.

REFERENCES

Section 4-1

Arbabi, M., Elzinga, J., and ReVelle, C. (1974). The Oxygen Sag Equation and a Linear Equation for the Critical Deficit. *Water Resour. Res.*, **10**, 921–929.

Di Toro, D. M. and O'Connor, D. J. (1968). The Distribution of Dissolved Oxygen in a Stream with Time Varying Velocity. *Water Resour. Res.*, **4**, 639–646.

Fair, G. M. and Geyer, J. C. (1965). *Water Supply and Waste-Water Disposal*. John Wiley, New York.

Liebman, J. C. (1965). The Optimal Allocation of Stream Dissolved Oxygen Resources. Ph.D. dissertation, Cornell Univ., Ithaca, N.Y.

Liebman, J. C. and Loucks, D. P. (1966). A Note on Oxygen Sag Equations. *J. WPCF*, **38**, 1963–1967.

Lin, S. H., Fan, L. T., and Hwang, C. L. (1973). Digital Simulation of the Effect of Thermal Discharge on Stream Water Quality. *Water Resour. Bull.*, **9**, 689–702.

Rinaldi, S. and Soncini-Sessa, R. (1976). Sensitivity Analysis of Streeter-Phelps Type Water Pollution Models (in Italian). *Ingegneria Ambientale*, **5**, 320–335.

Rinaldi, S. and Soncini-Sessa, R. (1978). Sensitivity Analysis of Generalized Streeter-Phelps Models. *Advances in Water Resources*, **1**, 141–146.

Stehfest, H. (1975). Decision Theoretical Remark on Sensitivity Analysis. Report IIASA RR-75-3, International Institute for Applied Systems Analysis, Laxenburg, Austria.

Streeter, H. W. and Phelps, E. B. (1925). A Study of the Pollution and Natural Purification of the Ohio River, vol. III, *Public Health Bulletin*, no. 146, United States Public Health Service, Reprinted by U.S. Department of Health, Education and Welfare, 1958.

Section 4-2

Braun, H. B. and Berthouex, P. M. (1970). Analysis of Lag Phase BOD Curves Using the Monod Equations. *Water Resour. Res.*, **6**, 838–844.

Camp, T. R. (1963). *Water and its Impurities*. Reinhold, New York.

Courchaine, R. J. (1963). The Significance of Nitrification in Stream Analysis—Effects on the Oxygen Balance. *Proc. of XVIII Industrial Waste Conference*, Purdue University, Lafayette, Indiana.

Di Toro, D. M. and O'Connor, D. J. (1968). The Distribution of Dissolved Oxygen in a Stream with Time Varying Velocity. *Water Resour. Res.*, 4, 639 646.

Dobbins, W. E. (1964). BOD and Oxygen Relationships in Streams. *J. San. Eng. Div., Proc. ASCE*, **90**, 53–78.

Gameson, A. L. H. (1959). Some Aspects of the Carbon, Nitrogen and Sulphur Cycles in the Thames Estuary, Part II. In *Effects of Pollution on Living Material*. Institute of Biology, London.

Li, W. H. (1972). *Differential Equations of Hydraulic Transients and Groundwater Flow*. Prentice-Hall, Englewood Cliffs, N. J.

Li, W. H. and Kozlowski, M. E. (1974). DO-sag in Oscillating Flow. *J. Env. Eng. Div., Proc. ASCE*, **100**, 837 854.

Liebman, J. C. and Loucks, D. P. (1966). A Note on Oxygen Sag Equations. *J. WPCF*, **38**, 1963–1967.

O'Connor, D. J. (1967). The Temporal and Spatial Distribution of Dissolved Oxygen in Streams. *Water Resour. Res.*, 3, 65–79.

O'Connor, D. J. and Di Toro, D. M. (1970). Photosynthesis and Oxygen Balance in Streams. *J. San. Eng. Div., Proc. ASCE*, 96, 547–571.

Rinaldi, S. and Soncini-Sessa, R. (1974). Modelling River Pollution (in Italian). In *Ingegneria Sistemistica Ambientale*. C.L.U.P., Milan.

Shastry, J. S., Fan, L. T., and Erickson, L. E. (1975). Non Linear Parameter Estimation in Water Quality Modeling. *J. Env. Eng. Div., Proc. ASCE*, 99, 315–331.

Thomas, H. A. (1948). Pollution Load Capacity of Streams. *Water and Sewage Works*, 95, 405.

Thomas, H. A. (1953). Personal communication, cited in Woodward, (1953). Deoxygenation of Sewage: A Discussion. *Sewage and Industrial Wastes*, 25, 518.

Westlake, D. F. (1968). A Model for Quantitative Studies of Photosynthesis by Higher Plants in Streams. *Air and Water Pollution Journal*, 10, 883–896.

Young, J. C. and Clark, J. W. (1965). Second Order Equation for BOD. *J. San. Eng. Div., Proc. ASCE*, 91, 43–58.

Section 4-3

Dobbins, W. E. (1964). BOD and Oxygen Relationships in Streams. *J. San. Eng. Div., Proc. ASCE*, 90, 53–78.

Tamura, H. (1974). A Discrete Dynamic Model with Distributed Transport Delays and its Hierarchical Optimization for Preserving Stream Quality. *IEEE Trans.*, SMC 4, 424–431.

Young, P. and Beck, B. (1974). The Modelling and Control of Water Quality in a River System. *Automatica*, 10, 455–468.

Section 4-4

Churchill, M. A., Elmore, H. L., and Buckingham, R. A. (1962). The Prediction of Stream Reaeration Rates. *Int. J. Air Wat. Pollution*, 6, 467–504.

Jannasch, H. W. (1972). New Approaches to Assessment of Microbial Activity in Polluted Waters. In *Water Pollution Microbiology* (R. Mitchell, ed.). John Wiley, New York.

Stehfest, H. (1973). Mathematical Modelling of Self-Purification of Rivers (in German; English translation available as report IIASA PP-77-11, International Institute for Applied Systems Analysis, Laxenburg, Austria). Report KFK 1654 UF, Kernforschungszentrum Karlsruhe, Karlsruhe, W. Germany.

Section 4-5

Abendt, R. W. (1975). Models in Water Quality Planning. *Ecological Modelling*, 1, 205–217.

Boes, M. (1975). Biocenotic Model for Simulating the Oxygen Balance of Rivers (in German). *GWF-Wasser/Abwasser*, 116, 339–407.

Gates, W. E., Marlar, J. T., and Westfield, J. D. (1969). The Application of Bacterial Process Kinetics in Stream Simulation and Stream Analysis. *Water Research*, 3, 663–686.

Kelley, R. A. (1975). The Deleware Estuary. In *Ecological Modelling in a Resource Management Framework* (C. S. Russell, ed.). Resources for the Future, Washington, D.C.

Kelley, R. A. (1976). Conceptual Ecological Model of the Delaware Estuary. In *Systems Analysis and Simulation in Ecology*, vol. IV (B. C. Patten, ed.). Academic Press, New York.

O'Connor, D. J. (1967). The Temporal and Spatial Distribution of Dissolved Oxygen in Streams. *Water Resour. Res.*, 3, 65–79.

O'Connor, D. J., Thomann, R. V., and Di Toro, D. M. (1976). Ecological Models. In *Systems Approach to Water Management* (A. K. Biswas, ed.). McGraw-Hill, New York.

Stehfest, H. (1973). Mathematical Modelling of Self-Purification of Rivers (in German; English translation available as report IIASA PP-77-11, International Institute for Applied Systems Analysis, Laxenburg, Austria). Report KFK 1654 UF, Kernforschungszentrum Karlsruhe, Karlsruhe, W. Germany.

Stratton, F. E. and McCarty, P. L. (1967). Prediction of Nitrification Effects on the Dissolved Oxygen Balance of Streams. *Environ. Sci. Technol.*, 1, 405–410.

Willis, R., Anderson, D. R., and Dracup, J. A. (1975). Steady-State Water Quality Modelling in Streams. *J. Env. Eng. Div., Proc. ASCE*, 101, 245–258.

Wolf, D. (1971). Incorporation of Latest Findings into Oxygen Budget Calculations for Rivers (in German). *GWF-Wasser/Abwasser*, 112, 200–203 and 250–254.

CHAPTER

FIVE

STATE AND PARAMETER ESTIMATION

5-1 GENERAL REMARKS

Problem Definition

The various models discussed previously are characterized by numerous parameters which cannot usually be determined theoretically or measured directly. Rather, they have to be determined on the basis of observations of the system output.

Confining ourselves, for the sake of simplicity, to the discrete time case, this means (see Eq. (1-2-20)) that the parameter vector $\theta = [\theta_1 \ \theta_2 \cdots \theta_q]^T$ in

$$x(t+1) = f(x(t), u(t), \theta, t) \tag{5-1-1a}$$

$$y(t) = \eta(x(t), \theta, t) \tag{5-1-1b}$$

has to be determined on the basis of observations of the vector y. This problem is called *parameter estimation*. Its solution obviously requires the knowledge of the system state x (or something equivalent). Therefore, if the state is neither measurable directly nor known for other reasons, the problem of *state estimation*, which is an important problem not only in the context of parameter estimation but also in its own right (see, for example, Sec. 5-4), has to be considered.

As already mentioned in Sec. 1-3, there exists a close relationship between state and parameter estimation. Parameters θ_i $(i = 1, \ldots, q)$ can always be considered as additional state variables for which equations of the type

$$\theta_i(t+1) = \theta_i(t)$$

hold. Hence, the problem of state and parameter estimation for a system (5-1-1) is equivalent to estimating the state of the system

$$z(t+1) = f'(z(t), u(t), t) \tag{5-1-2a}$$

$$y(t) = \eta'(z(t), t) \tag{5-1-2b}$$

with

$$z = \begin{bmatrix} x \\ \theta \end{bmatrix} \qquad f'(z, u, t) = \begin{bmatrix} f(x, u, \theta, t) \\ \theta \end{bmatrix}$$

$$\eta'(z, t) = \eta(x, \theta, t)$$

In general, the new model is nonlinear, even if the original one was linear.

If the parameters are to be estimated alone, an input–output description of the system (see Sec. 1-1) can be used in order to eliminate the state equations. Then the parameters have to be estimated from

$$\theta(t+1) = \theta(t) \tag{5-1-3a}$$

$$y(t) = \psi_{x_0,t_0}(u_{[t_0,t)}(\cdot), \theta(t), t)$$

where ψ_{x_0,t_0} is an input–output relationship. This formulation is again of the form (5-1-2). More generally, it can always be assumed in the following that a representation of type (5-1-2) in which the state z comprises exactly the quantities to be estimated has been found.

Unfortunately, estimation problems are, in practice, complicated by the fact that the system is randomly disturbed. The usual way of representing these disturbances is to add suitable noise terms to the model equations. Thus, for example, Eq. (5-1-2) is modified to give

$$z(t+1) = f'(z(t), u(t), t) + v(t) \tag{5-1-4a}$$

$$y(t) = \eta'(z(t), t) + w(t) \tag{5-1-4b}$$

where v and w are called *process* and *measurement noise*, respectively. Equations (5-1-1) and (5-1-3) may be modified in a similar way. Of course, the addition of v and w is not the most general way of taking into account the random disturbances; but usually one does not know exactly the characteristics of the noise and so the most simple representation is chosen. If the noise terms are added in Eqs. (5-1-1)–(5-1-3), these equations are, in general, no longer equivalent, as they are in the deterministic case. However, since the usual way of taking noise into account in water pollution modeling is in one equation as arbitrary as in the other, the estimation problem is always assumed to be of type (5-1-4). The state estimation problem can be formulated precisely in the following way: given two sets U_τ and Y_τ of input and output observations of a system over the time interval $[0, \tau]$, and given a state model of the system, find a "suitable" *estimate* for the actual value of the state z at the prescribed time t_s. (For time-varying systems the observation interval ought to be defined more generally, but this minor loss of generality is not essential for what follows.) The argument t_a will be left out in the following if there is no danger of confusion. The "suitable" estimate of $\mathbf{z}$ is denoted by $\hat{\mathbf{z}}$, the set of all possible $\mathbf{z}$ is denoted by $\mathbf{Z}$, and the rule for calculating $\hat{\mathbf{z}}$, i.e.,

$$\hat{\mathbf{z}} = \hat{\mathbf{z}}(\mathbf{U}_\tau, \mathbf{Y}_\tau) \tag{5-1-5}$$

will be called the *estimator*. The notion "suitable" in the problem statement will be specified through the selection of the function $\hat{\mathbf{z}}(\cdot,\cdot)$ appearing in Eq. (5-1-5).

The literature on the problem formulated just now is fairly well developed. More or less broad overviews of the area can be found in Åström and Eykhoff (1971), Eykhoff (1974), Isermann (1974), Unbehauen et al., (1974), and Strobel (1975). Many articles on particular topics are given in the proceedings of the IFAC Symposia on Identification and System Parameter Estimation.

The estimate $\hat{\mathbf{z}}$ is a random variable because of the random disturbances. Its statistical properties (which are determined by the characteristics of $\mathbf{v}$ and $\mathbf{w}$) are very important for selecting a suitable estimator. The most desirable ones are

Unbiasedness: $E[\hat{\mathbf{z}}] = \mathbf{z}$, where $E[\cdot]$ denotes expectation.
Consistency: $\lim_{\tau\to\infty} p(\|\hat{\mathbf{z}} - \mathbf{z}\| > \varepsilon) = 0 \ \forall\, \varepsilon > 0$, where $\|\cdot\|$ denotes norm.
Efficiency: $\operatorname{cov}[\hat{\mathbf{z}}] = E[(\hat{\mathbf{z}} - \mathbf{z})(\hat{\mathbf{z}} - \mathbf{z})^T] \le \operatorname{cov}[\boldsymbol{\zeta}]$ for all unbiased estimators $\boldsymbol{\zeta}$, where $\operatorname{cov}[\cdot]$ denotes covariance. (The statement $\mathbf{A} \le \mathbf{B}$, where $\mathbf{A}$ and $\mathbf{B}$ are matrices, means that $\mathbf{x}^T\mathbf{A}\mathbf{x} \le \mathbf{x}^T\mathbf{B}\mathbf{x}$ for all vectors $\mathbf{x}$.)

Selection of Estimators

The essential assumption for all statistical estimation techniques is that the *probability density function* (pdf) of the observations is known, apart from the unknown value $\mathbf{z}$. This means, the function

$$p(\mathbf{Y}_\tau \mid \mathbf{z})$$

is known, where the bar denotes *conditional upon*. (For the sake of notational simplicity the same symbol $\mathbf{z}$ is used for both the random variable and its actual value, and the input observations are omitted. In the applications shown in the following sections $\mathbf{u}(t)$ is assumed to be known exactly, anyway.) For estimation the *a posteriori probability*

$$p(\mathbf{z} \mid \mathbf{Y}_\tau)$$

is of interest, i.e., the probability for the different $\mathbf{z}$-values given certain observations $\mathbf{Y}_\tau$. The relationship between a priori and a posteriori probabilities is given by *Bayes' rule* (see, for instance, Raiffa, 1968):

$$p(\mathbf{z} \mid \mathbf{Y}_\tau) = \frac{p(\mathbf{Y}_\tau \mid \mathbf{z})\,p(\mathbf{z})}{\int_{\mathbf{z}} p(\mathbf{Y}_\tau \mid \mathbf{z})\,p(\mathbf{z})\,d\mathbf{z}} \tag{5-1-6}$$

The *a priori probability* $p(\mathbf{z})$ for $\mathbf{z}$ might reflect very vague, subjective knowledge. Since the integration in the denominator of Eq. (5-1-6) extends over all $\mathbf{z}$, the denominator equals $p(\mathbf{Y}_\tau)$. A natural choice for an estimator $\hat{\mathbf{z}}$ would be the solution of the maximization problem

$$\max_{\mathbf{z}}\,[p(\mathbf{z} \mid \mathbf{Y}_\tau)] \tag{5-1-7}$$

i.e., $\hat{\mathbf{z}}$ is defined as that value of $\mathbf{z}$ which maximizes the a posteriori probability given by Eq. (5-1-6). This kind of estimator is called *Bayes' estimator*, because of the use of Bayes' formula. It can still be refined, if one knows the costs associated with a deviation of the estimate from the true value of $\mathbf{z}$. If $\mathscr{C}(\mathbf{z}', \mathbf{z})$ indicates the costs to be incurred if $\mathbf{z}'$ is used instead of the true value $\mathbf{z}$, it is reasonable to use as an estimate that value of $\mathbf{z}'$ which minimizes the expected costs, i.e., to use the solution of the minimization problem

$$\min_{\mathbf{z}'} \int \mathscr{C}(\mathbf{z}', \mathbf{z})\,p(\mathbf{z} \mid \mathbf{Y}_\tau)\,d\mathbf{z} \tag{5-1-8}$$

In general, $\mathscr{C}(\mathbf{z}', \mathbf{z})$ is known only after the model has been applied to the problem causing the modeling effort (see Sec. 1-3 and 10-1). Hence, if the estimator is given by expression (5-1-8) no use is made of the *separation hypothesis* mentioned in Sec. 1-3.

In most cases, however, even less a priori knowledge than required by Eq. (5-1-6) is available. If nothing is known about $p(\mathbf{z})$, the assumption usually made is

$$p(\mathbf{z}) = \text{const.}$$

for all $\mathbf{z} \in \mathbf{Z}$. Then Eq. (5-1-7) yields the same $\hat{\mathbf{z}}$ as

$$\max_{\mathbf{z}}\,[p(\mathbf{Y}_\tau \mid \mathbf{z})] \tag{5-1-9}$$

The function $p(\mathbf{Y}_\tau \mid \cdot)$ (which is not a pdf!) is the so-called *likelihood function*; corresponding to this, the estimate from Eq. (5-1-9) is called *maximum likelihood estimate*. It gives the value of $\mathbf{z}$ for which the observed values $\mathbf{Y}_\tau$ have maximum probability.

The statistical properties of the maximum likelihood estimator have been extensively studied. If there is no process noise and certain other general assumptions are fulfilled the maximum likelihood estimator can be shown to be (Eykhoff, 1974) asymptotically unbiased (i.e., $E[\hat{\mathbf{z}}] \to \mathbf{z}$ as $\tau \to \infty$), consistent, and asymptotically efficient. Moreover, it is asymptotically normally distributed and the covariance matrix is given by

$$\operatorname{cov}[\hat{\mathbf{z}}] = -\left[E\left[\left.\frac{\partial^2 \ln p(\mathbf{Y}_\tau \mid \mathbf{z})}{\partial \mathbf{z}\,\partial \mathbf{z}^T}\right|_{\mathbf{z}=\hat{\mathbf{z}}}\right]\right]^{-1} \tag{5-1-10}$$

The matrix within the brackets on the righthand side of Eq. (5-1-10) is called *information matrix* (see Sec. 5-3).

If also the conditional probability density $p(\mathbf{Y}_\tau | \mathbf{z})$ is unknown it is usually assumed that it can be characterized completely by its expectation and covariance and that only the expectation depends on $\mathbf{z}(t_a)$. In other words, a $(\tau + 1)p$-variate Gaussian (normal) distribution is assumed for $p(\mathbf{Y}_\tau | \mathbf{z})$:

$$p(\mathbf{Y}_\tau | \mathbf{z}) = C \cdot \exp(-\tfrac{1}{2}(\mathbf{Y}_\tau - E[\mathbf{Y}_\tau])^T (\mathrm{cov}\,[\mathbf{Y}_\tau])^{-1}(\mathbf{Y}_\tau - E[\mathbf{Y}_\tau]) \qquad (5\text{-}1\text{-}11)$$

where C is a normalizing constant and $\mathbf{Y}_\tau$ has to be interpreted as the vector

$$\mathbf{Y}_\tau = [\mathbf{y}(0)^T\ \mathbf{y}(1)^T \ldots \mathbf{y}(\tau)^T]^T$$

If the system (5-1-4) is linear and both $\mathbf{v}(t)$ and $\mathbf{w}(t)$ are uncorrelated ("white") Gaussian disturbances, the observations $\mathbf{Y}_\tau$ are exactly a sample from such a distribution (see Sec. 5-4). Since the logarithm is a monotonic function, maximization of $p(\mathbf{Y}_\tau | \mathbf{z})$ from Eq. (5-1-11) with respect to $\mathbf{z}$ yields the same estimate $\hat{\mathbf{z}}$ as

$$\min_{\mathbf{z}} (\mathbf{Y}_\tau - E[\mathbf{Y}_\tau])^T (\mathrm{cov}\,[\mathbf{Y}_\tau])^{-1} (\mathbf{Y}_\tau - E[\mathbf{Y}_\tau]) \qquad (5\text{-}1\text{-}12)$$

The rule (5-1-12) for calculating the estimate $\hat{\mathbf{z}}$ is called *Markov estimator*. For reasons which will become obvious in the following, it is occasionally also called *generalized least-squares estimator*.

Often even the knowledge about cov $[\mathbf{Y}_\tau]$ is defective. Then one may assume that the covariance matrix is diagonal and that the diagonal elements (variances) for each component of $\mathbf{y}$ are the same for all t. This particular covariance matrix is obtained if there is no process noise in system (5-1-4) and $\mathbf{w}(t)$ is a white Gaussian noise with covariance matrix

$$\mathrm{cov}\,[\mathbf{w}] = \begin{bmatrix} \sigma_1^2 & 0 & \ldots & 0 \\ 0 & \sigma_2^2 & \ldots & 0 \\ \vdots & \vdots & & \vdots \\ 0 & 0 & \ldots & \sigma_p^2 \end{bmatrix} \qquad (5\text{-}1\text{-}13)$$

Under this simplifying assumption maximization of $p(\mathbf{Y}_\tau | \mathbf{z})$ becomes equivalent to

$$\min_{\mathbf{z}} \sum_{i=1}^{p} \frac{1}{\sigma_i^2} \sum_{t=0}^{\tau} (y_i(t) - E[y_i(t)])^2 \qquad (5\text{-}1\text{-}14)$$

i.e. equivalent to minimizing the sum of the squared deviations of $y_i(t)$ from the undisturbed output, where the squares are weighted by $1/\sigma_i^2$. If nothing is known about the σ_i^2 the most natural choice is to assume that they are all equal. An estimator which minimizes the sum of squared deviations between actual measurements and the output of a model is called *least-squares estimator*. It is the most widely used type of estimator.

Maximum likelihood, Markov, and least-squares estimator all have been derived as simpler and simpler special cases of the Bayes' estimator. As already indicated they are usually applied not because the assumptions made for their derivation are fulfilled, but because the knowledge about the noise characteristics is not sufficient, or a more sophisticated estimate is too complicated to be determined. In these cases the estimator has, in general, poorer statistical properties than a more sophisticated one. However, quite often it is possible to transform the output $\mathbf{y}(t)$ through a filter into a signal which has exactly the characteristics required for the derivation of a simpler estimator (Åström and Eykhoff, 1971).

Numerical Techniques

Once an expression either for $p(\mathbf{z} | \mathbf{Y}_\tau)$ or $p(\mathbf{Y}_\tau | \mathbf{z})$ has been derived the problem of determining the maximum over $\mathbf{z}$ remains. In general, this is a difficult task for which iterative numerical techniques have usually to be used (see e.g., Eykhoff, 1974). If, however, the function to be maximized is quadratic in the components of $\mathbf{z}$, and $\mathbf{z}$ is unconstrained the maximization can easily be done by putting all derivatives of the function with respect to z_i equal to zero, which yields a system of linear algebraic equations. This way of solving the maximization problem is feasible with the least-squares estimator, if $E[y_i(t)]$ in Eq. (5-1-14) is a linear function of $\mathbf{z}(t_a)$.

In any case, there are two strategies for numerically calculating the estimate. They might be called *accumulative* and *recursive estimation*. Accumulative procedures are designed for calculating the estimate from a fixed set of observations, while recursive schemes are suited for estimates which are to be updated as new observations become available. Hence, accumulative procedures are appropriate for off-line use and in particular for estimation of parameters which are supposed not to vary in time. Recursive methods are used for on-line estimation, where usually t_a increases at each recursion in accordance with the sampling interval. Each recursion may be interpreted as an application of Bayes' rule (5-1-6) for combining the information on $\mathbf{z}(t_a)$ which has been extracted from the previous measurements (a priori probability) with the information on $\mathbf{z}(t_a)$ obtained by the new measurement. To start a recursive estimation scheme one can either use an estimation result from an accumulative scheme or a subjective guess with an appropriately large variance. Recursive schemes are used, for example, for real-time state estimation in feedback control problems (see Sec. 9-1) or for estimation of parameters which can be expected to drift. They may also be used as a tool for determining the structure of a model: observation of how a parameter estimate changes under repeated updating may yield hints for improving the model structure, or confirm the structure proposed (see Sec. 5-5).

A critical problem for all estimation techniques is the problem of "*identifiability*." It is not at all obvious a priori whether the value of $\hat{\mathbf{z}}(t_a)$ can be determined uniquely from the available observations. If we try, for instance, to estimate too many parameters, which means that the dimension of $\mathbf{z}$ is high, there will be many completely different combinations of parameter values with about the same a posteriori probability, or in other words, $[\mathrm{cov}\,[\hat{\mathbf{z}}]]^{-1}$ becomes singular (see also Eq. (5-1-10)). This means, only certain combinations of the originally proposed parameters can be estimated uniquely. The result may be physically meaningless parameter values or difficulties in the numerical calculations. Similar things may happen with too short observation sequences or too large noise variances. Very little can be said on a theoretical basis, and even the definition of "*identifiability*" (in probabilistic terms) is problematic. Therefore, numerical experimentation is often the only way to solve the problem of identifiability (see, for example, Mehra and Tyler, 1973, and Sec. 5-3). In the case of linear systems without noise, conditions under which $\mathbf{z}(t_s)$ can be determined uniquely (conditions for "*observability*") can be specified theoretically; they are discussed in Sec. 5-4.

Classification of the Applications

In the following sections four examples of estimation techniques, which have been applied to river quality models, are given in detail; two are of the accumulative and two of the recursive type. Both accumulative techniques use the least-squares criterion. In Sec. 5-2 the parameters of a modified Streeter-Phelps model are estimated by a direct search in the parameter space. In Sec. 5-3 state and parameters are estimated simultaneously for the ecological model described in Sec. 4-4 by solving the estimation problem for a sequence of linear approximations to the original model.

The recursive technique described in Sec. 5-4 calculates a Markov estimate for the state of a linear system at time $t_s = \tau$. The algorithm, which is known as *Kalman filter*, is also obtained if the estimation result for $\mathbf{z}(\tau - 1)$ and the new observation $\mathbf{y}(\tau)$ are to be combined in such a way that

$$E\left[(\mathbf{z}(\tau) - \hat{\mathbf{z}}(\tau))^T(\mathbf{z}(\tau) - \hat{\mathbf{z}}(\tau))\right]$$

is minimal.

The Kalman filter is also used in Sec. 5-4 for estimating solely the parameters of a linear system. As already mentioned, system (5-1-4) need not be linear even if the parameters appeared linearly in the original model. A linear system may be obtained, however, by applying the following trick. The single input–single output linear state model is transformed into a model of type (1-2-17) (in discrete time)

$$y(t) + a_1 y(t-1) + \cdots + a_n y(t-n) = b_1 u(t-1) + b_2 u(t-2) + \cdots + b_n u(t-n) \tag{5-1-15}$$

following the procedure indicated in Sec. 1-2. (In general, however, the parameters a_i and b_i are not identical with the original parameters but with certain combinations of them.) If the state vector $\mathbf{z}$ is now defined as

$$\mathbf{z} = [a_1 \cdots a_n \quad b_1 \cdots b_n]^T$$

and the output matrix

$$\mathbf{h}^T(t) = [-y(t-1) \cdots -y(t-n) \quad u(t-1) \cdots u(t-n)]$$

Eq. (5-1-15) can be put into the form

$$\mathbf{z}(t+1) = \mathbf{z}(t) \tag{5-1-16a}$$

$$y(t) = \mathbf{h}^T(t)\mathbf{z}(t) \tag{5-1-16b}$$

System (5-1-16) is a time-varying linear system and if the random disturbances, which are not included in Eq. (5-1-16), have the appropriate characteristics, the Kalman filter may be applied (Åström and Eykhoff, 1971). This technique could not have been applied in a straightforward manner to the problem treated in Sec. 5-2, since the observations were not regularly spaced. A discrete time model like (5-1-15) would be time-varying in this case and therefore Eq. (5-1-16a) could not be used.

In Sec. 5-5 a recursive technique for state estimation in nonlinear models is described and applied to combined state and parameter estimation. It is an extension of the Kalman filtering technique described in Sec. 5-4. Finally, in Sec. 5-6 a few other applications of estimation techniques to water quality models are reviewed.

5-2 NONLINEAR PARAMETER ESTIMATION OF STREETER-PHELPS MODELS

The aim of this section is to describe a very simple least-squares estimator for the parameters of linear models such as those described in Secs. 4-1 and 4-2 (see Rinaldi et al., 1976). The estimation scheme is nonlinear and accumulative and requires that steady state BOD and/or DO values have been sampled in a certain number of points along the river. For the sake of clarity, reference to the particular case of the Bormida river (Italy), to which the estimation scheme has been applied, will be made.

The stretch of the river which has been considered is 68 km long and shown in Fig. 5-2-1; the numbers (0, 1, ..., 6) indicate the points in which measurements of temperature, BOD, and DO were taken. Because of the very high BOD load discharged by a factory in point 0 the downstream dissolved oxygen concentration was very low and some control action had to be taken in order to satisfy some required steady state stream standards. The installation of a wastewater treatment plant and/or the use of the upstream reservoir (see Fig. 5-2-1) for low flow augmentation were the two feasible alternatives open to the local authority. In order to make the decision on a rational basis a mathematical model was needed which could allow the computation of the steady state dissolved oxygen concentration at any point of the stretch under different hydrological, thermal, and biological conditions. Since algae had been observed in the final part of the stretch and sedimentation was supposed to take place in all the stretch (see Marchetti and Provini, 1969) a modified Streeter-Phelps model of the Dobbins kind (see Eq. (4-2-1)) was selected for further investigation.

Moreover, dispersion was neglected together with some minor distributed BOD load so that the model was given by

$$\frac{\partial b}{\partial t} + v\frac{\partial b}{\partial l} = -\left[k_1(T) + (k_3(v(Q))/A(Q))\right]b \tag{5-2-1a}$$

$$\frac{\partial c}{\partial t} + v\frac{\partial c}{\partial l} = -k_1(T)b + \frac{k_2(T,Q)}{H(Q)}(c_s(T) - c) + \frac{k_4}{A(Q)} \tag{5-2-1b}$$

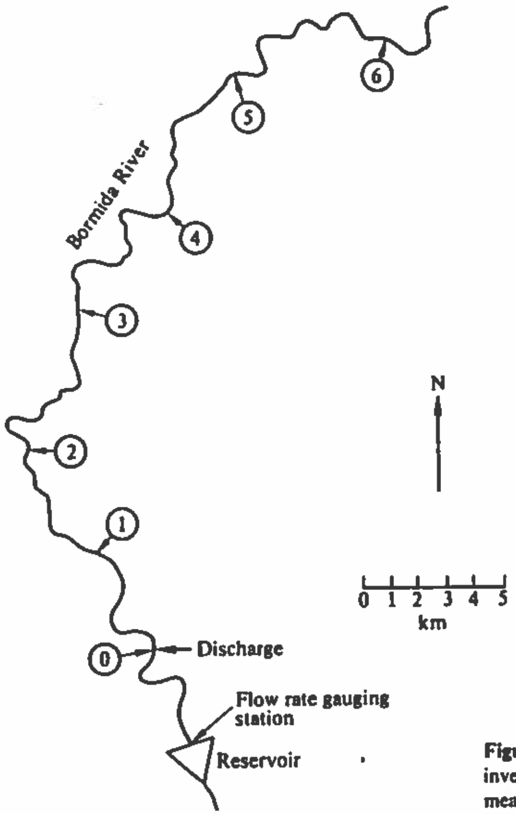

Figure 5-2-1 The reach of the Bormida river investigated, and locations of point (0) and measurement stations (1–6).

where, as usual, T is the water temperature, A the cross-sectional area, v the average stream velocity ($v = Q/A$) and $H(Q)$ is the mean river depth as a function of flow rate Q. Notice that the parameters are defined differently than in model (4-2-1, 4-2-2) in order to make clear the dependence on T and Q. The selection of a particular model among this class is, strictly speaking, a functional problem since the functions $k_1(T)$, $k_2(T, Q)$, $k_3(v)$, and k_4 (deoxygenation, reoxygenation, suspended BOD sedimentation, and photosynthetic oxygen production rate) are unknown. Moreover, the functions $v(Q)$, $A(Q)$, and $H(Q)$ are also unknown in the majority of the applications.

Thus, a more convenient set up must be obtained, and this is possible if a particular isothermical regime, characterized by constant BOD load and constant flow rate Q, is considered. Under these assumptions the daily average BOD and DO concentrations satisfy the following differential equations

$$\frac{\mathrm{d}b}{\mathrm{d}l} = -K_1 b \tag{5-2-2a}$$

$$\frac{\mathrm{d}c}{\mathrm{d}l} = -K_2 b + K_3(c_s - c) + K_4 \tag{5-2-2b}$$

where the functions K_h, $h = 1, \ldots, 4$, depend upon the two independent variables Q and T, i.e.,

$$K_1(T, Q) = k_1(T)/v(Q) + k_3\big(v(Q)\big)/Q \tag{5-2-3a}$$

$$K_2(T, Q) = k_1(T)/v(Q) \tag{5-2-3b}$$

$$K_3(T, Q) = k_2(T, Q)/H(Q)v(Q) \tag{5-2-3c}$$

$$K_4(Q) = k_4/Q \tag{5-2-3d}$$

In order to further simplify the estimation problem the structure of these unknown functions is specified in terms of a finite dimensional parameter vector $\theta = (\theta_1, \ldots, \theta_q)$, so that the functional estimation problem is reduced to a much more simple finite dimensional parameter estimation problem (determination of the optimal value of θ). Thus, from now on, the four functions $K_h(\theta, T, Q)$, $h = 1, \ldots, 4$ are assumed to be given.

The solution of Eq. (5-2-2) is well known and is given by (see Sec. 4-2)

$$b(l, K_1, b_0) = b_0\, \mathrm{e}^{-K_1 l} \tag{5-2-4a}$$

$$\begin{aligned} c(l, K_1, \ldots, K_4, b_0, c_0) = {} & c_s + K_4/K_3 - [c_s + (K_4/K_3) - c_0]\, \mathrm{e}^{-K_3 l} \\ & + [K_2 b_0/(K_1 - K_3)][\mathrm{e}^{-K_1 l} - \mathrm{e}^{-K_3 l}] \end{aligned} \tag{5-2-4b}$$

where b_0 and c_0 are the concentrations at the upstream end of the stretch ($l = 0$).

Consider n different steady state regimes characterized by n pairs (Q^i, T^i), $i = 1, \ldots, n$ of flow rate and water temperature and assume that the daily average concentrations of BOD and DO have been measured for each one of the above regimes at the initial point ($l = 0$) and at r fixed points (stations) $j = 1, \ldots, r$ along the river. Thus, a set of initial conditions

$$(b_0^i, c_0^i) \qquad i = 1, \ldots, n$$

and a set of measurements along the river

$$(b_j^i, c_j^i) \qquad i = 1, \ldots, n \qquad j = 1, \ldots, r$$

are available together with the distance l_j, $j = 1, \ldots, r$, of each station from the origin of the stretch. The square of the deviations for each station and for each regime can therefore be defined as

$$\varepsilon_b^{ij} = [b(l_j, K_1, b_0^i) - b_j^i]^2$$

$$\varepsilon_c^{ij} = [c(l_j, K_1, \ldots, K_4, b_0^i, c_0^i) - c_j^i]^2$$

so that the square error J^i associated with the i-th regime is given by

$$J^i = \sum_{j=1}^{r} [\lambda \varepsilon_b^{ji} + (1-\lambda)\varepsilon_c^{ji}] \qquad 0 \le \lambda \le 1 \tag{5-2-5}$$

and the total square error of J is

$$J = \sum_{i=1}^{n} J^i$$

Thus the least-squares estimation problem can be formulated as follows:

Problem A

> *Assume that the structure of the functions K_h is known, i.e., let $K_h = K_h(\theta, T, Q), h = 1, \dots, 4$, where θ is a q-dimensional vector of parameters. Then determine the value of θ which minimizes the total error J.*

This problem could be solved by applying a suitable searching algorithm in the q-dimensional vector space of the parameters. Unfortunately, reasonable values for q are quite high (about 10–12) which is probably the reason why this problem has never been dealt with in the literature.

A suboptimal solution of Problem A can be obtained by solving the following two problems in series:

Problem B-1

> *For each regime $i = 1, \dots, n$, determine the four-dimensional parameter vector $\mathbf{K}^i = (K_1^i, K_2^i, K_3^i, K_4^i)$ which minimizes the error J^i.*

Problem B-2

> *Determine the parameter vector θ which solves the following regression problem*
>
> $$\min_{\theta} \sum_{i=1}^{n} \sum_{h=1}^{4} (K_h(\theta, T^i, Q^i) - K_h^i)^2$$

Problems B-1 and B-2 are, in general, simpler to solve than Problem A and the dimensionality of Problem B-1 can be reduced by taking advantage of the particular structure of the model. Moreover, if data and estimates of Problem B-1 are highly correlated for all regimes the solution of Problem B-2 may be expected to be similar to that of Problem A. In the following, these correlations are computed for the Bormida river. They turn out to be very high, from which the conclusion may be drawn that Problem B is, in general, a meaningful problem. This result also justifies the fact that Problem B-1 is the only one which has been dealt with until now in the literature.

Solution of Problem B-1

Problem B-1 is a four-dimensional problem since four parameters must be determined. Nevertheless, the dimensionality of the problem can be reduced to two. In fact, from Eqs. (5-2-4) and (5-2-5) it follows that J^i is quadratic in K_2 and K_4, so that the stationarity conditions

$$\frac{\partial J^i}{\partial K_2} = 0, \qquad \frac{\partial J^i}{\partial K_4} = 0 \tag{5-2-6}$$

are linear in the same parameters. It is therefore possible to obtain two functions from Eq. (5-2-6)

$$K_2 = K_2(K_1, K_3), \qquad K_4 = K_4(K_1, K_3)$$

which can be substituted into the expression for J^i. Thus J^i becomes a function only of the two parameters K_1, K_3 and a searching method in the parameter space (K_1, K_3) must therefore be used to solve Problem B-1. Since nonlinear searching algorithms are described in some detail in Sec. 6-2 the reader is referred to that section for this point.

The two limit cases $\lambda = 1$ and $\lambda = 0$, which correspond to weighting only BOD or DO errors in the performance, are of particular interest. The first case ($\lambda = 1$) implies that the estimation of the parameters can in fact be performed in two separate and very simple steps, while the second case ($\lambda = 0$) requires only DO data to be collected, which is a definite advantage considering the effort needed for measuring BOD.

Two-step estimation ($\lambda = 1$) For $\lambda = 1$ Eq. (5-2-5) gives

$$J_b^i = \sum_{j=1}^{r} \varepsilon_b^{ji} = \sum_{j=1}^{r} [b(l_j, K_1^i, b_0^i) - b_j^i]^2 \tag{5-2-7}$$

from which the estimate K_1^i can be obtained by applying a one-dimensional search algorithm (see Sec. 6-2). The three remaining parameters can be obtained by minimizing the DO error

$$\sum_{j=1}^{r} \varepsilon_c^{ji} = \sum_{j=1}^{r} [c(l_j, K_1^i, K_2^i, K_3^i, K_4^i, b_0^i, c_0^i) - c_j^i]^2$$

where K_1^i is the value determined in the first step of the procedure (minimization of (5-2-7)). As mentioned above, the two parameters K_2^i and K_4^i can be eliminated, thus reducing the problem to a simple one-dimensional search with respect to K_3^i. In conclusion, the four parameters $(K_1^i, K_2^i, K_3^i, K_4^i)$ can be estimated by means of two successive one-dimensional search procedures. Because of its simplicity this is the estimation scheme which has been used for the Bormida river case.

Estimation from DO measurements ($\lambda = 0$) For $\lambda = 0$ the objective function (5-2-5) becomes

$$J_c^i = \sum_{j=1}^{r} [c(l_j, K_1^i, K_2^i, K_3^i, K_4^i, b_0^i, c_0^i) - c_j^i]^2$$

from which it is still possible to derive estimates of the four parameters by means of a two-dimensional search.

It must be noticed that one BOD measurement is used in the estimation procedure. If this measurement is not available only three parameters can be identified. In fact, if only DO data are available the analysis must be based on the second order differential equation derived from Eq. (5-2-2) (see Eq. (1-2-17))

$$\frac{d^2c}{dl^2} = -(K_1 + K_3)\frac{dc}{dl} + K_1K_3(c_s - c) + K_1K_4 \tag{5-2-8}$$

in which the parameter K_2 does not appear. From this equation, the solution $\tilde{c}_j^i$ can be obtained in each point l_j, $j = 2, \ldots, r$, as a function of the two measurements c_0^i and c_1^i, i.e.,

$$\tilde{c}_j^i = \tilde{c}(l_j, K_1, K_3, K_4, c_0^i, c_1^i)$$

This expression can be used to define the objective function

$$J_c^i = \sum_{j=2}^{r} [\tilde{c}_j^i - c_j^i]^2$$

which must be minimized in order to obtain the three best estimates (K_1^i, K_3^i, K_4^i) of the parameters appearing in Eq. (5-2-8). Again this minimization can be performed in a two-dimensional vector space since $\tilde{c}_j^i$ is linear in K_4.

The conclusion is that the deoxygenation rate K_2 cannot be identified from DO measurements: at least one BOD measurement (e.g., b_0^i) is necessary to estimate this parameter. The only trivial exception is when sedimentation effects are a priori known to be negligible since in this case $K_1 = K_2$.

Estimation Results

Returning to the problem of the Bormida river, the BOD, DO, and water temperature were measured in six stations and at the wastewater outlet at monthly intervals for four years, while the flow rate Q was continuously recorded at an upstream station. Thus, 48 sets of data were available from which fifteen regimes corresponding to roughly stationary hydrological and thermal conditions were selected in order to apply the algorithms described above (see Table 5-2-1).

The flow rate Q^i was taken as the average value of the flow rate during the three days immediately preceding the moment in which the data of the i-th regime were collected. The temperature T^i was chosen as the average of the measurements obtained in the six stations at the same time as BOD and DO were sampled. Since these measurements were not taken at the same time of the day this average value T^i is not very significant. Finally, since continuous records of BOD and DO were not available, the samples were assumed to be equal to the average daily values.

Using these very rough assumptions concerning the data, Problem B-1 has been solved for different values of λ for the first thirteen regimes of Table 5-2-1, the main result being that sedimentation and photosynthesis could reasonably be neglected, i.e., $K_1 \cong K_2$ and $K_4 \cong 0$.

Then, the estimation of the two parameters (K_1, K_3) of the Streeter-Phelps model was carried out again for the same thirteen regimes by means of the

Table 5-2-1 The data of the 13 regimes used for parameter estimation and of the two regimes used for the model validation (the first row of each regime refers to BOD (mg/l), the second one to DO (mg/l)).

Station number	0	1	2	3	4	5	6	Flow rate	Water Temperature (°C)	
Distance (km)	0.00	1.75	4.20	14.00	25.00	40.00	68.00	$(10^3\ m^3/day)$	Average	Range
Regime										
1	196.0	180.0	200.0	118.0	64.0	38.0	10.0	55	17.5	4.2
	2.5	3.0	0.0	4.5	5.5	6.5	9.0			
2	149.0	118.0	120.0	92.0	72.0	58.0	24.0	60	9.0	5.1
	4.0	4.5	3.0	5.5	9.0	9.5	9.5			
3	222.0	220.0	162.0	126.0	110.0	66.0	40.0	125	0.5	5.0
	5.0	0.0	1.0	3.0	5.0	6.5	10.5			
4	116.0	105.0	105.0	84.0	70.0	44.0	38.0	100	19.0	3.0
	3.0	3.5	2.0	5.0	5.5	6.0	7.5			
5	155.0	160.0	125.0	78.0	46.0	18.0	14.0	75	18.0	3.2
	1.5	0.0	1.5	3.5	4.5	5.5	7.0			
6	129.0	150.0	125.0	86.0	70.0	46.0	20.0	80	17.0	3.3
	3.0	3.5	2.0	5.0	6.0	6.0	6.5			
7	86.0	70.0	68.0	56.0	50.0	34.0	24.0	225	5.0	2.5
	8.0	0.0	2.0	6.0	7.0	9.5	12.0			
8	171.0	160.0	145.0	72.0	68.0	30.0	16.0	100	25.0	3.7
	1.5	0.0	0.0	1.2	2.2	3.6	5.8			
9	205.0	200.0	200.0	104.0	98.0	60.0	58.0	55	10.0	8.9
	1.0	0.0	0.0	4.0	6.0	6.0	7.0			
10	101.0	100.0	90.0	70.0	68.0	58.0	22.0	200	1.8	3.5
	7.0	5.0	4.0	4.0	8.0	9.0	9.0			
11	84.0	80.0	80.0	60.0	50.0	36.0	24.0	250	3.5	2.4
	8.0	3.0	6.0	8.0	10.0	10.5	11.0			
12	163.0	150.0	135.0	100.0	85.0	62.0	50.0	125	11.8	2.4
	4.5	0.0	0.5	4.0	5.0	6.0	8.0			
13	74.0	80.0	70.0	60.0	44.0	46.0	22.0	200	16.0	2.5
	5.5	5.5	3.0	6.0	7.0	7.5	8.0			
14	106.0	90.0	85.0	70.0	55.0	40.0	20.0	200	11.5	5.5
	7.5	3.0	3.0	6.0	7.0	9.0	9.5			
15	90.0	75.0	80.0	40.0	30.0	20.0	12.0	150	16.0	6.0
	6.0	5.5	2.5	5.0	7.0	8.5	9.0			

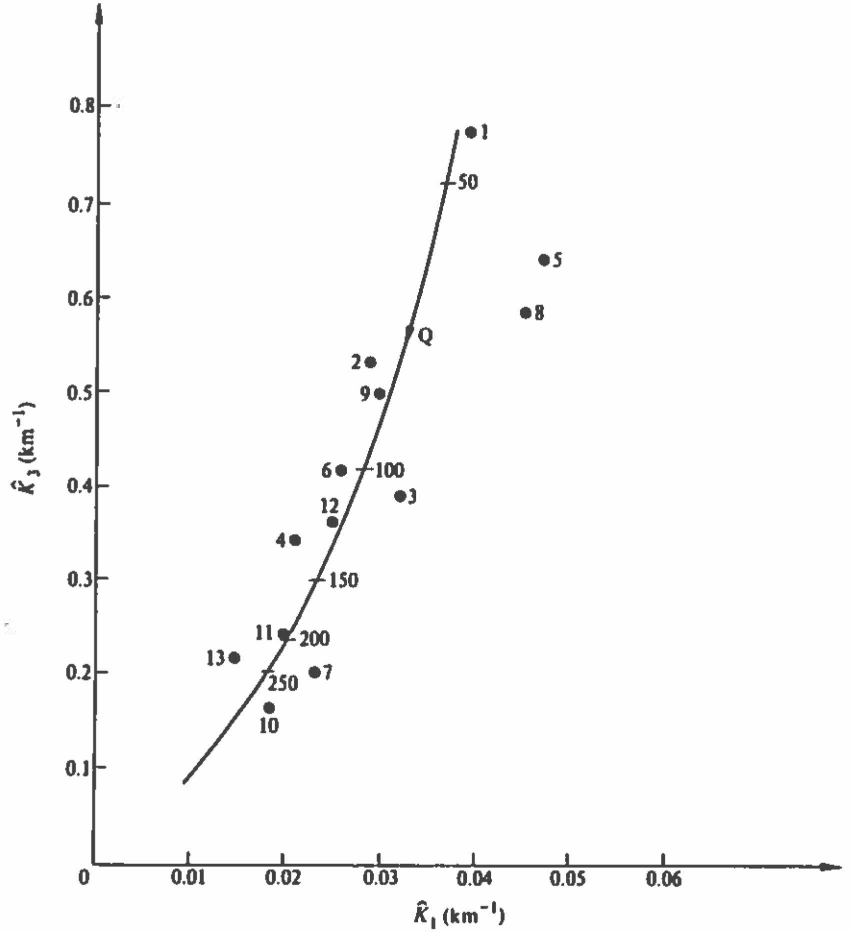

Figure 5-2-2 Estimates of parameters K_1 and K_3 for the 13 considered regimes and curve (5-2-10).

two-step procedure outlined above. The estimates of the parameters are shown in Fig. 5-2-2 where each number refers to the corresponding regime of Table 5-2-1. The correlation coefficient between estimated and measured BOD turned out to be greater than 0.95 for all regimes (average value 0.98), while for the DO concentrations the minimum correlation coefficient was 0.75 (average value 0.90). These high correlation coefficients justify the interest in Problem B-1, since the solution of Problem B-2 can now be expected to be similar to that of Problem A. Unfortunately, as could be predicted from the uncertainties of T^l, the regression problem B-2 did not give satisfactory results as far as the dependence of the parameters (K_1^l, K_3^l) upon T^l is concerned. Nevertheless, disregarding the dependence upon T^l and letting

$$K_1 = \theta_1 Q^{\theta_2} \qquad K_3 = \theta_3 Q^{\theta_4}$$

the solution of problem B-2 gives

$$K_1 = 0.2Q^{-0.43} \qquad K_3 = 16.4Q^{-0.8} \tag{5-2-9}$$

with correlation coefficients $r = 0.68$ and $r = 0.89$ respectively. Then, by eliminating Q in the two preceding expressions the following relationship is obtained

$$K_3 = 327.5K_1^{1.86} \tag{5-2-10}$$

which is represented in Fig. 5-2-2, while the ratio K_3/K_1 is given by

$$K_3/K_1 = 82.0Q^{-0.37} \tag{5-2-11}$$

This relationship can be proved to be approximately satisfied even if the temperature is taken into account. In fact, consider Eq. (5-2-3) with $k_3 = k_4 = 0$ and, disregarding the dependence of k_2 upon turbulence (see, for example, Metcalf and Eddy, 1972), let (see Eq. (3-5-9))

$$k_1(T) \propto \alpha^{(T-20^\circ)} \qquad k_2(T, Q) \propto \beta^{(T-20^\circ)}$$

where α and β are suitable parameters and $\propto$ denotes proportionality.

Then, from Eq. (5-2-3)

$$K_3/K_1 \propto (\alpha/\beta)^{(T-20^\circ)}/H(Q) \tag{5-2-12}$$

Since (α/β) is approximately unity (see, for instance, Metcalf and Eddy, 1972) the ratio K_3/K_1 should only depend upon Q, as it does in fact in Eq. (5-2-11). Moreover, from Eqs. (5-2-11) and (5-2-12) one can derive

$$Q \propto H^{2.78}$$

which is convex, as a stage-discharge relationship must be (see Sec. 3-3).

The result of the parameter estimation phase is that the Bormida river is described by a Streeter-Phelps model with the parameters K_1 and K_3 dependent on the flow rate Q as indicated by Eq. (5-2-9). These equations have been used to validate the model by means of the last two regimes of Table 5-2-1. The results of the validation turned out to be satisfactory and are shown in Fig. 5-2-3.

The problem of the sensitivity of the estimates with respect to the data of the first measurement point and with respect to the BOD data is now briefly discussed.

As is well known, BOD and DO data collected in the vicinity of a discharge point are often not very useful, since the waste and the river are not yet completely mixed at that point (with the measurement of the Bormida river this was not the case). Therefore, it is of interest to know if the parameters (K_1, K_3) can still be estimated without using the data of the first measurement point. The results obtained from the Bormida using only the data of stations 1,...,6 are highly consistent with the preceding ones (see Fig. 5-2-4). Therefore, it is possible to state that in doubtful cases it would be better to omit unreliable initial data,

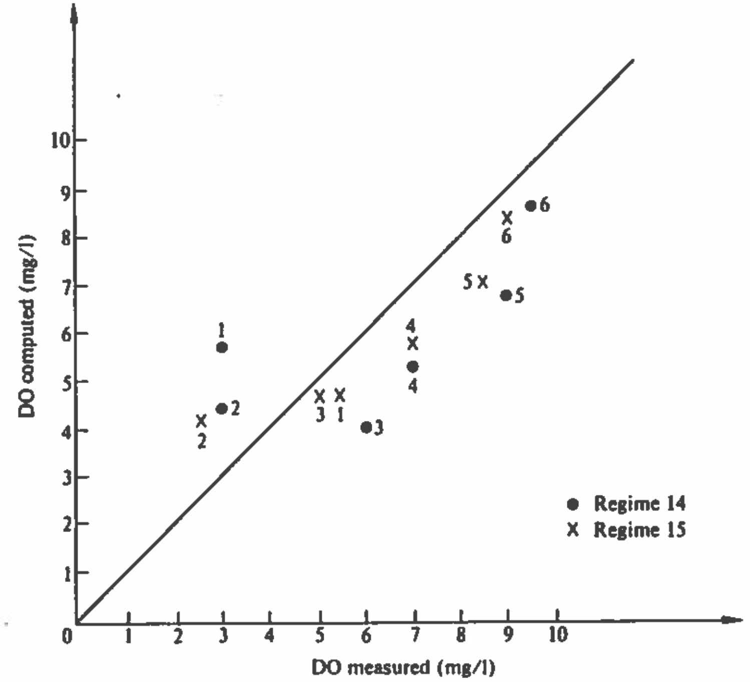

Figure 5-2-3 Measured and computed values of DO for the two regimes used to validate the model.

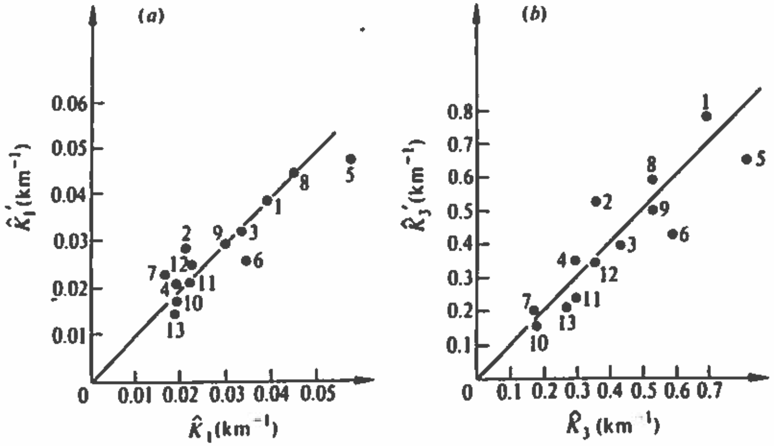

Figure 5-2-4 Effect of the first measurement point on: (a) estimate of deoxygenation rate, (b) estimate of reoxygenation rate (the primed parameters are estimated without data of the first section).

even if this entails the new initial point being approximately on the minimum of the DO sag curve (as it is in many of our regimes).

Finally, the parameters (K_1, K_3) have also been estimated by means of DO measurements only, as indicated on page 152. The estimates which have been obtained are relatively consistent for the decay rate K_1 as shown in Fig. 5-2-5, while the estimates of K_3 were found to be, in general, very inconsistent with the preceding ones. This fact can easily be explained, since it follows from Eq. (5-2-8) with $K_1 \ll K_3$ (as it is in the case under discussion) that the final part of the DO sag can be approximated by

$$c(l) = c_s - (c_s - c_0)\,e^{-K_1 l}$$

which depends only upon the deoxygenation rate K_1. Thus, if station 2 is not located around the minimum of the DO curve a good estimate for K_1, and a poor estimate for K_3, may be expected, and this is indeed what happened for the majority of the thirteen regimes. On the other hand, for the two regimes in which station 2 was around the point of the minimum DO (see regimes 10 and 13) highly consistent estimates for K_1 (see Fig. 5-2-5) and quite satisfactory estimates for K_3 were obtained. In conclusion, if only DO measurements are available the two parameters of the Streeter-Phelps model can still be estimated provided that at least three data points are in the critical part of the DO curve.

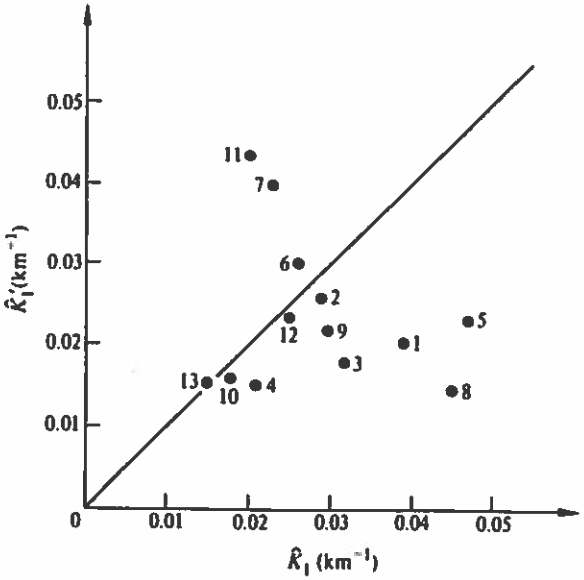

Figure 5-2-5 Estimates of decay rate K_1 with BOD and DO measurements ($\hat{K}_1$) and with DO measurements only ($\hat{K}_1'$).

5-3 QUASILINEARIZATION TECHNIQUE WITH APPLICATION TO THE RHINE RIVER

Another application of an accumulative estimation technique to a real case is the identification of two water quality models for a major part of the *Rhine river* in Germany (Stehfest, 1973). The Rhine river, which is depicted in Fig. 5-3-1, is one of the most heavily polluted, large rivers in the world. At the same time, its water is extensively used for drinking water production, and also for other purposes such as navigation, recreation, etc. In view of this situation, the need for a river quality model is obvious. In order to be able to estimate the level of model complexity necessary to obtain a realistic river management tool, two models were used: the ecological model described in Sec. 4-4 and a Streeter-Phelps model. The part of the river modeled extends from the cities of Mannheim and Ludwigshafen to the Dutch-German border. Upstream from Mannheim/Ludwigshafen the river pollution is considerably less severe, and downstream from the Dutch-German border the estuary part, which has to be modeled in a different way, begins.

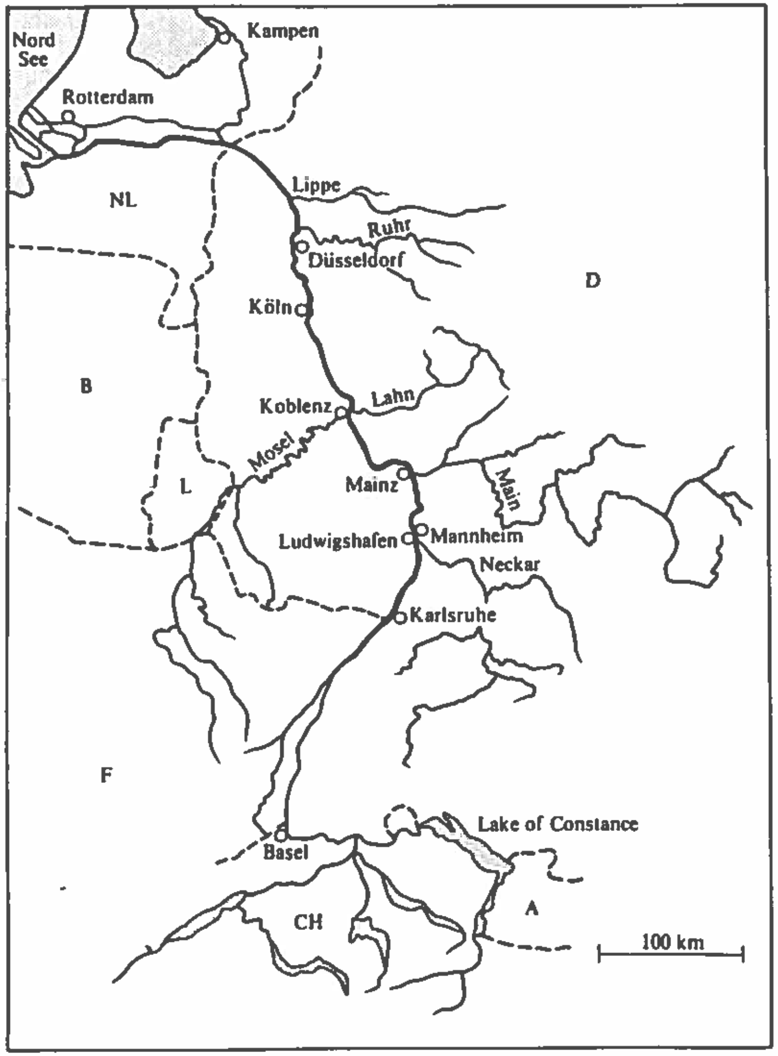

Figure 5-3-1 The Rhine river basin.

Quasilinearization Technique

The technique used for the estimation part of the system identification (see Sec. 1-3) is the quasilinearization technique for solving nonlinear *multi-point boundary value problems*, described in detail by Bellman and Kalaba (1965) and Lee (1968) (see also Eykhoff, 1974). Looking at the estimation problem as a boundary value problem means that the parameters are treated as additional state variables, as described in Sec. 5-1. Then the initial values of the augmented state are determined such that the sum of the squared differences between the measurements and the output of the model is minimal. Confining ourselves to time-invariant systems and linear observation equations, the problem can be formulated as follows (see Eq. (5-1-14))

$$\min_{\mathbf{x}(0)} J(\mathbf{x}(0)) = \min_{\mathbf{x}(0)} \left[\sum_{i=1}^{p} \frac{1}{2\sigma_i^2} \sum_{k=0}^{K_i} (y_{ik} - \mathbf{h}_i^T \mathbf{x}(t_{ik}))^2 \right] \qquad (5\text{-}3\text{-}1a)$$

subject to

$$\dot{\mathbf{x}} = \mathbf{f}(\mathbf{x}) \qquad (5\text{-}3\text{-}1b)$$

$$\mathbf{y} = \mathbf{H}\mathbf{x} + \mathbf{w} \qquad (5\text{-}3\text{-}1c)$$

where

σ_i^2 = variance of w_i
t_{ik} = time at which the k-th measurement of y_i was taken
y_{ik} = measurement of y_i at time t_{ik}
$\mathbf{h}_i^T$ = i-th row of the output transformation matrix $\mathbf{H}$
$\mathbf{w}$ = measurement noise

The input $\mathbf{u}$ has been omitted from Eq. (5-3-1b) for notational simplicity. As explained in Sec. 5-1, the least-square criterion used here is optimal in the maximum likelihood sense only if there is no process noise. But it is a reasonable substitute for the maximum likelihood criterion if the knowledge on the noise characteristics is not sufficient.

The method of quasilinearization for solving problem (5-3-1) consists of calculating better and better approximations $\mathbf{x}^j(0)$ to $\mathbf{x}(0)$ by solving iteratively a modified version of problem (5-3-1) obtained by substituting Eq. (5-3-1b) with its linearized form

$$\dot{\mathbf{x}}^j = \mathbf{f}(\mathbf{x}^{j-1}) + \mathbf{F}^{j-1}(t)(\mathbf{x}^j - \mathbf{x}^{j-1}) \tag{5-3-2}$$

where $\mathbf{F}^j(t)$ is the *Jacobian matrix* of $\mathbf{f}$ (see Sec. 1-2) evaluated at $\mathbf{x}^j(t)$, i.e.,

$$\mathbf{F}^j(t) = \left[\frac{\partial \mathbf{f}}{\partial \mathbf{x}}\right]_{\mathbf{x}^j}$$

The initial solution $\mathbf{x}^0(t)$ may be the solution of Eq. (5-3-1b) with an initial guess for $\mathbf{x}(0)$.

The optimal solution of the problem defined by Eqs. (5-3-1a) and (5-3-1c) (with $\mathbf{x}^j$ instead of $\mathbf{x}$) and Eq. (5-3-2) can be determined relatively easily, since $\mathbf{x}^j(t)$ is linear in the initial values $\mathbf{x}^j(0)$. The solution of Eq. (5-3-2) can be written in the form (see Eq. (1-2-4))

$$\mathbf{x}^j(t) = \mathbf{\Phi}^j(t)\mathbf{x}^j(0) + \mathbf{a}^j(t) \tag{5-3-3}$$

where $\mathbf{\Phi}^j$ is the transition matrix of system (5-3-2) and is the solution of

$$\dot{\mathbf{\Phi}}^j = \mathbf{F}^j(t)\mathbf{\Phi}^j \tag{5-3-4}$$

with initial condition

$$\mathbf{\Phi}^j(0) = \mathbf{I}$$

and $\mathbf{a}^j(t)$ is that solution of Eq. (5-3-2) which satisfies $\mathbf{x}^j(0) = \mathbf{0}$. The minimization in Eq. (5-3-1a) can easily be performed by putting all derivatives with respect to $x_r^j(0)$, $r = 1, \ldots, n$, equal to zero and solving the resulting linear algebraic system (see Sec. 5-1). The linear algebraic system is

$$\frac{\partial}{\partial x_r^j(0)} J(\mathbf{x}(0)) = \sum_{i=1}^{p} \frac{1}{\sigma_i^2} \sum_{k=0}^{K_i} \left[\mathbf{h}_i^T(\mathbf{\Phi}^j(t_{ik})\mathbf{x}^j(0) + \mathbf{a}^j(t_{ik})) - y_{ik}\right]\mathbf{h}_i^T \boldsymbol{\phi}_r^j = 0$$

$$r = 1, \ldots, n \tag{5-3-5}$$

where $\boldsymbol{\phi}_r^j$ denotes the r-th column of $\mathbf{\Phi}^j$. It can be solved easily using one of the standard techniques.

The main advantage of the quasilinearization technique is its fast convergence. However, whether or not the series of the $\mathbf{x}^j(0)$ converges normally cannot be ascertained from the outset, but has to be decided through numerical experimentation. If it converges, then it is certain that at least a local minimum of $J(\mathbf{x}(0))$ has been reached. But if the procedure does not converge, then it is not possible to infer that the parameters and the state of the system are not identifiable (see Sec. 5-1). Usually, inspection of $\mathbf{x}^j(0)$ and $J(\mathbf{x}^j(0))$ *for different* j yields some indication of whether there are identifiability problems. If, for instance, $\mathbf{x}^j(0)$ varies greatly over j while the value of $J(\mathbf{x}^j(0))$ remains almost constant, then it is probable that the estimate is not unequivocal. The same is the case if the coefficient matrix of system (5-3-5) becomes singular, since this means that there is a whole variety of solutions of Eq. (5-3-5). (The coefficients matrix of Eq. (5-3-5) is the information matrix of the linearized estimation problem, see Eq. (5-1-10).) In general, it is fair to say that application of any nonlinear estimation technique, and hence also of quasilinearization, is an art, at least to a certain extent. It is always advisable experimenting with various initial guesses and, if possible, with different estimation techniques also in order to get an estimate in which one has confidence. In practice, convergence can always be forced by treating a sufficient number of components of the initial guess $\mathbf{x}^0(0)$ as measurements. This can be quite reasonable since often the numerical value of a parameter is roughly known. One can then pretend to have a measurement of that value and change the matrix $\mathbf{H}$ in Eqs. (5-3-1a) and (5-3-1c) accordingly (see page 167). The confidence in that guess can be expressed by selecting appropriately the value of the corresponding variance.

Several time series of observations which have been obtained from the same system under different circumstances may be used for the estimation; steady state observations along a river for different flow rates and/or temperatures can be used, for instance. In this case the variables which are affected by a change of circumstances, have simply to be split into as many variables as there are observation series.

When determining $\mathbf{x}^j(\cdot)$ from Eq. (5-3-2) the preceding approximation $\mathbf{x}^{j-1}(\cdot)$ has to be available for the entire range of t. This can be achieved by storing $\mathbf{x}^{j-1}(\cdot)$ as a sufficiently dense table function, though with large systems or long observation periods the storage requirement may become prohibitive. Integration at each iteration of all previously used equations of type (5-3-2) may be made instead, thereby trading storage for computing time.

The quasilinearization technique may be modified in the following way: for the evaluation of $\mathbf{f}$ and $\mathbf{F}$ in Eq. (5-3-2), the solution of the original system (5-3-1b) may be used instead of $\mathbf{x}^{j-1}(t)$, which is defined by the previous optimal values $\mathbf{x}^{j-1}(0)$ as initial values. This technique is known as *Gauss-Newton algorithm* (see Mataušek and Milovanović, 1973). In this case the columns of $\mathbf{\Phi}^j$ in Eq. (5-3-4) are the sensitivity vectors of the original system with respect to the initial values, and the nominal solution is defined by $\mathbf{x}(0) = \mathbf{x}^{j-1}(0)$ (see Sec. 4-1). Finally, it should be mentioned that the quasilinearization technique can also be applied to distributed parameter models.

The Models

As mentioned above, the initial states and the parameters of two models, the Streeter-Phelps model and the ecological model described in Sec. 4-4, were to be estimated for a section of the Rhine river. Dispersion was not taken into account because of the relatively high velocity (see Sec. 4-3). Both models were augmented by an additional equation for the concentration w_3 of nondegradable pollutants, which simply describes the accumulation of those pollutants. Since the amount of nondegradable waste discharged into the river is assumed to be known (although its definition is problematic, see Sec. 3-5) these equations are not at all involved in the estimation procedure. In the final results, however, this waste component is always included (see, for example, Fig. 5-3-5), since later on (Sec. 8-4) it must be taken into account. In principle, it would be possible to dispense with the nondegradable waste fraction as a separate variable and include it instead in the slowly degradable fraction. What is said on identifiability of the models in the following would essentially remain true in this case, and the fit to the measured data would deteriorate only slightly. The models were also augmented by an additive constant in the oxygen equation, to account for biogenic aeration (see Fig. 5-3-5).

The measurements on which the estimation had to be based were total COD, bacterial mass density, protozoan mass density, and oxygen concentration (see Sec. 4-4). They are very fragmentary and in several cases they even had to be derived from other measurements (Stehfest, 1973). The total COD measurements, for instance, had to be derived from measurements of the dissolved COD and measurements of particulate organic matter, the COD of the latter having to be estimated.

The wastewater discharged into the river was assumed to contain dead matter only. The total amount and the proportion which is nondegradable was assumed to be known, while the ratio between easily and slowly degradable components in the ecological model, which is not measurable, was subject to the estimation procedure. Figure 5-3-2 depicts the assumptions on the BOD of pollutants entering the river per river-km and hour. The river section between Mannheim/Ludwigshafen and the Dutch–German border was divided into 12 reaches within which the discharge was assumed to be equally distributed along the river. In Fig. 5-3-2 the major pollution sources along the Rhine river are clearly recognizable: the cities of Mannheim and Ludwigshafen at the mouth of the heavily polluted Neckar river, with large chemical industries and pulp mills; the cities of Mainz and Wiesbaden at the mouth of the Main river which is extremely polluted by chemical industries and pulp mills; the area of Bonn, Cologne, and Leverkusen also having many chemical industries; and finally the heavily industrialized Ruhr district. The pollutants brought in by the affluents are included in Fig. 5-3-2. The composition of the wastewater, i.e., the proportions between easily, slowly, and nondegradable components, are assumed to be constant everywhere, which is quite a rough approximation. The total amounts of COD production in Fig. 5-3-2 are also relatively rough estimates; they refer to 1970. On the assumption that all discharges in Fig. 5-3-2 are due to the domestic, industrial, and agricultural activity of 35 million inhabitants (which is realistic), a production of approximately 600 g COD/(capita · day) results. This seems to be fairly high, in particular, in view of the fact that the values of Fig. 5-3-2 are lower than the actual production, since part of the COD produced has already been removed by treatment plants and by self-purification in the affluents. In Löffler-Ertel and Reichert (1975) considerably lower estimates are given, but the authors emphasize the great uncertainties in the data. In Roberts and Kreijci (1975) a daily TOC production (see Sec. 3-5), for the Glatt valley in Switzerland, of 200 g per capita was estimated for the year 2000, which corresponds roughly to 600 g COD. The main industries in this region are metal working and machine building industries, which produce less organic pollution than the chemical and pulp industries, which determine the pollutional situation of the Rhine river.

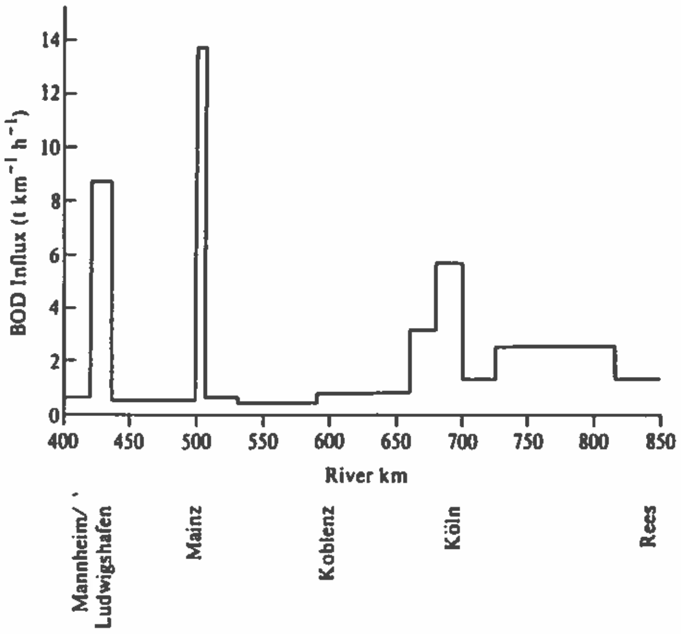

Figure 5-3-2 Estimated discharge of degradable COD into the Rhine river between Mannheim/Ludwigshafen and the Dutch–German border.

The quantities characterizing the hydrology, namely, the lateral inflow q and velocity v, were also assumed to be given and constant within the reaches. Figure 5-3-3 shows some of the hydrologic characteristics of the Rhine river.

The two models, written in flow time, are as follows:

Streeter-Phelps model

$$\dot{b} = -k_{11}b + \frac{v}{Q}(L - qb) \tag{5-3-6a}$$

$$\dot{w}_3 = \frac{v}{Q}(\alpha L - qw_3) \tag{5-3-6b}$$

$$\dot{c} = (k_{21} + k_{22}v)(c_s - c) - k_{11}b + \frac{v}{Q}(L_c - qc) + \beta \tag{5-3-6c}$$

$$\dot{Q} = qv \tag{5-3-6d}$$

$$b(0) = k_{01}, w_3(0) = w_{30}, c(0) = k_{03}, Q(0) = Q_0$$

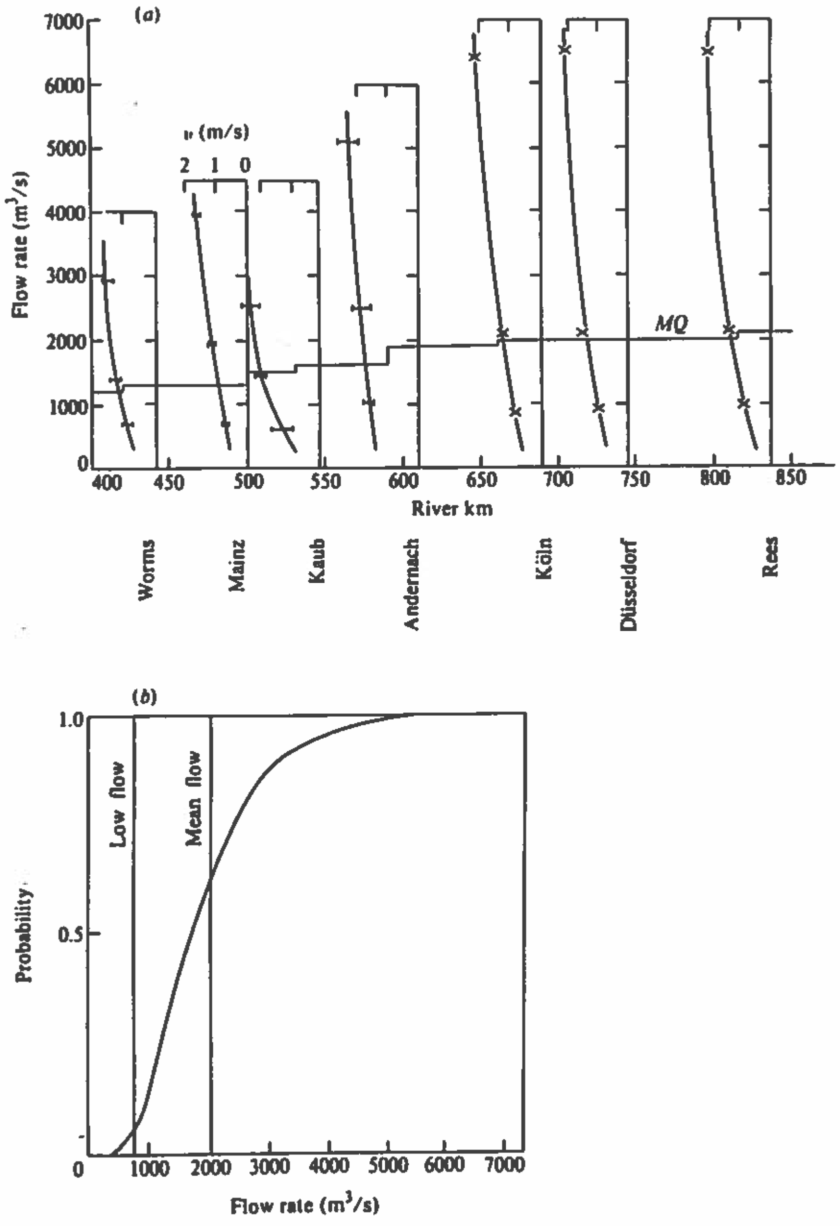

Figure 5-3-3 Hydrologic characteristics of the Rhine river:
(*a*) mean flow rate *MQ* (approximated by a step function) and relationship between v and Q in selected points
(*b*) distribution function of flow rate at Köln.

Ecological model

$$\dot{w}_1 = -k_{11}g_1B + \frac{v}{Q}(k_{12}L - qw_1) \tag{5-3-7a}$$

$$\dot{w}_2 = -k_{21}g_2B + \frac{v}{Q}((1 - k_{12})L - qw_2) \tag{5-3-7b}$$

$$\dot{w}_3 = \frac{v}{Q}(\alpha L - qw_3) \tag{5-3-7c}$$

$$\dot{B} = (g_1 + g_2 - k'_{46})B - k'_{47}g_3P + \frac{v}{Q}(L_B - qB) \tag{5-3-7d}$$

$$\dot{P} = (g_3 - k_{53})P + \frac{v}{Q}(L_P - qP) \tag{5-3-7e}$$

$$\begin{aligned}\dot{c} = {} & (k'_{61} + k_{62}v)(c_s - c) - (k_{63}g_1 + k_{64}g_2 + k'_{65}k'_{46})B \\ & - (k'_{66}g_3 + k'_{67}k_{53})P + \beta + \frac{v}{Q}(L_c - qc)\end{aligned} \tag{5-3-7f}$$

$$\dot{Q} = qv \tag{5-3-7g}$$

where

$$g_1 = \frac{k'_{41}w_1}{k_{42} + w_1} \qquad g_2 = \frac{k_{43}w_1}{k'_{44} + w_2 + k'_{45}w_1} \qquad g_3 = \frac{k'_{51}B}{k'_{52} + B}$$

$$w_1(0) = k_{01},\ w_2(0) = k_{02},\ w_3(0) = w_{30},\ B(0) = k_{04},\ P(0) = k_{05},$$
$$c(0) = k_{06},\ Q(0) = Q_0$$

All k_{ij}'s are quantities which are subject to optimal estimation. The primes on some of the k_{ij}'s will be explained later. The quantities L, L_B, L_P, and L_c denote the distributed loads (in flow time) of pollutants, bacterial mass, protozoan mass, and dissolved oxygen, respectively, which are added to the river as components of all kinds of affluxes. All these functions are assumed to be reachwise constant. The quantity α gives the ratio between the COD of the nondegradable pollutants and L, so that $(1 + \alpha)L$ is the total COD distributed load of the pollutants. The constant β in Eq. (5-3-7f) accounts for biogenic aeration and its numerical value was derived from measurements during summertime.

The composition of the pollution input is defined by the values of the parameters α and k_{12}. For all reaches which do not receive major tributaries these values were assumed to be the same, i.e., the assumption is made that the wastewater has the same composition everywhere and is directly discharged into the Rhine river. For reaches 2, 4, and 7, where major tributaries flow in, the values of α and k_{12} were modified empirically for the effects of self-purification of the tributaries (k_{12} becomes smaller, while α increases). Similarly, the values of L_c for those three reaches were chosen according to the quality of the tributaries.

In all other cases, the admixture terms (i.e., the last terms in Eqs. (5-3-6c), (5-3-7d)–(5-3-7f)) were assumed to vanish, which means that any lateral inflow has the same concentration of bacterial mass, protozoan mass, and oxygen as the receiving river.

Estimation Results

Figure 5-3-4 shows the result of the estimation for the Streeter-Phelps model. The quasilinearization technique converged to a unique set of initial values k_{ij} over a wide range of initial guesses. Flow rate Q and temperature T were chosen to be the same as for the ecological model. This was done in order to be able to consistently compare the two models (see Sec. 8-4). For the same reason the BOD measurements used were the sum of the $(w_1 + w_2)$ values used for the ecological model and the chemical oxygen demand of bacterial and protozoan mass; the oxygen observations used are exactly the same as for the ecological model. The parameter estimates turned out to be

$$\hat{k}_{11} = 0.045\ \mathrm{h}^{-1}, \qquad \hat{k}_{21} = 0.28\ \mathrm{h}^{-1}, \qquad \hat{k}_{22} \simeq 0$$

The negligible value of k_{22} means that the physical reaeration rate does not depend significantly upon the velocity variations along the river. The value of k_{21} seems to be somewhat high, which is consistent with the statement made above that the estimates for the input of pollutants are a little high. But it is still within the range marked by numerous publications about reaeration rates of comparable rivers (see, for example, Negulescu and Rojanski, 1969; Bansal, 1973). There is also very dense shipping traffic on the Rhine river, which considerably enhances physical reaeration. The fit of the measured data is not very good, and a recursive estimation (see Sec. 5-5) would clearly have shown variations of the parameter values along the river.

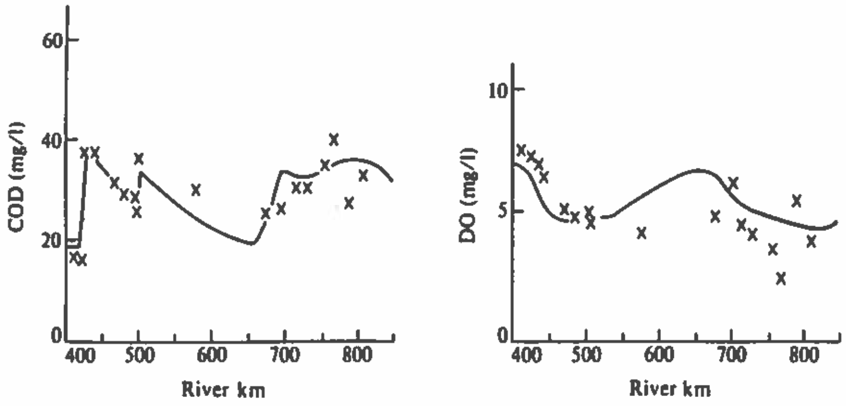

Figure 5-3-4 Description of the self-purification of the Rhine river by the Streeter-Phelps model.

An unambiguous estimation for the ecological model was possible only if the initial guesses for numerous parameters were treated as observations, because the number and accuracy of the observations was not sufficient. The optimal model output together with the measurements is shown in Fig. 5-3-5. Under the conditions selected for that figure ($Q = 1.25MQ$, $T = 20\,°\mathrm{C}$), a relatively large number of accurate measurements were taken along a characteristic line in the upper part of the river section. For other Q and T values even fewer measurements were available, and therefore the use of several measurement series (see p. 161) would not have removed the identifiability problems. The ecological model obviously fits the observations considerably better than the Streeter-Phelps model. The validation tests described below also indicate that the ecological model is more adequate than the Streeter-Phelps model.

The dashed oxygen sag curve in Fig. 5-3-5 shows that the influence of biogenic aeration on the oxygen balance is relatively small in this part of the Rhine river. The reasons for this have already been discussed in Sec. 4-4. One of them is the great depth of the river: because of this the phytoplankton receives on the average very little sunlight; this effect is particularly important because of the high turbidity of the Rhine river. Other reasons for the relative unimportance of biogenic aeration are high velocity and high turbulence of the river. High velocity simply means that the time for the development of a dense phytoplankton population is short. Finally, high turbulence is unfavorable for algal reproduction.

If the measurements from a system are not sufficient to obtain state and parameter estimates under satisfactory conditions, as in the case described, the estimation technique may be used as a tool for planning additional measurements (see Bellman et al., 1966). Numerical experimentation may show which variables have to be measured, where, and with what accuracy in order to obtain an unambiguous state and parameter estimate. The quasilinearization technique was applied to the ecological model for this purpose: under the assumption of reasonably dense and accurate measurements of $w_1 + w_2$, B, P, and c the estimation of the initial values of all variables and of the parameters for model (5-3-7) was attempted. Parameters k_{62} and β, all input and admixture terms, and the equation for nondegradable pollutants were left out. The measurements were generated on a computer using a river quality model much more complex than the one given by Eq. (5-3-7). This model, which is described in Stehfest (1973), contains 30 different pollutants, all of them having different degradation kinetics (mutual inhibitions according to Eqs. (3-5-21) and (3-5-22), purely additive degradation, formation of exoenzymes, see Sec. 3-5), as well as two protozoa types with different metabolic dynamics. The kinetic parameters were generated within realistic ranges by a random number generator. It turned out that the estimation was not possible in a unique way if all parameters were left completely free. But if, for instance, a priori estimates for the primed parameters in Eq. (5-3-7) were considered as measurements, the estimation technique converged, even with very high variances of the parameter guesses and very noisy measurements. In selecting the parameters, for which approximate values are to be prescribed, it is necessary to question whether reasonable guesses for the parameters concerned

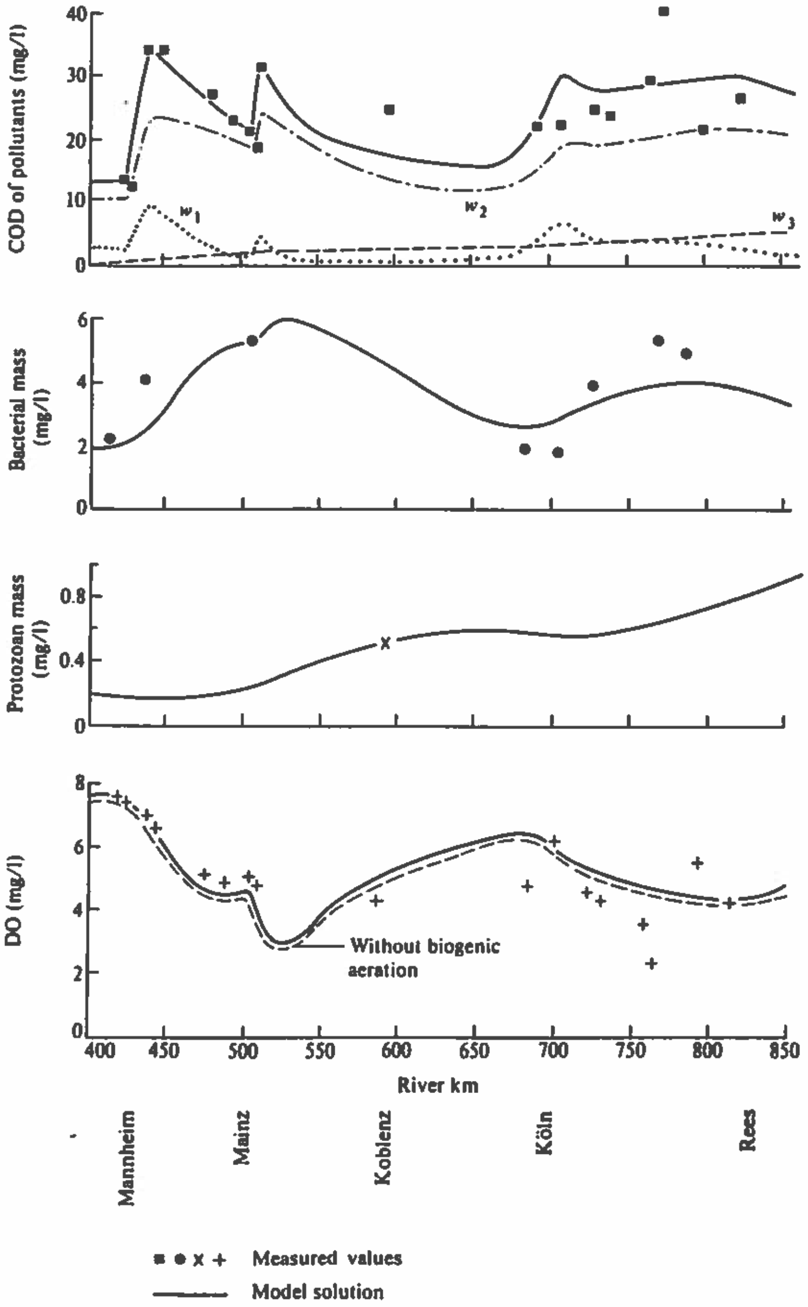

Figure 5-3-5 Description of self-purification of the Rhine river by the ecological model.

are available. It is better, for example, to use an approximate value for k_{41}, rather than for k_{42}, because k_{41} would not be expected to be very much smaller than the largest known growth rate of bacteria at the given temperature, while for a complex nutrient mixture, very little can be predicted about k_{42}. Kinetic parameters for the interaction between bacteria and protozoa which have been found in laboratory experiments can also be used as measured values for the estimation; but it is desirable to have the parameter k_{53} totally free, since the term $k_{53}P$ is to account approximately for the unknown influence of higher order links of the food chain.

Figure 5-3-6 shows the optimal model solution for noise-free measurements (*a*), and measurements distributed by a reasonable noise (*b*). In Fig. 5-3-6a the initial solution $x^0(t)$ is given, which was also used for Fig. 5-3-6b. It can be seen that the estimation is possible, even if the initial estimate is quite wrong. It should be emphasized again that the ratio between w_1 and w_2 is determined through the estimation procedure on the basis of measurements of $w_1 + w_2$, B, P, and c only.

Validation Tests

As explained in Sec. 1-3 model validation is an indispensable step for building any model: good fit to an observation series alone is not yet very meaningful, in particular if there are many parameters to be adjusted. It is always necessary to check if the optimal model is able to reproduce measurements which were taken independently of the ones used for estimation.

Figure 5-3-7 gives an example: in Fig. 5-3-7a that solution of model (5-3-7) is given which best fits the measurements generated by the complex river model. In Fig. 5-3-7b both models with the same parameter values but with completely different initial values for the variables are checked against each other. Since model (5-3-7) describes well the "observations" also under changed initial conditions, it may be concluded that the simple model (5-3-7) is a good approximation of the complex one.

Some validation tests could also be carried out for the ecological model as applied to the Rhine river, although the measurements are so sparse (see also Stehfest, 1978). Figure 5-3-8 shows, for instance, the changes of the model behavior if temperature is lowered from 20 °C to 10 °C. Two most remarkable changes have been confirmed by real measurements: the COD increases more in the upstream part than in the lower Rhine; and bacterial mass density is almost constant from river km 550 to 700 at $T = 10\,°C$, while at $T = 20\,°C$ there was a decline along this river section. The latter effect has already been mentioned and explained in Sec. 2-3.

Figure 5-3-9 shows the changes in the model behavior if the flow rate decreases from $1.25MQ$ to $0.77MQ$. The consequences of this decrease are governed by two effects: the dilution ratio for the discharged pollutants is changed, and the flow times between the pollution sources are changed. Both effects result in an increase of the pollutants removal over a fixed river section. This can be seen from the figure and has also been observed in practice. The

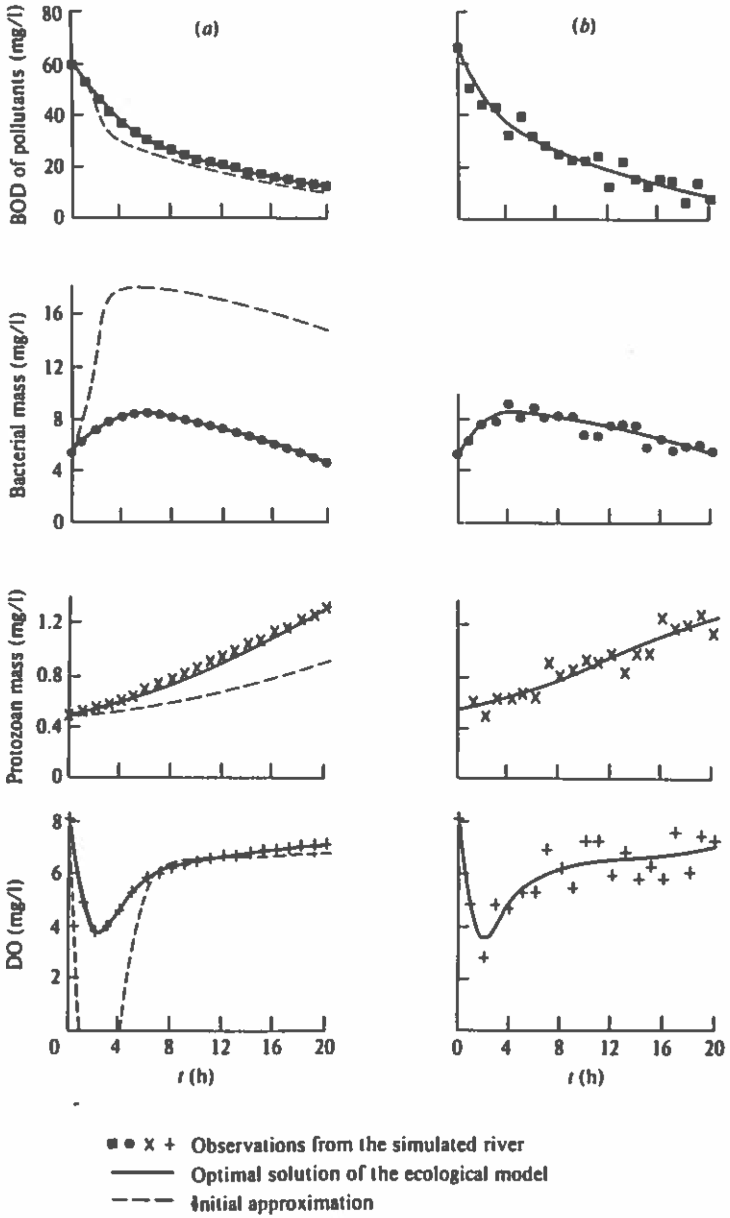

Figure 5-3-6 State and parameter estimation for the ecological model, using synthetic data:
(*a*) noise-free observations
(*b*) noise-corrupted observations.

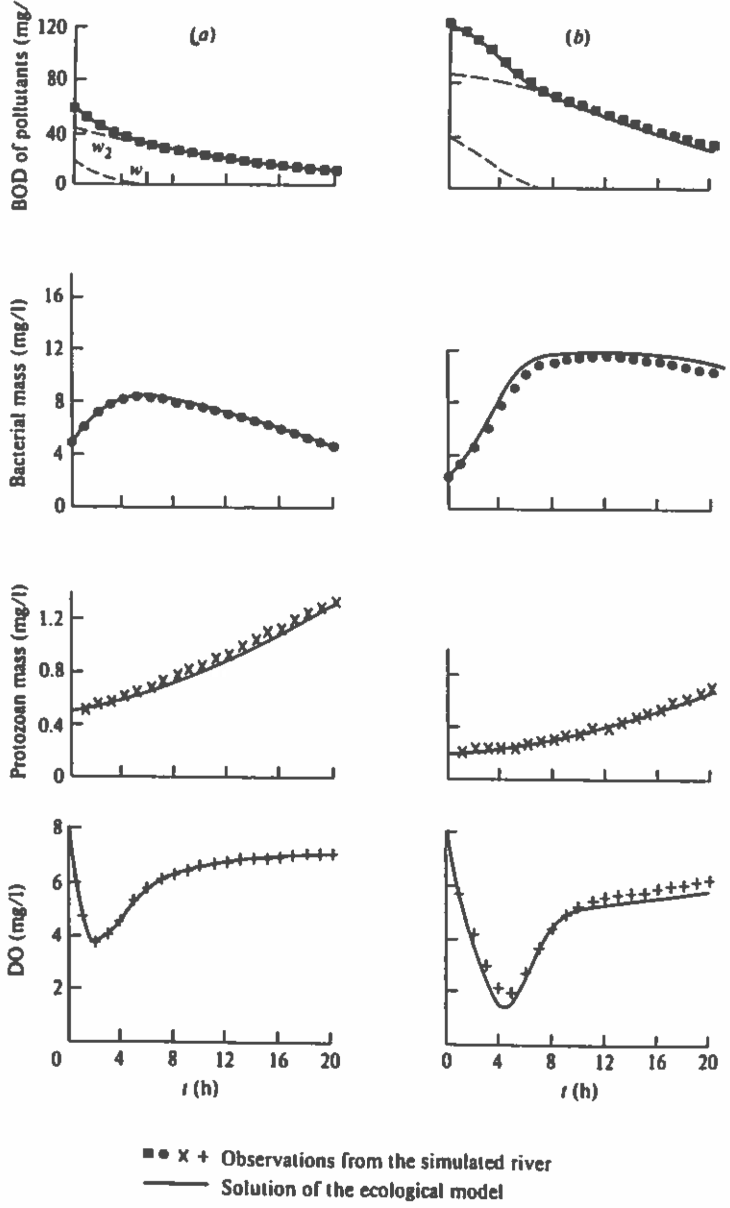

Figure 5-3-7 Model validation for the ecological model using synthetic data:
(*a*) estimation result
(*b*) comparison between observations and model solution under changed initial values.

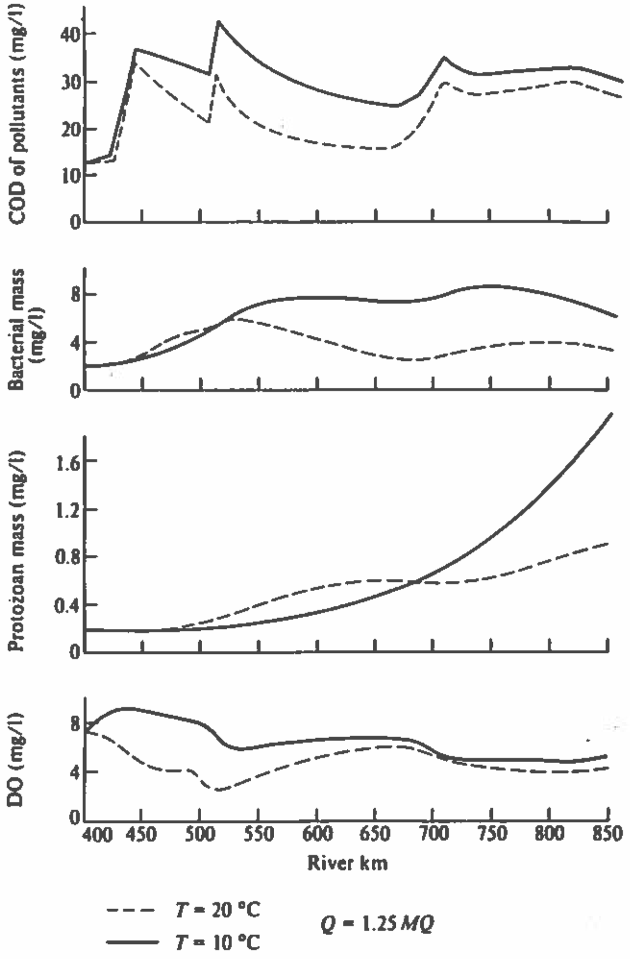

Figure 5-3-8 Changes in the self-purification behavior of the Rhine river when temperature is lowered.

serious deterioration of the oxygen conditions shown by Fig. 5-3-9 also corresponds to real observations.

Finally, Fig. 5-3-10 gives the model behavior in the case that 50 percent of the easily degradable component of the wastewater is removed before discharge. Although this means that as much as about 25 percent of the total COD had been removed, the COD concentration did not decrease considerably anywhere, and in certain parts even increased. The reason for this is the decrease of the growth rate of the bacteria relative to the protozoan consumption rate and to endogenous respiration. This result might be considered as a kind of validation, since a reduction of the easily degradable components is achieved by biological treatment plants. The fact that the quality of the Rhine river has not improved during the last years in spite of remarkable efforts at building biological treatment plants could possibly be attributed to this effect.

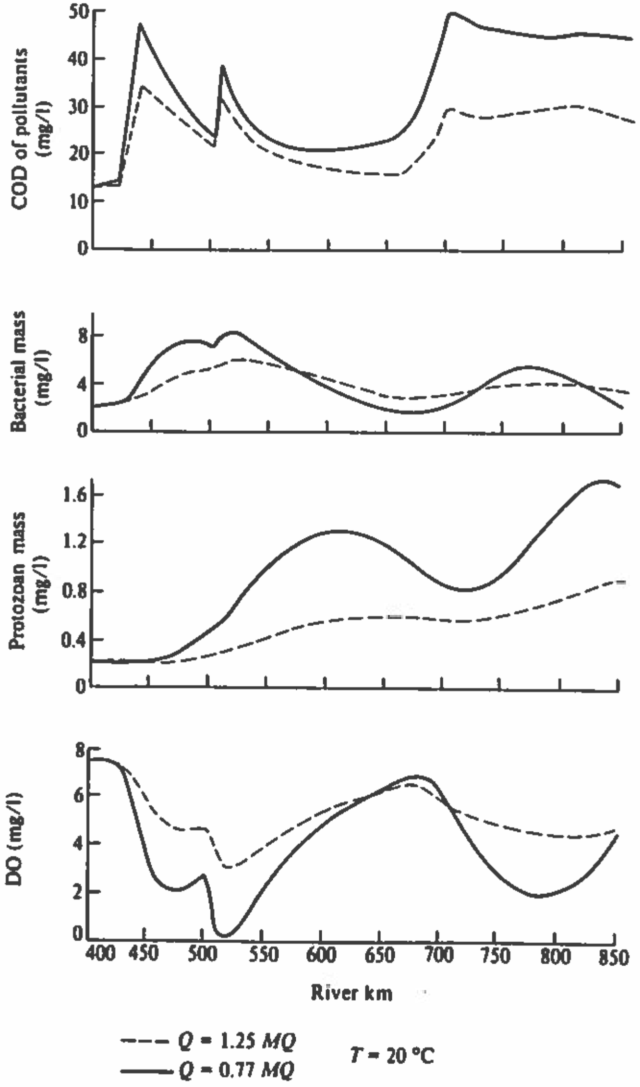

Figure 5-3-9 Changes in the self-purification behavior of the Rhine river when flow rate is lowered.

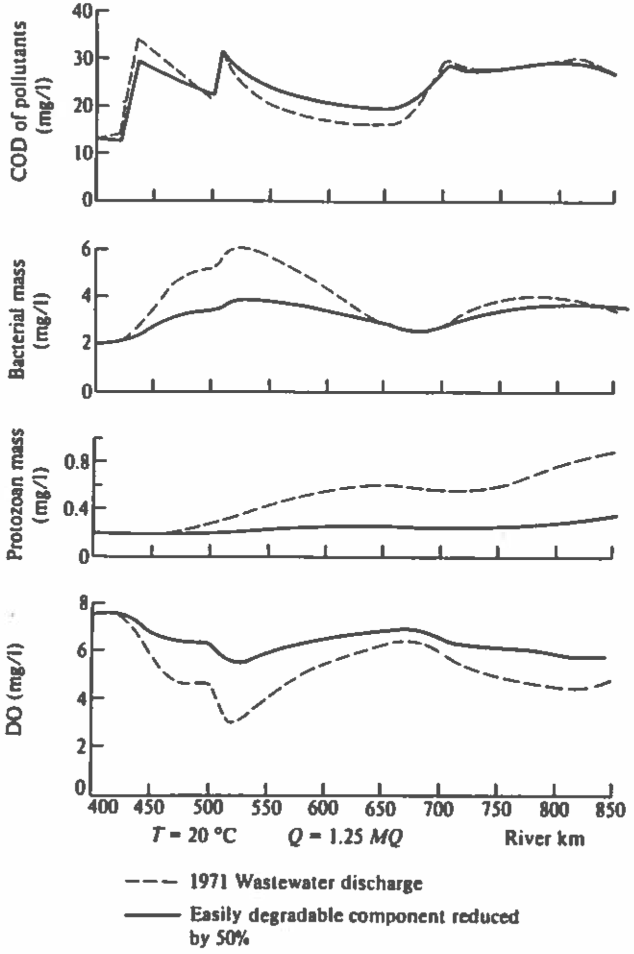

Figure 5-3-10 Changes in the self-purification behavior of the Rhine river due to removal of part of the easily degradable component from sewage.

REFERENCES

Section 5-1

Åström, K. J. and Eykhoff, P. (1971). System Identification: A Survey. *Automatica*, 7, 123–162.

Eykhoff, P. (1974). *System Identification.* John Wiley, London.

Isermann, R. (1974). *Process Identification* (in German). Springer, Berlin.

Mehra, R. K. and Tyler, J. S. (1973). Case Studies in Aircraft Parameter Identification, In *Identification and System Parameter Estimation, Part 1, Proc. 3rd IFAC Symposium, The Hague/Delft, The Netherlands. 12–15 June 1973.* North-Holland, Amsterdam.

Raiffa, H. (1968). *Decision Analysis: Introductory Lectures on Choices under Uncertainty.* Addison-Wesley, Reading, Mass.

Strobel, H. (1975). *Experimental Systems Analysis* (in German). Akademie-Verlag, Berlin.

Unbehauen, H., Göhring, B., and Bauer, B. (1974). *Parameter Estimation Techniques for Systems Identification* (in German). R. Oldenbourg, München, W. Germany.

Section 5-2

Marchetti, R. and Provini, A. (1969). Dissolved Oxygen Profile in Streams under Different Pollution Loads (in Italian). *Aria Acqua*, 7, 1–12.

Metcalf and Eddy, Inc. (1972). *Wastewater Engineering.* McGraw-Hill, New York.

Rinaldi, S., Romano, P., and Soncini-Sessa, R. (1976). Parameter Estimation of a Streeter-Phelps Type Water Pollution Model. In *Identification and Systems Parameter Estimation, Proc. 4th IFAC Symposium on Identification and System Parameter Estimation, Tbilisi, USSR, Sept. 1976.* Pergamon Press. London (to be published in *J. Env. Eng. Div., Proc. ASCE*).

Section 5-3

Bansal, M. K. (1973). Atmospheric Reaeration in Natural Streams. *Water Research*, 7, 769–782.

Bellman, R. E., Kagiwada, H., and Kalaba, R. E. (1966). Inverse Problems in Ecology. *J. Theoret. Biol.*, 11, 164–167.

Bellman, R. E. and Kalaba, R. E. (1965). *Quasilinearization and Nonlinear Boundary-Value Problems.* American Elsevier, New York.

Eykhoff, P. (1974). *System Identification.* John Wiley, London.

Lee, S. E. (1968). *Quasilinearization and Invariant Imbedding.* Academic Press, New York.

Löffler-Ertel, I. and Reichert, J. (1975). *Data Collection on the Water Balance of the Federal Republic of Germany* (in German). Institut für Systemtechnik und Innovationsforschung der Frauenhofer-Gesellschaft, Karlsruhe, W. Germany.

Mataušek, M. R. and Milovanović, M. D. (1973). Identification by Pseudosensitivity Functions and Quasilinearization. In *Identification and System Parameter Estimation, Part II (P. Eykhoff, ed.), Proc. 3rd IFAC Symposium, The Hague, 12–15 June 1973.* North-Holland, Amsterdam.

Negulescu, M. and Rojanski, V. (1969). Recent Research to Determine Reaeration Coefficient. *Water Research*, 3, 189–202.

Roberts, P. V. and Kreijci, V. (1975). *Cost-Benefit Analysis for Water Protection Planning* (in German). Eidg. Anstalt für Wasserversorgung, Abwasserreinigung und Gewässerschutz, Zürich, Switzerland.

Stehfest, H. (1973). Mathematical Modelling of Self-Purification of Rivers (in German; English translation available as report IIASA PP-77-11, International Institute for Applied Systems Analysis, Laxenburg, Austria). *Report KFK 1654 UF*, Kernforschungszentrum Karlsruhe, Karlsruhe, W. Germany.

Stehfest, H. (1978). On the Relationship Between Flow Rate and Organic Pollution Load of the Rhine River (in German). *GWF-Wasser/Abwasser*, 119, 302–305.